

**AWARD NUMBER:** W81XWH-19-1-0109

**TITLE:** Validating Epigenetic and Genetic Biomarkers for Diagnosis of Bladder Pain of Interstitial Cystitis

**PRINCIPAL INVESTIGATOR:** Jayoung Kim, PhD

**CONTRACTING ORGANIZATION:** Cedars-Sinai Medical Center, Los Angeles, CA

**REPORT DATE:** May 2022

**TYPE OF REPORT:** Annual

**PREPARED FOR:** U.S. Army Medical Research and Development Command  
Fort Detrick, Maryland 21702-5012

**DISTRIBUTION STATEMENT:** Approved for Public Release;  
Distribution Unlimited

The views, opinions and/or findings contained in this report are those of the author(s) and should not be construed as an official Department of the Army position, policy or decision unless so designated by other documentation.

# REPORT DOCUMENTATION PAGE

Form Approved  
OMB No. 0704-0188

Public reporting burden for this collection of information is estimated to average 1 hour per response, including the time for reviewing instructions, searching existing data sources, gathering and maintaining the data needed, and completing and reviewing this collection of information. Send comments regarding this burden estimate or any other aspect of this collection of information, including suggestions for reducing this burden to Department of Defense, Washington Headquarters Services, Directorate for Information Operations and Reports (0704-0188), 1215 Jefferson Davis Highway, Suite 1204, Arlington, VA 22202-4302. Respondents should be aware that notwithstanding any other provision of law, no person shall be subject to any penalty for failing to comply with a collection of information if it does not display a currently valid OMB control number. **PLEASE DO NOT RETURN YOUR FORM TO THE ABOVE ADDRESS.**

<b>1. REPORT DATE</b> May 2022		<b>2. REPORT TYPE</b> Annual		<b>3. DATES COVERED</b> 01Apr2021-31Mar2022	
<b>4. TITLE AND SUBTITLE</b>  Validating Epigenetic and Genetic Biomarkers for Diagnosis of Bladder Pain of Interstitial Cystitis				<b>5a. CONTRACT NUMBER</b>	
				<b>5b. GRANT NUMBER</b> W81XWH-19-1-0109	
				<b>5c. PROGRAM ELEMENT NUMBER</b>	
				<b>5d. PROJECT NUMBER</b> PR180579	
<b>6. AUTHOR(S)</b>  Jayoung Kim  E-Mail: jayoung.kim@csmc.edu				<b>5e. TASK NUMBER</b>	
				<b>5f. WORK UNIT NUMBER</b>	
				<b>8. PERFORMING ORGANIZATION REPORT</b>	
<b>7. PERFORMING ORGANIZATION NAME(S) AND ADDRESS(ES)</b>  Cedars-Sinai Medical Center 8700 Beverly Blvd. Los Angeles 90048				<b>10. SPONSOR/MONITOR'S ACRONYM(S)</b>	
<b>9. SPONSORING / MONITORING AGENCY NAME(S) AND ADDRESS(ES)</b>  U.S. Army Medical Research and Development Command Fort Detrick, Maryland 21702-5012				<b>11. SPONSOR/MONITOR'S NUMBER(S)</b>	
				<b>12. DISTRIBUTION / AVAILABILITY STATEMENT</b>  Approved for Public Release; Distribution Unlimited	
<b>13. SUPPLEMENTARY NOTES</b>					
<b>14. ABSTRACT</b> The goal of this study is to determine the biosignature consisting of DNA methylation and gene expression status detected in urine from interstitial cystitis/painful bladder syndrome (IC) patients will stratify IC patients from healthy controls. In this funding year, we have focused on (1) identification on baseline of urine collection, (2) expansion of database for better urine biomarker discovery, and (3) technology application to further identify the DNA methylation markers associated with IC. In particular, we were able to optimize the DNA methylation and gene expression assays, which were designed for high-throughput screening (HTS).					
<b>15. SUBJECT TERMS</b> None listed.					
<b>16. SECURITY CLASSIFICATION OF:</b>			<b>17. LIMITATION</b>	<b>18. NUMBER OF PAGES</b> 183	<b>19a. NAME OF RESPONSIBLE PERSON USAMRDC</b>
<b>a. REPORT</b> Unclassified	<b>b. ABSTRACT</b> Unclassified	<b>c. THIS PAGE</b> Unclassified			<b>19b. TELEPHONE NUMBER</b> (include area code)

# TABLE OF CONTENTS

	<u>Page</u>
1. Introduction	4
2. Keywords	4
3. Accomplishments	4
4. Impact	80
5. Changes/Problems	82
6. Products	83
7. Participants & Other Collaborating Organizations	87
8. Special Reporting Requirements	89
9. Appendices	89

## 1. INTRODUCTION:

The goal of this study is to determine the biosignature consisting of DNA methylation and gene expression status detected in urine from interstitial cystitis/painful bladder syndrome (IC) patients will stratify IC patients from healthy controls.

## 2. KEYWORDS:

interstitial cystitis, DNA methylation, biosignature, gene expression

## 3. ACCOMPLISHMENTS:

**What were the major goals of the project?**

The **overall goals** of this study are to improve the methodology for diagnosis of IC and progression of disease and to develop new insight into the underlying mechanisms that trigger this condition. In this project, we will determine if urine-based DNA methylation and gene expression signatures associates with pain severity, health-related quality of life, and other comorbid conditions in IC patients.

### **Approved SOW (by 12months)**

#### **Milestone(s) Achieved:**

Quantification of epigenetic and genetic biomarker candidates

#### **Subtask 1. Quantification of DNA methylation**

1.1. Sample preparation and protocol optimization

1.2. Targeted DNA methylation analysis

#### **Subtask 2. Quantification of gene expression**

1.1. Sample preparation and protocol optimization

1.2. High throughput gene expression analysis

#### **Subtask 3. Pipeline establishment for computational analysis to test a statistical model**

In this funding year, we have focused on (1) identification on baseline of urine collection, (2) expansion of database for better urine biomarker discovery, and (3) technology application to further identify the DNA methylation markers associated with IC.

**What was accomplished under these goals?**



## (1) Major activities

- The subject protocol (version dated 12/03/2019) was approved by the Cedars-Sinai Institutional Review Board (IRB) on 12/3/19.
- The U.S. Army Medical Research and Development Command (USAMRDC), Office of Research Protections (ORP), Human Research Protection Office (HRPO) reviewed the protocol and found that it complies with applicable DOD, U.S. Army, and USAMRDC human subjects protection requirements.
- We got an Approval Memorandum (Proposal Number PR180579, Award Number W81XWH-19-1-0109) in March 4, 2020.
- Trained personnel who will perform biochemical analyses for this project.

## (2) Significant results or key outcomes

- We made significant key scientific outcomes since the previous funding period. Several full research papers and review articles were published in this funding period. **Please refer to the APPENDICES.**
- After March 4, 2020 when we got an approval from DoD, we started to establish a laboratory-based protocol and assembled a cohort for this particular study.
- Due to this delay on HPRO approval, we were able to initiate actual lab work a little later than we originally expected.
- Urine samples from IC and healthy controls were pre-processed by the trained lab personnel.
- We optimized the DNA extraction protocols using human urine samples.
- We performed the gene expression analysis using urine samples as planned.
- We were able to optimize the DNA methylation and gene expression assays, which were designed for high-throughput screening (HTS). They include CNR2 as planned in the proposed study.
- To perform a pilot study for the MethyLight assay optimization (Dr. Kim).
- Using this optimized assay system, we found that CNR2 DNA methylation is significantly altered in IC patients compared to controls.
- Our pilot study began with evaluating the top five genes (*CNR2*, *PR2Y14*, *GRM6*, *F2R* and *CHRM3*), for which MethyLight assays have already been designed.
- Our ultimate goal is to evaluate the DNA methylation levels of the 20 most hypomethylated genes from preliminary work.

- Our project is conducted through a close collaboration with core facilities in University of Southern California and Genomics Core at CSMC.
- We initiated a contract with NanoString Research team for this particular study. NanoString gene expression analysis is a novel digital technology that is based on direct multiplexed quantification of nucleic acids and offers high levels of precision and sensitivity, in this proposal. NanoString technology employs molecular “barcodes” and single molecule imaging to detect and count target gene expression in a single reaction.
- Unfortunately, due to the current COVID-19 pandemic, we were not able to submit our pro-processed samples to facilities which will perform the HTP analysis.
- Many of my lab personnel were not able to come to work since our lab facility is closed due to the California’s statewide lockdown order.
- Facilities, clinical research center, and all other laboratories were closed or minimally maintained since late March, leading to a project hold.
- We have established new collaboration with a big biomarker discovery group at our own institute for further validation of target candidates. While our preliminary are based on small numbers and require validation in a large dataset, they nonetheless demonstrate the feasibility of the current study and provide strong support to the fact that we are likely to identify many clinically and biological important linkages with IC and the various IC phenotypes within this study.
- Luckily, we were able to publish a series of papers relevant to this proposed study. Our recent review paper summarized the underlying mechanisms that induce the chronic pain associated with IC and vulvodynia and explain why these two conditions often coexist. We also developed a statistical model to determine whether the biosignatures to be enhanced by additional systemic changes, such as widespread pain or associated clinical depression.
- We are sorry that this project may be a little bit delayed to complete. It’s because that we got the HRPO approval later than we originally expected and the COVID-19 pandemic hold the necessary lab work.
- Starting from April 2021, we were able to maintain 50% of full activity in laboratory setting. Slowly but surely the research activity is recovering.
- We were able to ship the samples to facility for analysis. Due to the high volume of COVID-19 samples, it is anticipated to experience the delay.
- We have worked on the validation of biomarker signatures of IC and found additional urinary biomarkers.
- In the following sections, we will update our progress in detail for your reference.

## ACHIEVEMENT 1: Advances in Urinary Biomarker Discovery in Urological Research

### OBJECTIVES

- Identify urine metabolites driving IC disease status.
- Identify urine metabolites affected by gender and/or year of collection.

### Deliverables

- A report summarizing the methods and results supporting this project.

### INTRODUCTION & METHODS

This report summarizes the Interstitial Cystitis (IC) analyses to identify IC biomarkers by analyzing urine metabolites for a cohort of 300 (case and control) IC patients. An initial pilot investigation of 39 (20 control and 19 cases) female subjects from this cohort identified 4 biomarkers of interest; purine, phenylalanine, 5-oxoproline and 5-hydroxyindole acetic acid (Figure 1A).

<b>PURINE</b>	<b>-1.128</b>	<b>&lt; 0.001</b>	<b>0.873</b>
<b>PHENYLALANINE</b>	<b>-1.226</b>	<b>&lt; 0.001</b>	<b>0.85</b>
<b>5-OXOPROLINE</b>	<b>-1.606</b>	<b>0.093</b>	<b>0.817</b>
<b>5-HYDROXYINDOLEACETIC ACID</b>	<b>0.938</b>	<b>0.12</b>	<b>0.817</b>

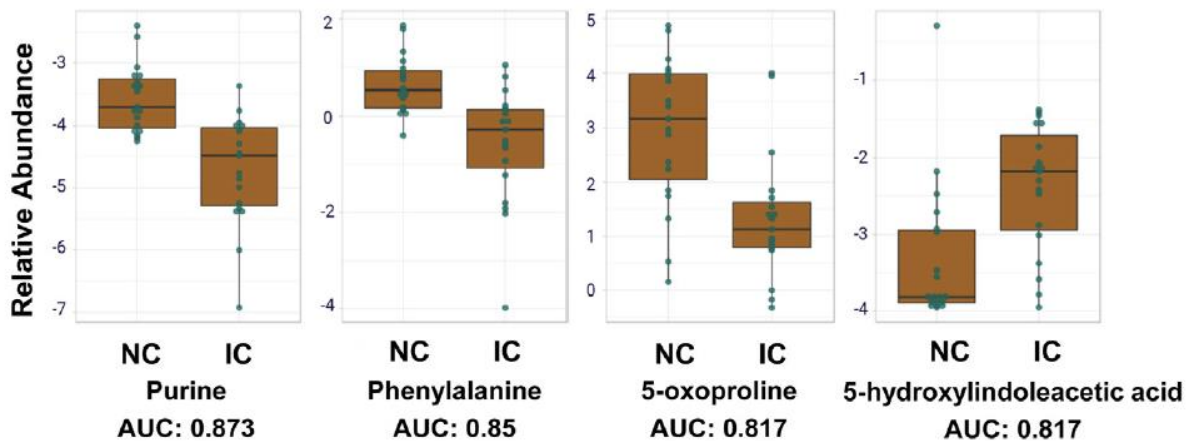


Figure 1: A) 4 Biomarkers identified from the panel of case/control female subjects in the pilot study. Top panel shows the statistics from the Metabolomics analysis. The bottom panel depicts the abundance of each metabolite between case (IC) and control (NC) subjects.

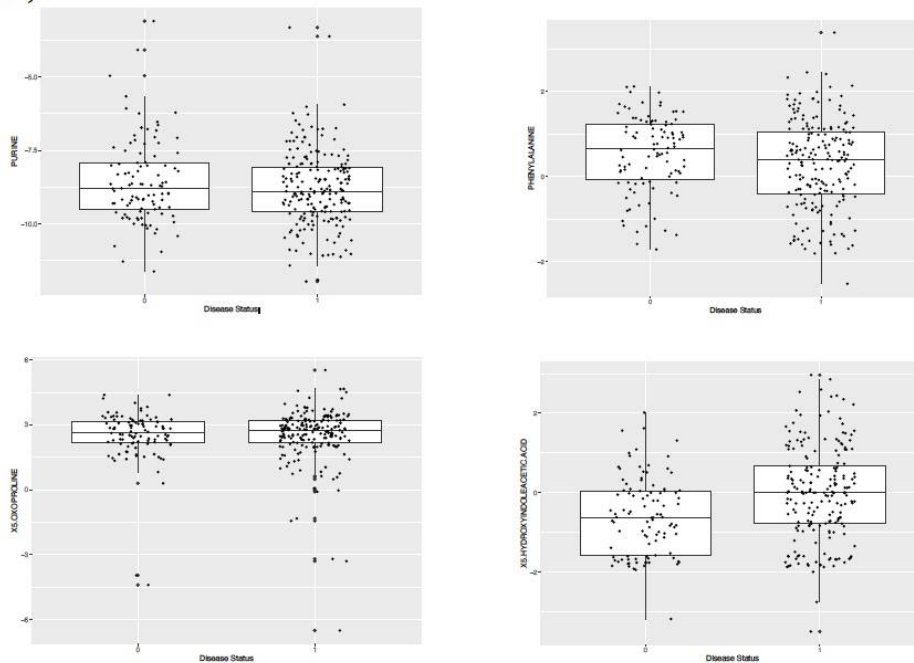
Subsequently, we were able to replicate findings for 5-hydroxyindole acetic acid when analyzing the entire population (n= 300) (Figure 2A). Furthermore, the Omics team showed evidence of a gender effect on a subset of metabolite abundances Figure 2C. Omics had a concern for the accuracy of these results given the known degradation of some metabolites in urine over time. The urine collection times for these samples range over a period of 5 years. Importantly, the Omics team's analysis tools did not provide the option to adjust their process for the impact of confounding variables (collection age or gender) on their differential results.

Described in this report are results of a bAlcis analysis investigating drivers of IC status. With these bAlcis results and results from several additional regression approaches, described below, we aim to 1) explore/validate further the relationship of the 4 biomarkers with IC Status and 2) to potentially identify additional drivers of disease status.

**A)**

Metabolite	FC	p value
5-HYDROXYINDOLEACETIC ACID GC	1.61	2.61E-05
5-AMINO-3-OXOHEXANOIC ACID	0.65	9.51E-05
4-GUANIDINOBUTANOATE	0.66	0.00012986
GLUCURONIC ACID	1.37	0.0001727
D-GLUCARATE	1.34	0.00029902
ANDROSTERONE GLUCURONIDE	0.83	0.0003542
BENZOATE	0.75	0.00052744
GLUCURONIC ACID LACTONE	1.41	0.0011362
OCTOPINE	0.79	0.0011933
AMP	1.27	0.0013454
1,3-PROPANEDIOL	0.77	0.0016584
3-METHOXYBENZENEPANOIC ACID	0.75	0.0021935
CARBAMOYL PHOSPHATE	1.35	0.0026907
3-HYDROXYHIPURIC ACID	1.65	0.0029907
GMP	1.37	0.0036623
GALACTARIC ACID	1.57	0.0037474
INDOLELACTIC ACID	0.60	0.0042832
N-ACETYLRNITHINE	0.78	0.0043964
3-METHYLGLUTACONIC ACID	1.37	0.0045693
3-AMINOISOBUTANOIC ACID	0.78	0.0052105

**B)**



**C)**

Metabolite	FC	p value
ASPARTATE	1.3041	1.11E-12
N-ACETYLASPARTIC ACID	1.3308	2.28E-12
SARCOSINE	1.9195	2.91E-08
AMP	1.5114	3.24E-08
ALANINE	1.8964	4.20E-08
N-ACETYL-GLUTAMATE	1.2613	8.32E-08
CREATINE	1.9493	9.11E-08
N-ACETYALANINE	1.5313	3.00E-07
ALLANTOATE	0.73484	5.15E-07
ISOBUTYRYLGLYCINE	1.6091	1.25E-06
N-ACETYLCARNOSINE	0.77701	3.28E-06
2-KETOGLUTARIC ACID	1.6995	4.07E-06
GLIANDINEACETIC ACID	1.4746	4.81E-06
DOCOSAHEXAENOATE	0.74479	1.38E-05
2-FUROIC ACID	1.3303	1.65E-05
2-HYDROXYGLUTARATE	1.2272	3.03E-05
BENZOATE	1.3658	3.65E-05
S-2-HYDROXYETHYL-N-ACETYLCYSTEINYLCARNITINE	0.81095	6.84E-05
2-KETOBUTYRIC ACID	1.3056	7.10E-05
TAURINE	0.78183	7.48E-05

Figure 2: A) Differential abundance results from Metaboanalyst between IC and Control groups (n = 300). Note only 5-hydroxyindole acetic acid replicates from pilot study. B) Distribution of 4 pilot biomarkers in the total population (n = 300). C) Differential abundance

results from Metaboanalyst between Male and Female groups (n = 300).

In addition, we have performed a differential abundance analysis using a method that allows us to adjust the regression model for the potentially confounding variables of gender and year of collection (YOC). By accounting for the effect of these variables on metabolite abundance we aim to produce a clear view of those features relating to IC Status for which Omics has shown evidence for concern.

## Results and Discussion

### QC analysis

After filtering and normalization of Omics data no batch effect or outliers were detected. Figure 3 shows summary stats on clinical and demographic features. Note, a majority of the clinical data was composed of qualitative questionnaire tables. There were only 11 traditional demographic and clinical features available after filtering in this study (Figure 3A). Clinical data was assessed for missingness.

A)

No	Variable	Stats / Values	Freqs (% of Valid)	Graph	Valid	Missing
1	CohortID [numeric]	Min : 0 Mean : 0.3 Max : 1	0 : 200 (66.7%) 1 : 100 (33.3%)		300 (100.0%)	0 (0.0%)
2	HeightAtDiagnosis [numeric]	Mean (sd) : 66.7 (3.6) min ≤ med ≤ max: 56 ≤ 66 ≤ 76 IQR (CV) : 5.2 (0.1)	56 : 1 ( 0.4%) 57 : 1 ( 0.4%) 58 : 1 ( 0.4%) 59 : 1 ( 0.4%) 61 : 10 ( 4.1%) 62 : 13 ( 5.3%) 63 : 21 ( 8.6%) 64 : 21 ( 8.6%) 65 : 30 (12.3%) 66 : 27 (11.1%) 67 : 20 ( 8.2%) 68 : 19 ( 7.8%) 69 : 18 ( 7.4%) 70 : 20 ( 8.2%) 71 : 17 ( 7.0%) 72 : 14 ( 5.7%) 73 : 3 ( 1.2%) 74 : 3 ( 1.2%) 75 : 2 ( 0.8%) 76 : 2 ( 0.8%)		244 (81.3%)	56 (18.7%)
3	WeightAtDiagnosis [numeric]	Mean (sd) : 186.6 (44) min ≤ med ≤ max: 102 ≤ 182 ≤ 326 IQR (CV) : 60 (0.2)	133 distinct values		243 (81.0%)	57 (19.0%)
4	AgentOrange [numeric]	Min : 0 Mean : 0.1 Max : 1	0 : 196 (93.3%) 1 : 14 ( 6.7%)		210 (70.0%)	90 (30.0%)
5	ServiceBranchID [numeric]	Mean (sd) : 2.4 (1.4) min ≤ med ≤ max: 1 ≤ 2 ≤ 5 IQR (CV) : 2 (0.6)	1 : 76 (25.9%) 2 : 143 (48.6%) 3 : 2 ( 0.7%) 4 : 22 ( 7.5%) 5 : 51 (17.3%)		294 (98.0%)	6 (2.0%)
6	Gender [numeric]	Min : 1 Mean : 1.5 Max : 2	1 : 153 (51.0%) 2 : 147 (49.0%)		300 (100.0%)	0 (0.0%)
7	RaceID [numeric]	Mean (sd) : 2.8 (1.4) min ≤ med ≤ max: 1 ≤ 3 ≤ 13 IQR (CV) : 0 (0.5)	1 : 59 (19.9%) 3 : 232 (78.1%) 10 : 5 ( 1.7%) 13 : 1 ( 0.3%)		297 (99.0%)	3 (1.0%)
8	EthnicityID [numeric]	Min : 1 Mean : 1.9 Max : 2	1 : 17 ( 5.9%) 2 : 271 (94.1%)		288 (96.0%)	12 (4.0%)
9	Deceased [numeric]	Min : 0 Mean : 0 Max : 1	0 : 298 (99.3%) 1 : 2 ( 0.7%)		300 (100.0%)	0 (0.0%)
10	HandAbstractedTobaccoUse [numeric]	Min : 0 Mean : 0.1 Max : 1	0 : 224 (93.3%) 1 : 16 ( 6.7%)		240 (80.0%)	60 (20.0%)
11	HandAbstractedFormerSmoker [numeric]	Min : 0 Mean : 0.5 Max : 1	0 : 125 (46.6%) 1 : 143 (53.4%)		268 (89.3%)	32 (10.7%)

Figure 3B shows a missingness heatmap for the Demographics table where 0s (in blue) indicate a missing value and 1s (in red) indicate a present value for each feature on the Y-axis. Not shown, are additional heatmaps for the clinical questionnaire tables. All clinical features showing more than 30% missingness were removed from subsequent analysis.

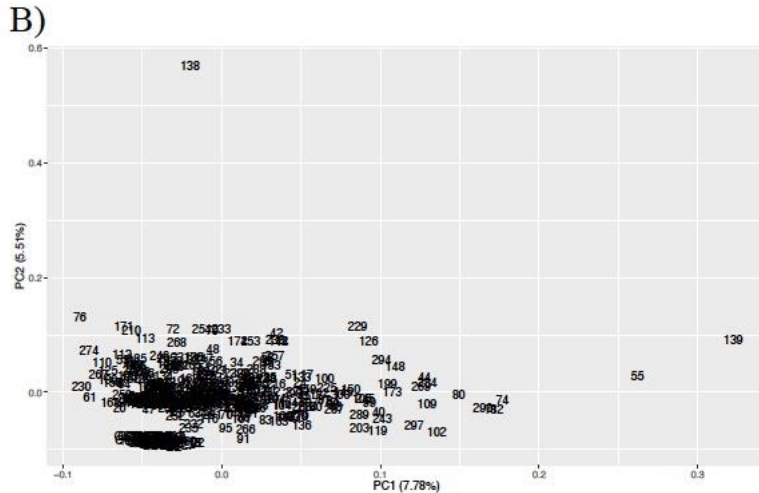


Figure 3C shows a PCA of all filtered and normalized urine metabolomics samples. Table 1 lists all features used in analyses after filtering and normalization. In total, a combined 587 clinical and Omics features remained after processing.

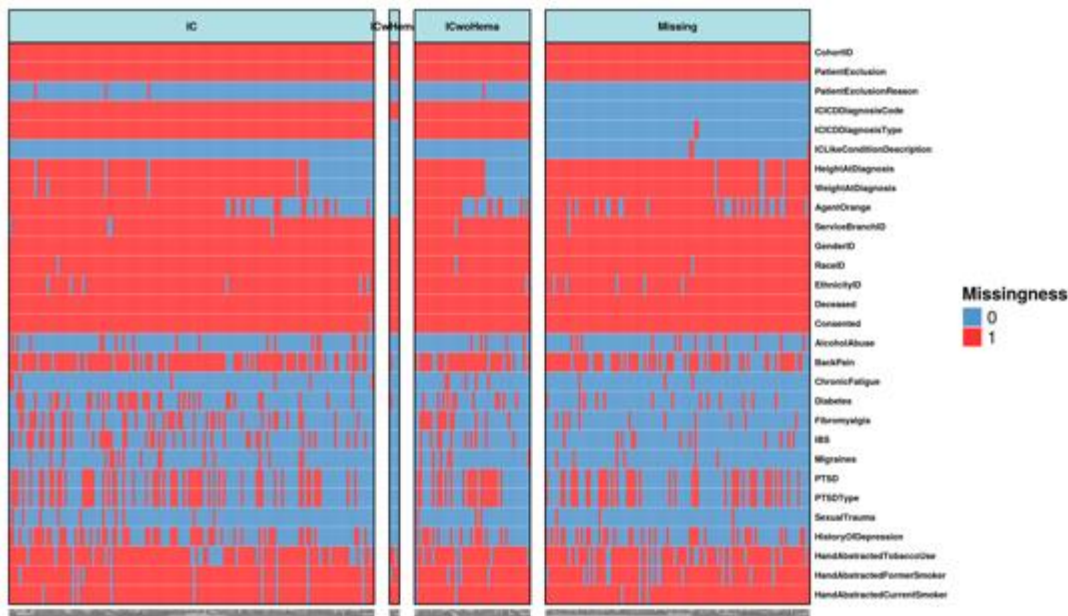


Figure 3: A) Summary stats of demographic features considered in this analysis. Not shown are additional questionnaire summary data. B) PCA of filtered and normalized metabolite samples. C) An example missingness heatmap of the Demographics table showing the degree of missing values across patients.



### bAlcis

Using the filtered clinical data a clinical bAlcis network was run to identify those feature driving IC status outcome (Figure 4A). One node, "Problem Pain" showed a first-degree connection to IC Status (Figure 4B). A list of all nodes within 2 degrees is provided in Table 2. Subsequently, an IC bAlcis network was created using all 587 features, both Clinical and Omics features to identify which ones may be driving the IC status outcome. Similar to the clinical only network, only one feature, "Problem Pain" was shown to connect to IC status (Figure 4C). No Omics feature showed connection with the IC status outcome. Furthermore, no Omics feature was found in the 2nd-degree connections (Figure 4C). None of the 4 biomarkers initially identified in the pilot study were identified by bAlcis.

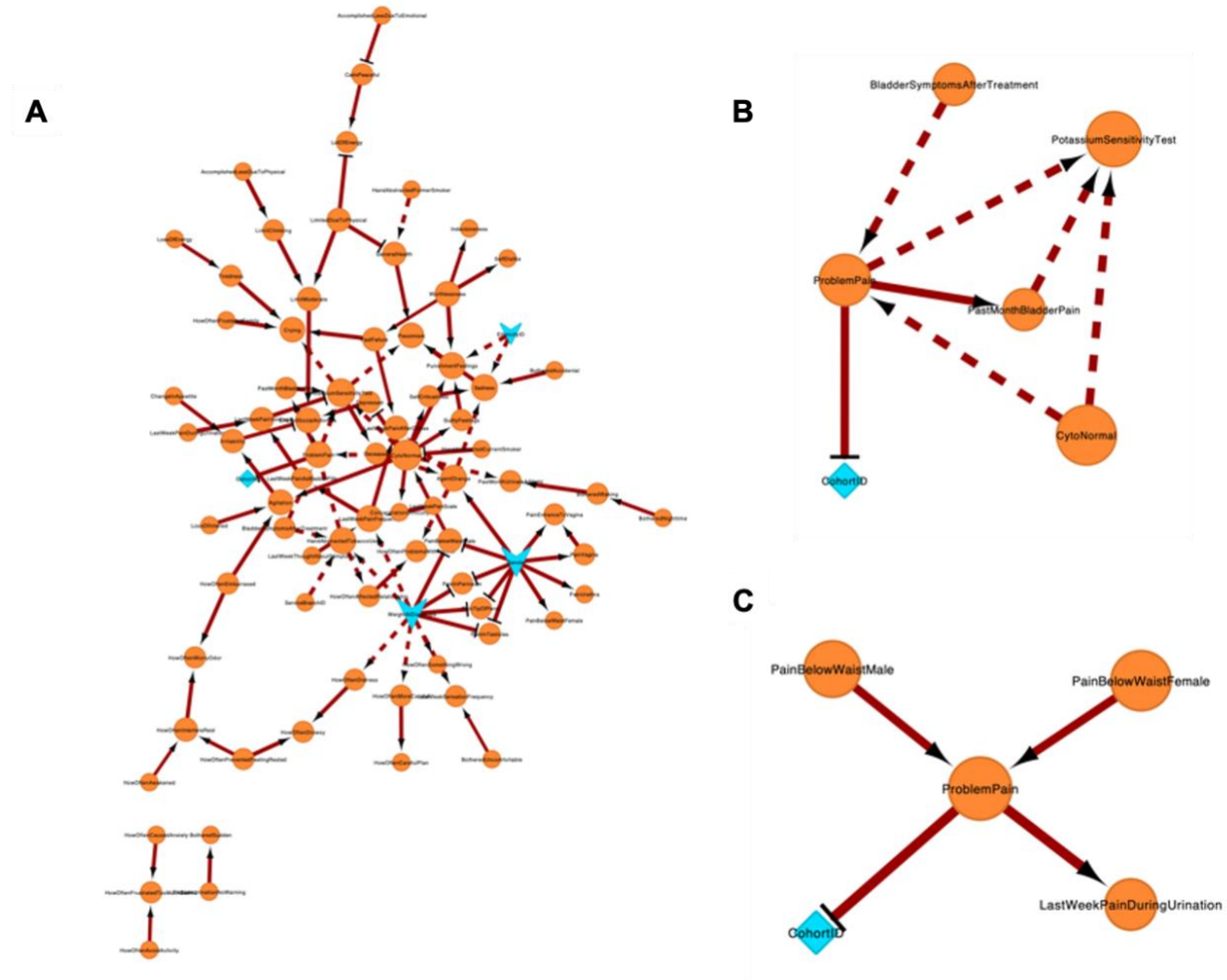


Figure 4: A) A hairball representation of the clinical network. B) A blown up section of the clinical network showing connections to CohortID up to 2-degrees out. C) A blown up section of the clinical and Omics network showing connections to CohortID up to 2-degrees out.

## Univariate regression analyses

A univariate regression was run assessing each metabolite and clinical feature for association with IC status. After FDR correction for multiple testing 133 clinical and metabolomic features showed significance having a qvalue < 0.05 (Table 3).

Feature (Clinical or Omic)	Estimate	StdError	pvalue	qval
LastWeekThoughtAboutSymptoms	-1.5854	0.1787	0.0000	0.0000
ProblemPain	-1.6852	0.1916	0.0000	0.0000
LastWeekPainFrequency	-1.4947	0.1724	0.0000	0.0000
LastWeekPainScale	-0.6997	0.0811	0.0000	0.0000
LastWeekHowAboutRestOfLife	-0.9759	0.1133	0.0000	0.0000
ProblemUrinationFrequency	-1.0991	0.1287	0.0000	0.0000
PastMonthBladderPain	-1.5815	0.1857	0.0000	0.0000
LastWeekUrinatingTwoHrs	-1.0646	0.1277	0.0000	0.0000
LastWeekPainVoiding	-3.0421	0.3685	0.0000	0.0000
BotheredUncomfortable	-1.2337	0.1497	0.0000	0.0000
LastWeekSensationFrequency	-1.0453	0.1290	0.0000	0.0000
HowOftenInterfereRest	-0.8486	0.1049	0.0000	0.0000
HowOftenFrustrated	-1.0255	0.1272	0.0000	0.0000
PastMonthEveryTwoHrs	-0.7833	0.0981	0.0000	0.0000
LastWeekPainAsBladderFills	-3.0299	0.3813	0.0000	0.0000
LastWeekHowOftenLimited	-1.6977	0.2135	0.0000	0.0000
BotheredFrequency	-1.1271	0.1417	0.0000	0.0000
ProblemUrinationNight	-0.8753	0.1118	0.0000	0.0000
ProblemUrinationNoWarning	-0.9456	0.1213	0.0000	0.0000
HowOftenAwakened	-0.8702	0.1116	0.0000	0.0000
HowOftenInterfereSleep	-0.8383	0.1079	0.0000	0.0000
HowOftenPreventedFeelingRested	-0.9274	0.1205	0.0000	0.0000
PastMonthStrongNeedUrinate	-0.7716	0.1034	0.0000	0.0000
BotheredSudden	-1.0655	0.1438	0.0000	0.0000
HowOftenLocateRestroom	-0.8162	0.1110	0.0000	0.0000
HowOftenCarefulPlan	-0.9568	0.1305	0.0000	0.0000
BotheredUncontrollable	-1.0604	0.1454	0.0000	0.0000
HowOftenDecreasedExercise	-0.9376	0.1290	0.0000	0.0000
BotheredWaking	-0.7543	0.1042	0.0000	0.0000
HowOftenEscapeRoutes	-1.1031	0.1533	0.0000	0.0000
HowOftenDistress	-1.1554	0.1608	0.0000	0.0000
HowOftenMoreCareful	-1.2559	0.1750	0.0000	0.0000
HowOftenFrustratedTooMuchBathro	-0.9673	0.1352	0.0000	0.0000
HowOftenSomethingWrong	-0.8617	0.1216	0.0000	0.0000
BotheredNighttime	-0.7278	0.1033	0.0000	0.0000
HowOftenCausedAnxiety	-1.0319	0.1508	0.0000	0.0000
HowOftenAvoidActivity	-1.1424	0.1679	0.0000	0.0000
HowOftenAdjustTravel	-0.9688	0.1427	0.0000	0.0000
PastMonthUrinateAtNight	-0.7171	0.1064	0.0000	0.0000
HowOftenUncomfortableTravelingO	-0.7963	0.1233	0.0000	0.0000
HowOftenPreferStayHome	-1.0129	0.1592	0.0000	0.0000
LastWeekPainDuringUrination	-2.6174	0.4173	0.0000	0.0000
HowOftenDrowsy	-0.8007	0.1373	0.0000	0.0000
HowOftenDecreaseSocialActivitie	-0.9645	0.1692	0.0000	0.0000
HowOftenEmbarrassed	-0.7637	0.1347	0.0000	0.0000
PainInterfered	-0.6678	0.1212	0.0000	0.0000
HowOftenWorryOdor	-0.5650	0.1045	0.0000	0.0000
HowOftenFrustratedFamily	-1.1761	0.2180	0.0000	0.0000
LossOfInterestInSex	-0.7267	0.1358	0.0000	0.0000
BotheredLoss	-0.6733	0.1258	0.0000	0.0000



A second univariate regression was run assessing only Omics features for association with IC status. After FDR correction for multiple testing 24 metabolomic features showed significance having a qvalue < 0.05 (Table 4).

Metabolite	Estimate	StdError	pvalue	qval
X5.HYDROXYINDOLEACETIC.ACID	-0.4796	0.1183	0.0001	0.0148
GLUCURONIC.ACID.LACTONE	-0.4409	0.1192	0.0002	0.0157
D.GLUCARATE	-0.5321	0.1401	0.0001	0.0157
SUCCINYLADEOSINE	-0.9068	0.2442	0.0002	0.0157
GLUCURONIC.ACID	-0.3602	0.1038	0.0005	0.0190
X5.AMINO.3.OXOHEXANOIC.ACID	0.4629	0.1302	0.0004	0.0190
AMP	-0.5606	0.1594	0.0004	0.0190
GUANIDINEBUTYRIC.ACID	0.4640	0.1335	0.0005	0.0190
ANDROSTERONE.GLUCURONIDE	0.5094	0.1577	0.0012	0.0347
X3.METHYLGLUTARYLCARNITINE	-0.5477	0.1748	0.0017	0.0347
BAIBA	0.4554	0.1458	0.0018	0.0347
CARBAMOYL.PHOSPHATE	-0.3426	0.1068	0.0013	0.0347
GLUCOSYLGALACTOSYLHYDROXYLYSINE	-0.6809	0.2123	0.0013	0.0347
GMP	-0.3419	0.1079	0.0015	0.0347
PIMELYLCARNITINE	-0.5034	0.1602	0.0017	0.0347
BENZOIC.ACID	0.4158	0.1368	0.0024	0.0433
X2.HYDROXY.2.METHYLBUTANEDIOIC.ACID	-0.6192	0.2094	0.0031	0.0454
CYTIDINE	-0.7350	0.2452	0.0027	0.0454
GLUTACONYLCARNITINE	-0.4025	0.1347	0.0028	0.0454
OCTOPINE	0.3528	0.1189	0.0030	0.0454
GAMMA.GLU.GLN	-0.3894	0.1335	0.0035	0.0483
HOMOCYSTEIC.ACID	-0.5238	0.1801	0.0036	0.0483
IMP	-0.4240	0.1470	0.0039	0.0493
SN.GLYCEROL.3.PHOSPHATE	-0.2924	0.1017	0.0041	0.0493

After correction for multiple testing in both clinical and Omics and Omics alone the 5-hydroxyindole acetic candidate biomarker showed significant association with IC status. The other 3 biomarkers of interest showed no association with IC status.

### Multivariate regression analyses

Results from the stepForward multivariate regression analysis is shown in Figure 5. Note, this analysis took the top 24 metabolites surpassing FDR correction from the univariate approach. It subsequently used this to build a multivariate model best predicting IC status. Eight of the 24 metabolites input from the univariate results, when combined, were shown to differentiate IC status (Figure 5A). Figure 5B shows the AUC curve for these predictors.

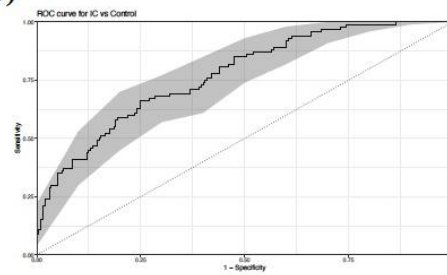
The panel underneath provides the AUC statistic for this result. Note, that 5-hydroxyindole acetic acid is included in the variables best predicting IC status outcome.

We next ran the stepForward analysis with both the clinical and omics data using the top 133 metabolites surpassing FDR correction from the univariate approach (Table 3). Figure 6A shows the ten features when combined best predict IC status. The corresponding AUC plot using these features is shown in Figure 6B. Note, there were many more significant clinical features than omic in this list resulting in the list skewing towards clinical features.

A)

X5.HYDROXYINDOLEACETIC.ACID
AMP
X5.AMINO.3.OXOHEXANOIC.ACID
GLUTACONYLCARNITINE
GAMMA.GLU.GLN
SUCCINYLADEOSINE
HOMOCYSTEIC.ACID
GLUCOSYLGALACTOSYLHYDROXYLYSINE

B)



Model	Cutoff	AUC	Sensitivity	Specificity	PPV	NPV	OR	(CI)	pval
all	0.1805113	0.77	0.91	0.4	0.4312796	0.8988764	6.7	(3.14-16)	8.41E-09

C)

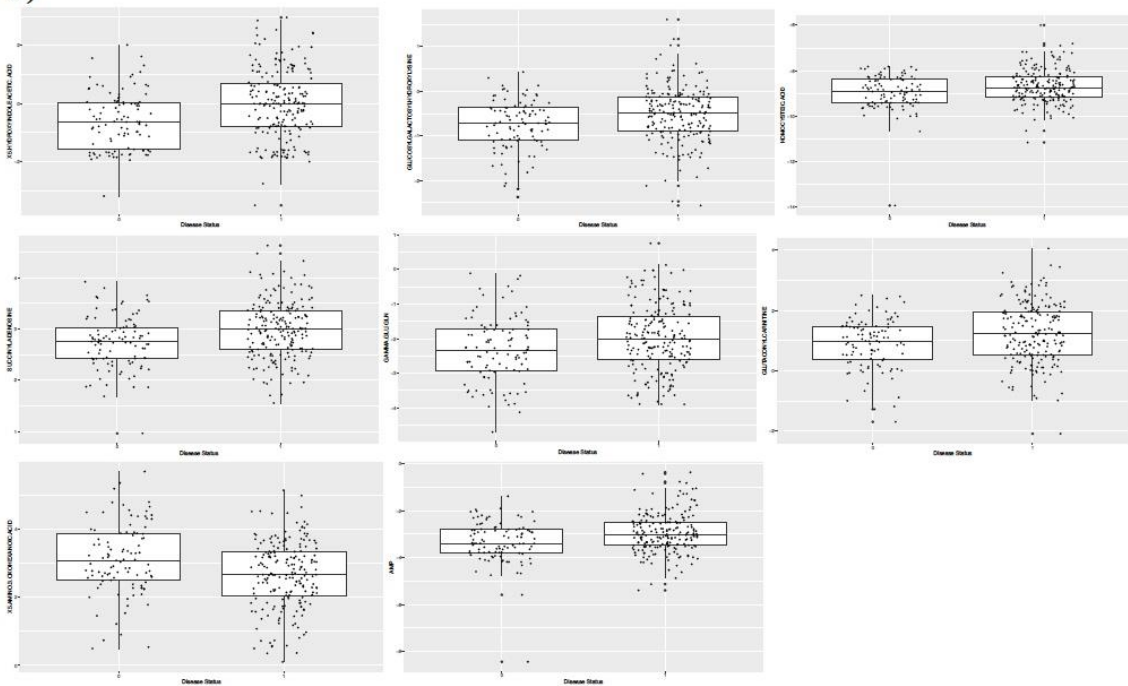


Figure 5: A) 8 metabolites, when combined, best predict the difference between IC status. B) AUC plot using these 8 metabolites. The second panel provides the AUC statistics. C) Boxplots of metabolites in controls (0) and cases (1) for the metabolites in the order of X5.HYDROXYINDOLEACETIC.ACID, GLUCOSYLGALACTOSYLHYDROXYLYSINE, HOMOCYSTEIC.ACID, SUCCINYLADEOSINE, GAMMA.GLU.GLN, X5.AMINO.3.OXOHEXANOIC.ACID and AMP.

### Differential expression analyses

Due to the concerns discovered and raised by the Omics team, a differential abundance analysis was performed to identify metabolites different between IC and control groups. Importantly, to address the potential confounding effects of YOC and gender on this analysis these variables were adjusted for in the regression model to account for their effect. The results of the LimmaDE regression results adjusted for YOC and gender are shown in Supplementary Table 1. Results from this analysis identified 34

metabolites significantly different (Qvalue < 0.05), between IC and Control groups. Note that no L2FC threshold was used here.

Metabolite	Adjusted Regression Model			Collection Year Effect		Gender Effect	
	Adjusted L2FC	Adjusted Pvalue	Adjusted Qvalue	Year Pvalue	Year L2FC	Gender Pvalue	Gender L2FC
X5.HYDROXYINDOLEACETIC.ACID	0.66024	0.00001	0.00301	0.12705	-0.09716	0.41954	0.11092
GLUCURONIC.ACID.LACTONE	0.57090	0.00005	0.00860	0.19236	-0.07905	0.03570	0.27584
SUCCINYLADENOSINE	0.28467	0.00007	0.00860	0.21501	-0.03827	0.93814	-0.00517
AMP	0.41952	0.00011	0.00868	0.53747	-0.02886	0.00000	-0.51960
D.GLUCARATE	0.48719	0.00011	0.00868	0.61027	-0.02779	0.62860	-0.05699
CHOLESTERYL.SULFATE	-0.74026	0.00020	0.01247	0.00097	0.28696	0.00000	-0.96656
CARBAMOYL.PHOSPHATE	0.55732	0.00029	0.01247	0.11575	-0.10491	0.41767	0.11664
GLUCOSYLGALACTOSYLHYDROXYLYSINE	0.28804	0.00028	0.01247	0.09400	-0.05757	0.38000	0.06511
X2.HYDROXY.2.METHYLBUTANEDIOIC.ACID	0.29820	0.00023	0.01247	0.01125	-0.08922	0.53137	-0.04737
N.ACETYL.GLUCOSAMINE.1.PHOSPHATE	0.54996	0.00038	0.01248	0.01788	-0.15965	0.00742	0.39056
X5.AMINO.3.OXOHEXANOIC.ACID	-0.47019	0.00032	0.01248	0.70792	0.02122	0.05104	0.23953
SN.GLYCEROL.3.PHOSPHATE	0.56479	0.00038	0.01248	0.02121	-0.15942	0.43034	0.11744
GLYCERYLPHOSPHORYLETHANOLAMINE	0.78610	0.00045	0.01336	0.00810	-0.25838	0.05393	-0.40531
GUANIDINEBUTYRIC.ACID	-0.44432	0.00049	0.01366	0.76609	0.01644	0.05671	0.22817
BENZOIC.ACID	-0.40494	0.00094	0.02285	0.35705	0.04896	0.00003	-0.48991
X3.METHOXYBENZENEPROPANOIC.ACID	-0.44436	0.00100	0.02285	0.07797	0.10351	0.22179	-0.15485
BAIBA	-0.61788	0.00094	0.02285	0.01071	0.20796	0.26593	-0.19505
GLUCURONIC.ACID	0.53530	0.00108	0.02332	0.73160	0.02437	0.04978	0.30216
NAD.	0.40411	0.00117	0.02405	0.33017	-0.05266	0.00000	-0.99247
GMP	0.47649	0.00136	0.02650	0.90881	0.00740	0.00000	-0.80864
GALACTOSYLHYDROXYLYSINE	0.27142	0.00158	0.02932	0.15744	-0.05282	0.87975	-0.01219
X3.FORMYLINDOLE	-0.43618	0.00206	0.03490	0.01551	0.14954	0.01492	0.32504
IMP	0.38268	0.00202	0.03490	0.82968	-0.01158	0.00003	-0.49760
X4.HYDROXYBENZENEACETIC.ACID	0.46427	0.00270	0.04378	0.30264	-0.06937	0.16948	0.19995
DEOXYGUANOSINE	-0.44460	0.00293	0.04391	0.01144	0.16510	0.02490	-0.31605
X3.PHOSPHOGLYCERATE	0.61091	0.00316	0.04391	0.16279	-0.12574	0.05456	0.37482
X3..3.HYDROXYPHENYL.3.HYDROXYPROPIOIC.ACID	0.70472	0.00306	0.04391	0.00101	-0.34300	0.14158	0.32908
OCTOPINE	-0.41998	0.00305	0.04391	0.71462	0.02253	0.52055	0.08557
N.ACETYLPUTRESCINE	-0.29877	0.00334	0.04485	0.13660	0.06600	0.00441	-0.27417
X3.METHYLGUTARYLCARNITINE	0.28785	0.00366	0.04751	0.76525	0.01286	0.35784	-0.08562
X2.PHENYLGLYCINE	0.82066	0.00392	0.04820	0.06583	-0.22816	0.23287	0.31923
CYTIDINE	0.19794	0.00396	0.04820	0.90361	-0.00362	0.98290	-0.00138
ANDROSTERONE.GLUCURONIDE	-0.31725	0.00421	0.04822	0.32353	-0.04762	0.00073	0.35544
D.GLUCONATE	0.31076	0.00420	0.04822	0.02744	-0.10450	0.29206	0.10755

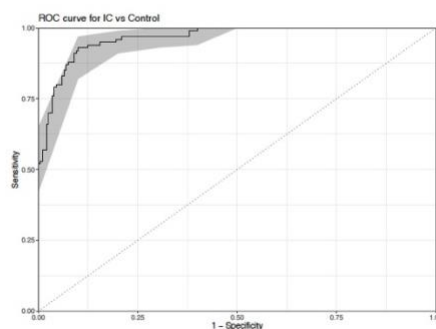
Supplementary Table 1.

Figure 6 shows a volcano plot of these results using a Qvalue threshold of < 0.05 and a L2FC < 0.5. Note, that the top hit here is the biomarker candidate 5-hydroxyindole acetic acid.

A).

X5.HYDROXYINDOLEACETIC.ACID
ProblemPain
LastWeekPainFrequency
HowOftenEscapeRoutes
Irritability
X1.3.PROPANEDIOL
LossOfInterestInSex
THREONIC.ACID
HOMOCYSTEIC.ACID
LastWeekUrinatingTwoHrs

B)



Model	Cutoff	AUC	Sensitivity	Specificity	PPV	NPV	OR (CI)	pval
all	0.4106186	0.96	0.91	0.91	0.8348624	0.9528796	98.9 (41.7 - 262)	3.12e-47

Figure 6: A) 10 metabolite and clinical features, when combined, best predict the difference between IC status. B) AUC plot using these 10 features. The second panel provides the AUC statistics.

Supplementary Table 1 contains 2 additional columns of information for the effect of YOC and gender. For each, a column exists describing the P value and another the L2FC of each metabolite between case and control in this analysis. These columns inform us if the metabolite is significantly different across YOC or between genders (p value) and how large the difference is (L2FC). To determine which metabolomic features are significantly upregulated in males compared to females we filter Supplementary Table 1 on gender P value with < 0.05 and sorted the results by gender L2FC by ascending. This filtering identifies 76 metabolites significantly more abundant in males compared to females (Table 5, Figure 7B). The remaining 76 metabolites, with a “-“ L2FC, are shown to be less abundant in males compared to females (Table 6, Figure 7C). To determine which metabolomic features are significantly less abundant in samples as years progress we filter.

Supplementary Table 1

Metabolite	Base L2FC	Base Pvalue	Base Qvalue
X5.HYDROXYINDOLEACETIC.ACID	0.58543	0.00002	0.00744
D.GLUCARATE	0.46580	0.00008	0.01071
GLUCURONIC.ACID.LACTONE	0.51004	0.00012	0.01071
SUCCINYLADEOSINE	0.25520	0.00014	0.01071
AMP	0.39730	0.00020	0.01214
X5.AMINO.3.OXOHEXANOIC.ACID	-0.45385	0.00025	0.01232
GUANIDINEBUTYRIC.ACID	-0.43167	0.00035	0.01341
GLUCURONIC.ACID	0.55406	0.00036	0.01341
ANDROSTERONE.GLUCURONIDE	-0.35392	0.00087	0.02848
CARBAMOYL.PHOSPHATE	0.47654	0.00098	0.02848
GLUCOSYLGALACTOSYLHYDROXYLYSINE	0.24370	0.00108	0.02848
GMP	0.48219	0.00114	0.02848
PIMELYLCARNITINE	0.31701	0.00135	0.03012
X3.METHYLGLUTARYLCARNITINE	0.29775	0.00140	0.03012
BENZOIC.ACID	-0.36724	0.00191	0.03602
IMP	0.37376	0.00192	0.03602
GLUTAONYLCARNITINE	0.35361	0.00228	0.03778
HOMOCYSTEIC.ACID	0.28077	0.00233	0.03778
CYTIDINE	0.19516	0.00249	0.03778
OCTOPINE	-0.40263	0.00251	0.03778
X2.HYDROXY.2.METHYLBUTANEDIOIC.ACID	0.22950	0.00279	0.03991
GAMMA.GLU.GLN	0.34935	0.00301	0.04117
SN.GLYCEROL.3.PHOSPHATE	0.44204	0.00322	0.04201
N.ACETYL.GLUCOSAMINE.1.PHOSPHATE	0.42703	0.00371	0.04644
X3.METHOXYBENZENEPROPANOIC.ACID	-0.36465	0.00414	0.04973
GALACTOSYLHYDROXYLYSINE	0.23075	0.00431	0.04979
X4.HYDROXYBENZENEACETIC.ACID	0.41085	0.00478	0.05323
NOREPINEPHRINE	0.50527	0.00588	0.06091
X2.ISOPROPYLMALIC.ACID	0.30729	0.00606	0.06091
NAD.	0.36356	0.00622	0.06091
GLYCERYLPHOSPHORYLETHANOLAMINE	0.58715	0.00628	0.06091
SAICAR	0.67595	0.00689	0.06414
GLUCOSE	0.64932	0.00704	0.06414
X2.OCTENDIOIC.CARNITINE	0.28443	0.00753	0.06582
CHOLESTERYL.SULFATE	-0.51930	0.00767	0.06582
X1.3.PROPANEDIOL	-0.35654	0.00827	0.06707
L.ARGININO.SUCCINATE	0.21069	0.00828	0.06707
X3.PHOSPHOGLYCERATE	0.51408	0.00848	0.06707
INDOLELACTIC.ACID	-0.44941	0.00876	0.06745
FAD	0.42286	0.00910	0.06832
X3.METHYLPHENYLACETIC.ACID	-0.64354	0.00955	0.06832
BAIBA	-0.45775	0.00955	0.06832

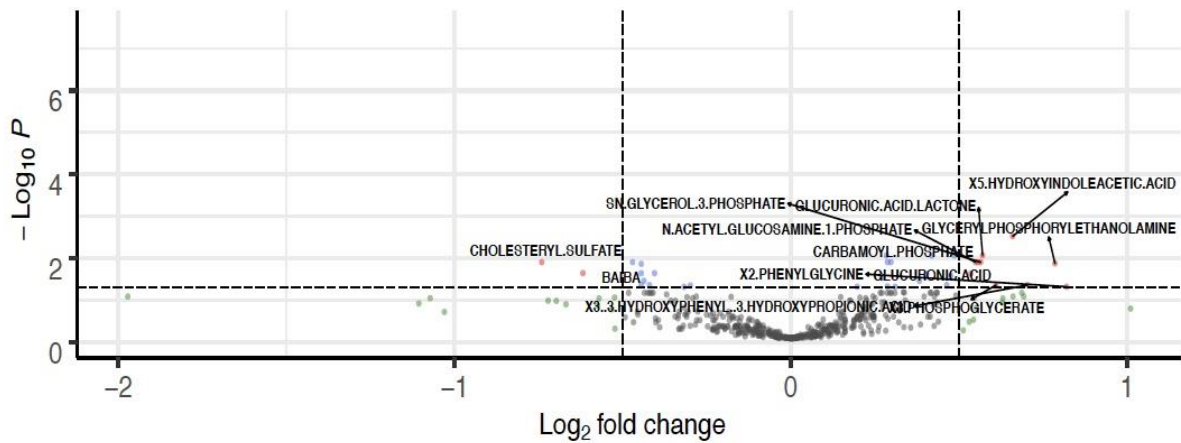
Supplementary Table 1 on Year P value with < 0.05 threshold and selected those L2FC values with a negative value. This resulted in 15 metabolites showing significant degradation over YOC time (Table 7). We also provide Supplementary Table 2 to show the base DE regression model in which no metabolites were adjusted for gender or YOC.

A)

**Volcano plot**

L2FC > 10.51, q-val < 0.05

● NS ● Log<sub>2</sub> FC ● p-value ● p-value and log<sub>2</sub> FC



Total = 479 variables

B)

Metabolite	Adjusted L2FC	Adjusted Pvalue	Adjusted Qvalue	Gender Pvalue	Gender L2FC
ALLANTOATE	-0.00110	0.97337	0.96988	0.00000	0.46970
D1.HYDROXYMETHYL-5-GLYOXYL-3-PHOSPHOCHOLINE	-0.23962	0.42378	0.45460	0.00000	0.36837
N.ACETYLCAINE	-0.09990	0.33413	0.46896	0.00000	0.37600
5.2.HYDROXYMETHYL-3-ACETYLCHOLINE	0.02769	0.78143	0.74886	0.00003	0.40222
DIOXYGENAMINE	0.14026	0.42381	0.46863	0.00004	0.09636
DIOXYTHIONE	0.43367	0.00811	0.06004	0.00007	0.53823
DECAHYDROEPIANDRONE	-0.06100	0.44849	0.56379	0.00011	0.30660
16.HYDROXYMETHYL-2-AMINO-2-DEOXYRIBOSE	0.23914	0.23774	0.42804	0.00019	0.65890
MALONICACID	0.00513	0.93497	0.80337	0.00024	0.22122
ANDROSTRIENE	-0.06996	0.54666	0.57518	0.00028	0.34120
TRIGLYCERINE	0.00278	0.97537	0.96988	0.00032	0.30880
X5.HYDROXYMETHYL-2-FURFURYLCAINE	0.03325	0.84798	0.76029	0.00035	0.53905
BENZYLCAINE	0.02395	0.84943	0.76756	0.00036	0.37330
HEXAMETHYLDISAZINE	0.00940	0.93847	0.80713	0.00044	0.36320
ALPHA-HYDROXYISOBUTYRICACID	0.06204	0.62133	0.76036	0.00044	0.52387
ANDROSTRIENE-GLUCURONIDE	-0.18720	0.06421	0.04832	0.00073	0.30346
TETRAHYDROXYMETHYLCAINE	0.27845	0.02431	0.13400	0.00085	0.39170
TRIMETHYLSULFAMETHYLCAINE	0.04621	0.83827	0.80519	0.00088	0.24803
TRICHOCLICACID	0.13028	0.46010	0.53982	0.00091	0.57123
SPERMINE	-0.09153	0.62189	0.66889	0.00105	0.58370
BISAMINOCAINE	0.06820	0.46990	0.53702	0.00113	0.28794
GABOSINE	-0.19798	0.34967	0.45458	0.00114	0.53268

C)

Metabolite	Adjusted L2FC	Adjusted Pvalue	Adjusted Qvalue	Gender Pvalue	Gender L2FC
NAL	0.40411	0.00117	0.02605	0.00000	-0.99247
ASPARTATE	-0.04043	0.45559	0.56987	0.00000	-0.35562
N.ACETYLASPARTICACID	0.06137	0.33619	0.46004	0.00000	-0.39493
CMP	0.04951	0.64413	0.67930	0.00000	-0.66313
CMP	0.07649	0.00136	0.02555	0.00000	-0.30564
ALANINE	-0.41413	0.00716	0.06744	0.00000	-0.81785
SARCOSINE	0.00870	0.00870	0.06744	0.00000	-0.82757
CREATINE	-0.43897	0.00872	0.06744	0.00000	-0.84228
CHOLESTERYLSULFATE	-0.74026	0.00000	0.01347	0.00000	-0.96656
N.ACETYLALANINE	-0.28095	0.01314	0.08245	0.00000	-0.55193
AMP	0.41352	0.00011	0.00968	0.00000	-0.51960
N.ACETYL-GLUTAMATE	-0.28177	0.20880	0.40668	0.00000	-0.30080
ISOBUTYRYLGLYCINE	0.33968	0.07078	0.23338	0.00000	-0.58736
X1.METHYLADENOSINE	-0.06664	0.34366	0.49536	0.00000	-0.31131
UDP-B-GLUCOSE	-0.02118	0.88970	0.79055	0.00002	-0.34512
IMP	0.38268	0.00202	0.03490	0.00003	-0.49790
BENZOCACID	-0.40494	0.00094	0.02285	0.00003	-0.48991
GUANINEACETICACID	-0.51616	0.03861	0.15229	0.00004	-0.60075
ADENINE	-0.30157	0.01461	0.06029	0.00007	-0.40511
BIOTIN	-0.45604	0.05321	0.18813	0.00008	-0.88896

Figure 7: A) Volcano plot of adjusted DE. A Qvalue of < 0.05 and a L2FC threshold of < 0.5 were used. B) Top 20 metabolites having significantly greater abundance in males than females. C) Top 20 metabolites having significantly greater abundance in females than males.

Overall the provided clinical data for this study was well represented among patients. While we had 108 clinical features available in > 70% of subjects 97 of these features were derived from self-reported patient questionnaires. There are 11 more traditional clinical features described in Figure 3A.

We were able to replicate one biomarker identified in the pilot study, 5-hydroxyindole acetic acid, as differentiating IC case vs control in the larger cohort of 300 subjects. Furthermore, 5-hydroxyindole acetic acid was significant in all three of our regression-based tests, but not found



in our bAlcis analysis. It is worth noting that 5-Oxyproline appears to have a modest gender effect in the Limma analysis where 5-Oxyproline level are more abundant in Females. However, 5-Oxyproline is not significantly different in either Males or Females as independent cohorts. We must consider the limited power of the pilot study with an  $n=39$ . In this analysis utilizing an  $n=300$ , nearly 8x greater, 5-Oxyproline is not significant. Neither of the remaining two candidates, purine and phenylalanine, showed a significance in any analyses using the cohort of 300 subjects (Summary Table 1). It is noteworthy that we identified metabolites of interest (Tables 4-7) that appear to be influenced by gender and/or YOC. These metabolites may be of interest for future studies.

There were 33 biomarkers, in addition to 5-hydroxyindole acetic acid, identified using the differential abundance analysis adjusting for gender and YOC (Supplementary Table 1). These may be filtered down to a more conservative subset by introducing a L2FC threshold. These candidates may be of interested as additional biomarkers.

Overall, the provided clinical data for this study was well represented among patients. While we had 108 clinical features available in > 70% of subjects 97 of these features were derived from self-reported patient questionnaires. There are 11 more traditional clinical features described in Figure 3A.

We were able to replicate one biomarker identified in the pilot study, 5-hydroxyindole acetic acid, as differentiating IC case vs control in the larger cohort of 300 subjects. Furthermore, 5-hydroxyindole acetic acid was significant in all three of our regression-based tests, but not found in our bAlcis analysis. It is worth noting that 5-Oxyproline appears to have a modest gender effect in the Limma analysis where 5-Oxyproline level are more abundant in Females. However, 5-Oxyproline is not significantly different in either Males or Females as independent cohorts. We must consider the limited power of the pilot study with an  $n=39$ . In this analysis utilizing an  $n=300$ , nearly 8x greater, 5-Oxyproline is not significant. Neither of the remaining two candidates, purine and phenylalanine, showed a significance in any analyses using the cohort of 300 subjects (Summary Table 1).

It is noteworthy that we identified metabolites of interest (Tables 4-7) that appear to be influenced by gender and/or YOC. These metabolites may be of interest for future studies.

There were 33 biomarkers, in addition to 5-hydroxyindole acetic acid, identified using the differential abundance analysis adjusting for gender and YOC (Supplementary Table 1). These may be filtered down to a more conservative subset by introducing a L2FC threshold. These candidates may be of interested as additional biomarkers.

## **ACHIEVEMENT 2: PATHOPHYSIOLOGY AND CLINICAL BIOMARKERS IN INTERSTITIAL CYSTITIS**

### **Synopsis**

IC/BPS is a poorly understood yet prevalent condition accounting for a significant proportion of urology office visits. Identification of reliable biomarkers for disease remains an important yet challenging area of research given the heterogeneity of disease presentation and pathophysiology. Our review of the literature revealed a handful of original investigations which revealed promising biomarkers within various physiologic processes or organ systems including immunity, inflammation, neural pathways, urothelial integrity, and anesthetic bladder capacity. While no perfect biomarker has yet been identified for IC/BPS, research in this area has greatly expanded our understanding of disease.

**Key words:** Interstitial cystitis, bladder pain syndrome, biomarkers, autoimmune, inflammation.

### **Key points:**

1. IC/BPS is a heterogeneous disease both in presentation and pathophysiology, making characterization and reliable biomarker identification challenging.
2. The emergence of omics research and collaboration by the MAPP Network has allowed for rapid expansion of our understanding of IC/BPS pathophysiology and introduced numerous candidate biomarkers of disease.
3. There still exists no perfect biomarker for diagnosis of IC/BPS or response to treatment.

### **ABSTRACT**

Interstitial cystitis/ bladder pain syndrome (IC/BPS) is a poorly understood chronic pain condition that affects 2.5 – 6.7% of American women and accounts for roughly 2.5% of urology office visits. Patients present with pain, pressure, or discomfort of the urinary bladder with associated lower urinary tract symptoms (LUTS) for more than six weeks without an identifiable cause. IC/BPS is highly comorbid with other chronic pain conditions suggesting a common pathophysiology. Due to the heterogeneous nature of disease, identification of a reliable biomarker in IC/BPS has been a challenging and active area of research. Candidate biomarkers include abnormally expressed bladder epithelial proteins, mast cells, neurotransmitters, and inflammatory proteins, among others. As our understanding of IC/BPS pathophysiology continues to expand, so too does the search for the ideal biomarker.

### **INTRODUCTION**

Interstitial cystitis/ bladder pain syndrome (IC/BPS) is a poorly understood yet prevalent disease that urologists face in daily practice. Prevalence estimates range from 2.5 – 6.7% of American women, with lower estimates among men [1-2]. Approximately 2.5% of urologist visits are related to IC/BPS, and its detrimental impact on patient quality of life leading to missed work, depression, and impaired sexual function is well-studied in the literature [3-7]. IC/BPS symptoms are wide-ranging and often overlap with other conditions; symptoms include bladder/ pelvic pain and associated urinary frequency, urgency, nocturia, dyspareunia, in the setting of sterile urine [8-10]. Patients can experience chronic symptoms every day for years, intermittent symptoms with periods of acquiescence, or a combination of acute-on-chronic symptoms flares [9-10].

Given the heterogeneous presentation and manifestations of disease, identifying the true IC/BPS population has been a challenge, placing increased importance on ruling out other symptom etiologies [10]. Common conditions that can often masquerade as IC/BPS include endometriosis, non-infectious cystitis, vulvodynia, pudendal nerve entrapment, pelvic floor dysfunction, and prostatitis in men [10]. Perhaps the most important and difficult condition to distinguish from IC/BPS is overactive bladder (OAB), as nearly all IC/BPS patients present with urinary urgency and frequency [11]. As knowledge of IC/BPS has evolved and become more nuanced, we now understand that IC/BPS patients void

frequently to avoid pain from overdistention, whereas OAB patients tend to void frequently to avoid incontinence [11]. IC/BPS was once considered to be a disease of the bladder alone – on the spectrum of OAB – but is now considered to be a chronic pain syndrome with pelvic manifestations [8-10].

The Society for Urodynamics and Female Urology (SUFU) officially defines IC/BPS as an unpleasant sensation (pain, pressure, discomfort) perceived to be related to the urinary bladder, associated with lower urinary tract symptoms (LUTS) of more than six weeks duration, in the absence of infection or other identifiable causes [12]. This definition is the product of much refinement as understanding of IC/BPS has expanded through research and more accurately captures the true IC/BPS population [12-13]. It also acknowledges that IC/BPS may not be a primary bladder or urinary tract disorder, despite presenting symptoms being urologic in nature.

There is high concordance with IC/BPS and other idiopathic medical conditions such as fibromyalgia, irritable bowel syndrome, chronic fatigue syndrome, and chronic headaches [9-15] which suggests that there may be a unified underlying abnormality in certain patient groups. Thus, unsurprisingly, the pathophysiology of IC/BPS is poorly understood and remains an active area of research [8-10]. Several etiologic mechanisms have been proposed including intrinsic dysfunction of the protective GAG layer of the urothelial surface, mast-cell infiltration of urothelium, infection, neural changes causing hypersensitivity, and chronic inflammation due to autoimmune processes [16-20].

Identification of useful biomarkers for IC/BPS has been a challenging area of research given the heterogenous and likely multifactorial nature of disease. However as our understanding of IC/BPS continues to expand and as gene sequencing technology has improved leading to the emergence of omics research, candidate biomarkers are being frequently identified [21]. As with all disease processes, the ideal biomarker in IC/BPS would not only identify IC/BPS patients with suitable sensitivity and specificity but would also reflect response to treatment or disease progression [9]. Additionally, IC/BPS biomarkers would ideally be obtained via urine or blood specimen rather than tissue biopsy [9]. With these parameters in mind, herein we review the current literature pertaining to IC/BPS biomarker discovery with emphasis on recent, novel findings.

## **METHODS**

We performed a search of original articles available on PubMed using the search terms “IC/BPS” and “biomarker”. To capture the most current trends in biomarker research and application, we limited the search to articles published within the past 10 years. Only articles originally published in English were included in the initial screening. We excluded review articles and editorial comments. Finally, we excluded animal model studies and cadaver studies. (Figure 1)

## **RESULTS**

Prior to 2008, much of the research and understanding of IC/BPS pathophysiology was focused on bladder-centric processes [22]. Leading theories included “leaky epithelium,” mast cell activation, neurogenic inflammation, or some combination of these, among others [22]. The urothelium of IC/BPS patients has been shown to produce lower concentrations of glycosaminoglycans (GAGs) – which serve as a protective, impermeable barrier to noxious stimuli in urine – compared to controls [23]. This GAG deficiency causes a “leaky epithelium” and increases bladder susceptibility to infection and inflammatory proteins [24-26]. Mast cells are proinflammatory cells that excrete primarily histamine among other compounds when activated [27]. They are primarily involved allergic and acute inflammatory responses but have also been shown to infiltrate the urothelium of IC/BPS patients [27-28]. While unlikely the root cause of IC/BPS, mast cells are thought to serve as the final common pathway through which IC/BPS symptoms are mediated [27-29]. Increased sympathetic nervous system activity has been demonstrated in IC/BPS along with increased sensory nerve fiber density in the suburothelium [30-31]. This increased sympathetic tone within the bladder is thought to create a hypersensitive bladder mucosa and contribute to mast cell degranulation [30-31]. Each of these



theories helped elucidate features of IC/BPS that were previously unrecognized, however none provide a satisfactory explanation for the etiology of IC/BPS. Additionally, features of these mechanisms are implicated in other chronic pain syndromes such as irritable bowel syndrome and fibromyalgia – which commonly co-occur with IC/BPS – suggesting that there may be a shared, systemic mechanism of disease [32].

These insights have shifted the focus of IC/BPS research beyond the bladder alone. In 2008 the National Institute of Diabetes and Digestive and Kidney Diseases (NIDDK) established the Multidisciplinary Approach to the Study of Chronic Pelvic Pain (MAPP) Research Network. The network consists of six different research centers across the United States and a single Data Coordinating Center which manages and stores clinical data, and a Tissue and Technology Center to centrally process, store, and disburse clinical samples [33]. MAPP investigators represent a wide array of medical disciplines working together with the shared goal of improving our understanding of IC/BPS and its relationship to other pain conditions [33]. In this shared resource model, large-scale basic science and clinical research studies can be conducted in an efficient manner allowing for rapid advancement of our IC/BPS knowledge.

The MAPP Network has made significant strides in advancing our understanding of IC/BPS symptoms and pain. Studies have shown that approximately three-quarters of IC/BPS experience pain at other sites beyond the pelvis, one-third experience pain at more than three nonpelvic sites, and that only one-quarter of IC/BPS patients experience pain only in the pelvis [33-35]. Patients with widespread extra-pelvic pain are reported to have more severe pelvic pain symptoms and more psychosocial difficulties and depression [34]. MAPP investigators have also established the importance of differentiating IC/BPS symptoms and pelvic pain from urinary symptoms. IC/BPS symptoms, but not urinary symptoms, are associated with depression suggesting that urologic pain versus urinary symptoms differ in their overall impact on patient quality of life [33 36]. These findings encourage practitioners to assess IC/BPS symptoms and urinary symptoms with separate measurement tools and measure response to therapy separately [36-38]. The significant impact of non-pelvic and non-urinary symptoms on the lives of IC/BPS further support hypothesis that the pathophysiology of IC/BPS is likely more far-reaching than the bladder itself [33 39]. Some of the leading theories to explain the high prevalence of extra-vesical pain in IC/BPS include central sensitization and pelvic visceral organ cross-sensitization [33]. The central sensitization theory is based on evidence that nociceptive pathways in the brain and spinal cord have been shown to be tonically upregulated in IC/BPS patients [33 40]. Pelvic visceral organ cross-sensitization describes stimuli from one organ inducing physiological changes in other organs with shared sensory pathways, these changes can persist even after withdrawal of painful stimuli [33 41].

Also important in understanding IC/BPS symptoms is the role of flare symptoms – the acute worsening or intensifying of symptoms on top of a patient's chronic or steady-state symptom profile. Some of the early MAPP Network efforts sought to systematically study symptom flares and the influence of flares on patients as investigators performed both multicenter and single site focus groups of patients with IC/BPS to better elucidate the role of flare symptoms [42-44]. These studies revealed a heterogeneous mix of IC/BPS flare symptoms in terms of frequency, character, physical location, and intensity but did reveal a consistent negative impact on patient quality of life. Investigators found that anticipation and avoidance of flare symptoms are a significant source of stress for IC/BPS patients and even leads to social anxiety. Given the significant impact of flare symptoms on patient quality of life, identification of flare symptom triggers has naturally garnered the attention of IC/BPS investigators.

One of the more significant triggers of IC/BPS symptom flares identified in the literature is diet [33 45]. Diet modification is often among the earliest and simplest interventions recommended to IC/BPS patients with bothersome symptoms. Acidic foods are commonly reported to cause IC/BPS symptom exacerbation among survey studies despite evidence that acidic urinary pH alone does not appear to

cause symptom flares [46 47]. Caffeine and alcohol are also frequently reported to exacerbate IC/BPS symptoms. Several prospective studies on healthy subject have identified caffeine as a bladder irritant, causing de novo urinary frequency and in one study, urinary incontinence, however these effects are generally mild and wash out as patients develop caffeine tolerance [45 48 49]. In a survey of 535 IC/BPS patients, 94% reported exacerbation of bladder symptoms when consuming alcohol [45]. In other large survey studies directed towards IC/BPS patients, citrus fruits, tomatoes, vitamin C, coffee, tea, and alcoholic beverages continue to be common culprits for IC/BPS symptom exacerbation [50 51]. Based on findings such as these, practitioners frequently recommend that IC/BPS patients perform an elimination diet, in which patients carefully record their dietary intake and bladder symptoms, and iteratively remove then reintroduce triggering foods [45]. Dietary modification serves as simple, inexpensive, and potentially efficacious method of limiting IC/BPS symptom flare and quality of life.

Diet has also been implicated in the etiology of IC/BPS and explored as a potential therapy.

MAPP Network studies have contributed to the identification of several candidate biomarkers for IC/BPS including matrix metalloproteinase 2 (MMP2), MMP9, neutrophil gelatinase-associated lipocalin (NGAL), the MMP9-NGAL complex, vascular endothelial growth factor (VEGF) and VEGF receptor 1 (VEGFR), toll-like receptor 2 (TLR2), TLR4 and etiocholan-3 $\alpha$ -ol-17-one sulfate (Etio-S) [33 52-54]. Studies designed to identify candidate biomarkers for IB/BPS typically involve sampling bladder tissue or urine from IC/BPS patients and comparing its features to that of unaffected control patients. This paradigm has evolved over time from comparing urothelial histology under a light microscope and culturing urine specimens to performing genome sequencing on bladder biopsy, urine, serum, and saliva samples [33 55 56]. Both as part of the MAPP Network and within individual research centers, biomarker investigation has moved beyond the bladder to the realms of genomics, epigenomics, proteomics, and metabolomics [33 53 57 58].

One example of this paradigm shift is the evolution of our understanding of anti-proliferative factor (APF). While not quite pathognomonic for IC/BPS, urinary APF is generally considered the most promising biomarker for disease with reported sensitivity and specificity of 94% and 95% respectively for IC/BPS urine versus control urine [9 59]. First described in 1996 via urine culture, APF is present in the urine of IC/BPS patients and is associated with inhibition of urothelial cell proliferation; thereby contributing to the “leaky epithelium” mechanism of IC/BPS [60]. Further study has precisely characterized the structure of APF as a Frizzled-8 protein-related sialoglycopeptide and is secreted by bladder epithelial cells from patients with interstitial cystitis [60-62]. Taking a step further, proteomic analysis of urothelial cells exposed to APF compared to APF-naïve controls found approximately 100 differentially regulated proteins which formed a protein network involved in cell adhesion substantially altered by APF [63 64]. These findings help elucidate the mechanism of APF-induced urothelial damage on the cellular level.

In addition to bioinformatics techniques, given the neurological implications of IC/BPS, functional magnetic resonance imaging (fMRI) has also gained popularity as a methodology of interest in IC/BPS research and introduces the possibility of fMRI findings as biomarkers of disease [65 66]. MAPP Network investigators have identified fMRI alterations in IC/BPS patients compared to controls [65 66]. One study identified altered resting functional connectivity within centers related to pain; sensory, motor, and emotion regulation processes; reward; and higher executive functioning [65]. The authors also described “decoupling” of two brain regions from the brain’s resting network, which regulates undisturbed, task-free, introspective thought [65]. These findings suggest that while experiencing symptoms, IC/BPS patient are unable to focus on anything other than their symptoms and have diminished ability to regulate their neurological resting state [65].

We report examples of many of these techniques which have proposed candidate biomarkers. Results of our literature search yielded 43 articles, 20 of which were excluded based on our criteria: there were

two duplicate study results, 13 review articles, five animal studies, one editorial, one cadaver study, and one bench study of human bladder cells. The 20 studies included in our analysis reported on original clinical data proposing candidate biomarkers for IC/BPS (Table 1). We also report sensitivity and specificity of biomarkers for which these data were either reported or calculable (Table 2).

## **DISCUSSION**

### **Clinical biomarkers – anesthetic bladder capacity**

One of the cardinal symptoms thought to be specific for IC/BPS - especially when differentiating between IC/BPS and OAB - is pain associated with bladder filling or bladder distention [67]. Urinary urgency and frequency associated with IC/BPS is believed to be the result of fear of a full bladder rather than intrinsic detrusor overactivity [11]. Along these lines, IC/BPS patients are thought to have a lower bladder capacity than patients without IC/BPS. Several studies have explored this hypothesis by comparing anesthetic bladder capacity between IC/BPS patients and controls [68-70]. Plair, et al reported their findings from a retrospective case series of 257 women with a diagnosis of IC/BPS who underwent bladder hydrodistension at their center [69]. The authors found on multiple regression analysis that patients with normal bladder capacities were more likely to carry a concomitant diagnosis of pelvic pain syndrome, endometriosis, or one of several neurologic, autoimmune, system pain diagnoses [69]. Meanwhile, patients with low bladder capacity were more likely to have bladder-specific and voiding symptoms, suggesting that decreased bladder capacity provides specificity for the diagnosis of bladder-centric IC/BPS rather than diagnosing pain syndromes with associated pelvic symptoms [69].

Schachar, et al built upon this hypothesis and sought to provide histological supporting evidence for low bladder capacity as a biomarker for bladder-centric IC/BPS [70]. The authors performed a retrospective review of bladder biopsy pathology slides from 41 patients with IC/BPS and anesthetic bladder capacity below 400cc compared to 41 IC/BPS patients with anesthetic bladder capacity above 400cc. Pathology review was performed by a single, blinded pathologist using a standardized, predefined grading scale. The authors found that the low bladder capacity group demonstrated more severe acute inflammation, more severe chronic inflammation, and more erosion than the normal capacity cohort [70]. They also noted that mast cell counts between the two groups were roughly equal. The authors concluded that these findings lend further support to the hypothesis that low bladder capacity serves as a reliable biomarker for differentiation bladder-centric IC/BPS from IC/BPS as a manifestation of a systemic pain syndrome [70].

Colaco, et al explored this hypothesis on an even more basic level by searching for differential gene expression in the bladder tissue of IC/BPS with low bladder capacity (<400 ml) compared to IC/BPS patients with normal bladder capacity (≥400 ml) and control subjects with normal bladder capacity [68]. The authors performed RNA extraction and microarray assay to determine differentially expressed RNA transcripts (DETs) between the groups [68]. In all, 193 DETs were identified between the low bladder capacity IC/BPS and control group, and fewer DETs between the normal bladder capacity IC/BPS and control groups. Most of the up-regulated transcripts were involved in inflammatory cell signaling while most down-regulated transcripts were involved in epithelial integrity proteins such as uroplakin [68]. Choi, et al performed Reverse Transcriptase Polymerase Chain Reaction (RT-PCR) analysis of biopsy specimen from 25 IC/BPS patients and 5 controls [71]. Their goal was to assess expression of WNT family genes, which when downregulated, are associated with fibrotic changes. The authors found silencing of WNT11, WNT 2B, WNT 5A, and WNT 10A in IC/BPS patients compared to controls [71]. These findings support that the epithelium of IC/BPS is more prone to fibrosis than that of healthy controls, perhaps contributing to decreased bladder capacity and improper response to mucosal injury or irritation [71]. Taken together, these data support the hypothesis that anesthetic bladder capacity is not only different between IC/BPS patients and controls, but it may also

represent distinct disease phenotypes within IC/BPS. Based on these findings low anesthetic bladder capacity offers promise as a biomarker for bladder-centric IC/BPS and more accurate stratification of patients along the IC/BPS spectrum of disease.

Given the longstanding “leaky epithelium” hypothesis of IC/BPS pathogenesis, it is unsurprising that alterations in proteins related to urothelial structural integrity and permeability have become attractive biomarkers of disease. While our literature review did not necessarily reveal novel urothelial barrier biomarkers, the studies included in our review highlight unique clinical scenarios or modalities of assessing for these biomarkers. Cho, et al sought to compare urothelial uroplakin expression in IC/BPS patients who had were scheduled to undergo augmentation ileocystoplasty, an indication of severe disease [72]. Uroplakin is a urothelial protein that helps for an impermeable plaque on the surface of healthy urothelium [73]. Bladder tissue samples were collected from 19 subjects with ulcerative subtype IC/BPS and five controls; tissue was specifically collected from non-ulcerated urothelium from study subject. Presence of uroplakin was assessed by immunofluorescence staining and degree of uroplakin expression was measure by Western blot. The authors found that uroplakin expression was elevated in study subjects compared to controls [72]. This finding is contrary to the prior reports of uroplakin as a biomarker for IC/BPS; in which uroplakin is decreased leading to hyperpermeable urothelium [74-76]. The authors hypothesize that this may be the result of a positive feedback loop between the diseased, ulcerated tissue and the surrounding healthy tissue in which uroplakin is compensatorily upregulated [77]. As such, this finding would provide some specificity in differentiating between ulcerative and non-ulcerative subtypes of IC/BPS beyond cystoscopic inspection and biopsy.

Lui et al, sought to measure differential expression of different biomarkers of varying physiologic origins in the bladder tissue of IC/BPS patients. In this study the authors compared 17 IC/BPS subjects not only to 10 healthy controls, but to 15 bladder outlet obstruction (BOO), 13 ketamine cystitis (KC), 12 spinal cord injury (SCI), and 12 recurrent urinary tract infection (UTI) patients as well [78]. Bladder biopsy specimens were analyzed for expression of E-cadherin, a urothelial junction protein, as well as mast cell activation and presence of apoptotic cells, measures of inflammation [79 80]. IC/BPS patients were found to have significantly decreased E-cadherin expression compared to controls, again supporting the hypothesis of structurally deficient urothelium in these patients. KC and UTI patients also demonstrated decreased E-cadherin expression, implying that there may be a shared pathogenesis between these conditions and IC/BPS [78]. All subjects with lower urinary tract pathology demonstrated greater mast cell activity and greater presence of apoptotic cells compared to healthy controls, highlighting the sensitive, but not specific role of inflammation within the urothelium in these disease processes [78].

## **Inflammatory biomarkers**

The pathophysiology of IC/BPS is characterized by chronic inflammation and urothelial dysfunction. During states of inflammation, detrusor smooth muscle cells and urothelial cells produce chemokines, which are measurable in the urine. Early studies have demonstrated an elevation of inflammatory proteins in patients with IC/BPS. Inflammatory biomarkers therefore represent an important area of investigation. Tonyali et. al demonstrated elevated levels of urinary nerve growth factor (NGF) in patients with IC/BPS compared to controls. Furthermore, normalized NGF levels were significantly correlated with more severe symptoms in those with IC/PBS [81]. Similarly, Jiang et. al analyzed the urinary specimens of 127 patients with IC/BPS compared to controls, testing 31 candidate cytokines [82]. The authors found five urinary cytokines with high diagnostic value, including eotaxin-1, CXCL10, RANTES, and MCP-1. Identifying urinary biomarkers with high sensitivity and specificity carries important diagnostic value. Equally important is identifying which inflammatory biomarkers are differentially expressed, as this provides better insight into the specific pathophysiology of IC/BPS. For instance, eotaxin is a chemoattractant for eosinophils and its differential expression in patients with

IC/BPS suggests an immune response to allergy-related inflammation. Elevated NGF identified in Tonyali et al points to the role of peripheral nerve proliferation in IC/BPS and may explain persistent hyperalgesia in the absence of inflammation.

Perhaps even more clinically important is the ability to distinguish between IC/BPS and conditions with similar symptomatic presentation. In a subsequent study, Jiang, et. al identified urinary macrophage inflammatory protein 1 $\beta$  (MIP-1 $\beta$ ) as having high sensitivity for distinguishing between patients with IC/BPS and health controls [83]. Furthermore, the authors identified several urinary cytokines as differentially expressed in IC/BPS samples compared to samples from patients with OAB, including three cytokines identified in their prior study: CXCL10, eotaxin, and RANTES. The authors proposed a diagnostic algorithm wherein MIP-1 $\beta$  is used in initial screening and the latter three are used in confirmatory testing. Subsequent validation of this and similar diagnostic algorithms could generate a series of accepted urinary assays for diagnosis that would avoid more invasive diagnostic testing. Ma, et al similarly identified serum MIP-1 $\beta$  as a promising biomarker for IC/BPS, among others [84]. The authors also identified serum interleukin-4 (IL-4), tumor necrosis factor alpha (TNF- $\alpha$ ), Tie2, and serum amyloid A (SAA) as promising biomarkers, with SAA demonstrating the greatest area under curve (AUC) on receiver-operator characteristic (ROC) of 0.85 [84]. All of these proteins represent inflammatory cytokines or chemokines [84]. Vera et. al identified a urinary biomarker, macrophage migration inhibitory factor (MIF) that not only is significantly elevated in patients with IC/BPS compared to controls but is also differentially elevated in patients with IC/BPS with Hunner's lesions, compared to IC/BPS patients without Hunner's lesions [85]. Although OAB and IC/BPS share similar symptoms, their pathophysiology and treatment are different. Identification of IC/BPS biomarkers distinct from OAB can help avoid misdiagnosis and inappropriate or delayed treatment.

### **Neurogenic/ neurologic biomarkers**

As previously discussed, neurogenic or neurologic alterations in IC/BPS patients have garnered interest in the realm of biomarker discovery. Given the heterogenous presentation of IC/BPS pain which often extends beyond the bladder or pelvis and can often persist after elimination of stimuli, there is almost certainly a neurologic component of IC/ BPS pain. Our literature search yielded one study by Pang, et al that described a novel technique to assess abnormalities of functional connectivity within the prefrontal cortex (PFC) of patients with IC/BPS [86]. Rather than resting state fMRI, the authors utilized resting state functional near-infrared spectroscopy (rs-fNIRS). fNIRS is a noninvasive, portable, optic-based functional brain imaging technology with few physical movement restrictions that detects changes in oxyhemoglobin signals in areas of the brain [86 87]. Comparison studies between fMRI and fNIRS have demonstrated the reliability of fNIRS and thus suitability for use in studying IC/BPS patients [86-89]. In their study, ten IC/BPS patients and 15 age and gender-matched controls were asked to empty their bladder prior to initiation of rs-fNIRS data collection to collect "empty bladder" PFC activity. Next, subjects were asked to drink water until they felt a strong urge to void at which point, they were assessed for urinary incontinence and PFC activity was recorded. Finally, subjects were allowed to void. In both the empty bladder and urge to void states, IC/BPS patients demonstrated significantly decreased functional connectivity in the dorsolateral prefrontal cortex, frontopolar area, and the pars triangularis regions of the PFC compared to controls [86]. These areas are intimately involved in sensory integration, motivational drive, mood-control, cognitive processing, and decision-making [86]. With regards to lower urinary tract activity, they contribute to integration and regulation of the urge to void; once the urge is sensed, the PFC can either encourage or discourage voiding based on other sensory inputs [86]. Decreased FC in these regions was also demonstrated in similar fNIRS studies in patients with OAB and UUI but not IC/BPS [86 90 91]. These findings are not only illustrative of the central nervous system's role in IC/BPS, but also demonstrate the feasibility of a new technology in the investigation of IC/BPS [86].

### **Genomic, proteomic, metabolomic biomarkers**

IC/BPS research has benefited greatly from the emergence of bioinformatics and omics research. Made possible by the large-scale storage and distribution of tissue and urine samples by the MAPP Network, sequencing and identification of differentially expressed genes, proteins, and metabolites as candidate biomarkers for IC/BPS has helped elucidate IC/BPS pathophysiology. Our review of the literature revealed several such studies both at single centers and as part of the MAPP Network using both urothelial biopsy tissue and urine samples from IC/BPS patients.

Parker, et al applied mass spectrometry-based global metabolite profiling to urine specimens from 40 female IC/BPS supplied by the MAPP Network and 40 age-matched controls [53]. Among multiple metabolites that discriminated IC/BPS subjects from controls, etiocholan-3 $\alpha$ -ol-17-one sulfate (Etio-S), a sulfo-conjugated 5- $\beta$  reduced isomer of testosterone, demonstrated better than 90% specificity for IC/BPS [53]. This is the first study to identify Etio-S as a urinary biomarker in IC/BPS and its mechanistic implications are unclear. The authors assert that high concentrations of Etio-S may stimulate acute phase reactants and local inflammatory effects; alternatively, they cite evidence that changes in Etio-S may have a GABA-ergic effects manifested as acute stress, depression, or nociception [53 92 93]. Further research is needed to elucidate the mechanism of Etio-S in IC/BPS but its specificity for disease is promising.

Saha, et al completed a bioinformatics study in which preexisting Gene Expression Omnibus (GEO) datasets were mined for IC/BPS-associated genes [94]. One dataset contained cell lines treated with and without APF as well as bladder tissue samples from IC/BPS patients and normal controls. Two datasets contained gene expression profiles of bladder biopsy tissues from IC/BPS patients and normal controls. One dataset contained the gene expression profiles of urine sediment from IC/BPS patients and normal controls. Differentially expressed genes (DEGs) that were significantly different between IC/BPS patients and controls were retrieved from all datasets and included for analysis; these were: CD5, CD38, ITGAL, IL7R, KLRB1, and PSMB9 [94]. After identification of significant DEGs, the authors then performed Real-Time Quantitative Polymerase Chain Reaction (RT-qPCR) analysis for these DEGs on newly obtained tissue from IC/BPS patients and controls. RT-qPCR results showed that all six genes were over-expressed in IC/BPS patients compared to controls. PSMB9, ITGAL, and KLRB1 were most significantly overexpressed in IC/BPS patients compared to controls making them the most promising candidate biomarkers among DEGs [94]. According to the authors, these genes are commonly, albeit nonspecifically, associated with autoimmune processes [94 95]. Autoimmunity is one of the many proposed pathophysiological etiologies for IC/BPS, supported by relatively strong association between IC/BPS and autoimmune conditions like Sjögren's syndrome [94]. There is some evidence to suggest that autoantibodies to the muscarinic M3 receptor are contributory to Sjögren's syndrome; the M3 receptor happens to also be expressed in detrusor cells of the bladder [94 96]. Wu, et al performed a similar GEO-based study in which they analyzed a database containing five IC/BPS patients and six controls for DEGs [97]. In all the authors identified 483 DEGs between IC/BPS patients and controls: 216 up-regulated and 276 down-regulated genes, however at conclusion of their analysis only three genes were considered possible core IC/BPS-related genes: CXCL8, CXCL1, and IL-6 [97]. All three of these genes produce chemokine or cytokine proteins involved in the inflammatory response, furthering the concept of dysregulated lower urinary tract inflammation in IC/BPS [97 98].

Finally, Bradley, et al performed an epigenomic study of voided urine samples to identify differentially methylated genes in IC/BPS [57]. Much like DEGs, differences in methylation, usually caused by environmental exposures, can both shed light on IC/BPS pathophysiology and potentially serve as a noninvasive biomarker. Urine samples from eight female IC/BPS patients and eight female age-matched controls were included for analysis. Genes were analyzed for addition of a methyl group to the 5' carbon of a cytosine moiety, generating 5-methylcytosine (5-mC), which occurs predominantly in the context of cytosines that precede guanine (5'-CpG-3') dinucleotides, or CpGs [57 99]. In all, over 1000 differentially methylated CpG sites between IC/BPS patients and controls were identified, however the most prominent pathway enriched for genes with differential methylation was the mitogen-activated

protein kinase (MAPK) pathway, which contained 22 differentially methylated sites. Additionally, one of the MAPK pathway genes, MDS1 and EVI1 complex locus (MECOM), contained multiple differentially methylated sites, increasing the likelihood of its significance. While not classically associated with IC/BPS, MAPK is associated with inhibition of cell growth, inflammation, and regulation of apoptosis [57 100]. The findings of Bradley, et al not only implicate MAPK signaling in the pathophysiology of IC/BPS, but they also support the idea that environmental exposures can cause fundamental epigenetic changes in IC/BPS patients. For example, changes secondary to chronic UTI have been thought to contribute to IC/BPS symptoms and altered epigenetic expression may be the mechanism by which these changes manifest [57 101].

### **Biomarkers in response to therapy**

Another area in which biomarkers prove useful is in assessing response to treatment. Numerous treatment modalities are available for IC/BPS. For patients who fail conventional therapies, several non-standard treatments have been explored. These treatments have had mixed success, and their mechanisms for improving symptoms associated with IC/BPS are still poorly understood. Studies on biomarker changes in response to novel therapies help improve our understanding of the therapeutic mechanisms.

Jiang et. al tested urinary biomarkers of 40 patients with IC/BPS symptoms refractory to conventional therapy who received four intravesical injections of autologous platelet-rich plasma (PRP) [102]. The authors found significant decreases in urinary levels of VEGF, NGF, and matrix metalloproteinase-13 alongside symptomatic improvement. These results suggest that the therapeutic effects of PRP are likely due to its ability to alleviate inflammation and reduce atypical angiogenesis [102]. Similarly, Peng et. al tested urinary markers of 21 patients with IC/BPS who had failed conventional therapy and went on to receive treatment with intravesical onabotulinumtoxinA injections every 6 months for 4 total treatments [103]. They too found a significant decrease in the expression of VEGF following treatment. Although these patients also experienced symptomatic improvement, clinical improvement did not directly correlate with VEGF expression [103]. Shen et. al also found a significant difference in VEGF as well as urinary chemokines IL-4 and IL-6 in 13 patients treated with extracorporeal shockwave for IC/BPS [104].

Finally, Peters et. al tested urinary markers in patients who experienced successful sacral neuromodulator device implant for refractory urinary symptoms associated with IC/BPS [105]. In this study, success was defined as 50% symptomatic improvement on the Interstitial Cystitis Symptom and Problem Index (ICSPI). The authors found a positive correlation between urinary levels of CXCL-1 and Soluble interleukin-1 receptor antagonist (sIL-1ra) and ICSPI and pain score, suggesting the ability of these markers to reflect severity of disease [105]. Furthermore, the authors demonstrated a reduction in urinary levels of MCP-1 and sIL-1ra after treatment, which was significantly associated with symptomatic response. sIL-1ra elevation in serum has been associated with pain and stiffness in fibromyalgia patients and MCP-1 is a potent chemotactic protein that helps maintain an inflammatory state in tissue [105]. Unlike in prior studies, these authors did not see a significant decrease in urinary levels of VEGF, suggesting that the mechanism by which sacral neuromodulation improves IC/BPS symptoms may differ from the therapeutic mechanisms of ESWL, PRP, and intravesical onabotulinumtoxin A. Changes in biomarkers following treatment are evidence to change in the actual bladder microenvironment, beyond subjective symptomatic improvement. In the future, biomarkers also have the potential to provide objective measures of improvement.

### **CONCLUSIONS**

IC/BPS remains a challenging disease for clinicians, researchers, and patients. The heterogeneity of disease presentation and the absence of reliable biomarkers of disease make patient counseling and disease management difficult. Impressively, the coordination of resources within the MAPP Network has expanded our understanding of IC/BPS over a relatively short period of time and has benefited

IC/BPS investigators both within the MAPP Network and at individual centers. Our review of literature highlighted several novel biomarkers for IC/BPS as well as cutting-edge methodologies for biomarkers identification. Identification of PFC changes supports the hypothesis that there is a central nervous system component to IC/BPS while omics work help elucidate differences between IC/BPS patients and controls at the genome level and beyond. While there remains no perfect biomarker for IC/BPS that is: non-invasive, sensitive and specific, and serves as a measure of disease progression/remission, there is reason for optimism as research in this area continues to meaningfully progress.

Figure 1. Flow diagram for literature review and study inclusion.

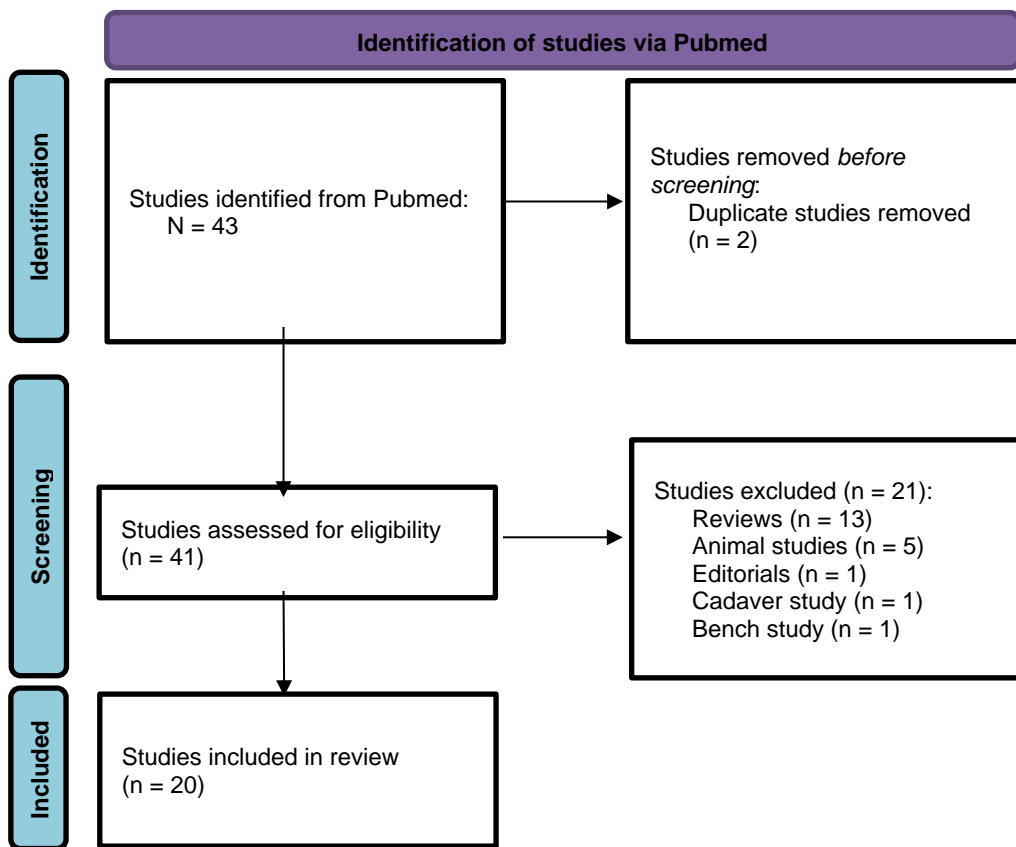




Table 1. Studies included from literature review with description of biomarkers.

	<b>Biomarker</b>	<b>Mechanism</b>	<b>Sample</b>	<b>Change</b>	<b>Reference</b>
1	Anesthetic bladder capacity	clinical	bladder capacity	decreased	Plair A, et al. 2021 [69].
2	Histology/ bladder capacity	clinical	bladder tissue	different	Schachar JS, et al. 2019 [70].
3	Gene expression/ bladder capacity	clinical	bladder tissue	increased	Colaco M, et al. 2014 [68].
4	WNT11	genomic	bladder tissue	decreased	Choi D, et al. 2018 [71].
5	MCP-1, CXCL10, eotaxin-1, RANTES	inflammatory	urine	increased	Jiang YH, et al. 2020 [82].
6	MIP-1 $\beta$ , eotaxin, CXCL10, and RANTES	inflammatory	bladder tissue/ urine	increased	Jiang YH, et al. Sci Rep. 2021 [83].
7	MIF	inflammatory	urine	elevated	Vera PL, et al. 2018 [85].
8	Apoptotic cells	inflammatory	bladder tissue	increased	Liu HT, et al. 2015 [78].
9	NGF, MMP-13, VEGF	inflammatory	urine	decreased s/p PRP	Jiang YH, et al. 2020 [102].
10	Uroplakin	urothelial barrier	urine	elevated	Cho KJ, et al. 2020 [72].
11	Prefrontal cortex changes	neurogenic	brain	different	Pang D, et al. 2021 [86].
12	NGF	neurogenic	urine	increased	Tonyali S, et al. 2018 [81].
13	Etio-S	metabolomic	urine	increased	Parker KS, et al. 2016 [53].
14	CD38, ITGAL, IL7R, KLRB1, and IL7R	inflammatory	bladder tissue/ urine	differently expressed	Saha SK, et al. 2020 [94].
15	CXCL8, CXCL1, IL6	inflammatory	bladder tissue/ urine	differently expressed	Wu H, et al. 2021 [97].
16	IL-4, TNF- $\alpha$ , MIP-1 $\beta$ , AAA, Tie2	inflammatory	urine	increased	Ma E, et al. 2016 [84].
17	MAPK pathway	genomic	urine	differentially methylated	Bradley MS, et al. 2018 [57].
18	IL-4, VEGF, IL-9	inflammatory	urine	decreased s/p LI-ESWT	Shen YC, et al. 2021 [104].
19	VEGF	inflammatory	bladder tissue	decreased s/p botox	Peng CH, et al. 2013 [103].
20	MCP-1	inflammatory	urine	decreased s/p interstim	Peters KM, et al. 2015 [105].

Table 2. Reported Areas under the Curve, Sensitivity, and Specificity of Inflammatory Biomarkers

Biomarker	AUC	Sensitivity	Specificity
IL-7	0.756	71.1	67.9
MCP-1	0.753	60.3	72.4
eotaxin-1	0.720	52.2	85.7
MIF	0.718	74.4	61.8
IL-4	0.703	54.4	86.2
CXCL10	0.685	66.2	65.5
MIP-1 $\beta$	0.674	92.2	44.8
RANTES	0.666	53.8	75.9
IL-10	0.637	38.9	92.9
IL-6	0.631	50.0	79.3
eotaxin	0.604	40.3	80.0
TNF- $\alpha$	0.527	41.1	71.4

### **ACHIEVEMENT 3:**

#### **Urobiome: An Outlook on the Metagenome of Urological Diseases**

The urinary tract likely plays a role in the development of various urinary diseases due to the recently recognized notion that urine is not sterile. In this mini review, we summarize the current literature regarding the urinary microbiome and mycobiome and its relationship to various urinary diseases. It has been recently discovered that the healthy urinary tract contains a host of microorganisms, creating a urinary microbiome. The relative abundance and type of bacteria varies, but generally, deviations in the standard microbiome are observed in individuals with urologic diseases, such as bladder cancer, benign prostatic hyperplasia, urgency urinary incontinence, overactive bladder syndrome, interstitial cystitis, bladder pain syndrome, and urinary tract infections. However, whether this change is causative, or correlative has yet to be determined. In summary, the urinary tract hosts a complex microbiome. Changes in this microbiome may be indicative of urologic diseases and can be tracked to predict, prevent, and treat them in individuals. However, current analytical and sampling collection methods may present limitations to the development in the understanding of the urinary microbiome and its relationship with various urinary diseases. Further research on the differences between healthy and diseased microbiomes, the long-term effects of antibiotic treatments on the urobiome, and the effect of the urinary mycobiome on general health will be important in developing a comprehensive understanding of the urinary microbiome and its relationship to the human body.

#### **INTRODUCTION: WHY UROBIOME?**

Although it was previously believed that urine was a sterile substance, new research indicates that it contains a host of microorganisms. This has left the urinary microbiome relatively unstudied, as it was not a part of the Human Microbiome Project which aimed to identify and categorize the microbiomes of the human body in healthy individuals. [1] However, research suggests that the urinary microbiome is extremely diverse and may play a role in a host of urinary diseases. [2-4, PMID: 32665990] While research remains relatively inconclusive, studies have indicated an association between certain bacterial and fungal species and various urinary diseases using new technologies like next-generation sequencing (NGS) and expanded quantitative urinary cultures (EQUC) that help identify a majority of the bacteria found in urinary microbiomes. [5] This review aims to provide a comprehensive understanding of select bladder diseases and their respectively identified bacterial signatures using NGS- and EQUC-based analysis from data compiled through previous studies and reviews surrounding the subject.

#### **Human Genome, Microbiome, and Mycobiome**

The human genome is complex and, although efforts have been made to fully sequence it, remains relatively unexplained regarding its mechanistic function. After the Human Genome Project, it was discovered that there was much left to understand regarding the human body, the relationship between DNA and protein function, and the interaction between these elements and the various microbiomes in the human body. [6] For urinary diseases specifically, the lack of research on the urinary microbiome has left much to be understood about its relationship with the human body. The microbiome, consisting of the microorganisms and their respective genomes that exist within a region of a host body, as well as their individual activity and formed micro-ecosystems, have been indicated to significantly affect the health of the host as changes occur due to situational and environmental factors.[7] Another factor to consider is the region's mycobiome, which is the fungal microbiota within an area. This also can significantly impact host health, as well as the microbiome of the region, making it important to investigate in combination with the bacterial microbiome. [8]

Although the urinary microbiome and mycobiome remain relatively unstudied, there is significant evidence indicating that the microbiome and mycobiome of other regions, like the lungs and gut, heavily

affect the overall health of the human body. [9] Evidence has linked lung and gut microbiome and mycobiome health to a host of issues, including asthma, colorectal cancer, alcoholic liver disease, cystic fibrosis, and hypoglycemia. [9-12, PMID: 34329692] This type of linkage between microbial health and host health indicates that the urinary microbiome and mycobiome play a similarly important role in the overall health of the human body.

## **The Gastrointestinal Microbiome and Indication of Urobiome Significance**

Traditionally, research has focused on the gut microbiota and its relationship to various disease. With its expansive surface area and constant processing of food, symbiosis of the gut microbiota have long been recognized as an important step in disease prevention. [13] Important for diseases related to diet and obesity, as well as atherosclerosis, Crohn's disease, ulcerative colitis, and autism, research has indicated that the balance of the gut microbiota is extremely significant to host health. [13, 14, PMID: 29093639] Studies have begun to indicate a similar importance for the health of an individual's urinary microbiota. With connections to prostate, gut, and renal health, dysbiosis of the urinary microbiota has indicated increased risk of various lower urinary tract diseases, prostate cancer, kidney disease, and increased risk of gastrointestinal dysbiosis as well. [15-19] Research of the urinary microbiome is thus extremely important in understanding these inter-system relationships and their effect on overall host health.

## **Urobiome, Microbiome and Mycobiome in Urine**

With the discovery of bacteria in urine, research into its relation to urological diseases began. Consequently, the urinary microbiome has become increasingly important, although it has been shown to vary significantly between individuals. This environment, consisting of all the bacterial microorganisms contained within the bladder, as well as the proteins and metabolites they produce, their genetic material, and the host proteins and metabolites within the region, has been shown to be increasingly more complex than previously believed. [20, 21] Together, with the urinary mycobiome, which is all the fungal microbiota and its subsequent genetic material, proteins, and metabolites within the bladder, evidence suggests that the balance of a healthy individual's urinary biome is important to prevent and protect against many urinary diseases. [22]

## **NGS Method and Culture-Based Validation of Urobiome**

The urinary microbiome is most effectively determined using a combination of next-generation gene sequencing and expanded quantitative urine culture. Because whole genome sequencing can be performed as a form of next-generation sequencing (NGS), DNA NGS is generally performed using PCR amplification and 16S rRNA gene high-throughput sequencing, which allows the entire genome to be sequenced. Although this process is much better than standard diagnostic methods of urine analysis, there are still several limitations. [5] This includes an inability to distinguish closely related bacterial taxa, confirm bacterial viability, and link the genotypic resistance to a specific organism. [5] In addition, bacterial abundance can be determined by 16S rRNA sequencing, but not precisely. [5]

EQUC is also important because it can detect bacterial growth as low as 10 CFU/ml by plating a urine sample on various media at different temperatures and under various atmospheric conditions for a longer period, resulting in detection of up to 92% of bacteria species not otherwise detected on a standard urine culture. This contrasts with the standard urine culture, which was designed to grow specific *E. coli* pathogens and can only detect about 33% of bacterial growth. [5, 23]

Both EQUC and NGS are important analysis techniques because they each provide data that the other one may not. [2, 24] Although sequencing allows for the bacterial populations to be studied, more specific technology must be used to determine the functional ability of these microbes, indicating that the specific metabolites, and not the species of microbe, are what will drive future research and therapies. [16]

## Microbial Diversity in Human Urine

There is substantial variation in an individual's microbial diversity, and the way subjects are grouped in studies may greatly affect the analysis of the results. For some populations, an increase in microbial diversity may be beneficial, and for others it may be harmful, which is why factors such as age and gender must be accounted for when organizing studies.[25-28] For example, studies have indicated that menopause causes a significant alteration in the female urinary microbiome. Although the *Lactobacillus* species is the most prevalent bacteria in pre-menopausal women, post-menopausal women have more significant levels of *Mobiluncus* and a general decrease in overall microbial diversity. [1, 29] This change in the microbiome of a healthy female can greatly affect studies when age is not accounted for. Similarly, the female microbiome is very different than that of a male, which has a high amount of the species *Corynebacterium* in most control groups. [2, 24, 30] Overall, the most common bacterial species found in sampled urine include *Lactobacillus* and *Streptococcus*, with *Gardnerella*, *Staphylococcus*, and *Corynebacterium* following closely and *Alloscardovia*, *Burkholderia*, *Jonquetella*, *Klebsiella*, *Saccharofermentans*, *Rhodanobacter*, *Prevotella*, and *Veillonella* also noted as prevalent.

In patients over seventy years old, one study indicated that there was again a change in the microbiome, detecting *Proteiniphilum*, *Saccharofermentans*, and *Parvimonas* in the microbiome, which are species not commonly found in samples from younger individuals. [2, 5, 24, 30-33] **Table 1** shows a compiled list of these bacterial species commonly found in the healthy human urinary microbiome. Similarly, **Table 2** is a list of the bacterial (and certain fungal) species commonly found in the urinary microbiome of individuals with the urinary diseases discussed in this article and is organized accordingly.

The sampling method also tends to affect the microbial diversity observed in urinary samples. Since there is not yet a standard method of collection and analysis for urine samples, it is often difficult to compare studies.[5, 34] Urine has a very low concentration of microbes within each sample, resulting in a high potential for contaminant amplification that leads to significant error rates and confounders. [34] This can be combated by larger volume samples, stricter lysis conditions, and new sequencing techniques with higher fidelity. For women it is difficult to collect urine samples without vaginal contamination. Several studies aimed at determining the optimal sampling method have been performed. Results indicated that collecting female urine via a transurethral catheter most closely resembled samples obtained via suprapubic aspiration, suggesting that this may be a better collection method than midstream voided urine. [34-36] For men, a subsequent study indicated that the male bladder, like the female bladder, is a low biomass environment, making catheterization a preferred urine sample collection method. [34] Another study also concluded that suprapubic aspiration and transurethral catheterization are the two best forms of sample collection because they avoid contamination from the genitals. [2] Trials have also indicated that, in males specifically, there is a difference in the beta microbial diversity when comparing voided and catheterized samples. It was hypothesized that this was likely due to the difference in urethra length between males and females, which likely allows for a greater difference between the bladder and the urethra microbiome in males than in females. This difference between collection methods in males raises the question of which would act as a stronger diagnostic method for diseases like bladder cancer because, while one may better represent the urinary microbiome, this may not be the best functional representation of urological microbes for therapeutic purposes. And voided urine has been served for initial identification of diagnostic, prognostic, and non-invasive biomarkers for diseases primarily at the microbe-urothelial interface.[25, 37, 38]

## Microbial Diversity in Bladder Cancer

The taxa *Fusobacterium*, *Sphingobacterium*, and *Enterococcus* are present in schistosomiasis-induced bladder cancer patients. [16, 39] This type of bladder cancer is also more prevalent in individuals with strains of bacteria that can mediate the formation of N-nitrosamines. Chronic UTIs are hypothesized to

leave an individual predisposed to developing bladder cancer, but there is conflicting epidemiological evidence surrounding this. It has not been determined whether the presence of these microbes is a result of or a cause for bladder cancer. One hypothesis is that the extracellular matrix is influenced by the urinary microbiome, which may either help prevent or induce cancer depending on the microbes present. This would be similar to the influence of microbiomes in intestinal cancer. However, studies have conflicting support for this hypothesis. Biofilms may be a cause for chronic inflammation in the genitourinary system, among other places, which has been indicated to correlate with a higher risk of developing cancer due to their interactions with epithelial cells. There is also evidence to suggest that the urinary tract's microbiome hosts commensal microorganisms, and the interaction between these microbes and bladder cancer cells may affect tumorigenesis. [40, 41] The presence of some species, like *Lactobacillus*, have been indicated to help aid in the prevention of disease in some women, dissuading from the growth of other, more commonly harmful species. However, the growth of too much of a commensal organism, like *Lactobacillus*, can become harmful to the surrounding environment by decreasing the overall microbial diversity, which has been indicated to promote tumorigenesis. [2]

Although bladder cancer is much more common in men, it is much more deadly in women. [40, 42] While this is likely affected by factors related to social inequality, it may also be due to the microbial differences between male and female urinary tracts. For bladder cancer, the genetic difference between male and female patients remains unknown. One specific example is the activity of glutathione-S-transferase M1, which affects the metabolizing of carcinogens. Studies also indicated that increased age, parity, premenopausal status, and use of estrogen and progestin are all associated with a lower risk of developing bladder cancer. In females, the *Lactobacillus* species is extremely common in the urinary microbiome, while in males *Corynebacterium* is most prevalent. Additionally, one study indicated that females with bladder cancer had higher levels of *Klebsiella* in urine samples than healthy women, and an increase in *Burkholderia* for bladder cancer patients was observed regardless of gender. [40, 43]

It has been suggested that 20-30% of cancers, like gastric cancer, liver cancer, urinary bladder cancer, cholangiocellular neoplasia, and cervical cancer are related to recurring microbial infections. [40, 44] Evidence has also indicated that abnormal microbiomes have been correlated with a higher risk of cancer, but it is unclear what the "normal" microbiome of the urinary tract is specifically. Various bacteria have been indicated to play a role in the relationship between bladder cancer and the urinary microbiome, but studies vary in the specific species associated. In one, it was an increase in *Streptococcus* in cancerous patients. In another, it was *Fusobacterium nucleatum*, which has known associations with carcinogenesis. [40, 41] This bacterium is gram-negative and anaerobic and is known to induce a chronic inflammatory response by promoting the beta-catenin pathway. There are several genes also associated with bladder cancer, with one of significance being *Acinetobacter*, which consists of several gram-negative, anaerobic species that are indicated to impair immune response to bovine papillomavirus type 2 and thus increase susceptibility to carcinogenesis.

The microbiome has a promising predictive ability for urinary cancer, with dysbiosis showing evidence of a relationship to anticancer therapy and a potential to predict Bacillus Calmette-Guerin (BCG) therapy response. *Lactobacillus iners*, which is more prevalent in females, may also play a role in BCG efficacy due to the competition between them for fibronectin binding. [40, 45] One notable difference in the urinary microbiome of individuals with urothelial cell carcinoma was an increase in *Streptococcus*. Associations between bladder cancer and *Mycobacterium tuberculosis* from the BCG vaccine have also been made, but the mechanistic reason for its success in bladder cancer inhibition remains unsure. [2, 46, 47]

BCG is used for bladder cancer treatment via direct insertion, but the induced immune response may be due to the interaction of BCG with urinary bacteria, and BCG may be competing with other bacteria, like *Lactobacillus iners*, for fibronectin-binding positions, potentially reducing its treatment efficacy (**Figure 1**). [16, 45, 48] BCG has been regularly used to deter cancer progression, and studies before treatment indicate that patients with bladder cancer were more likely to have increased levels of *Fusobacterium*.

[25, 41] Healthy women generally have higher levels of *Mycobacteria* and other *Actinomycetes*, which are suspected to help impede cancer progression, and some studies suggest that certain urinary microbial profiles may leave an individual predisposed to malignancies and affect treatment response. [25, 49] Additionally, *Lactobacillus casei* was previously believed to reduce the recurrence of bladder cancer, but human studies were stalled due to complications. [16, 50, 51] However, with new technology in the microbiome field, these studies should be reinvestigated because of their promising potential, and the *L. casei* strain Shirota may be a viable for non-muscle-invasive bladder tumors. [16, 50, 51]

Antibiotic treatments of patients with bladder cancer reduced the progression-free and overall survival of immunotherapy-treated patients, indicating that an alteration of the patient's microbiome may lead to a better therapeutic result. [16] The presence of certain bacteria (species of *Mycoplasma* and *Proteobacteria*) can metabolize the chemotherapy drug gemcitabine, rendering it ineffective. Other bacteria can reactivate irinotecan, causing drug toxicity. There is also evidence that certain bacteria can affect the efficacy of immunotherapy. [16, 52]

### **Microbial Diversity in Benign Prostatic Hyperplasia (BPH)**

BPH may be correlated to an increase in *Escherichia coli* in prostatic secretion, a decrease in *Escherichia coli* in urine, and an increase in *Enterococcus* in the seminal fluids, but it is unknown whether these changes in the microbiome are the cause for BPH or are a result of prostate cancer treatment. [53, 54] Several studies have indicated a correlation between chronic prostate inflammation and BPH, implicating that the urinary microbiota may play a role in its development due to the increase in proinflammatory cytokines observed in the urinary microbiome of individuals diagnosed with BPH. [55, PMID: 33858430] Additionally, this study suggested that inflammasomes may have a role in BPH development due to their involvement with activation of the immune system's inflammatory response. [55, 56] Factors such as oxidative stress, DNA damage, and signaling involving nuclear factor- $\kappa$ B (NF- $\kappa$ B) and cyclooxygenase-2 (COX2) have also been indicated to play a role in BPH onset and development. [53, 57-59] The species *Staphylococcus*, *E. coli*, *Micrococcus*, *Enterococcus*, *Serratia spp.*, *Pseudomonas aureginosa*, and *Pantoea spp.* were all identified in 22% to 2.8% of BPH samples from a study of 36 individuals, with the relatively high rate of 11.1% for *E. coli* matching the findings of previous studies, making this the most common bacteria associated with benign prostatic hyperplasia. [53, 57]

Although more individuals are being diagnosed with BPH, its overall severity has decreased with the usage of oral medication, leading to a reduction of surgical cases. [53] This combination therapy using an alpha-blocker and a 5-alpha-reductase inhibitor help reduce inflammation of the prostate to relax the organ and minimize BPH symptoms. [60, 61] This management of the chronic inflammation associated with BPH further indicates its importance in the disease pathology, suggesting that inflammation is not only a correlated factor, but possibly a causative factor as well. [60, 62]

### **Microbial Diversity in Urgency Urinary Incontinence (UUI)**

Although UUI is the most frequently studied bladder disease, there is little consistency or overlap between results. One study suggested that increased prevalence of *Actinomyces*, *Corynebacterium*, and *Streptococcus* correlated with better responses to medication. Another study suggested that the *Lactobacillus* species dominates the urinary microbiome in healthy controls, while diseased groups are more likely to have Lactobacilli within a diverse microbiome. [5, 63] This is especially interesting because *Lactobacillus* species are more common in the female urinary system, and young women tend to have less diverse urinary microbes, while older women tend to have more diverse ones. [25] Another study showed evidence that patients with evidence of bacterial DNA in their urine had fewer episodes of urgency urinary incontinence on a daily basis than those with no reported urinary bacterial DNA. In this study, *Actinobaculum*, *Actinomyces*, *Areococcus*, *Arthrobacter*, *Corynebacterium*, *Gardnerella*, *Oligella*, *Staphylococcus*, and *Streptococcus* were more prevalent in those experiencing UUI, and *Lactobacillus*

was once again present in decreased amounts. However, the use of either NGS or EQUC altered whether there was a significant overall difference in microbial diversity of the urinary system for those experiencing UUI and healthy individuals, although evidence suggests that there is some type of microbial component to UUI. [5, 25, 30, 63]

In the studies regarding UUI, women generally tended to have lower *Lactobacillus* and higher *Gardnerella* counts when experiencing this disease. Research concluded that there was a correlation between UUI symptom severity and decreased urinary microbial diversity, and one study additionally suggested that the use of solifenacin to treat UUIs was more effective when women had a lower microbial diversity in the urinary system. [2, 24]

### **Microbial Diversity in Overactive Bladder Syndrome (OAB)**

OAB, characterized by frequent urination, urinary urgency, and difficulty controlling bladder contractions, is a syndrome with a multitude of possible pathologies.[64] Sampling has indicated that in at least some cases, the urinary microbiome may play a role in overactive bladder syndrome. In one study analyzing the urinary microbiome in females, the most prevalent bacteria found in both healthy and OAB urinary microbiomes were *Staphylococcus*, *Streptococcus*, *Corynebacterium*, and *Lactobacillus*. There was also a statistically significant difference in the prevalence of *Lactobacillus* and *Proteus* between the control and the OAB samples, with *Lactobacillus* being much more prevalent in healthy individuals and *Proteus* in OAB samples. [64]

It is hypothesized that the presence of *Lactobacillus* bacteria in the urinary tract, especially in women, may help prevent overactive bladder syndrome because it promotes a more acidic environment that prevents more virulent bacteria from growing there. [2] Although the specific role of the microbiome is not yet known in relation to OAB, preliminary trials for several antimuscarinics and intradetrusor botulinum toxin injections have indicated that patients who respond to these treatments usually have a reduced microbial diversity in their urinary tract. [65] Furthermore, there is a possibility that the urinary microbiome is related to brain function, similar to the gut microbiome, which may affect neurotransmitter release and immune system stimulation to affect an individual's risk of experiencing overactive bladder syndrome.[65]

### **Microbial Diversity in Interstitial Cystitis and Bladder Pain Syndrome (IC/BPS)**

Not much is fully understood about the role microbes play in IC/BPS. Studies suggest that there is a decrease in diversity for the urinary microbiome in individuals suffering from IC/BPS, but an increase in levels of the *Lactobacillus* species. [2] One study also suggests that the level of inflammatory cytokines is increased in those affected with IC/BPS. However, there is not enough conclusive evidence to show that bacteria play a role in IC/BPS development, and some studies have even concluded that no significant role for the urinary microbiome can be determined for IC/BPS susceptibility. [1, 5] On the other hand, there may be an overall decrease in the urinary microbiome diversity for individuals suffering from IC/BPS, but an increase in levels of the *Lactobacillus* species, as well as the level of inflammatory cytokines in those affected with IC/BPS, with one study additionally concluding that an increase in *Lactobacillus* levels was associated with an increase in IC/BPS severity. [5, 32]

Some studies have also indicated that increased amounts of fungi in the bladder may influence IC/BPS. [2, 32] Although there was no significant difference in bacterial species composition when comparing patients with IC/BPS to healthy individuals, symptom flares indicated increased levels of the fungal species *Candida* and *Saccharomyces*, but subsequent studies did not observe a similar conclusion. Testing for IC/BPS is unfortunately extremely limited because 16S NGS is unable to detect eukaryotic microbes, and EQUC cannot identify several types of fungi, resulting in many negative tests using the current diagnostic standards due to culture testing inconsistency. [5, 32]



## Microbial Diversity in Chronic Urinary Tract Infections (UTI)

Although acute urinary tract infections are primarily caused by *E. coli*, when UTI is chronic and persistent, it is likely caused by a different microbe, which is why standard urine culture often misses this as a diagnosis. [5, 25, 66] Chronic lower urinary tract symptoms are likely caused by the formation of biofilms, which protect harmful bacteria from helpful immune mechanisms while simultaneously promoting mutations. It has been indicated that chronic UTIs can be perpetuated by treatment through antibiotics because the formation of biofilms can aid in increased resistance as well. [5, 35, 67, PMID: 34044483] It was previously believed that bacteriuria caused urinary tract infections, but evidence suggests that asymptomatic bacteriuria may help prevent chronic urinary tract infections by inhibiting the growth of certain *Escherichia coli*, especially those which are shown to be antibiotic resistant. Current diagnostic methods for urinary tract infections are effective, and further specification for diagnosis is unnecessary and would likely result in overtreatment. [25]

No longitudinal studies regarding the urinary microbiome and antibiotics have been performed. However, a general decrease in *Lactobacillus*, *Fingoldia*, *Gardnerella*, *Atopobium*, and *Sneathia* species were observed from various studies. [25, 68] One study in particular saw that after treatment from metronidazole, *Lactobacillus crispatus* was completely undetectable in urinary samples, despite being one of the most prevalent bacteria in the urinary samples of healthy young females. [1] The lack of *Lactobacilli* likely increased post-menopausal susceptibility to recurrent urinary tract infections. [1, 69]

Although antibiotic treatment is a popular method to combat UTIs, it has been associated with long-term problems by promoting antibiotic resistance. Probiotics, prebiotics, and diet alterations have been proposed as alternative preventative and general treatment methods to avoid this problem. This includes administration of the *L. rhamnosus* GR-1, *L. fermentum* RC-12, and *L. reuteri* B-54 for UTIs. [2, 16] The risk of recurrent urinary tract infections can be reduced using estrogen replacement treatment, which increases the *Lactobacillus* population in the vagina and likely the urinary tract as well. [1, 70, 71] Although certain *Lactobacillus* species may aid in UUI treatment, the presence of the specific *L. delbrueckii* and *L. gasseri* are indicated to be associated with increased UTI and urgency urinary incontinence severity. [2, 35] Another treatment method that has been investigated to replace antibiotic treatment is the consumption of cranberry juice supplements, although studies indicated that supplement use showed no significant decrease in UTI risk. However, intake of higher doses of D-mannose, which is found in cranberries, may be effective in UTI risk reduction. [2, 24]

## Microbiome Can be Altered by Procedures and Medications

There are several current potential procedures aimed at altering the urinary microbiome of individuals with urinary disease. For bladder cancer, *Mycobacterium tuberculosis* from the BCG vaccine has shown success in inhibiting the spread of bladder cancer despite the mechanistic understanding of this process remaining unknown. [2, 46, 47] Additionally, *Lactobacillus casei*, specifically the Shirota strain, has had promising results in preliminary testing regarding its ability to reduce the recurrence of non-muscular invasive bladder tumors. [16, 50, 51] In benign prostatic hyperplasia, relative success has come from a combination therapy treatment using alpha-blockers and 5-alpha-reductase inhibitors, but 12.6% of patients that receive this therapy still observe clinical progression and 5% still require surgery. [60, 61] Urgency urinary incontinence has most often been treated using solifenacin, a bladder relaxant, but its success has been indicated to be tied with the patient's relative urinary microbial diversity. [2, 24, PMID: 31119104] Similarly, treatment for overactive bladder syndrome has been indicated to depend on the patient's urobiome diversity, with preliminary trials using antimuscarinics and intradetrusor botulinum toxin injections showing potential primarily in individuals with reduced diversity. [65] Widespread clinical procedures and drug treatments for those with interstitial cystitis/bladder pain syndrome have been difficult to identify. A distinct pattern connecting the urinary microbiome to these diseases remains unknown, making the development of an effective treatment difficult as well. [1] For urinary tract infections,

a common treatment method involves the administration of antibiotics, but studies indicate that treatment using the *L. rhamnosus* GR-1, *L. fermentum* RC-12, and *L. reuteri* B-54 may be better options. [2, 16] Estrogen replacement therapies and D-mannose supplements have also shown potential in reducing the risk of recurrent urinary tract infections.[1, 2, 24, 70, 71]

## CONCLUSIONS

As research about the urinary microbiome and mycobiome continue, evidence regarding its relationship to urinary disease will expand and improve. Methods like NGS and EQUIC remain relatively limiting in their ability to analyze microorganisms present within the bladder microbiome, but they are still much improved from previous techniques. The use of antibacterial treatments for various bladder diseases and their effects on the balance of bacteria in a healthy bladder must be researched further to help elucidate whether changes in the urinary microbiome are primarily causative or correlative with bladder disease.

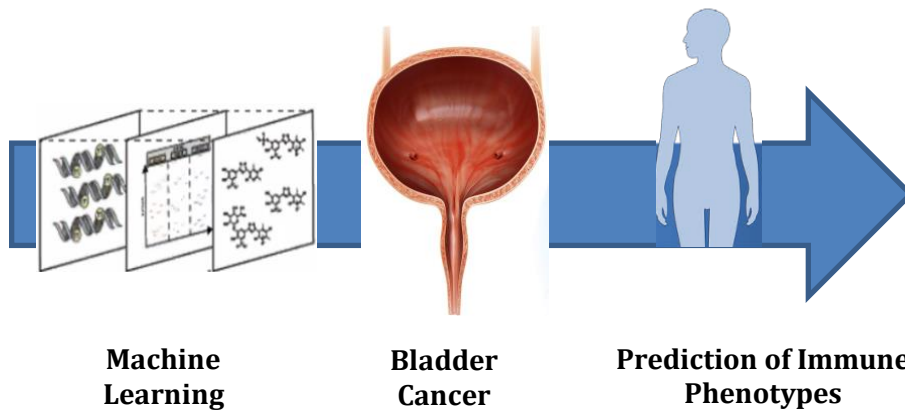
## CURRENT LIMITATIONS AND FUTURE PLANS

The potential benefits of understanding the urinary microbiome are numerous. Despite the current limitations due to lack of previous research, difficulties in standardizing sampling techniques and analysis methods, and problems with defining the scope of the urinary microbiome, much progress has already begun in the field. New challenges in this field include to develop the better identification methodologies of microbiome and to understand the pathological function of micro- and mycobiome include multi-omics-based and host-microbe interaction (**Figure 2**). [7] With further research and technological development, the relationship between the urinary microbiome and mycobiome health and the health of the human body will be understood, allowing for more specific clinical treatment of a variety of urinary diseases and a potential connection to diseases not directly associated with the urinary environment. It can also provide a stronger understanding regarding the use of antibiotics and their effects on the microbiomes of the body, as well as the potential efficacy of other treatments, including the use of probiotics and dietary supplements, in regard to various urinary diseases.

## ACHIEVEMENT 4:

### Machine Learning Approaches to Predict the Immune Phenotypes in Bladder

To develop a biosignature of immunotherapy-based responses using gene expression data, Deep Neural Networks (DNN), Support Vector Machines (SVM) together with boosting and feature selection methods were applied. DNN yielded the highest area under the curve (AUC) with receiver operating characteristic (ROC) curves and precision and recall (PR) curves for each phenotype ( $0.711 \pm 0.092$  and  $0.86 \pm 0.039$  respectively). Our results suggest significant potential to further develop and utilize machine learning algorithms for analysis of bladder cancer and its precaution.



## INTRODUCTION

Globally, bladder cancer (BC) is the ninth most common malignant tumor. BC also accounts for 4% of all cancer-related deaths in the United States, ranking it the fifth most deadly cancer [1]. According to the American Cancer Society, there will be approximately 83,730 new cases of BC (about 64,280 in men and 19,450 in women) and about 17,200 BC-related deaths (about 12,260 in men and 4,940 in women) in the United States, alone, in 2021. If your paper is intended for a conference, please contact your conference editor concerning acceptable word processor formats for your particular conference.

Based on the degree of bladder muscle wall infiltration, BC can be classified as either non-muscle invasive (NMIBC) or muscle invasive (MIBC). About 70% of BC patients have NMIBC, while the other 30% have MIBC or metastatic disease [2]. Treatment for NMIBC includes endoscopic resection of the tumor followed by adjuvant intravesical treatment to reduce the possibility of recurrence or progression. The risk of recurrence and progression is affected by many factors, including tumor grade, size, staging, multiplicity, recurrence rate, and the presence of carcinoma in situ (CIS). BC requires a lifetime of close monitoring and repeated treatments, which places an immensely heavy burden on patients and the social economy. MIBC treatment options include chemotherapy and radical cystectomy. The 5-year and 10-year survival rates of MIBC are approximately 50% and 36%, respectively. However, the 5-year survival rate of metastatic BC is only 15%, and the median overall survival (OS) is about 15 months following platinum-based chemotherapy.

Immunotherapies against BC have shown encouraging results. The first immunotherapy against BC was reported in 1976, when Alvaro Morales reported 9 cases of BC that were successfully treated with Bacillus Calmette-Guerin (BCG), demonstrating the immunogenicity of BC [3]. Immune checkpoint inhibitors (CPIs) are leading the field of immunotherapies against BC. It includes anti-cytotoxic T lymphocyte antigen 4 (CTLA4), anti-programmed cell death 1 (PD-1), and anti-programmed cell death 1 ligand 1 (PD-L1)

antibodies. Anti-CTLA4, anti-PD-1, and anti-PD-L1 CPIs can improve anti-tumor immune response by restoring T-lymphocyte activation [4]. With the rapid advancement of new immunotherapy drugs, the development and validation of biomarkers will be important. Established biomarkers can help clinicians predict whether treatments will be effective. Varying subtypes of BC may also have definitive biological differences, which can result in variable sensitivity to Immunotherapies. In order to fully optimize the benefits of immunotherapy in future treatments and to further improve its impacts, supplemental biomarkers capable of monitoring response should be integrated.

Despite the initial success of cancer immunotherapies[5], approximately 70% of patients with advanced urethral cancer are considered unresponsive to anti-PD-1 or anti-PD-L1 antibodies[6, 7].

Recent studies have employed a variety of biomarkers such as PD-L1 hyperexpression and tumor mutation burden (TMB) to distinguish the potential immunotherapy responders from non-responders[5]. There seems to exist a link between these biomarkers and immunotherapy outcomes, but neither PD-L1 expression nor TMB was sufficient to distinguish immunotherapy responder from non-responders[8, 9]. For example, the epithelial PD-L1 expression in BC has been shown to be unrelated to immunotherapy responses[10]. In addition, there has been difficulty predicting responses using TMB as a single marker[11], although increased TMB has been linked to improved clinical outcomes of immunotherapy in bladder cancer[12]. These previous works indicate the unmet needs to identify more reliable biomarkers for the stratification of immunotherapy responders from non-responders.

IMvigor210 was an open multicenter, single-arm phase 2 clinical study designed to study whether atezolizumab could become the standard treatment for advanced urothelial cancer. This study suggested that for patients with first-line platinum-based refractory metastatic urothelial carcinoma (mUC) checkpoint inhibitors seem to be more attractive than chemotherapy[13].

Atezolizumab is now suggested to prescribe for many patients who are ineligible for cisplatin therapy. In our study we used the publicly available IMvigor210 data. Previously, IMvigor210 data has been used to test the prognostic power of gene expression signatures for basal and luminal/differentiated BC subtypes [14]. Overall survival, prognosis and response to immunotherapy were also studied in the IMvigor 210 cohort [15]. A consensus molecular classification system for MIBC was suggested by analyzing the 1,750 MIBC transcriptomic profiles from datasets including IMvigor dataset, providing a tool for testing and validation of potential predictive MIBC biomarkers [16].

Big data-based ML has been increasingly used and successfully applied to preventive medicine, image recognition, diagnosis, personalized medicine, and clinical decision-making. Application of machine learning (ML) algorithms to determine the cancer-specific classifiers have been tried in a series of studies. To determine the multi-variate classifiers predicting response to paclitaxel-therapy, methylome and miRNome were used [16]. Not only in vivo multi-omics profiles [17] but also in vivo cancer molecular profiles were able to predict the drug-sensitive tumors using ML modeling approach [18].

Clinical application of conventional ML approaches has been performed for the more accurate clinical decision, which was benefited by an increased computational power and accumulated digital health data from patients [19, 20]. However, we are aware the limitations due to the complicated data processing (feature engineering) including knowledge-based training [21, 22]. ML algorithms derived from not-so-relevant data resources, low volume of patients, data with high sparsity and poor could significantly diminish enthusiasm and reduce the efficacy of ML approach [23].

Although ML is widely used in the context of BC, there are still limitations, including difficulties in quantitatively analyzing observed endpoints and the inapplicability of generalizability across data sets. Therefore, further verification is needed to improve the accuracy and versatility of ML in BC. Therefore, in this study, we aimed to search for the potential of using ML algorithms to investigate relationships between gene expression features with immunotherapies specific to BC and identify potentials to develop and use

ML algorithms for such studies. For this, we have adopted five different traditional but powerful ML classification methods (i.e., Random Forest, Deep Neural Network, Support Vector Machine, Adaboost and XGBoost) to predict BC immune phenotypes using high-dimensional gene features. With efforts to avoid pitfalls of these algorithms, e.g., overfitting, we managed to get successful classification performance identifying phenotype-specific gene features (see Section IV for detailed clinical and technical discussions). We see great possibility to further develop more sophisticated and task-specific ML algorithm for analyzing BC with gene data to provide diagnostic tool for individuals and identify BC in their early stages, or possibly even prevent the disease.

## II. MATERIALS AND METHODS

### A. ETHICS STATEMENT

For this paper, we used deposited datasets derived from previously published studies. Use of publicly deposited data does not require IRB approval.

### B. DESCRIPTION OF THE DATASET

For this study, we have used the IMvigor210 data that can be found in previous report [24] and the associated resource web site provided by Dorothee Nickles, Yasin Senbabaoglu, Daniel Sheinson at <http://research-pub.gene.com/IMvigor210CoreBiologies/>. The raw data are available at the European Genome-phenome archive (EGA) under the accession number EGAS00001002556. The IMvigor210CoreBiologies package can be downloaded at <http://research-pub.gene.com/IMvigor210CoreBiologies/IMvigor210CoreBiologies.tar.gz>. Code for data processing, analysis and plotting and the R script are available from this IMvigor210CoreBiologies package.

The IMvigor210 study was a phase 2, multicenter, single-arm, open-label, and 2 cohort trial that assessed atezolizumab as a treatment for metastatic urothelial cancer in cisplatin-ineligible patients [25]. Clinical data for the first-line cisplatin-ineligible IMvigor210 cohort was collected from 47 academic medical centers and community oncology practices across 7 countries in North America and Europe. All participants in the study consented.

The IMvigor210 dataset includes recorded responses to immune checkpoint blockade. This Illumina HiSeq 2500-based dataset contains 348 subjects (76 female and 272 male) with 17,692 gene expression biomarkers (i.e., features), which were derived from genes using Entrez gene ID and gene symbol. Archival tumor tissues were collected for biomarker assessments, and gene expression was designed to be quantified for a T-effector gene signature (consisting of CD8A, GZMA, GZMB, PRF1, INFG, and TBX21) [5]. The feature values of gene information were normalized using the trimmed mean of M-values (TMM) method. Each sample includes corresponding clinical labels, such as age, sex, PD-L1 status of immune cells, prior tobacco use, metastatic disease, best confirmed overall survival, overall response, Response Evaluation Criteria in Solid Tumor (RECIST), immune phenotype, and The Cancer Genome Atlas (TCGA) subtype. For this study, three specific immune phenotypes were investigated: immune deserts, immune-excluded, and inflamed.

All types of human cancers, including BC, can be categorized into three immune phenotypes. These phenotypes are distinguished by the strength and relationship of the immune response of T-cells acting on the tumors, and different treatments should be applied based on the individual immunological biology of each phenotype. The IMvigor210 dataset consists of 76, 134, and 74 samples of immune deserts, immune-excluded, and inflamed phenotypes, respectively. The immune desert subtype is absent of immune cells, with total lack of an immune response against the tumor. The immune-excluded subtype has an immune response with only peripheral invasion of T-cells that cannot completely overwhelm the tumor. The inflamed subtype involves an active immune response where inflammatory myeloid cells and activated CD8+ T-cells exist in the tumor [26, 27]. Since the remaining 64 samples in the dataset did not provide any information on immune phenotypes, they were disregarded for this study.

### **C. CLASSIFICATION METHOD**

Five powerful ML-based classification algorithms, i.e., Support Vector Machine (SVM), Random Forest, XGBoost, AdaBoost and deep neural network (DNN) were adopted to investigate immune phenotypes using gene expression features [28-32]. We performed a supervised learning task, where each data sample consists of a feature vector and class label. In our experiment, the algorithms were trained to learn optimized mapping between the features (i.e., gene expression) and target labels (i.e., immune phenotypes).

SVM is a well-known supervised classification algorithm that can learn a decision boundary, either linear or non-linear, in a feature space. Given data samples forming individual clusters in the feature space according to class labels, SVM learns a decision boundary that maximizes the margin of distance between the decision boundary and other clusters [33]. Such a criteria intuitively makes sense as the distance between individual clusters and the learned decision boundary will be balanced. To train a linear model when the data are not linearly separable, the model requires a regularizer with a user parameter (i.e., slack variable) that controls the margin and tolerable error within the margin. Training a non-linear model requires a kernel function (e.g., Gaussian and polynomial kernels) that can map the data onto a high-dimensional space where the data can become linearly separable. Taking the trained decision boundary back to the original space will then yield an optimized non-linear decision boundary [34].

Random Forest is one of the ensemble methods for classification and regression tasks. A sole Decision Tree can perform the same tasks on supervised learning problems by asking a series of questions regarding to the characteristics of input variables. To avoid overfitting with large trees [35, 36], Random Forest incorporates multiple Decision Trees and casts a majority vote from the results classified from each tree. This ensemble technique is known as Bagging [37], which is an abbreviation of Bootstrap Aggregation. It is a method of extracting samples multiple times (Bootstrapping [38]) and training each model to aggregate the results. Although some trees created by Random Forest can be overfitted, an overwhelming majority can suppress the flaw from having a significant impact on prediction of class labels, i.e., classification.

In addition, we adopted another ensemble method, Boosting algorithm [39], based on the Decision Tree architecture. Unlike to Bagging where each tree makes independent decisions, Boosting has a sequential prediction process in which one model influences the decision of the next tree. In this process, Boosting repeats multiple steps to create a new classification criterion by improving weights on misclassified data. Finally, it creates a strong classifier gathering weak classifiers altogether to result in the ensembled output. In this paper, we used XGBoost [40] and Adaptive Boost (AdaBoost) [41, 42]. The difference of two methods is the way to deliver information of misclassified data from previous models. For example, AdaBoost updates subsequent classifiers based on the weight values of the former models. However, the update of XGBoost is based on gradient descent with a greedy algorithm.

Lastly, for the deep learning (DL) approach, we used a DNN algorithm with multiple hidden layers [30]. This consisted of an input layer for the original data, output layer for prediction outcome (e.g., pseudo-probability for each class), and a varying number of hidden layers where the input data can be transformed and model parameters are trained to minimize prediction error, usually defined by cross-entropy. While the input and output layers contain nodes according to the input dimension and the number of class labels respectively, each hidden layer is composed of hidden nodes determined by a user. At each hidden node, the node from its previous layer becomes the input, which is connected to the hidden node via edges with corresponding edge weights. The input values and edge weights at each hidden node are first linearly combined and then fed into a non-linear activation function (e.g., sigmoid or rectified linear unit (ReLU)) to yield an output that goes into the following layer as an input. At the output layer, the outcome values from each node are normalized to yield a pseudo-probability that tells which class label is the most likely for a given data sample. The l1- and l2-regularizers were applied onto the model parameters for sparsity as in least absolute shrinkage and selection operator (LASSO [43, 44], depicting important features only by suppressing weights of unimportant features to 0) and to make the model stable [28].

#### **D. MODEL TRAINING**

In order to obtain unbiased results, we used 10-fold cross validation (CV) to conduct experiments with the ~~two~~ five classification algorithms [45]. For the SVM, we utilized both linear and non-linear models. An RBF kernel was used for the non-linear classifier. The slack variable C was varied from 0.01 to 1000 to find the best performance. For Decision Tree-based models, such as Random Forest, XGBoost and AdaBoost, the number of trees per fold was kept to the same rate for comparing all results under unbiased conditions. The number of Decision Trees per fold was set to 100 and all Decision Trees were generated by allowing random sampling with replacement. The final classification was decided by majority voting incorporating outputs from every single classifier. The number of Decision Trees in all Boosting methods was set to 100. As for learning rates, XGBoost and AdaBoost were set to 0.1 and 1.0 respectively, with the highest test accuracy score for each classifier. For the DNN, we tried multiple settings by adjusting the number of hidden layers, nodes, and regularizers. The number of hidden layers varied from 0 to 3, and the number of hidden nodes in each layer varied between 16 and 1,024. A drop rate ranging from 0.1 to 0.5 was applied. To measure the error of the model, cross-entropy was used. For the activation function, ReLU was used and Softmax was applied at the output layer to obtain the likelihood for each class. The overall model was trained by backpropagating the error from cross-entropy with gradient descent using the Adaptive Moment Estimation (Adam) optimizer [46].

#### **E. FEATURE SELECTION**

Since the data is compiled in a very high-dimensional space, statistical hypothesis tests were used to select effective features for distinguishing different groups. Statistical group analysis for each pair of phenotypes was applied on each feature, and resultant p-values were corrected for multiple comparisons using Bonferroni correction at the 0.05 confidence level. The feature selection process was applied only at the training stages (i.e., excluding test data) across each fold in CV where the phenotype labels were available; hence, avoiding circular analysis.

#### **F. EVALUATION**

To evaluate the performance of our classification results, we measured accuracy, precision, and recall. Accuracy was computed as the ratio of the number of correct predictions out of the total number of samples in a testing dataset. Precision and recall were considered for binary classification (i.e., positive vs. negative); precision measures how precise the prediction is for the positive class, while recall measures how much of the positive samples in the training dataset are correctly covered by the prediction. While accuracy is an intuitive and important measure for evaluation, precision and recall are also important for evaluating data with imbalanced class labels. Since precision and recall are computed for binary classification tasks, we computed them in a one-versus-all manner; out of the three immune phenotype classes, one of them is selected as positive. The other two were combined and considered the negative class. This is iterated for all the three classes as positive, yielding three individual results. We also plotted receiver operating characteristic (ROC) and precision and recall (PR) curves. The area under the curve (AUC) was computed for evaluation (higher AUC denotes better performance). To understand the effectiveness of a classifier on an imbalanced dataset, the AUC scores of both curves were used as quantified summaries of the model performance as well as Mathews Correlation Coefficient (MCC) at a threshold of 0.5 to determine positive and negative labels. These values ranged between 0.0 to 1.0, with larger scores suggesting that a model is more robust.

#### **G. IMPLEMENTATION ENVIRONMENT**

All experiments were implemented in Python on a Nvidia GeForce RTX 2070 SUPER graphic card. DNN was designed based on Keras and scikit-learn machine learning libraries were utilized for the other methods. As for statistical tests, scipy library was used to derive p-values.

### **III. RESULTS**

Classification results on Immune Phenotypes of BC using the five classification methods are demonstrated in this section.



## A. CLASSIFICATION OF IMMUNE PHENOTYPES WITH SVM

Immune phenotyping of BC from the Imvigor210 dataset resulted in three subtypes, inflamed, immune-excluded, and immune desert; all of which are characterized by distinct T lymphocyte infiltration patterns. Immune desert tumors have

TABLE I  
COMPARISON OF REPRESENTATIVE RESULTS IN DIFFERENT SETTINGS

Classifier	Mean Train Acc	Mean Test Acc	MCC (Threshold: 0.5)	Mean Precision (std)	Mean Recall (std)	Mean AUC of PR (std)	Mean AUC of ROC (std)
SVM (Linear)	1	0.655	0.457	0.667 (0.036)	0.645 (0.048)	0.674 (0.031)	0.799 (0.083)
SVM (RBF)	1	0.655	0.456	0.655 (0.018)	0.644 (0.048)	0.678 (0.034)	0.798 (0.083)
SVM (RBF) (feature selection)	0.963	0.68	0.495	0.701 (0.035)	0.663 (0.118)	0.688 (0.034)	0.822 (0.066)
Random Forest	1	0.496	0.344	0.752 (0.099)	0.473 (0.104)	0.670 (0.045)	0.795 (0.086)
Random Forest (feature selection)	1	0.570	0.404	0.737 (0.089)	0.558 (0.051)	0.691 (0.051)	0.817 (0.077)
XGBoost	1	0.623	0.406	0.647 (0.043)	0.606 (0.103)	0.646 (0.073)	0.793 (0.081)
XGBoost (feature selection)	1	0.605	0.380	0.623 (0.029)	0.598 (0.059)	0.616 (0.055)	0.770 (0.089)
AdaBoost	0.821	0.613	0.386	0.714 (0.144)	0.547 (0.287)	0.649 (0.094)	0.776 (0.135)
AdaBoost (feature selection)	0.810	0.577	0.314	0.632 (0.116)	0.528 (0.239)	0.576 (0.110)	0.726 (0.163)
DNN (feature selection)	0.715	0.641	0.473	0.679 (0.045)	0.626 (0.101)	0.755 (0.099)	0.875 (0.054)
DNN (l1 regularizer)	0.834	0.616	0.412	0.685 (0.069)	0.590 (0.109)	0.771 (0.118)	0.870 (0.027)
DNN (feature selection, l1 regularizer)	0.719	0.666	0.488	0.722 (0.084)	0.635 (0.134)	0.771 (0.092)	0.860 (0.039)

Evaluation measures were averaged across 10-fold. These values range between 0 and 1, with values closer to 1 indicating better performance. The area under the curve (AUC) of precision and recall (PR) curves accounts for the class imbalance in performance evaluation

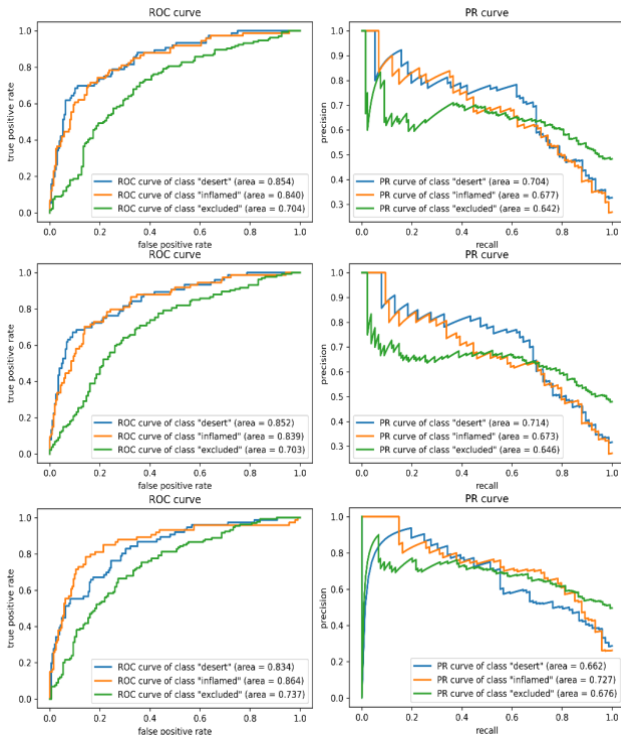


**Figure 1. Receiver operator characteristic (ROC) and precision and recall (PR) curves for each class using support vector machine (SVM).** Top: linear SVM, mid: SVM (RBF), bottom: SVM (RBF) with feature selection. Higher AUCs, closer to 1, indicate better performance. High AUCs with ROC curves for each phenotype indicate the model is predicting the phenotypes with low false positives. PR curves show that classification performance for the immune-excluded class is enhanced (green line) by feature selection.

poor infiltration of immune cells (absence of pre-existing antitumor immunity), immune-excluded tumors only exhibit retention of T lymphocytes in the reactive stroma, and inflamed tumors show infiltrated T lymphocytes [47, 48]. The overall results are summarized in Table I.

The classification process using an SVM-based system was implemented with two types of kernel functions (i.e., linear kernel and radical basis function (RBF)). As shown in Table 1, the best accuracy scores of both SVM experiments without feature selection were 0.655 while their training accuracies were 1. This indicates that there was a serious overfitting (i.e., the model worked perfectly on the training data but significantly failed to do so for testing data). The slack variable utilized in the two cases were 100. When statistical feature selection was applied to the input data of SVM with RBF kernel, the average test accuracy across CV scored the highest (0.68) throughout all experiments, which suggests that feature selection based on statistical group tests was effective. For slack variables, the score reached a peak at 10 and decreased slightly as the variables changed. On the other hand, linear SVM with feature selection yielded poor results. The accuracy was 0.588 regardless of the slack variable.

In Figure 1, PR and ROC curves for the three SVM experiments are described for the 3 classes, which are marked in blue (immune desert), orange (inflamed), and green (immune-excluded). Among the results with various SVMs, similar to the results of the test accuracy, SVM with RBF kernel and feature selection resulted in the highest average AUC scores for both metrics among SVM results; 0.688 and 0.812 for the PR and ROC curves, respectively. Accordingly, MCC of 0.495 for this case was the highest as well. Notably, all of the averaged AUC scores of the PR and ROC curves across SVM classes were recorded slightly smaller than the results from DNN models.

### B. CLASSIFICATION OF IMMUNE PHENOTYPES WITH RANDOM FOREST

Test accuracy of Random Forest scored the lowest throughout all experiments regardless of feature selection. Similar to SVM, training accuracies of Random Forest were 1, denoting that this algorithm has also overfitted to the input data and yielded poor test accuracy and MCC. But interestingly, we can see that mean precision recorded the highest score among all models as shown in Table 1, whether feature selection is applied or not. This highest precision value indicates that Random Forest was able to produce the lowest number of false positive samples. Notably, applying Bonferroni correction reduced the gap between precision and recall, so that the AUC scores of all classes in PR and ROC plot outperformed to those of non-feature selected Random Forest.

### C. CLASSIFICATION OF IMMUNE PHENOTYPES WITH XGBOOST AND ADABOOST

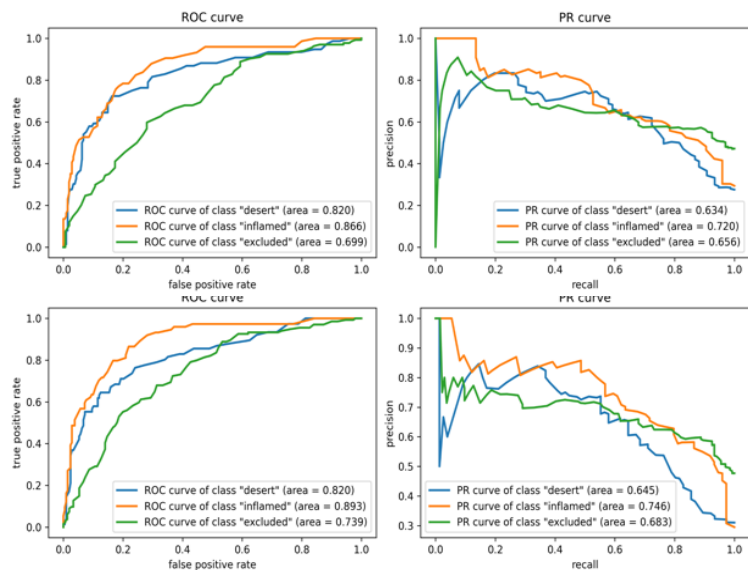


**Figure 2. Receiver operator characteristic (ROC) and precision and recall (PR) curves for each class using XGBoost and AdaBoost.** Top: XGBoost without feature selection, second row: XGBoost with feature selection, third row: AdaBoost without feature selection, bottom: AdaBoost with feature selection. Higher AUCs, closer to 1, indicate better performance. High AUCs with ROC curves for each phenotype indicate the model is predicting the phenotypes with low false positives. Almost all classes of both Boosting algorithms without feature selection shows better AUCs of PR and ROC curves than feature selected models.

For Boosting methods, the most representative Boosting algorithms, AdaBoost and XGBoost were employed. As shown in Table 1, the overall test accuracy and MCC of both Boosting algorithms scored higher than Random Forest but lower than SVM and DNN. Although XGBoost was overfitted for training data, on the contrary to AdaBoost, the test accuracy of XGBoost was slightly higher than for AdaBoost's. Also, applying feature selection to Boosting classifiers resulted a worse performance for all metrics compared to models without Bonferroni correction.

Therefore, we can see that the feature selection was invalid in respect of Boosting algorithms that focus weights on misclassified samples for improving accuracies. In other words, the eliminated features from Bonferroni correction have had a substantial influence on decision-making processes in Boosting models, especially for identifying the attributes of incorrectly classified dataset.

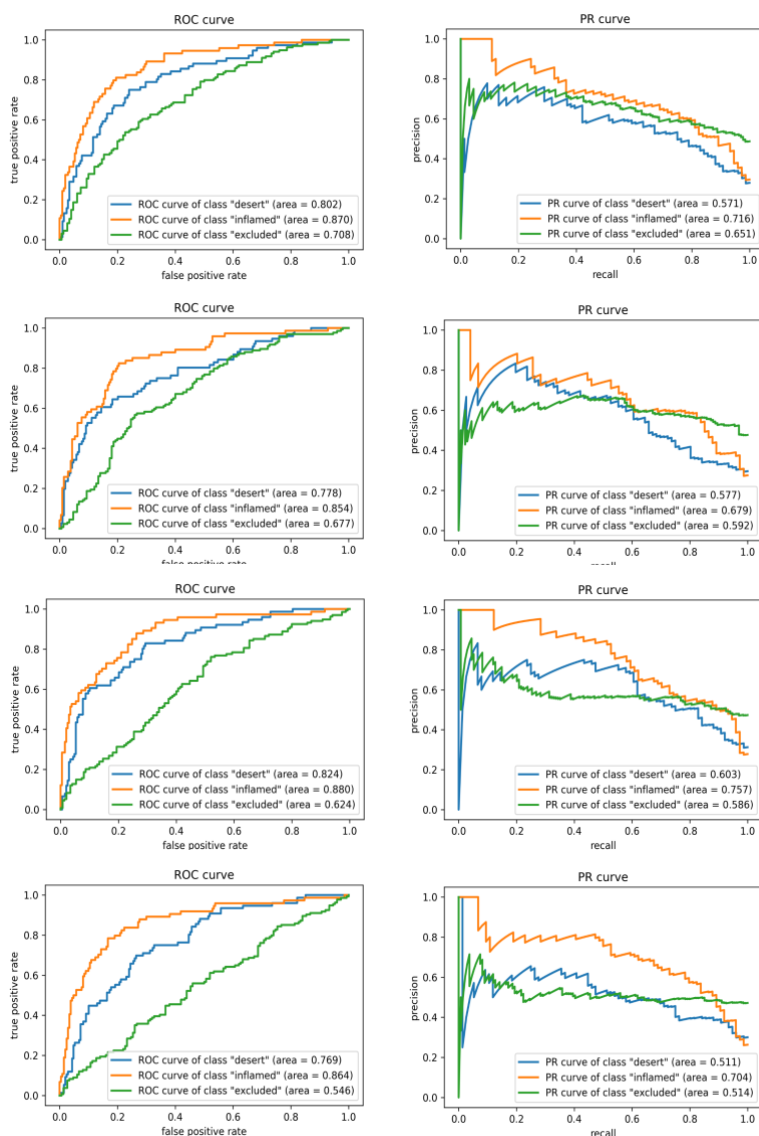


**Figure 3. Receiver operator characteristic (ROC) and precision and recall (PR) curves for each class using Random Forest.** Top: Random Forest without feature selection, bottom: Random Forest with feature selection. Higher AUCs, closer to 1, indicate better performance. High AUCs with ROC curves for each phenotype indicate the model is predicting the phenotypes with low false positives. ROC curves show that classification performance for the immune-excluded class is enhanced (green line) by feature selection. Likewise, comparing two PR curve plots illustrates that performance of all classes with feature selection has outperformed.

#### D. CLASSIFICATION OF IMMUNE PHENOTYPES WITH DNN

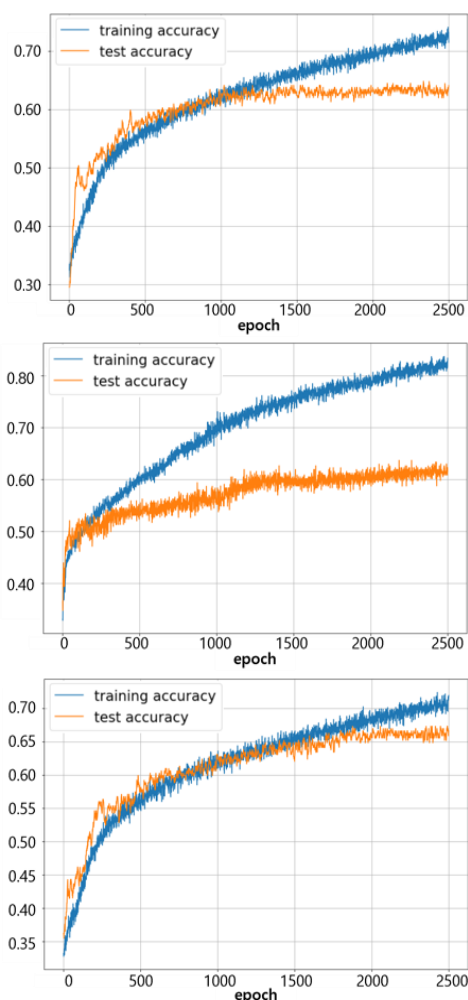


**Figure 4. Change of training / testing accuracy with respect to epoch in DNN training.** Top: DNN (feature selection), middle: DNN (L1-norm penalty), Bottom: DNN (L1-norm penalty and feature selection). Similar training (blue) and testing (orange) accuracies indicate better generalization of the trained model to unseen testing data. As seen in the middle panel, significant overfitting (large differences between training and testing accuracies) occurs without feature selection.

Various classification experiments using DNN were performed with the settings described in the Methods section. Representative results are summarized in Table 1. With a very naïve DNN model without any regularizers or techniques to make the model robust (i.e., dropout, batch normalization, and feature selection), the resultant accuracy averaged across all 10 folds was 0.549. Considering the baselines with random guess (0.33) and prediction as the dominant class (0.472), the model was properly learning to predict BC immune phenotypes. However, it suffered from overfitting and relatively low accuracy compared to the SVM-based models. Applying a dropout rate of 0.3, statistical feature selection, and l1-regularizer (with hyper parameters 0.01 and 0.08 for each layer) on two hidden layers with 32 hidden nodes, the accuracy increased to 0.666 with averaged respective precision and recall of 0.722 and 0.635 across different class labels.

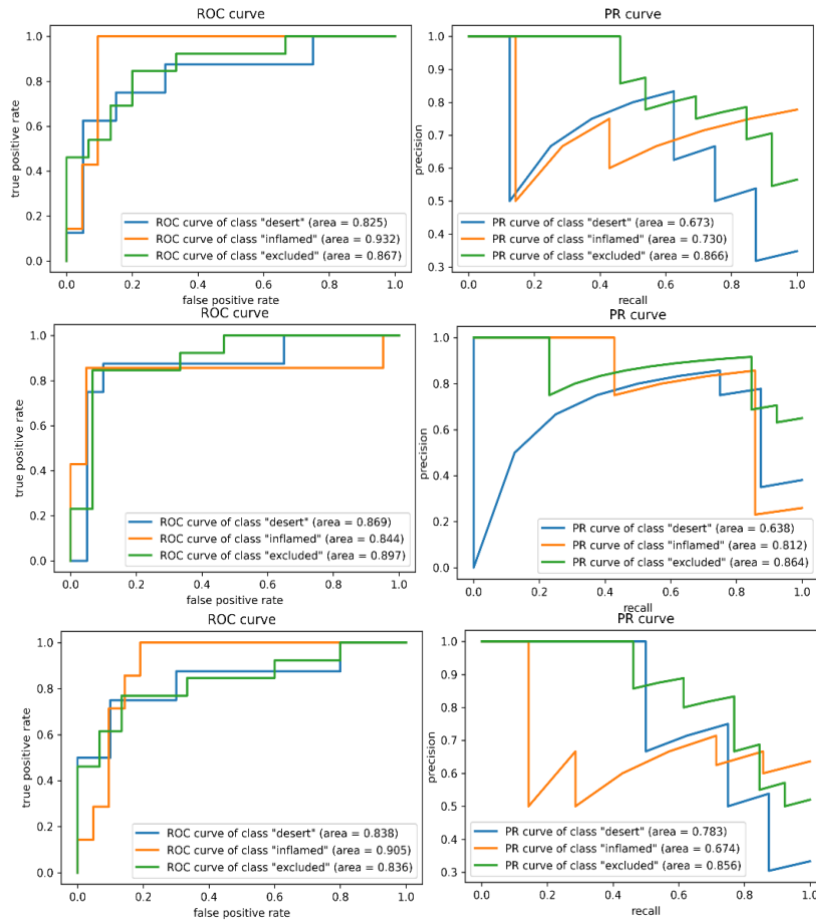


**Figure 5. ROC and PR curves (for each class) using deep neural network (DNN).** Top: DNN (feature selection), mid: DNN (L1-norm penalty), bottom: DNN (L1-norm penalty and feature selection). Higher AUC (closer to 1) indicates better performance. High AUCs with ROC curves for each phenotype indicate the model is predicting the phenotypes with low false positives. Overall AUCs of both ROC and PR curves are higher than those from SVM analysis.

The ROC and PR curves for individual experiments are shown in Fig. 4, where the curves for each class are given in blue (immune desert), orange (inflamed), and green (immune-excluded). All the ROC curves in the left column of Fig. 4 rapidly converged close to 1 in their true positive rate (TPR). Simultaneously, the PR curves in the right column of Fig. 4 maintained precision with respect to recall as much as possible. The respective AUCs of 0.77 and 0.87 for the PR and ROC curves demonstrated the model's feasibility in classifying different stages of immune phenotypes. The training and testing accuracies for different DNN settings are shown in Fig. 5, which demonstrates that both training (blue) and testing (orange) accuracies increase as the training progresses. After the model convergences, the middle subfigure (with l1-penalty) shows a large difference between the training and testing accuracies as opposed to the other two subfigures. These differences were due to the application of statistical feature selection using a t-test. For each fold, statistical testing at each gene feature on the training data with Bonferroni correction at 0.05 yielded 900~1300 significant features. Given the high dimensionality of the data, without feature selection for dimension reduction, the issue of overfitting was easily seen. Although not presented in these results, we also observed overfitting occurring with an increase in hidden layers or nodes. This overfitting behavior explains the differences in MCC. As seen in Table 1, the DNN with l1-penalty only showed the lowest MCC as it was highly overfitted. On the other

hand, the DNN with both l1-penalty and feature selection did not overfit and demonstrated the highest MCC of 0.488.

With the l1-regularizer at imposing sparsity at the input layer, many of the weights associated with each feature were suppressed to a value of or close to 0. From the DNN model with regularizer and feature selection, which yielded the highest accuracy and AUC for PR curves, the top 20 highest weighted gene features across all 10 folds were identified. Among them, 13 common features existed across all folds. These were named TMEM156 (Transmembrane Protein 156), TOX (Thymocyte Selection-associated High-mobility Group Box Protein), XAF1 (X-linked Inhibitor of Apoptosis-associated Factor-1), SPATC1 (Spermatogenesis and Centriole Associated 1), FOXP3 (Forehead Box P3), ARRB2 (Arestin Beta 2), TNFRSF9 (TNF Receptor Superfamily RNASE6 (Ribonuclease A Family Member K6), DBH-AS1 (DBH Antisense RNA 1), TENT5C (Terminal Nucleotidyltransferase 5C), ID3 (DNA-binding Protein Inhibitor), APOE (Apolipoprotein E), and LAX1 (Lymphocyte Transmembrane Adaptor 1).

#### **IV. DISCUSSION**

In recent years, immunotherapy has come to play an increasingly important role in oncology. Immunotherapy in cancer treatment involves modifying or adding defense mechanisms to the patient's immune system. Immunotherapy is often used as a supplement to conventional cancer treatment methods, such as surgery, chemotherapy, and radiation therapy. For some specific types of lung and colorectal cancer, immunotherapy is used as the first line of treatment [49]. In urological oncology specifically, immunotherapy is used as a supplemental treatment in addition to standard of care [50]. Immunotherapy in cancer treatment involves modifying or adding defense mechanisms to the patient's immune system. Currently, immunotherapy can be divided into several types, including immune CPIs, T cell transfer therapy, monoclonal antibodies, therapeutic vaccines, and immune system modulators [51].

Based on current research on BC therapies, immunotherapy seems to be the most promising. Because there are multiple regimens for immunotherapy, patients respond differently depending on the therapy. Currently, the US FDA has approved five anti-programmed death-1/ligand 1 (PD-1/L1) checkpoint inhibitors: atezolizumab, avelumab, durvalumab, nivolumab, and pembrolizumab [52]. Among them, atezolizumab was the first to pass approval. This approval was made based on the research results of IMvigor210. IMvigor210 was an open multicenter, single-arm phase II clinical study designed to study whether atezolizumab could become the standard treatment for advanced urothelial cancer. This study suggested that for patients with platinum-based refractory metastatic urothelial carcinoma (mUC), checkpoint inhibitors seem to be more attractive than chemotherapy [13]. Atezolizumab has shown encouraging long-term response rates, survival rates, and tolerability, supporting its therapeutic use in untreated mUC [53]. Based on the results of the study, the FDA approved atezolizumab as the first-line drug for the treatment of patients with advanced urothelial cancer who are not suitable for cisplatin chemotherapy.

Regarding Boosting methods, the key hyperparameters were the number of trees and learning rates. The number of estimators designates the scale of Random Forest. As more individual trees were included, the classification performance became better, but the whole model took longer time to be trained. A learning rate of Boosting algorithms denotes a coefficient applied to the weak classifiers when calibrating the error values sequentially. Since the learning rate directly affects the variation in the weight update, the difference in decision boundaries of multiple trees changed proportionally to the learning rate. However, it requires a large number of trees with a time-consuming ensemble process at the same time. Thus, the number of trees and learning rate has a trade-off relationship and coordinating the ratio between the two parameters was crucial to the performance of classification. Therefore, we had to manage the number of estimators at the same rate for fair comparison of the results.

In our study, Decision Tree based methods mostly tended to overfit as the training accuracies reached 1, and testing cases underperformed compared to SVM and DNN. Comparing the top-2

algorithms, although the accuracies with our DNN model were lower than that of our SVM model, the AUCs of evaluation curves (ROC and PR) were better. Specifically, the AUCs of PR curves in the DNN model were larger by 0.083 compared to the best of both models, which demonstrates that the DNN did better with imbalanced class labels. This is because the latent space for group separation found by DNN is better than SVM; while SVM with RBF kernel maps the data onto a higher dimensional space to find a linear decision boundary in that space, the DNN model mapped data onto a lower-dimensional space where group separation can be more effective and robust. The accuracy may be better in the high-dimensional space found by SVM with RBF kernel, but the actual separation of the three immune phenotypes was more effective with DNN. This was also seen in the overfitting trend of both models. Both SVM and DNN suffered from overfitting; it was more serious for the SVM model while the DNN model was able to mitigate this issue with common techniques, such as dropout and regularizers, and this behavior was observed in MCC of individual models. As a result, there was a trade-off between training accuracy and other measures. Although SVM achieved slightly better test accuracy and MCC than those from DNNs, the precision and AUCs were significantly higher in DNN models, which we believe are more important.

Regarding the effective biomarkers found by the DNN model, downstream statistical group tests across each phenotype pairs yielded many significant p-values. As the phenotype profiles are ordered by severity, all 13 features showed very low p-values ( $<1e-6$ ) for immune desert vs. inflamed and mostly effective (i.e.,  $<0.05$ ) for other group pairs. Perhaps this was expected as our feature selection process selected important features with statistical tests at the training stage, but it was still worth analyzing them over the entire data to confirm if these biomarkers are really statistically meaningful for group comparisons.

We further investigated the 13 significant features associated with immunotherapy responsiveness in BC. FOXP3 is widely known as a key regulatory transcription factor of regulatory T cells, contributing to immune system responses [27, 54, 55]. Expression of FOXP3 in BC has been reported to negatively associated with survival of patients [56]. Recent studies have reported that FOXP3 acts as a transcriptional regulator of HIF-1 $\alpha$  gene expression in BC, suggesting the potential contribution of the FOXP3/HIF-1 $\alpha$  pathway in poorer survival [57]. APOE, an apolipoprotein related to lipoprotein-mediated lipid transport, was also found in the immunotherapy responsive molecular features. The LXR (liver X receptor)/APOE axis has been reported to regulate innate immune suppression and activation. Since this axis blocks innate immune suppression in many cancer types, it has been suggested as a therapeutic target to allow better efficacy of immunotherapy for cancer patients [58]. TOX has been found to regulate innate immunity and the tumor microenvironment. TOX expression significantly increases immune infiltration levels and is downregulated in most cancer types. Lower expression of TOX is correlated with poorer prognoses, suggesting that TOX expression can be used for stratification of non-responders to immunotherapy [59, 60].

Findings from this study suggest that the experiment we designed using ML algorithms are effective in classifying immune phenotypes of BC with gene expressions and identifying associations between specific gene expressions and the phenotypes. It also demonstrates the potential of our DNN model after improving overfitting via utilization of more samples. In addition, this study found 13 features associated with response to immunotherapy, which may all be biologically relevant.



## ACHIEVEMENT 5:

### Classification of the Urinary Metabolome Using Machine Learning and Potential Applications to Diagnose Interstitial Cystitis

#### Summary

With the advent of artificial intelligence (AI) in biostatistical analysis and modeling, machine learning can potentially be applied into developing diagnostic models for interstitial cystitis (IC). In the current clinical setting, urologists are dependent on cystoscopy and questionnaire-based decisions to diagnose IC. This is a result of a lack of objective diagnostic molecular biomarkers. The purpose of this study was to develop a machine learning-based method for diagnosing IC and assess its performance using metabolomics profiles obtained from a prior study. To develop the machine learning algorithm, two classification methods, support vector machine (SVM) and logistic regression (LR), set at various parameters, were applied to 43 IC patients and 16 healthy controls. There were 3 measures used in this study: accuracy, precision (positive predictive value), and recall (sensitivity). Individual precision and recall (PR) curves were drafted. Since the sample size was relatively small, complicated deep learning could not be done. We achieved a 76-86% accuracy with cross validation depending on the method and parameters set. The highest accuracy achieved was 86.4% using SVM with a polynomial kernel degree set to 5, but a larger area under the curve (AUC) from the PR curve was achieved using LR with a  $l_1$ -norm regularizer. The AUC was greater than 0.9 in its ability to discriminate IC patients from controls, suggesting that the algorithm works well in identifying IC, even when there is a class distribution imbalance between the IC and control samples. This finding provides further insight into utilizing previously identified urinary metabolic biomarkers in developing machine learning algorithms that can be applied in the clinical setting.

Interstitial cystitis (IC), also known as painful bladder syndrome or bladder pain syndrome, is a chronic visceral pain syndrome of unknown etiology that presents itself as a constellation of symptoms, including bladder pain, urinary frequency, urgency, and small voided volumes, in the absence of other identifiable diseases<sup>100-102</sup>. Urine is in direct contact with the bladder epithelial cells that could be giving rise to IC; as a result, metabolites released from bladder cells may be enriched in urine<sup>103</sup>.

The urinary metabolome was previously investigated by our group for potential IC diagnostic biomarkers<sup>104-106</sup>. We attempted to identify IC-associated metabolites from urine specimens obtained from IC patients and controls using nuclear magnetic resonance (NMR). Our findings provided preliminary evidence that metabolomics analysis of urine can potentially segregate IC patients from controls. We sought to capture the most differentially detected NMR peaks and discern if there was a significant difference in the peak distribution between IC and control specimens. Based on multivariate statistical analysis, principal component analysis (PCA) suggested that the urinary metabolome of IC patients and controls were clearly different; 140 NMR peaks were significantly altered in IC patients (FDR < 0.05) compared to controls<sup>104</sup>.

Machine learning (ML), originally described as a program that learns to perform a task or make decisions based on data, is a valuable and increasingly necessary tool for modern healthcare<sup>107</sup>. However, this definition is broad and could cover nearly any form of data-driven needs. ML is not a magical approach that can turn data in immediate benefits, even though many news outlets imply that it can. Rather, it is natural extension to traditional statistical approaches. In our present study, we utilized ML and automated performance metrics to evaluate the clinical value of our 140 identified NMR peaks. We used ML algorithms examine the relationship between metabolic expression and disease. We applied logistic regression (LR)<sup>108</sup> and support vector machine (SVM)<sup>109,110</sup>, which are traditionally known to work well even with small sample sizes, to our metabolomics signatures and used this data together with patient clinicopathological features to

diagnose IC. We used our dataset of 59 cases to train, test, and validate the model. The results showed that our ML-based algorithms were able to successfully identify IC patients from healthy subjects.

This study aimed to address the question of, “Does utilizing metabolic data in ML play a role in diagnosing IC?”. ML is a form of artificial intelligence (AI) and learns from past data in order to predict the future. Our NMR-based ML algorithm was able to collectively distinguish the IC patient urinary profile from that of controls.

## **MATERIALS AND METHODS**

### **Ethics Statement**

For this paper, we used the deposited dataset derived from the published data. This study used the publicly deposited data, which does not need IRB approval.

### **Dataset**

There are 59 samples in total in the IC dataset. In order to acquire IC-associated metabolites, urine samples were collected from 43 IC patient group and 16 healthy control group. Each urine specimen was analyzed using nuclear magnetic resonance (NMR) and biomarkers were identified with 140 NMR peaks. The 140 NMR peak feature was utilized to apply the dataset to ML algorithms for classification of IC patients in this paper <sup>104</sup>.

### **Machine Learning**

#### ***Method.***

Due to limited sample size, we adopted two machine learning algorithms, i.e., Support Vector Machine (SVM) <sup>109,110</sup> and Logistic Regression (LR) <sup>108</sup>, that are traditional but work well even with small number of samples. These are supervised learning algorithms, where each data sample is represented by a number of features and comes with a label that tells which group the sample belongs to.

When data is represented as scattered data points in a feature space that consists of two clusters representing individual groups, SVM finds a decision boundary (either linear or non-linear) that separates the different groups. Training an SVM optimizes the decision boundary to maximize the margin between the clusters, and it requires a kernel function train a kernel SVM that learns a non-linear decision boundary, i.e., a non-linear classifier <sup>111</sup>. The model contains a user parameter known as ‘slack variable’ that controls the width of the margin.

LR is also a classifier that learns via a linear model. By feeding a set of training samples with a number of features, it learns specific weights associated with features. When a data sample is input into to a LR model, a classification is made by a linear combination between the weights and the data; together with a sigmoid function, the combined value is mapped to a probability between 0 and 1. The predicted label is assigned according to the probability, and by minimizing the classification error (usually formulated using cross-entropy) in the training dataset, the weights are learned. One can add additional regularization terms in the model, such as  $l_1$  or  $l_2$ -norm of the weights, where  $l_1$ -norm controls the sparsity of the weights <sup>112</sup>, which will select the most important features, while  $l_2$ -norm controls the smoothness of the weights to make the model more robust <sup>112,113</sup>.

Both SVM and LR were implemented using the sklearn package in Python.

#### ***Training.***

Because the sample size was very small, the leave-one-out cross validation (CV) <sup>114</sup> method was utilized to make full use of the data set and to obtain unbiased result from the classifiers.

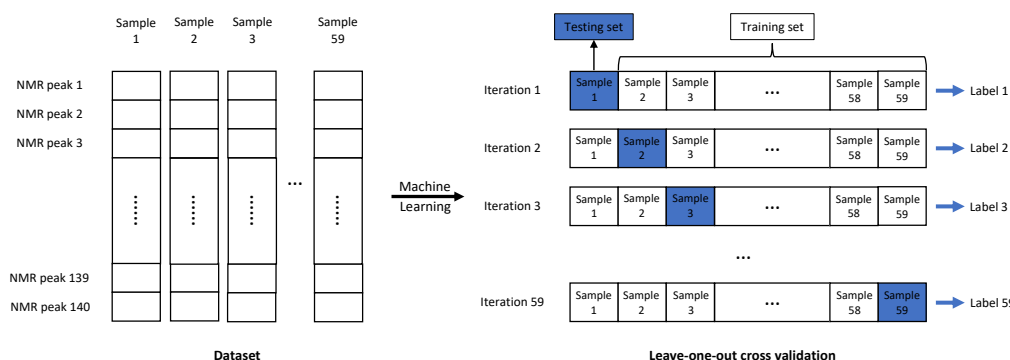
With leave-one-out, we picked one sample as a testing set while using the rest of samples as a training set to train and test the model. The same process was iterated for every sample in the dataset. An illustration of the leave-one-out CV workflow is given in the **Figure 1**.

For SVM, we performed a set of experiments with a linear model, radial basis function (RBF) kernel, polynomial kernel with degree being 3, 5, 7. The slack variable was set to 1 for all cases. For LR, we tried  $l_1$  and  $l_2$  penalties with different strengths; i.e. the inverse of regularization strength  $C$  was set to 1, 5, and 10.

### Evaluation.

After repeating training and testing the model 59 times with leave-one-out CV, each sample was assigned a predicted label. By comparing these 59 predicted labels with the true labels, we constructed a confusion matrix by counting numbers of True Positive (TP), True Negative (TN), False Positive (FP) and False Negative (FN). From these numbers, accuracy, precision and recall were calculated to evaluate the performances of the models. Receiver operating characteristic (ROC) curve and precision-recall (PR) curve are plotted, and their area under the curve (AUC) are reported in the result section. Especially when the distribution of labels in the dataset is skewed, the AUC of the PR curve is a suitable measure for evaluating to account for the imbalance.

**Figure 1.** IC classification experimental scheme with leave-one-out cross validation



## RESULTS

### Classification of IC Samples with SVM.

SVM was applied to the IC dataset with the leave-one-out CV scheme to classify IC samples from controls. The result varied depending on user parameters (i.e., kernel type and kernel parameters) as shown in **Figure 2** and **Table 1**. Comparing the numbers, it was found that SVM with polynomial kernel resulted in the best performance when the degree of the polynomial kernel was 3 with 86.4% accuracy, 0.88 AUC of PR curve, and 0.85 AUC of ROC curve. Although the accuracy was the highest when the degree was 5, the AUCs of ROC and PR curves with degrees set to 3 was the highest. Moreover, the degree equal to 3 has less chance of overfitting than a degree of 5.

Here, the usage of linear kernel did not perform well. It may be because the data were not linearly separable or simply the sample size ( $N=59$ ) was too small compared to the dimension of the data (i.e., 140 features). Performance of RBF kernel was also poor; looking at the accuracy using RBF kernel with SVM shown in **Table 1** (i.e., 72.9%), it was the same as the proportion of IC samples

in the dataset (i.e., 43 IC subjects out of 59 subjects) and its recall was 1. This means that the classifier was simply predicting that all the samples belong to IC group and was not able to handle the class distribution imbalance problem.

**Figure 2.** Classification result evaluation curves using SVM. (a) the Precision-Recall curve, (b) ROC curve. The values of AUC are calculated for each curve and larger values indicate better performance.

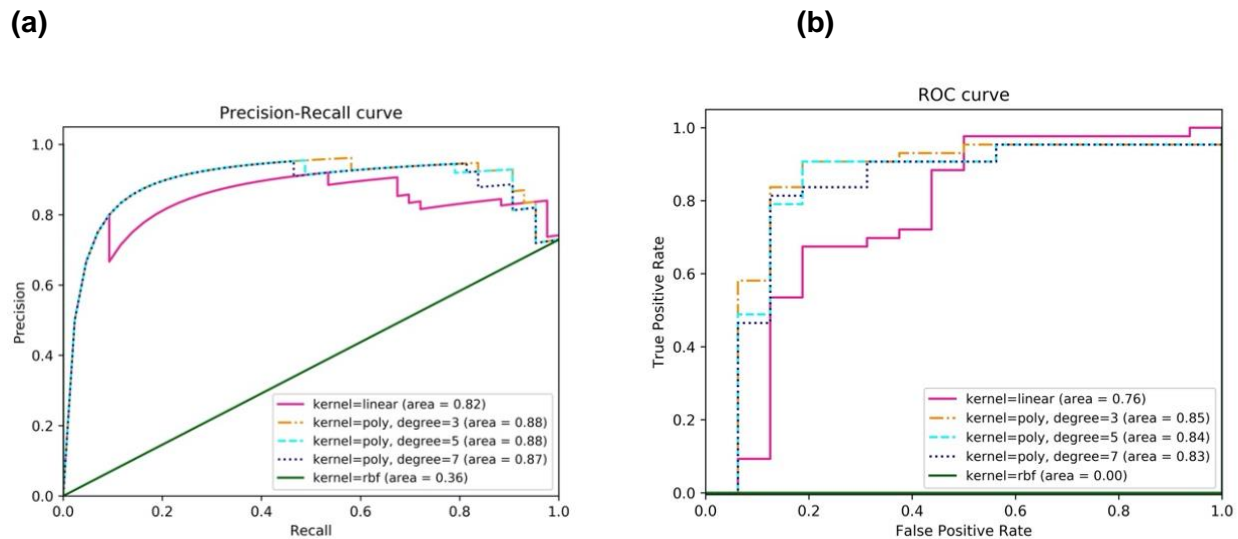


**Table 1.** The comparison of results from SVM with different set of parameters. TP: True Positive, TN: True Negative, FP: False Positive, and FN: False Negative.

Parameters	TP	TN	FP	FN	Accuracy	Precision	Recall	AUC of PR	AUC of ROC
kernel=linear	36	9	7	7	0.763	0.837	0.837	0.82	0.76
kernel=poly, degree=3	39	11	5	4	0.847	0.886	0.907	0.88	0.85
kernel=poly, degree=5	39	12	4	4	0.864	0.907	0.907	0.88	0.84
kernel=poly, degree=7	39	11	5	4	0.847	0.886	0.907	0.87	0.83
kernel=rbf	43	0	16	0	0.729	0.729	1.000	0.36	0.00

### Classification of IC Samples with LR.

In addition to SVM experiment, LR was used to classify IC samples and the results are shown in **Figure 3** and **Table 2** with different user parameter settings. LR with  $l_1$ -penalty yielded the best performance when its penalty parameter was set to 10 with 84.7% accuracy, 0.91 for AUC of PR curve and 0.86 for the AUC of ROC curve, which was slight better than the results from SVM. These numbers are the best among several trials because of its randomness with the initial weights being trained, and the results from other trials did not differ much from those reported in **Figure 3** and **Table 2**.

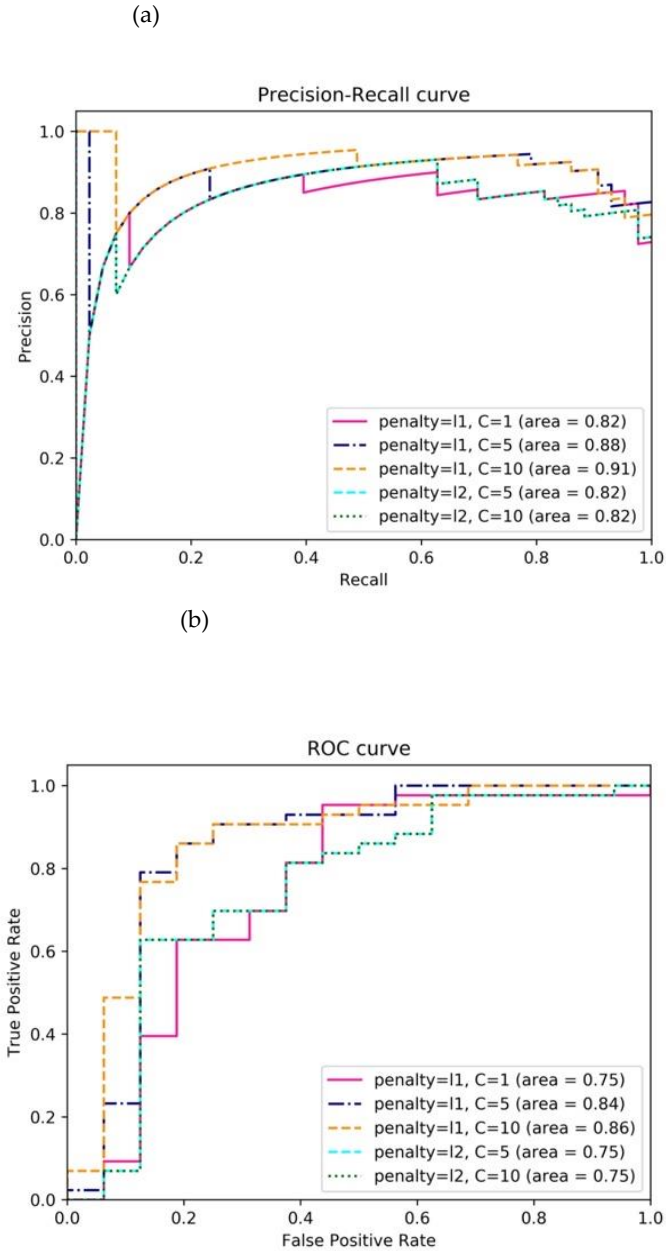
**Table 2. The comparison of results from LR with different set of parameters. TP: True Positive, TN: True Negative, FP: False Positive, and FN: False Negative.**

LR	TP	TN	FP	FN	Accuracy	Precision	Recall	AUC of PR	AUC of ROC
penalty=l1, C=1	39	9	7	4	0.814	0.848	0.907	0.82	0.75
penalty=l1, C=5	39	10	6	4	0.831	0.867	0.907	0.88	0.84
penalty=l1, C=10	38	12	4	5	0.847	0.905	0.884	0.91	0.86
penalty=l2, C=5	38	7	9	5	0.763	0.809	0.884	0.82	0.75
penalty=l2, C=10	38	7	9	5	0.763	0.809	0.884	0.82	0.75

It was observed that LR worked well despite being a linear model. Notice that the performance of linear SVM was poor in **Table 1**; this is because of the  $l_1$ -norm penalty applied to the trained parameter imposing sparsity and behaving as a natural feature selector. When we checked the trained weight of features, most of the weights converged to 0 (a very small number on average of absolute values across the leave-one-out process). When the penalty parameter was 10, the average weights of 133 features was less than or equal to 0.1. This means that we only need a few critical features to predict correct label. In our experiment, feature id = 73, 4, 129, and 35 were the most dominant features with the highest weights regardless of the random initialization. In other words, they were the four most useful NMR features. We have performed further statistical group analysis on these four NMR peaks using two-sample t-test, which resulted in  $p$ -values of 0.003, 0.001, 0.057, and 0.036 respectively. It was interesting to see that there were many other NMR peaks with even lower  $p$ -values and the peak ID=129 had a  $p$ -value greater than 0.05. While these statistical tests are performed independently, our classification results were derived by taking all the peaks at the same time for the analysis and it demonstrates that a linear combination of the features can be more powerful to distinguish IC from controls.

The  $l_2$ -norm constraint did not contribute much in these experiments. This is because the model can robustly operate even without the  $l_2$ -norm regularizer, which typically degrades performance of models in exchange for model robustness. Especially with the  $l_1$ -norm regularizer significantly lowering the dimension of the data (with 133 redundant features), the sample size ( $N=59$ ) was sufficient to make robust and correct predictions for IC samples.

**Figure 3.** Classification result evaluation curves using LR. (a) the Precision-Recall curve, (b) ROC curve. The values of AUC are calculated for each curve and larger values indicate better performance.



## DISCUSSION

It comes with no surprise that medicine is awash with claims that ML applications into big healthcare data will create extraordinary revolutions<sup>107,115,116</sup>. Recent examples have demonstrated how big data and ML can create algorithms that can perform on par with human physicians. AI is one ML approach without prerequisites. Various AI techniques already exist, and successful metabolomics analysis has been reported in previous studies<sup>117-119</sup>. Conventional statistical analysis and AI-based methods were used to assess the discrimination capability of quantified metabolites. A multiple logistic regression (MLR) model, alternative decision tree (ADTree), neurofuzzy modelling (NFM), artificial neural network (ANN), and SVM machine learning methods were used<sup>120,121</sup>.

Modern advancements in computational and data science, with its most popular implementation in ML, has facilitated novel complex data-driven research approaches. Combined with biostatistics, ML aims at learning from data. It accomplishes this by optimizing the performance of algorithms with immediate previous knowledge. ML can be applied in either a supervised or unsupervised fashion. Supervised learning entails monitoring of the algorithm while it is being trained to learn a correct class assignment from a set of parameters, such as how to make a correct diagnosis from clinical and laboratory information<sup>117</sup>.

Current biomarkers for IC diagnosis and prognosis are insufficiently robust for clinical practice using AI. Instead, we used AI to identify IC-related metabolites in an NMR metabolomics dataset from our previous study<sup>104</sup>, which was able to collectively distinguish IC patient urinary profiles from that of healthy controls. The development of diagnostic tools using ML may be useful for more accurately identifying IC patients. AI has the potential to manage the imprecision and uncertainty that is common in clinical and biological data. AI or ML-based algorithms can take several different forms. The icons in the presented figures in this paper represent typical ML methods. These include multilayer neuronal networks, decision tree-based algorithms, SVM, and related algorithms that separate classes by placing hyperplanes between them, and prototype-based algorithms, such as k-nearest neighbors that compare feature vectors carried by a case with those carried by other cases and assign classes based on similarities. ML-based algorithms are not being actively applied to IC research. Such applications could lead to a better understanding and deeper knowledge of metabolomics data, which would then provide insights into biomarker discovery.

Although this is out of scope for this study, AI algorithms can be used to predict IC progression or therapeutic responses, too<sup>122,123</sup>. Patient clinicopathological features are commonly used to train AI algorithms to predict patient outcomes in other diseases, such as cancer<sup>124-126</sup>. For instance, Wong et al. developed a prostate cancer patient-specific ML algorithm based on clinicopathological data to predict early biochemical recurrence after prostatectomy<sup>127</sup>. The resulting 3 ML algorithms were trained using 338 patients and achieved an accuracy of 95-98% and AUC of 0.9-0.94. When compared to traditional Cox regression analysis, the 3 ML algorithms had superior prediction performance. This study demonstrated how AI algorithms, trained with clinicopathological data, imaging radiomic features, and genomic profiling, outperformed the prediction accuracy of D'Amico risk stratification, single clinicopathological features, and multiple discriminant analysis, a type of conventional multivariate statistics<sup>127</sup>. There is also a role for AI in selecting effective drugs for cancer treatment<sup>128</sup>. Using an ML-based algorithm, Saeed et al. quantified the phenotypes of castration-resistant prostate cancer cells and tested their response to over 300 emerging and established clinical cancer drugs<sup>129</sup>.

We are aware that one of the limitations of this study includes the novelty of using crowdsourcing in medical biomarker development. To our knowledge, there is no previous reference for comparison. Additionally, this study was limited to participants in South Korea and to a 1-time



point collection. A major problem associated with medical datasets is a small sample size<sup>104</sup>. Given that sufficiently large datasets are important when creating classification schemes for disease modeling, a relatively larger dataset can result in reasonable validation due to sufficient partitioning of training and testing sets. On the contrary, a smaller training dataset can lead to misclassifications and may result in unstable or biased models. For our study, a major problem was the small sample size. However, the reason for this is that it takes an immense amount of time, effort, and cost to collect a larger amount of medical research data. Furthermore, medical research data is often inconsistent, incomplete, or noisy in nature; thereby, reducing sample sizes even more. Such small sample size for high-dimensional data often leads to 'curse of dimensionality', i.e., failing to properly estimate necessary parameters due to lack of samples, which we also faced with only 59 samples for 140 NMR features. In this work, we have used SVM and LR as classifiers. For SVM, when casting its objective function as a dual form using Lagrangian multiplier, the optimization problem seeks for a sparse solution that identifies a few 'support vectors' and thus greatly reduces the dimension of problem. For the LR, we used two different regularizers on the parameters to estimate, i.e., L1 and L2-norms, to avoid curse of dimensionality and obtain feasible solutions. As demonstrated in the results, as L1-norm constraint behaved as a data-driven feature selector reducing the dimension of the problem, the classifier avoided the curse of dimensionality. Although we were able to stay away from the curse of dimensionality in this study, poor analysis may lead to data overfitting and irreproducible results. ML-based algorithms may be manipulated by datasets containing dominant but irrelevant features when the sample number is limited. Also, AI cannot be used as an end-all solution to any question. There are instances where traditional statistics has outperformed AI or where additional AI does not improve results.

In summary, we have found that ML-based algorithms can be applied to developing diagnostic models for IC patients. In the current clinical setting, urologists are generally dependent on cystoscopy and questionnaire-based decisions to diagnose IC due to a lack of objective molecular biomarkers. The purpose of this study was to develop machine learning methods for diagnosing IC and assess their performance using metabolomics data. Considering how ML techniques for analyzing omics data can play a role in predicting the diagnosis and prognosis of diseases, future studies should integrate use of a larger multidimensional and heterogenous dataset, application of more accurate validation results, and use of different techniques for classifying and selecting features to pave a promising way toward clinical applications.

## **ACHIEVEMENT 6: BRINGING MACHINE LEARNING TO PICK OUT HIDDEN CLINICAL VALUES FROM BIG DATA IN UROLOGY**

Suppose you are asked to select one the most important information technology revolution of our time that can give your decision-making processes a massive upgrade. Many of us will choose machine learning (ML). A definition of ML is “gives computers the ability to learn without being explicitly programmed.” The main premise of ML is to introduce algorithms that ingest input data, apply computer analysis to predict output values within an acceptable range of accuracy, identify patterns and trends within the data and finally learn from previous experience. ML is often applied to complicated, poorly understood phenomena in nature, such as complex biological systems, climate change, astronomy, or particle physics.

Let us tell you the mathematics and methodological of ML. The two major pathways in machine learning are supervised learning and unsupervised learning. In supervised learning, an algorithm is often provided with data  $X_{N \times P}$  (N samples with P features) related to the learning objective and a desired target measure  $y$ . The goal is to train a classifier (i.e., learn a decision function)  $f$  that can perform prediction on the target  $y$  for unseen data  $X$ , i.e.,  $f(X) = y$ , and identify links between the features and the target measures. Supervised learning primarily deals with classification and regression problems. In unsupervised learning, an algorithm is provided with data  $X$  without any class label / annotation to find any latent patterns, sometimes producing both answers and questions that may not have been conceived by the investigators. Unsupervised learning typically deals with clustering and dimensionality reduction problems. The patterns identified in unsupervised learning often need to be evaluated for utility either by human interrogation or via application within a supervised learning task.

While validation of unsupervised algorithm can only be performed based on a dataset with ground truth that is hidden during the training process, the performance of a supervised learning algorithm can be evaluated by various metrics based on the objective of a task. For supervised learning algorithms, a dataset is typically divided into two independent sets, i.e., training set and testing set, where training of an algorithm is performed using the training set and then the trained model is evaluated using the testing set. In order to remove any bias that may have been introduced in a single division of training and testing sets, Cross Validation (CV) is often used to evaluate a supervised learning algorithm. CV divides a dataset into  $k$  subsets, also known as  $k$ -folds, and iterates through  $k$  number of training and testing phases that use  $i$ -th subset as a testing set and the rest of subsets for training. Such iterations yields  $k$  different results with different training-testing set pairs and aggregating the results let us avoid those cases that may have performed successfully or poorly by bias or coincidence.

The performance of a supervised learning algorithm is often measure by accuracy, precision and recall. While accuracy being the main measure of interest, it does not consider class distribution imbalance in a dataset which is quite common in many biomedical studies. For example, when a dataset consists of two class, e.g., positive and negative, where the number of normal subjects dominates, then simply predicting all samples in a testing set as normal will yield high accuracy with significant false-positives. That is why one needs to consider precision and recall together, where precision measures how precise the prediction made by a trained model is and recall measures how much of the total positive examples in the testing set the trained model can predict as true positive. F1-score is also a common measure, which accounts for both precision and recall simultaneously.

**How ML is applied to develop precision medicine for us?**

Many of us may agree with this statement - "big data will transform medicine". In recent years, a large amount of data has been accumulated in big omics studies of genomes, epigenomes, transcriptomes, proteomes, metabolomes and other sources. This big data needs to be analyzed, interpreted and manipulated to provide the biological meaning. Where ML shines is in handling enormous numbers of predictors. ML has become ubiquitous and indispensable for solving complex problems in most sciences. ML will become an indispensable tool for clinicians seeking to truly understand their patients. Yet, we are aware that ML has shortcomings in dealing with big data<sup>130</sup>. First, algorithms might "overfit" predictions to spurious correlations in the data; multicollinear, correlated predictors could produce unstable estimates. Second, ML algorithms often require millions of observations to reach acceptable performance levels. Third, biases in data collection can substantially affect both performance and generalizability. Finally, ML does not solve any of the fundamental problems of causal inference in observational data sets.

Precision medicine is one of the important developments in current medicine. It helps doctors with early intervention by using advanced diagnostic procedures and customizes reasonable and better personalized treatment methods for patients. Many scientists and physicians are convinced by the importance of information technology and ML for the implementation of precision medicine, which includes data storage and analysis for determining the association between disease outcome, identification of patient characteristics and optimal treatment. Utilizing ML approaches for pattern recognition and development of statistical models, creating a knowledge base of all existing phenotype categories and disease, organization of clinical datasets of population size and open software platform development for statistical analysis of high-dimensional healthcare and multi-omics data are crucial for practical realization of precision medicine.

As you can imagine, ML will have a huge impact in disease (especially cancer) diagnostics and prognostics, specifically on the development of novel computational tools for stratification, grading, and prognostication of patients with the goal of improving patient care. There are many different ML techniques and algorithms, which have been widely used in disease prediction, diagnosis and prognosis. A series of studies show how ML could improve diagnostic performance and prediction accuracy in clinically relevant patient cohorts<sup>131</sup>. A study demonstrates how ML can improve well established standards such as the Gleason, thus yielding to more precise prognostication. Another study developed a ML system to predict Microsatellite instability (MSI) in patients with gastrointestinal cancer and endometrial cancers, both accuracies are higher than the prediction of molecular markers. Some studies have shown that ML can get higher accuracy of drug response prediction. ML methods have become a popular tool for medical researchers, which is able to effectively predict future outcomes of disease.

So how ML is involved in current clinical research? For digitalized pathology field, various applications incorporating ML are being developed to assist the process of pathologic diagnosis. Major applications that have been studied so far include detection of specific objects such as cancer cells, cell nuclei, cell divisions, ducts, and blood vessels, classification and grading of tumors, and quantitative evaluation of immunostaining. The major obstacle facing ML of pathological images is inadequate image dataset annotation. At present, many technologies have been developed<sup>132</sup>. For example, generative adversarial networks (GAN), the techniques for learning and generating color tones using "generative model" technology, is used for pathological data analysis to automatically prepare image datasets necessary for subsequent DL. Pathologists are looking forward to a gold standard technology to process pathological images.

ML applications in radiology are designed to help computers identify medical imaging data and support diagnosis by associating with clinical data, such as treatment or outcome. These radiomics techniques can predict diseases with higher accuracy than human eyes. Using ML to recognize and analyze image data will fundamentally change our understanding of disease risk

and treatment. ML can also use the image information that human eyes can't recognize, so as to find new disease patterns and predictive markers.

At present, it is very popular to find cancer biomarkers through omics research. Because of the large data set, people need to use advanced information technology (such as machine learning technology) to analyze and understand the data. ML has been applied to mass spectrometry (MS) data from different biological disciplines, particularly for various cancers. ML can be useful in determining which proteins, from MS data, could be used as biomarkers to differentiate between samples of different classes. Metabolomics can also be considered as a method complementary to proteomics. ML is the most useful for the interpretation of large genomic data sets and has been used to annotate a wide variety of genomic sequence elements, in the process, to identify potentially valuable disease biomarkers.

### **Then, how about ML application in urological research?**

For prostate cancer (PC) many technology platforms for diagnosis, prognosis, and treatment demonstrated the potential benefits of ML. In diagnostic imaging, ML can read cross-sectional radiographic images reproducibly and rapidly to make a diagnosis. The ML methods described for diagnostic imaging can be extended to treatment planning and interventions by augmenting the surgeon's display with information such as cancer localization and other image-guided interventions. Computer-assisted diagnosis of PC in histopathological slides could be achieved by ML in order to optimize accuracy. ML method is also used in genomics research. By identifying specific genes or genes, we can develop diagnostic and risk stratification tools, determine the best individualized treatment methods and generate targeted drug treatment schemes.

ML can read radiological / pathological images of bladder cancer to provide diagnostic, treatment and prognostic information. Some studies have shown that by using ML model to analyze MRI data of bladder cancer, low-grade and high-grade bladder cancer can be identified before operation, with an accuracy of 83%. ML-based methods have been further applied to accurately quantify tumor buds from immunofluorescence-labeled slides of muscle-invasive bladder cancer (MIBC) patients. ML algorithms have been employed to create recurrence and survival predictive models from imaging and operative data. ML algorithms used to identify genes at initial presentation that are most predictive of recurrence can be applied as molecular signatures to predict the risk of recurrence within 5 years after TURB<sup>133</sup>.

More and more ML technology has been used to analyze the clinical and imaging data of renal cell carcinoma to provide doctors with disease diagnosis, prognosis information and help to make treatment plans. Previous studies have shown that ML model can accurately distinguish high-grade and low-grade renal clear cell carcinoma by analyzing CT image features<sup>133</sup>. In recent years, identifying biomarkers and multiple gene expression-based signatures by ML have been developed to predict survival and disease prognosis in ccRCC. Moreover, some studies have demonstrated that noninvasive ML and DL models constructed from radionics features have comparable performance to percutaneous renal biopsy in predicting the International Society of Urological Pathology (ISUP) grading.

ML has been also applied in various modalities of urinary stone therapy. Computer-assisted detection using image features can support radiologists in identifying stones. With multiple layers on large datasets, artificial neural networks (ANN) can predict outcomes after various forms of endourologic intervention. ANN has been used to differentiate ureteral stones from phleboliths in thin slice CT volumes due to their similarity in shape and intensity. ANN also can be used for the early detection of kidney stone type and most influential parameters to provide a decision-support system. The model resulted in 97.1% accuracy for predicting kidney stone type. Recently, ML

algorithms have been used to predict treatment success after a single-session shock wave lithotripsy (SWL) in ureteral stone patients.

Furthermore, ML can be applied to benign bladder diseases, such as overactive bladder (OAB) syndrome<sup>134</sup>. A ML model using a random forest-based algorithm was studied to identify patients for whom anticholinergic medications are likely to fail. A validated ML prediction model can predict the treatment failure of a 3 months standard anticholinergic treatment experiment, and the accurate rate is more than 80%.

### **How ML will be evolved in tomorrow's urology?**

In today's fast-moving technologically enhanced world, ML is still in its evolution. The steps needed to integrate ML into the clinic are still unknown. How the new algorithms will influence the diagnosis and management of our patients remains our decision. Future research should focus on the construction of larger medical databases and further development of AI techniques. The predictive precision of ML will continue to provide and enhance personalized medicine with the further inclusion of data and model retraining. There are limitless future applications for artificial intelligence in the field of urology.

## **ACHIEVEMENT 7:**

### **Research Progress of Urine Biomarkers in the Diagnosis, Treatment, and Prognosis of Bladder Cancer**

#### **1 Introduction**

##### **1.1 Bladder cancer (BC) incidence, epidemiology, and risk factors**

Bladder cancer (BC) is the fourth most common cancer in the U.S. and the second most common cancer of the urinary system, accounting for 7% of all new cancer cases. It also accounts for 4% of all cancer-related deaths in the U.S., ranking it the fifth deadliest cancer. The male to female ratio of morbidity and mortality was about 3:1 [1]. Risk factors are related to the environment, diet, and lifestyle, especially smoking, exposure to aromatic amines, and genetic factors [2-4]. Other known risk factors include the ingestion of high levels of arsenic or significant usage of pain relievers containing finazepine [4, 5].

##### **1.2 Economic burden of BC**

The European Organization for Research and Treatment of Cancer (EORTC) has established recommended plans for low to moderate-risk BC patients. This involves a cystoscopy every three months during the first two years, every four months during the following two years, and once a year thereafter [6]. Because BC treatment is continuous, the lifetime cost of treatment and monitoring increases with time. Studies have shown that the cumulative cost of health insurance for long-term survivors (those over 16 years) is \$172,426 [7]. As a result of this need for lifelong monitoring, the cost per patient when treating BC is the highest of all other cancers [8].

##### **1.3 Classical Classification of BC**

Based on the degree of invasion in the bladder muscle wall, BC is divided into either non-muscle invasive BC (NMIBC) or muscle invasive BC (MIBC) [9]. There may be different genetic variation underlying the difference between the two types of BC [10]. When histologically subtyping BC, there are several types. Transitional cell carcinoma (TCC), also known as urothelial carcinoma, accounts for about 90% of all BC. Squamous cell carcinoma (SCC) and adenocarcinoma account for about 10% [11]. There are various other rare types of BC as well [12]. BC can also be divided pathologically into low-grade (LG) and high-grade (HG) tumors. LG tumors are usually well-differentiated, while HG tumors are poorly differentiated [13].

##### **1.4 Molecular phenotyping of BC**

Recent genome mRNA expression analysis demonstrated that BC can be classified into molecular subtypes. These different subtypes of BC have distinct progression patterns, biological and clinical properties, and response to chemotherapies. There are currently five published classification methods; these include guidelines from the University of North Carolina (UNC), MD Anderson Cancer Center (MDA), The Cancer Genome Atlas (TCGA), Lund University (Lund), and Broad Institute of Massachusetts Institute of Technology and Harvard University (Broad) (Table 1)

The classifications by UNC define two molecular subtypes of high-grade BC, “luminal” and “basal”, with molecular features reflecting different stages of urothelial differentiation [14]. Luminal BC expresses terminal urothelial differentiation markers, such as those seen in umbrella cells (UPK1B, UPK2, UPK3A, and KRT20), whereas basal BC expresses high levels of genes that are typical in urothelial basal cells (KRT14, KRT5, and KRT5B). The UNC study created a gene signature, BASE47, that accurately discriminates intrinsic bladder subtypes. Identified basal

tumors had significantly decreased disease-specific and overall survival. In addition, among the clinicopathological features available in the MSKCC dataset, only subtypes identified by BASE47 were found to be significant in disease-specific survival by univariate analysis. This study also found that females have an increased incidence of basal-like BC, which is associated with a worse prognosis.

The classification system by MDA identified three molecular subtypes of MIBC: “basal”, “luminal”, and “P53-like” [15]. Basal MIBC was associated with shorter disease-specific and overall survival, presumably because these patients tend to have more invasive and metastatic disease at presentation. Transcription factor P63 plays a central role in controlling basal gene signatures and preliminary data suggests that EGFR, Stat-3, NFκB, and Hif-1α are also involved. Luminal MIBC displays active ER/TRIM24 pathway gene expression and were enriched for FOXA1, GATA3, ERBB2, and ERBB3. Luminal MIBC contains active PPAR gene expression and activating FGFR3 mutations; thereby, PPARγ- and FGFR-3-targeted agents may be active in this subtype. Because luminal MIBC responds well to neoadjuvant chemotherapy (NAC), targeted therapies should be combined with conventional chemotherapy for maximum efficacy. The P53-like MIBC responded very poorly to NAC and were consistently resistant to frontline neoadjuvant cisplatin-based combination chemotherapy. Additionally, comparative analysis of matches gene expression profiles before and after chemotherapy revealed that all resistant tumors expressed wild-type P53 gene expression signatures. These results indicate that “P53-ness” may play a central role in BC chemoresistance.

The classification by TCGA identified four clusters (clusters I–IV) by analyzing RNA-seq data from 129 tumors [16]. Cluster I (papillary-like) is enriched in tumors with papillary morphology, FGFR3 mutations, FGFR3 copy number gain, and elevated FGFR3 expression. Cluster I samples also had significantly lower expression of miR-99a, miR-100, miR-145 and miR-125b. Tumors with FGFR3 alterations and those that share similar cluster I expression profiles may respond well to inhibitors of FGFR and its downstream targets. Clusters I and II express high levels of GATA3 and FOXA1. Markers of urothelial differentiation, such as uroplakins, epithelial marker E-cadherin, and members of miR-200 miRNAs are also highly expressed in clusters I and II. Clusters I and II express high HER2 levels and an elevated estrogen receptor beta signaling signature, which suggests potential targets for hormone therapies, such as tamoxifen or raloxifene. Cluster III (basal/squamous-like) express characteristic epithelial lineage genes, including KRT14, KRT5, KRT6A, and EGFR. Many of the samples in cluster III express cytokeratins (KRT14 and KRT5). Integrated expression profiling analysis of cluster III revealed a urothelial carcinoma subtype with cancer stem-cell expression features, perhaps providing another avenue for therapeutic targeting.

The Lund classification system defines five major urothelial carcinoma subtypes: urobasal A, genomically unstable, urobasal B, squamous cell carcinoma-like (SCC-like), and infiltrated tumor class [17]. This was established using gene expression profiles from 308 tumor cases. These different molecular subtypes show significantly different prognosis. The best prognosis is the urobasal A, and the worst prognosis are urobasal B and SCC-like. The prognosis of genomically unstable and infiltrated class are between them. Urobasal A tumors were characterized by elevated expression of FGFR3, CCND1, TP63, as well as expression of KRT5 in cells at the tumor–stroma interface. The majority of urobasal A tumors were non-muscle invasive and of low pathologic grade. The genomically unstable subtype was characterized by expression of ERBB2 and CCNE, low expression of cytokeratin, and frequent mutations of TP53. Genomically unstable cases represented a high-risk group, as close to 40% were MIBC. This subtype also showed low PTEN expression. The SCC-like subtype was characterized by high expression of basal keratins, which are normally not expressed in the urothelium; these include KRT4, KRT6A, KRT6B, KRT6C, KRT14, and KRT16. SCC-like tumors also had markedly bad prognoses. Furthermore, this group showed a comparatively different proportion of female/male patients, reminiscent of the 1:1 proportion seen in patients diagnosed with bladder SCC, suggesting that females are more likely



to develop urothelial carcinomas with a keratinized/squamous phenotype, which is associated with an adverse prognosis. Urobasal B tumors showed several similarities to urobasal A tumors, such as a high FGFR3 mutation frequency, elevated FGFR3, CCND1, and TP63 levels, and expression of the FGFR3 gene signature. However, this group also showed frequent TP53 mutations and expression of several keratins specific for the SCC-like subtype. Additionally, 50% of the cases were MIBC; including 5 of 9 FGFR3 mutated cases. The infiltrated subtype demonstrated a pronounced immunologic and extracellular membrane (ECM) signal, indicating the presence of immunologic and myofibroblast cells. This subtype most likely represents a heterogeneous class of tumors; immunohistochemistry (IHC) revealed the presence of tumors with genomically unstable, urobasal B, and SCC-like protein expression patterns in this group.

The Broad classification identified four different subtypes: luminal, immune undifferentiated, luminal immune, and basal[18]. Approximately 41% of invasive BC was in the luminal subtype, with high expression of KRT20 and UPKs 2/1A/1B/3A as well as moderate to high expression of multiple pertinent transcription factors (KLF5, PPARG, and GRHL5). The luminal subtype was enriched for in male patients, papillary histology, and stage II tumors. A third (29%) of invasive BC was in the basal subtype, with high expression of KRT14, KRT5, KRT6A/B, and KRT16, and low expression of uroplakins, which is consistent with basal or undifferentiated cytokeratin expression patterns. Consistent with prior studies, the basal subtype expressed TP63, TP73, MYC, EGFR, TGM1, and SCEL, which is indicative of some degree of squamous differentiation. The basal subtype was enriched in female patients and tumors with nonpapillary histology. The basal subtype also expressed many immune genes at intermediate and somewhat variable levels. These genes include CTLA4 and CD274, which encodes for PD-L1, suggesting that there may be immune cell infiltration of tumors. A smaller percentage of cancers (11%) were grouped into a novel subtype called immune undifferentiated. These cancers showed very low expression of luminal markers, variable expression of basal cytokeratins, and relatively high expression of immune genes, including CTLA4 and CD274, which further suggests significant immune cell infiltration and possible immune evasion. Lastly, the luminal immune subtype group constitutes about 18% of all cases and is characterized by the expression of luminal genes (cytokeratins and uroplakins) and intermediate expression of immune genes. This group was notably enriched for stage N+ tumors. The luminal subtype was enriched for in cancers with FGFR3 mutations and amplification events involving PVRL4 and YWHAZ. The basal subtype was enriched for NFE2L2 mutations. Both the luminal immune and immune undifferentiated subtypes had high expression levels of ZEB1, ZEB2, and TWIST1, which is characteristic of epithelial-mesenchymal transition (EMT).

Gottfrid et al. proposed five major tumor-cell phenotypes in advanced BC: urothelial-like, genomically unstable (GU), basal/SCC-like, mesenchymal-like, and small-cell/neuroendocrine-like[19]. Urothelial-like tumors express FGFR3 and CCND1 and frequently demonstrate a loss of 9p21 (CDKN2A). GU tumors express FOXM1, but not KRT5, and frequently show loss of RB1. Basal/SCC-like tumors were found to express KRT5 and KRT14, but not FOXA1 and GATA3. The mesenchymal-like BC is a new subtype that shows a tumor-cell phenotype that starkly contrasts with previously defined subtypes and is biologically different from the basal/SCC-like cases that they are clustered with. The tumor cells are mesenchymal-like and express typical mesenchymal genes, such as ZEB2 and VIM. The tumor cells were themselves mesenchymal-like and expressed the typical mesenchymal genes ZEB2 and VIM. The consensus cluster Sc/NE-like turned out to harbor two very distinct tumor-cell phenotypes. One-half of these tumors expressed markers that are typical for neuroendocrine differentiation. This part of the Sc/NE consensus cluster also showed an absence of PPARG, FOXA1, and GATA3 expression, as well as of uroplakin and KRT20 expression.

Kardos et al. reported the discovery of a claudin-low molecular subtype of high-grade BC that shares characteristics with the homonymous subtype of breast cancer[20]. Although there has



been much work done on the molecular phenotyping of BC, the different emphases of different classification methods have made it difficult to consolidate a widely accepted classification method. As a result, the molecular phenotyping of BC remains to be further studied. The claudin-low subtype can be considered a subpopulation of the basal-like subtype (UNC classification system). Claudin-low bladder tumors are rich in a variety of genetic characteristics, including increased mutation rates of RB1, EP300, and NCOR1, increased the frequency of EGFR amplification, decreased mutation rates of FGFR3, ELF3, and KDM6A, and decreased the frequency of PPARG amplification. These characteristics define a molecular subtype of BC with distinct molecular features and an immunological profile that is theoretically primed for an immunotherapeutic response.

**Figure 1** summarizes the classification of BC.

**Table 1. Different classifications of BC based on molecular phenotyping. This table does not contain classifications based on Gottfrid’s research.**

UNC	MDA	Lund	TCGA	Broad
Basal	Basal	UroA	Cluster I	Basal
Luminal	Luminal	UroB	Cluster II	Luminal
	P53-like	GU	Cluster III	Luminal immune
		SCCL	Cluster IV	immune undifferentiated
		Infiltrated		

## 2 Biomarker Discovery in BC

More than 75% of patients are diagnosed and treated for NMIBC. At the time of initial evaluation, its recurrence rate can be as high as 70%[\[21\]](#). Currently, the standard and most important examination method for BC is cystoscopy, However, this procedure is invasive, uncomfortable, and expensive[\[22\]](#). Furthermore, cystoscopy may miss certain lesions, particularly smaller areas of carcinoma in situ[\[23\]](#). Molecular biosignatures indicative of altered cellular landscapes and functions have been casually linked to pathological conditions, suggesting the promise of BC-specific biomarkers. However, a noninvasive biomarker that is as sensitive and specific as standard cystoscopy has yet to be discovered. As we progress through the 21<sup>st</sup> century, we now have access to a number of ways to analyze diagnostic markers in-depth. The evolution of omics platforms and bioinformatics to allow for analysis of the genome, epigenome, transcriptome, proteome, lipidome, metabolome et al. enables the development of more sensitive biomarkers. These discoveries will broaden understanding of the complex biology and pathophysiology of bladder diseases, which can then be clinically translated. Biomarkers of interest can be detected in different types of samples, including serum, tissue, and urine. Urinary biomarkers are particularly attractive due to cost, time, and minimal effort. As a result, studies on urinary BC biomarkers continue to expand.

**Figure 2** shows the overview of the multi-OMICS strategies for urine-based biomarker discovery and translational application.

## 2.1 Proteomics-based BC biomarkers

In patients with hematuria, aurora A kinase (AURKA) can discriminate low-grade BC patients vs. normal patients [24]. After adjusting for patients, clinical features, and treatment with Bacillus Calmette-Guerin, the activated leukocyte cell adhesion molecule (ALCAM) is positively correlated with tumor stage and overall survival (OS) [25]. Nicotinamide N-methyltransferase has been shown to be elevated in BC patients and is correlated with histological grade [26]. Apurinic/aprimidinic endonuclease 1/redox factor-1 (APE/Ref-1) levels are higher in BC, with respect to non-BC, and is correlated with tumor grade and stage; moreover, it has been shown to be significantly increased in patients with historical BC recurrence [27]. The urinary cytokeratin-20 (CK20) RT-PCR assay shows that the sensitivity of urothelial BC detection was 78-87%, and the specificity was 56-80%, with improved diagnostic accuracy in tumor progression [28]. However, its performance is relatively poor in low-grade tumors. Higher urinary levels of CK8 and CK18 have been detected via UBC Rapid Test in high vs. low-grade BC [29].

There are multiple markers that can potentially be used for BC detection; increased urinary levels of apolipoproteins, A1, A2, B, C2, C3, and E (APOA1, APOA2, APOB, APOC2, APOC3, APOE) were found in BC compared to healthy controls [30, 31]. A signature of 4 urinary fragments of uromodulin, collagen  $\alpha$ -1 (I), collagen  $\alpha$ -1 (III), and membrane-associated progesterone receptor component 1 may be able to discriminate MIBC from NMIBC [32]. Other panels employ IL-8, MMP-9/10, ANG, APOE, SDC-1,  $\alpha$ 1AT, PAI-1, VEGFA, and CA9 to indicate BC from urine samples. The advantage of these multi-urinary protein biomarkers is evident in high and low-grade and high and low-stage diseases [33]. Combined with urine markers, including midkine (MDK), MDK, synuclein G, CEACAM1, ZAG2 [34], clusterin (CLU) and angiogenin (ANG), the sensitivity and specificity of NMIBC diagnosis can be improved through immunoassay and urine cytology [35]. CK20 and insulin-like growth factor II (IGF-II) levels were found to be increased in the urine sediments of NMIBC patients compared to controls [36]. Increased levels of urinary HAI-1 and epithelial cell adhesion molecule (EpCAM) are prognostic biomarkers in high-risk NMIBC patients [37]. Urine survivin have been proved by chemiluminescence enzyme immunoassay that it is a potential biomarker for BC, which has been shown to be related to tumor stage, lymph node metastasis, and distant metastasis. [38]. Snail overexpression represents an independent prognostic factor for tumor recurrence in NMIBC [39]. CD44 in urine was found to be elevated in high-grade MIBC by glycan-affinity glycoproteomics nanoplateforms. [40].

Proteomics-based BC biomarkers were summarized in **Table 2**.

## 2.2 Metabolomics-based BC biomarkers

Urinary metabolomics signature may be useful in detecting early stage BC. Jin X et al. analyzed urinary metabolites by high-performance liquid chromatography-quadrupole time-of-flight mass spectrometry (HPLC-QTOFMS), and found 12 metabolites that help to identify BC. [41]. Zhou Y et al. developed a urinary pseudotargeted method based on gas chromatography-mass spectrometry (GC-MS) which has been validated by a BC metabolomics study [42]. Using binary logistic regression analysis, a four-biomarker panel was defined for the diagnosis of BC. The results revealed that the urinary four-biomarker panel can be used to diagnose NMIBC or low-grade BC. Among the four metabolites, cholesterol levels were significantly increased in the BC group, while 5-hydroxyvaleric acid, 3-phosphoglyceric acid, and glycolic acid levels were markedly decreased in the BC group.

X. Cheng et al. carried out a study based on metabolomics with liquid chromatography-high resolution mass spectrometry (LC-HRMS) to discover novel biomarkers for detecting early-stage

BC. [43]. A total of 284 subjects were enrolled in the study including 117 healthy adults and 167 BC patients. Metabolite panels are known to have more predictive power than a single metabolite [44]. A metabolite panel consisting of dopamine 4-sulfate, MG00/1846Z,9Z,12Z,15Z/00, aspartyl-histidine, and tyrosyl-methionine was found to have the best predictive accuracy in diagnosing NMIBC.

**Table 2. Summary of proteomics-based BC biomarkers**

Sample s	Proteins	Reference s
urine	AURKA	24
	ALCAM	25
	Nicotinamide N-methyltransferase	26
	APE/Ref-1	27
	CK20	28
	CK8, CK18	29
	APOA1, APOA2, APOB, APOC2, APOC3, APOE	30,31
	uromodulin, collagen $\alpha$ -1 (I), collagen $\alpha$ -1 (III), and membrane-associated progesterone receptor component 1	32
	IL-8, MMP-9/10, ANG, APOE, SDC-1, $\alpha$ 1AT, PAI-1, VEGFA, and CA9	33
	midkine (MDK), synuclein G or MDK, ZAG2, CEACAM1 and angiogenin, clusterin	34,35
	CK20, IGFII	36
	HAI-1, Epcam	37
	survivin	38
Snail	39	
CD44	40	

A study by Yumba Mpanga A et al. developed and validated an analytical method for the simultaneous quantitative determination of metabolites using reversed phase high-performance liquid chromatography coupled with triple quadrupole mass spectrometry (RP-HPLC-QQQ/MS)[45]. The optimized and validated method was applied to urine samples from 40 BC patients and 40 healthy matched controls. Statistical analysis was done using the Student's t-test or U-Mann Whitney test. This identified 10 compounds that participate in different metabolic pathways, such as gut flora metabolism, RNA degradation, purine metabolism, etc., as being significantly different in urine between BC and control groups ( $p < 0.05$ ). These 10 compounds

include acetyllysine, N-acetylneuraminic acid, pseudouridine, uridine, xanthine, 7-methylguanine, gluconic acid, glucuronic acid, 1,7 dimethylxanthine, and hippuric acid. Moreover, acid trehalose, nicotinic acid, and AspAspGlyTrp peptide were upregulated; inosinic acid, ureidosuccinic acid, and GlyCysAlaLys peptide were downregulated in BC, but not in healthy controls[46].

Metabolomics-based BC biomarkers were summarized in **Table 3**.

**Table 3. Summary of metabolomics-based BC biomarkers**

<b>Metabolites</b>	<b>Alteration</b>	<b>References</b>	
<i>Succinate</i>	↑	41	
<i>Pyruvate</i>	↑		
<i>Oxoglutarate</i>	↑		
<i>Carnitine</i>	↑		
<i>Phosphoenolpyruvate</i>	↑		
<i>Trimethyllysine</i>	↑		
<i>Melatonin</i>	↓		
<i>Isovalerylcarnitine</i>	↑		
<i>Glutaryl carnitine</i>	↓		
<i>Octenoylcarnitine</i>	↑		
<i>Decanoylcarnitine</i>	↑		
<i>Acetyl-CoA</i>	↑		
<i>Cholesterol</i>	↑		42
<i>5-hydroxyvaleric acid</i>	↓		
<i>3-phosphoglyceric acid</i>	↓		
<i>glycolic acid</i>	↓		
<i>dopamine 4-sulfate</i>	↑	43	
<i>MG00/1846Z,9Z,12Z,15Z/00</i>	↓		
<i>aspartyl-histidine</i>			
<i>tyrosyl-methionine</i>		45	
<i>acetyllysine</i>	↑		
<i>N-acetylneuraminic acid</i>	↑		
<i>pseudouridine</i>	↑		
<i>uridine</i>	↑		
<i>xanthine</i>	↑		
<i>7-methylguanine</i>	↑		
<i>gluconic acid</i>	↑		
<i>glucuronic acid</i>	↑		
<i>1,7 dimethylxanthine</i>	↓		
<i>hippuric acid</i>	↓		
<i>acid trehalose</i>	↑		46
<i>nicotinuric acid</i>	↑		
<i>AspAspGlyTrp peptide</i>	↑		

<i>inosinic acid</i>	↓	
<i>ureidosuccinic acid</i>	↓	
<i>GlyCysAlaLys peptide</i>	↓	

## 2.3 Genomics-based BC biomarkers

### 2.3.1 DNA methylation

Using urine sediments from BC patients, Sun and her group demonstrated that SOX-1, IRAK3, and Li-MET gene methylation status have higher recurrence predictivity than urine cytology and cystoscopy (80 vs. 35 vs. 15%, respectively) [47]. Methylated genes, such as those for APC and cyclin D2, were found to be significantly prevalent in the urine from malignant vs. benign cases[48]. Hypermethylation of the GSTP1 and RAR $\beta$ 2 and APC genes have been identified in the urine of BC patients[49]. Evaluation of Twist Family BHLH Transcription Factor 1 (TWIST1) and NID2 genes methylation status in urine has been shown to differentiate primary BC patients from controls with 90% sensitivity and 93% specificity[50]. Additionally, evaluation of the methylation status of NID2, TWIST1, CFTR, SALL3, and TWIST1 genes in urinary cells in combination with urine cytology has been found to increase sensitivity and have high negative predictive value in BC patients[51, 52]. Urinary methylation levels of POU4F2 and PCDH17 is able to distinguish BC from normal controls with 90% sensitivity and 94% specificity[53]. Promoter hypermethylation of HS3ST2, SEPTIN9, and SLIT2 combined with FGFR3 mutation showed 97.6% sensitivity and 84.8% specificity in the diagnosis, surveillance, and risk stratification of low- and high-risk NMIBC patients[54]. Lastly, the methylation status of p14ARF, p16INK4A, RASSf1A, DAPK, and APC has been found to be correlated with BC grade and stage[55].

### 2.3.2 miRNAs

Urinary levels of miR-146a-5p are significantly increased in high-grade BC[56]. MiR-126 urinary levels were found to be elevated in BC compared to healthy controls [57]. Low miR-200c expression has been shown to be correlated with tumor progression in NMIBC [58]. Chen et al. detected 74 miRNAs, of which 33 were upregulated and 41 were downregulated in BC compared to healthy patients; the most notable of these include let-7miR, mir-1268, miR-196a, miR-1, miR-100, miR-101, and miR-143[59]. By screening patients with negative cystoscopy, Eissa et al. identified miR-96 and miR-210 as being associated with BC[60]. MiR-125b, miR-30b, miR-204, miR-99a, and miR-532-3p were downregulated in the urine supernatant of BC patients[61]. MiR-9, miR-182, and miR-200b have been shown to be correlated with MIBC aggressiveness, recurrence-free, and overall survival (OS)[62]. MiR-145 distinguishes NMIBC from non-BC[63]. MiR-144-5p inhibits BC proliferation, affecting CCNE1, CCNE2, CDC25A, and PKMYT1 target genes[64]. Cell-free urinary miR-99a and miRNA-125b were found to be downregulated in the urine supernatants of BC patients (sensitivity 86.7%; specificity 81.1%)[65]. Urinary levels of miR-618 and miR-1255b-5p were increased in MIBC patients compared to healthy controls[66]. Whole genome analysis determined increased miR-31-5p, miR-191-5p and miR-93-5p levels in the urine of BC patients compared to controls[67].

Genomics-based BC biomarkers were shown in **Table 4**.

**Table 4. Summary of genomics-based BC biomarkers**

	<b>Biomarkers</b>	<b>Alteration</b>	<b>References</b>
<b>DNA Methylation</b>	SOX-1, IRAK3, and Li-MET		47
	APC and cyclin D2		48
	GSTP1 and RAR $\beta$ 2 and APC		49
	TWIST1 and NID2		50
	NID2 and TWIST1 or CFTR, SALL3 and TWIST1		51,52
	POU4F2 and PCDH17		53
	HS3ST2, SEPTIN9 and SLIT2		54
	p14ARF, p16INK4A, RASSF1A, DAPK, and APC tumor suppressor		55
<b>miRNAs</b>	miR-146a-5p	↑	56
	MiR-126	↑	57
	miR-200c	↓	58
	let-7miR, mir-1268, miR-196a, miR-1, miR-100, miR-101, and miR-143		59
	miR-96 and miR-210		60
	MiR-125b, miR-30b, miR-204, miR-99a, and miR-532-3p	↓	61
	MiR-9, miR-182 and miR-200b		62
	MiR-145		63
	MiR-144-5p		64
	miR-99a and miRNA-125b	↓	65
	miR-618 and miR-1255b-5p	↑	66
	miR-31-5p, miR-191-5p and miR-93-5p	↑	67

**Metabolomics and metabolic phenotypes of BC**

In biological research, the omics approach includes genomics, proteomics, and metabolomics. It probes physiological and malignant processes at the cellular and molecular levels; thereby, characterizing the global molecular quantity, structure, function, and dynamic changes within an organism. Although genomics and proteomics have helped subtype many cancers based on gene mutation or receptor status, considerable heterogeneity is observed in tumor behavior and patient outcome, even within a genomic subtype. This is due to the unique cellular processes and metabolic profiles that can only be elucidated through metabolomics [68]. Metabolomic analysis is less complex compared to genomics, transcriptomics, and proteomics due to fewer endpoints. Metabolomics measures the entire set of small molecule products of metabolic processes in a biological system. By focusing on the downstream products of genomic and proteomic processes, metabolomics summarizes the effects of other omics methods and most closely represents a system's phenotype [69].

Metabolomic studies are either untargeted, aiming to comprehensively include all measurable analytes without a prior hypothesis, or targeted, measuring only select predefined groups of metabolites [70]. Although untargeted studies deal with large complex data sets and carry the risk



of false positives due to multiple testing of variables, the advantage is that they are free from assumptions. Targeted studies, on the other hand, are hypothesis-driven and offer measurements of high precision and accuracy. In metabolomic biomarker research, targeted studies are often used to validate findings from prior untargeted studies [71].

The field of blood-based genomic and proteomic cancer biomarkers are more developed than that of urine-based metabolomics because blood is considered to be an active participant in biological processes unlike urine, which is a contrast to waste product. With the advancement of urine analysis technology, urinalysis techniques have improved considerably. There are a number of methods that now enable in-depth analysis of diagnostic markers. In particular, NMR and MS-based identification of urinary metabolites are powerful techniques that can potentially diagnose a number of conditions. At present, urine metabolomic biomarker studies are being primarily conducted by either NMR or MS. Both of these tools have their strengths and limitations. The major advantage of MS is its accuracy and specificity in regard to metabolite detection. MS is more accurate compared to NMR spectrometry; however, the analytes need to be separated for detection and assimilation. In contrast, NMR-based spectrometry is more expensive and has lower sensitivity, generally limited to less than 100 analytes in biological fluids. Furthermore, NMR does not require the segregation of analytes for detection. The major advantage of NMR is that samples are not destroyed and can actually be reused [72-74].

BC has profound metabolic abnormalities. Several altered metabolic pathways play a role in bladder tumorigenesis. As a result, metabolomics can contribute substantially to understanding the relevant alterations of catabolic and anabolic metabolic processes impaired in cancer through the identification of tumor-specific metabolic biomarkers with potential diagnostic, prognostic, or predictive value [75]. Metabolomic studies have already identified various metabolites of diverse pathways (glucose, lipid, amino acid, nucleotide metabolites) as probable BC biomarkers [76].

However, caution must be applied; clinical metabolic phenotypes (metabotypes) may be altered due to age, gender, diet, race, lifestyle, surgical intervention, and underlying pathophysiological conditions [77]. In the context of BC metabolomics, baseline characteristics, such as tumor stage and grade, hematuria (gross or micro), surgical interventions, and smoking habit should additionally be taken into consideration [78].

#### **4. Metabolomic Platforms**

Contrary to the genome or proteome, the human metabolome composition is still not fully defined. There are few research approaches, all of which have emerged in metabolome analysis; these include metabolic profiling, metabolic fingerprinting and metabolic footprinting [79].

Metabolic profiling is an example of a targeted approach, focusing on identifying and quantifying predetermined groups of metabolites with similar physicochemical properties (e.g., carbohydrates, amino acids, organic acids, nucleosides) or under the same biochemical pathway (e.g., glycolysis, gluconeogenesis,  $\beta$ -oxidation or citric acid cycle) [80]. Metabolic profiling is considered to be an extension of metabolite targeted analysis, which relies on analyzing a single compound or small subset of metabolites to determine the influence of the specific stimuli on metabolism. Metabolic fingerprinting is an untargeted approach that is not driven by any preliminary assumption and aims to define changes in the whole metabolome, which occurs at a specific state in the cell, tissue or organism. Therefore, the main purpose of metabolic fingerprinting is to identify and qualify as many possible metabolites in samples. Metabolic fingerprinting is frequently used in a comparative analysis of two subject groups (i.e., healthy vs disease, one disease vs another

disease), which makes it a promising tool in studies focused on disease diagnosis and prognosis[81]. Metabolic footprinting is often applied in microbiological or biotechnological studies. Compared to the other methods, this approach does not concern intracellular metabolites but focuses on compounds that are secreted or failed to be used by cells in specific media. Due to the close relationship between intracellular and extracellular metabolism, metabolic footprinting can provide an integrative interpretation of the metabolic network in a specific living system[82].

Due to both the physicochemical diversity of the metabolome and complexity of the biological systems, no single analytical platform is able to determine all metabolites present in complex biofluids. Therefore, numerous analytical platforms are commonly used in both targeted and untargeted metabolomic studies [83]. NMR or MS coupled with different separation techniques currently dominates in metabolomics. There are at least four major analytical platforms with proven utility for metabolomic applications: NMR, GC-MS, LC-MS, and LCECA [84]. Each of these platforms has specific advantages and disadvantages (**Table 5**).

Modern NMR makes it possible to perform rigorous structural analysis of many metabolites in crude extracts, cell suspensions, intact tissues, or whole organisms. Structural determination of known metabolites using various one-dimensional (1D) or 2D NMR methods is straight forward; in fact, de novo structural analysis of unanticipated or even unknown metabolites is also feasible. NMR has high throughput capability and is particularly capable of determining the structure of metabolites, including the location of isotope labeled atoms in different isotopes produced during stable isotope tracing studies [85-88]. As a result, metabolic pathways can now be systematically mapped by NMR with unprecedented speed. In summary, NMR offers essentially universal detection, excellent quantitative precision, and the potential for high-throughput (>100 samples/day is possible). NMR is an unbiased, robust, reproducible, non-destructive and selective analytical platform. In NMR analysis almost no sample pretreatment is required. However, the main disadvantages of this technique include low sensitivity and lack of analyte separation. Another disadvantage is its high initial cost; NMR instruments can cost well over a million dollars.

MS represents a universal, sensitive tool that can be used to characterize, identify, and quantify a large number of compounds in biological samples where metabolite concentrations may constitute a broad range[89]. Liquid chromatography coupled with mass spectrometry (LC-MS), gas chromatography coupled with mass spectrometry (GC-MS) or capillary electrophoresis coupled with mass spectrometry (CE-MS) has a significantly wider application in metabolome analysis[83].

GC, which employs high-resolution capillary columns and is combined with MS detection, is a powerful platform for determining the metabolome. GC-MS often employs either an electron impact (EI) or chemical ionization (CI) mode, which provides putative identification based on the highly reproducible mass spectra of metabolites and availability of universal structural and mass spectral libraries[90]. GC-MS can provide structural information (more informative if the compounds are present in existing libraries), reasonable quantitative precision, and high-throughput (>100 samples/day is possible). Sensitivity is at least 2 orders of magnitude higher than NMR. One limitation of GC-MS is its inability to study molecules that cannot be readily volatilized. Another limitation is its relatively low mass accuracy (unit resolution). GC-MS is a technique of choice for volatile and thermally stable analytes. Therefore, complex and time-consuming sample derivation is necessary; however, this can lead to undesirable metabolite loss. The recent development of multidimensional GC (GC x GC) has improved resolution, robustness, and sensitivity compared to conventional GC-MS.



LC-MS is the most suitable technique for analyzing non-volatile, thermally unstable, high or low-molecular-weight compounds with a wide polarity range. Most compounds can be analyzed by LC-MS. LC-MS is commonly used in the metabolomic analysis of various biofluids (urine, blood or tissue extracts)[91, 92]. One limitation of LC-MS is its relative difficulty in obtaining consistent quantitative precision. The development of the LC-NMR-MS systems combines the high-throughput capability of NMR with the high sensitivity and resolution of LC-MS[93, 94]. To improve the sensitivity of conventional LC-MS technique, nanoLC-MS was implemented in metabolomics studies[95, 96].

Compared to LC-MS or GC-MS, CE-MS is rarely applied in metabolomic studies. However, recent significant improvements have opened CE-MS application in metabolomics. This technique is particularly useful in analyzing highly polar ionogenic metabolites in biological fluids [97]. CE-MS is a suitable method for urinary metabolomic analysis, which can be performed with relatively minimal sample preparation. However, extensive research is also being conducted in applying CE-MS to serum metabolomics [98]. CE-MS is a technique dedicated to water-soluble and charged molecules, which makes it a highly complementary platform to other separation methods, like LC-MS or GC-MS. The main advantages of CE-MS include high resolution power and small sample or reagent requirements. Its main limitation is the unstable electroosmotic flow phenomenon, which can result in notable migration time shifts during analyses[99].

LCECA is ideal for studies on the tryptophan and tyrosine pathways that lead to monoamine neurotransmitters because many metabolites within these two pathways can be measured quantitatively with LCECA. The robust nature of this platform, its reproducibility, and sensitivity have been well described in a series of peer-reviewed publications[100-104]. Preliminary experiments described later in this review demonstrate the power and promise of electrochemistry-based platforms for metabolomics analysis in defining signatures for central nervous system (CNS) disorders and treatments. The LCECA system is extremely sensitive, perhaps 2–3 orders of magnitude higher than that of GC-MS, and displays strong run-to-run precision over long periods of time. The disadvantages include the lack of structural information and low throughput (12 samples/day is the most commonly used metabolomic configuration). The system can detect molecules, such as tyrosine and tryptophan metabolites, as well as antioxidants and oxidative damage products, but it is “blind” to other molecules, such as glucose, ketoglutarate, and most fatty acids.

**Table 5** shows the advantages and limitations of different metabolomics platforms.

**Table 5. Summary of the advantages and limitations of different metabolomics platforms**

	<b>STRENGTHS</b>	<b>DRAWBACKS</b>
NMR	Rapid	Lack of sensitivity
	reproducible	Multiplicity of the resonance
	Nondestructive	Difficulty of quantification-chemical noise and signal overlapping
	High-throughput	lack of an analyte separation component
	Minimal sample manipulation	high instrument cost (over one million dollars)
	Possible tissue analysis	
MS	High sensitivity	Low quantitation
	Wide detection range	Low reproducibility
	Easy metabolite	Destructive

	identification-databases availability	High sample volume requirements
GC-MS	Possibility to couple with separation techniques reasonable quantitative precision high throughput	Can't study nonvolatile molecules low mass accuracy (often unit resolution)
	low instrumentation costs (\$100–\$300,000) High sensitivity	undesirable metabolite losses
LC-MS	volatile and thermally stable analytes high flexibility	high instruments cost(\$100,000-over one million dollars) difficulty in obtaining consistent quantitative precision
	tailor separations to the compounds enable low, medium, or high mass accuracy Can trade off sensitivity for throughput Can determine the exact molecular composition	
CE-MS	various biofluids analytes highly polar ionogenic metabolites analytes minimal sample preparation high resolution power	notable migration time shift during analyses
LCECA	extremely sensitive strong run-to-run precision high specificity (tryptophan and tyrosine pathways)	lack of structural information low throughput low cost (under \$100,000)

## 5. Metabolomics in BC Diagnosis and Prognosis and Predicting Response to Therapies

BC has profound metabolic anomalies that play central roles in tumor progression[105]. Metabolic pathways, such as the tricarboxylic acid (TCA) cycle, lipid synthesis, amino acid synthesis, nucleotide synthesis, and glycolysis pathway, are known to be increased in BC tissue compared to adjacent benign tissue[106].

### a. Tricarboxylic acid cycle

A significant decrease in citrate concentration was consistently observed in the urine and serum of BC patients[107]. One possible explanation for this is the active uptake of citrate from the extracellular medium into the tumor cell [108]. Citrate is important for lipid biosynthesis, which is crucial for tumor proliferation [109]. Therefore, the decrease in citrate levels in the urine or serum may illustrate the increased utilization of citrate in lipogenesis for the rapid proliferation of tumor cells[2].

### b. Lipid metabolism

Up or downregulation of carnitine species, including carnitine, carnitine C8:1, carnitine C9:0, carnitine C9:1, carnitine C10:1, carnitine C10:3, isobutyryl carnitine, acetylcarnitine, 2,6-dimethylheptanoylcarnitine, isovalerylcarnitine, glutarylcarnitine, and decanoylcarnitine, has been reported in BC[41, 110, 111]. The carnitine system plays a central role in lipid metabolism; it facilitates the entry of long-chain fatty acids into the mitochondria for utilization in energy-generating processes and removes short-chain and medium-chain fatty acids that accumulate as a byproduct[112]. It has been postulated that the dysregulation of lipid metabolism provides an environment that is beneficial to the development of BC. Additionally, altered fatty acid transportation, fatty acid  $\beta$ -oxidation, or energy metabolism might partially explain why BC patients are prone to lethargy[2].

### c. Amino acid metabolism

#### i. Glutathione metabolism

Elevated glutathione (GSH) level was reported in BC tissues and cell lines via metabolomic studies [2]. Oxidative stress results in elevated GSH and overexpression of antioxidant enzymes, such as glutathione peroxidase, glutathione reductase, and glutathione-S transferase[113]. While GSH is involved in the detoxification of carcinogens, its elevation in tumors may promote chemotherapy resistance in cancer cells via conjugation with pharmacologically active drugs or metabolites[114].

#### ii. Tryptophan metabolism

Upregulation of tryptophan metabolism in BC was observed with increased levels of anthranilic acid, N-acetylanthranilic acid, kynurenine, 3-hydroxykynurenine, and malonate[115-117]. The proposed underlying mechanisms include autoxidation and interaction with nitrite or transition metals to form reactive intermediates, binding as ligands to aryl hydrocarbon receptor (AHR) that plays a role in carcinogenesis[118]. Notably, Opitz et al. demonstrated that tryptophan-2,3-dioxygenase (TDO)-derived kynurenine suppresses antitumor immune responses and promotes tumor-cell survival through AHR, which in turn suggests TDO as a potential cancer therapeutic target[119].

### iii. Hippuric acid & taurine metabolism

Downregulation of hippuric acid was generally observed in BC patients and taurine was found to be elevated in BC patients compared to benign and healthy controls [107]. Taurine inactivates hypochlorous acid, which is a strong oxidant and cytotoxic agent, by forming stable taurine chloramine (Tau-Cl). In turn, Tau-Cl downregulates immunological responses via production of proinflammatory cytokines, leading to tumor progression [120].

### iv. Nucleotide metabolism

Purine and pyrimidine metabolism has been found to be perturbed in BC, leading to upregulation of guanine, hypoxanthine, cytidine monophosphate, thymine, uracil, uridine, and pseudouridine [111, 115]. Nucleosides, particularly modified nucleosides (e.g., pseudouridine), are elevated and suggested as potential biomarkers in various cancers [121]. Such elevation nucleoside levels have been postulated to be the result of increased DNA synthesis associated with enhanced cell cycle activity in cancer [122]. Modified nucleosides are excreted in urine because they cannot be recycled as nucleosides [123]. Thus, levels of modified nucleosides in urine reflect oxidative DNA damage and RNA turnover in the body.

### v. Glycolysis

Lactate, an important end product of glycolysis, was found to be elevated in BC tissue and urine [115, 124], indicating an increased rate of glycolysis rate. The upregulation of glycolysis, resulting in increased glucose consumption, is a universal phenomenon in cancer and is termed the “Warburg effect” [125, 126]. Gatenby and Gillies proposed that the upregulation of glycolysis is an adaptation of premalignant lesions to intermittent hypoxia, but requires evolution to the resultant proliferative and invasive phenotypes where resistance to acid-induced cell toxicity is also observed [125].

Diagnosis and prognosis of various diseases are enhanced by the identification of biomarkers, which can differentiate individuals with the disease from those without. Ideal markers are easily detectable in tissue, serum, and urine, and have a high sensitivity and specificity. There are several potential applications of metabolomics in BC and other cancers; this includes improving detection, providing prognostic information, and impacting treatment.

## 6. Clinically applicable BC biomarkers-based tools

At present, the FDA has approved six tests for detecting or monitoring BC. NMP22, NMP22 BladderChek, and UroVysion have FDA approval for BC diagnosis and surveillance; Immunocytology (uCyt+), BTA-TRAK, and BTA-STAT have been approved only for surveillance [127-131]. There are also many metabolites that can be considered as potential tumor biomarkers for BC.

By ultra-performance liquid chromatography time-of-flight mass spectrometry, imidazole-acetic acid was evidenced in BC [132]. A metabolite panel consisting of indolylacryloylglycine, N2-galacturonyl-L-lysine, and aspartyl-glutamate can discriminate high- vs. low-grade BC [133]. In addition, alterations in the metabolisms of phenylalanine, arginine, proline, and tryptophan were evidenced by UPLC-MS in NMBIC [134]. Jin X et al. confirmed through their study that carnitine

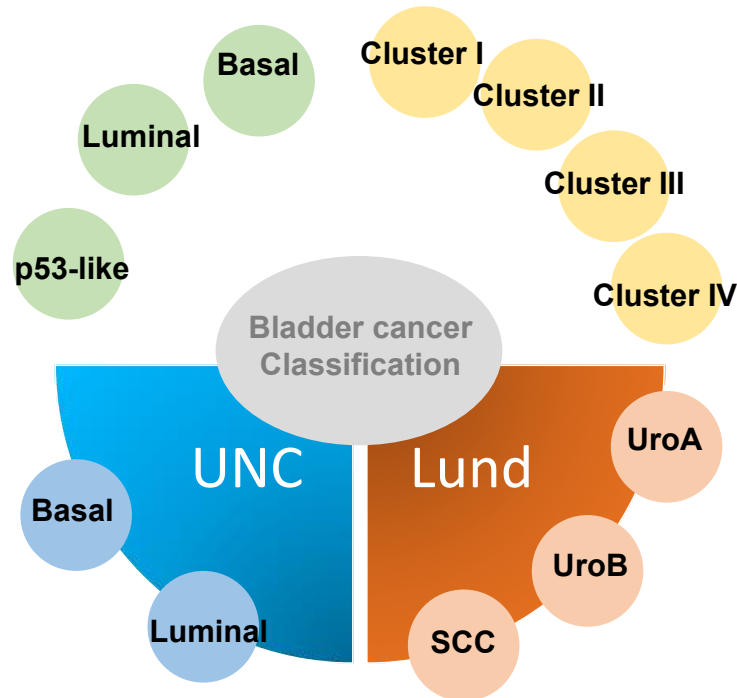
acyltransferase and pyruvate dehydrogenase complex expressions are significantly altered in cancer[41]. Alberice JV et al. propose that metabolites related to the tryptophan metabolism pathway, such as kynurenine and tryptophan, are potential urinary biomarkers and therapeutic targets of BC therapy[116]. Wittmann et al. performed unbiased metabolomics on a set of urine samples from BC patients, revealing nearly 1000 distinct metabolic signatures, of which 587 have a chemical identity[135]. The authors chose a set of 25 potential biomarkers from this group and tested this panel on a second independent cohort to validate its predictive power. A new group of metabolites, including lactate, adenosine, succinate, and palmitoyl sphingomyelin, were proposed as urinary biomarkers; thus, showing the involvement of lipid metabolism in BC progression.

## **7. Conclusions and Perspectives**

At present, there is much research on biomarkers of BC. Biomarkers can be identified in tissue, blood, urine, etc. and include genes, proteins, metabolites, etc. In this paper, we summarized the research progress of BC biomarkers in recent years. Due to the advantages of urine collection, including non-invasive procedures, simplicity, easy storage, low-cost, and direct contact with bladder cancer tissue, we focused particularly on urinary biomarker research progress. Compared to genomics and proteomics, metabonomics of BC is still in its early stages. However, because of the great progress in metabonomics research in BC using NMR, GC-MS, and LC-MS, metabonomics has been widely used to propose new biomarkers. These may be applied to screening, diagnosing, treating, evaluating, and monitoring BC. Although the potential of metabonomics to improve detection and treatment of BC may be great, the main limitation is the lack of reliable validation for a large population. Current research has so far been limited to smaller samples without validation and metabolites can be easily affected by various factors. For future metabonomics research, experimental design and analysis methods need to be standardized to eliminate the systemic influence of confounding variables on the measurement of metabolites, make results more comparable, verify potential biomarkers, and assist in clinical applications against BC.

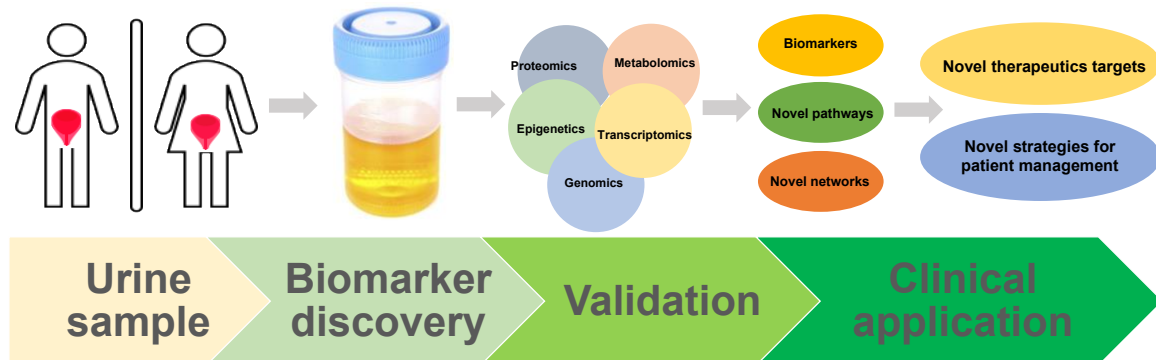
**Figure 1. Schematic illustration of molecular subtypes of bladder cancer.** Based on Whole-genome mRNA expression profiling, several molecular subtypes of muscle-invasive bladder cancer (MIBC) have been identified. Molecular subtypes of MIBC might have important implications for patient prognosis and response to conventional chemotherapy and targeted agents. Four groups have shown great similarities among tumor subtype. Lund, University of Lund; MDA, MD Anderson Cancer Center; TCGA, The Cancer Genome Atlas; UNC, University of North Carolina.

Figure 1



**Figure 2. Overview of the multi-OMICS strategies for urinary bladder cancer biomarker discovery and their clinical implication.** A typical integrated multi-omic technologies workflow showing to probe the complexity of bladder cancer biology. Integration of several of omics data sources use systems biology approach build biomarker discovery.

Figure 2



*If the project was not intended to provide training and professional development opportunities or there is nothing significant to report during this reporting period, state "Nothing to Report."*

*Nothing to Report*

**How were the results disseminated to communities of interest?**

*Nothing to Report*

**What do you plan to do during the next reporting period to accomplish the goals?**

In coming funding period, we will focus on quantification of levels of DNA methylation and gene expression for the IC diagnostic marker panel. We will further analyze patients' outcomes and construct a statistical model predicting the IC-associated pain severity and to evaluate its association with co-morbid conditions, patient-reported outcomes, and health-related quality of life.

**4. IMPACT:**

**What was the impact on the development of the principal discipline(s) of the project?**



- State-of-the-art technologies emerging from recent omics studies of urine specimens of IC, including the innovative concept that the urine plays an active role modulating bladder microenvironment as a reliable diagnostic biofluid, providing epigenetic resource associated with bladder pain.
- A robust statistical and machine learning model to obtain comprehensive mechanistic insights into the IC etiology
- Translating omics biomarkers into routine clinical diagnostics for IC risk will be aided by developing automatic quality controls and absolute quantifications for biomarkers in these panels by working with an industry partner who is committed to commercial development and clinical implementation of molecular tests.

**What was the impact on other disciplines?**

*Nothing to Report*

**What was the impact on technology transfer?**

*Nothing to Report*

**What was the impact on society beyond science and technology?**

*Nothing to Report*

**5. CHANGES/PROBLEMS:**

**Changes in approach and reasons for change**

*Nothing to Report*

**Actual or anticipated problems or delays and actions or plans to resolve them**

*Nothing to Report*

**Changes that had a significant impact on expenditures**

*Nothing to Report*

**Significant changes in use or care of human subjects, vertebrate animals, biohazards, and/or select agents**

**Significant changes in use or care of human subjects**

*Nothing to Report*

**Significant changes in use or care of vertebrate animals**

**Significant changes in use of biohazards and/or select agents**

*Nothing to Report*

**6. PRODUCTS:**

- **Publications, conference papers, and presentations**

- Journal publications.**

- **Publications since last funding period**

1. Shoemaker R, **Kim J.** (2021) Urobiome: An outlook on the metagenome of urological diseases, *Investig Clin Urol.* 62(6):611-622. doi: 10.4111/icu.20210312.PMID: 34729961
2. Lee RJ, Madan RA, **Kim J,** Posadas EM, Yu EY (2021) Disparities in cancer care and the Asian American population, *Oncologist*, Online ahead of print, PMID: 33683795, doi: 10.1002/onco.13748

3. Park S, Lee H-Y, **Kim J\***, Park H, Ju YS, Kim E-G, Kim J (2021) Cerebral cavernous malformation 1 determines YAP/TAZ signaling dependent metastatic hallmarks of prostate cancer cells, *Cancers*, 13(5):1125, \*, **co-first author** PMID: **33807895**, doi: 10.3390/cancers13051125, PMID: **33807895**
4. Laden BF, Bresee C, De Hoedt A, Scharfenberg A, Saxena R, Senechal JF, Barbour KE, **Kim J**, Freedland SJ, Anger JT (2021) Comorbidities in a Nationwide, Heterogenous Population of Veterans with Interstitial Cystitis/Bladder Pain Syndrome, *Urology*, S0090-4295(21)00343-5 PMID: **33901534**  
DOI: [10.1016/j.urology.2021.04.015](https://doi.org/10.1016/j.urology.2021.04.015)
5. Kim SJ, **Kim J**, Na YG, Kim KH (2021) Irreversible Bladder Remodeling Induced by Fibrosis, *Int Neurourol J*, 25(Suppl 1): S3-7, PMID: 34053205
6. **Kim J**, Yeon A, Parks S, Shahid M, Thiombane A\*, Cho E\*, You S, Emam H, Kim D-G, Kim M (2021) Alendronate-induced Perturbation of the Bone Proteome and Microenvironmental Pathophysiology, *International Journal of Medical Sciences*, 18(14):3261-3270. PMID: **34400895**, PMCID: [PMC8364444](https://pubmed.ncbi.nlm.nih.gov/PMC8364444/), DOI: [10.7150/ijms.61552](https://doi.org/10.7150/ijms.61552), \* **UCLA mentees**
7. Yang J S-W, Qian C, You S, Rotinen M, Posadas EM, Freedland SJ, Di Vizio D, **Kim J**, Freeman MR (2021) Scaffold attachment factor B1 regulates androgen degradation pathways in prostate cancer, *Am J Clin Exp Urol* 2021;9(4):337-349. PMID: 34541032
8. Eun SJ, **Kim J**, Kim KH (2021) Applications of artificial intelligence in urological setting: a hopeful path to improved care. *J Exerc Rehabil*. 2021 Oct 26;17(5):308-312. doi: [10.12965/jer.2142596.298](https://doi.org/10.12965/jer.2142596.298). PMID: 34805018
9. **Kim J\***, Yeon A, Kim W-K, Kim K-H, Ohn T. (2021) Stress-Induced Accumulation of HnRNP K into Stress Granules, \* corresponding author, *Journal of Cancer Science and Clinical Therapeutics*, 2021; 5 (4): 434-447
10. Dallas KB, Bresee C, De Hoedt A, Senechal JF, Barbour KE, **Kim J**, Freedland SJ, Anger JT. (2021) Demographic Differences and Disparities in the Misdiagnosis of Interstitial Cystitis/Bladder Pain Syndrome in a National Cohort of VA Patients. *Urology*, S0090-4295(21)00709-3. doi: [10.1016/j.urology.2021.07.019](https://doi.org/10.1016/j.urology.2021.07.019), PMID: **34348123**

11. Yin LY, Li Q, Mrdenovic S, Chu G, Wu B, Bu H, Duan P, **Kim J**, You S, Lewis M, Liang G, Wang R, Zhau H, Chung LWK (2022) KRT13 promotes stemness and drives metastasis in breast cancer through a plakoglobin/c-Myc signaling pathway. *Breast Cancer Res.* 24(1):7. doi: 10.1186/s13058-022-01502-6. PMID: 35078507
12. Dubinskaya A, Tholemeier LN, Erickson T, De Hoedt AM, Barbour KE, **Kim J**, Freedland SJ, Anger JT. (2022) Prevalence of Overactive Bladder Symptoms Among Women With Interstitial Cystitis/Bladder Pain Syndrome. *Female Pelvic Med Reconstr Surg.* 28(3):e115-e119. doi: 10.1097/SPV.0000000000001166. PMID: 35272344
13. Tholemeier LN, Bresee C, De Hoedt AM, **Kim J**, Freedland S, Anger JT. (2022) Do medication prescription patterns follow guidelines in a cohort of women with Interstitial Cystitis/Bladder Pain Syndrome? *Neurourol Urodyn*, doi: 10.1002/nau.24923
14. Anger J, Dallas KB, Bresee C, De Hoedt A, Barbour KE, Hoggatt K, Goodman MT, Kim J, Freedland S. National Prevalence of IC/BPS in Women and Men Utilizing Veterans Health, *Administration Data Frontiers In Pain Research*
15. Cho H, Tong F, You S, Jung S, Kim WH, Kim J (2022) Prediction of the Immune Phenotypes of Bladder Cancer Patients for Precision Oncology, *IEEE Open Journal of Engineering in Medicine and Biology*, VOLUME 3, 47-57, Print ISSN: 2644-1276, Digital Object Identifier 10.1109/OJEMB.2022.3163533

**Peer-Reviewed (Submitted)**

1. Masterson JM, Castaneda PR, **Kim J** (2022) PATHOPHYSIOLOGY AND CLINICAL BIOMARKERS IN INTERSTITIAL CYSTITIS, *Urologic Clinics of North America* (Invited paper, in review)

**Books or other non-periodical, one-time publications.**

1. Jin F, Shahid M, Kim J. Research Progress of Urine Biomarkers in the Diagnosis, Treatment, and Prognosis of Bladder Cancer, *Springer, Nature, Translational Urinomics*, Advances in Experimental Medicine and Biology 1306, [https://doi.org/10.1007/978-3-030-63908-2\\_5](https://doi.org/10.1007/978-3-030-63908-2_5)  
<https://www.springer.com/gp/book/9783030639075>  
**acknowledgement of federal support (yes).**

**Other publications, conference papers and presentations.**

*Nothing to Report*

**Website(s) or other Internet site(s)**

*Nothing to Report*

**Technologies or techniques**

*Nothing to Report*

**Inventions, patent applications, and/or licenses**

*Nothing to Report*

## Other Products

*Nothing to Report*

## 7. PARTICIPANTS & OTHER COLLABORATING ORGANIZATIONS

What individuals have worked on the project?

Name: *Mary Smith*  
Project Role: *Graduate Student*  
Researcher Identifier (e.g. ORCID ID): *1234567*  
Nearest person month worked: *5*

Contribution to Project: *Ms. Smith has performed work in the area of combined error-control and constrained coding.*

Funding Support: *The Ford Foundation (Complete only if the funding support is provided from other than this award.)*



Name:	Jayoung Kim
Project Role:	PI <i>no change</i>
Name:	Jennifer Anger
Project Role:	Co-Investigator <i>no change</i>
Name:	Catherine Breese
Project Role:	Co-Investigator <i>no change</i>
Name:	Muhammad Shahid
Project Role:	Post-doctoral fellow <i>no change</i>

**Has there been a change in the active other support of the PD/PI(s) or senior/key personnel since the last reporting period?**

**What other organizations were involved as partners?**

*Nothing to Report*

*Describe partner organizations – academic institutions, other nonprofits, industrial or commercial firms, state or local governments, schools or school systems, or other organizations (foreign or domestic) – that were involved with the project.*

*Nothing to Report*

**8. SPECIAL REPORTING REQUIREMENTS**

**COLLABORATIVE AWARDS:**

**QUAD CHARTS:**

**9. APPENDICES:**

## REFERENCE

- 1 Siegel, R. L., Miller, K. D. & Jemal, A. Cancer statistics, 2018. *CA Cancer J Clin* **68**, 7-30, doi:10.3322/caac.21442 (2018).
- 2 Abrams, P. *et al.* The standardisation of terminology of lower urinary tract function: report from the Standardisation Sub-committee of the International Continence Society. *Am J Obstet Gynecol* **187**, 116-126, doi:10.1067/mob.2002.125704 (2002).
- 3 Choe, J. H. *et al.* Prevalence of painful bladder syndrome/interstitial cystitis-like symptoms in women: a population-based study in Korea. *World J Urol* **29**, 103-108, doi:10.1007/s00345-010-0536-4 (2011).
- 4 Temml, C. *et al.* Prevalence and correlates for interstitial cystitis symptoms in women participating in a health screening project. *Eur Urol* **51**, 803-808; discussion 809, doi:10.1016/j.eururo.2006.08.028 (2007).
- 5 Patnaik, S. S. *et al.* Etiology, pathophysiology and biomarkers of interstitial cystitis/painful bladder syndrome. *Arch Gynecol Obstet* **295**, 1341-1359, doi:10.1007/s00404-017-4364-2 (2017).
- 6 Berry, S. H. *et al.* Prevalence of symptoms of bladder pain syndrome/interstitial cystitis among adult females in the United States. *The Journal of urology* **186**, 540-544, doi:10.1016/j.juro.2011.03.132 (2011).
- 7 Zhu, F. *et al.* Gene mutation detection of urinary sediment cells for NMIBC early diagnose and prediction of NMIBC relapse after surgery. *Medicine (Baltimore)* **98**, e16451, doi:10.1097/MD.00000000000016451 (2019).
- 8 van Rhijn, B. W. *et al.* FGFR3 and P53 characterize alternative genetic pathways in the pathogenesis of urothelial cell carcinoma. *Cancer Res* **64**, 1911-1914 (2004).
- 9 Ecke, T. H., Sachs, M. D., Lenk, S. V., Loening, S. A. & Schlechte, H. H. TP53 gene mutations as an independent marker for urinary bladder cancer progression. *Int J Mol Med* **21**, 655-661 (2008).
- 10 Goebell, P. J., Groshen, S. G., Schmitz-Drager, B. J. & International Study-Initiative on Bladder, C. p53 immunohistochemistry in bladder cancer--a new approach to an old question. *Urol Oncol* **28**, 377-388, doi:10.1016/j.urolonc.2010.03.021 (2010).
- 11 Malats, N. *et al.* P53 as a prognostic marker for bladder cancer: a meta-analysis and review. *Lancet Oncol* **6**, 678-686, doi:10.1016/S1470-2045(05)70315-6 (2005).
- 12 Sidransky, D. *et al.* Identification of p53 gene mutations in bladder cancers and urine samples. *Science* **252**, 706-709, doi:10.1126/science.2024123 (1991).
- 13 Traczyk-Borszynska, M. *et al.* Genetic diversity of urinary bladder cancer and the risk of recurrence based on mutation analysis. *Neoplasma* **63**, 952-960, doi:10.4149/neo\_2016\_614 (2016).
- 14 Junker, K. *et al.* Fibroblast growth factor receptor 3 mutations in bladder tumors correlate with low frequency of chromosome alterations. *Neoplasia* **10**, 1-7, doi:10.1593/neo.07178 (2008).
- 15 van Rhijn, B. W. *et al.* Molecular grade (FGFR3/MIB-1) and EORTC risk scores are predictive in primary non-muscle-invasive bladder cancer. *Eur Urol* **58**, 433-441, doi:10.1016/j.eururo.2010.05.043 (2010).
- 16 Ploussard, G. *et al.* The prognostic value of FGFR3 mutational status for disease recurrence and progression depends on allelic losses at 9p22. *Am J Cancer Res* **1**, 498-507 (2011).
- 17 Rebouissou, S. *et al.* CDKN2A homozygous deletion is associated with muscle invasion in FGFR3-mutated urothelial bladder carcinoma. *J Pathol* **227**, 315-324, doi:10.1002/path.4017 (2012).
- 18 Fernandez-Medarde, A. & Santos, E. Ras in cancer and developmental diseases. *Genes Cancer* **2**, 344-358, doi:10.1177/1947601911411084 (2011).
- 19 Beukers, W., Hercegovic, A. & Zwarthoff, E. C. HRAS mutations in bladder cancer at an early age and the possible association with the Costello Syndrome. *Eur J Hum Genet* **22**,

- 837-839, doi:10.1038/ejhg.2013.251 (2014).
- 20 Knowles, M. A., Habuchi, T., Kennedy, W. & Cuthbert-Heavens, D. Mutation spectrum of the 9q34 tuberous sclerosis gene TSC1 in transitional cell carcinoma of the bladder. *Cancer Res* **63**, 7652-7656 (2003).
- 21 Knowles, M. A., Platt, F. M., Ross, R. L. & Hurst, C. D. Phosphatidylinositol 3-kinase (PI3K) pathway activation in bladder cancer. *Cancer Metastasis Rev* **28**, 305-316, doi:10.1007/s10555-009-9198-3 (2009).
- 22 Pymar, L. S., Platt, F. M., Askham, J. M., Morrison, E. E. & Knowles, M. A. Bladder tumour-derived somatic TSC1 missense mutations cause loss of function via distinct mechanisms. *Hum Mol Genet* **17**, 2006-2017, doi:10.1093/hmg/ddn098 (2008).
- 23 Goebell, P. J. & Knowles, M. A. Bladder cancer or bladder cancers? Genetically distinct malignant conditions of the urothelium. *Urol Oncol* **28**, 409-428, doi:10.1016/j.urolonc.2010.04.003 (2010).
- 24 Solomon, D. A. *et al.* Frequent truncating mutations of STAG2 in bladder cancer. *Nat Genet* **45**, 1428-1430, doi:10.1038/ng.2800 (2013).
- 25 Aquila, L., Ohm, J. & Woloszynska-Read, A. The role of STAG2 in bladder cancer. *Pharmacol Res* **131**, 143-149, doi:10.1016/j.phrs.2018.02.025 (2018).
- 26 Guo, G. *et al.* Whole-genome and whole-exome sequencing of bladder cancer identifies frequent alterations in genes involved in sister chromatid cohesion and segregation. *Nat Genet* **45**, 1459-1463, doi:10.1038/ng.2798 (2013).
- 27 Balbas-Martinez, C. *et al.* Recurrent inactivation of STAG2 in bladder cancer is not associated with aneuploidy. *Nat Genet* **45**, 1464-1469, doi:10.1038/ng.2799 (2013).
- 28 Taylor, C. F., Platt, F. M., Hurst, C. D., Thygesen, H. H. & Knowles, M. A. Frequent inactivating mutations of STAG2 in bladder cancer are associated with low tumour grade and stage and inversely related to chromosomal copy number changes. *Hum Mol Genet* **23**, 1964-1974, doi:10.1093/hmg/ddt589 (2014).
- 29 Lelo, A. *et al.* STAG2 Is a Biomarker for Prediction of Recurrence and Progression in Papillary Non-Muscle-Invasive Bladder Cancer. *Clin Cancer Res* **24**, 4145-4153, doi:10.1158/1078-0432.CCR-17-3244 (2018).
- 30 Carbone, M. *et al.* BAP1 and cancer. *Nat Rev Cancer* **13**, 153-159, doi:10.1038/nrc3459 (2013).
- 31 Lin, M. *et al.* Common, germline genetic variations in the novel tumor suppressor BAP1 and risk of developing different types of cancer. *Oncotarget* **8**, 74936-74946, doi:10.18632/oncotarget.20465 (2017).
- 32 Segovia, C. *et al.* Opposing roles of PIK3CA gene alterations to EZH2 signaling in non-muscle invasive bladder cancer. *Oncotarget* **8**, 10531-10542, doi:10.18632/oncotarget.14453 (2017).
- 33 Duenas, M. *et al.* PIK3CA gene alterations in bladder cancer are frequent and associate with reduced recurrence in non-muscle invasive tumors. *Mol Carcinog* **54**, 566-576, doi:10.1002/mc.22125 (2015).
- 34 Beukers, W. *et al.* FGFR3, TERT and OTX1 as a Urinary Biomarker Combination for Surveillance of Patients with Bladder Cancer in a Large Prospective Multicenter Study. *J Urol* **197**, 1410-1418, doi:10.1016/j.juro.2016.12.096 (2017).
- 35 Holyoake, A. *et al.* Development of a multiplex RNA urine test for the detection and stratification of transitional cell carcinoma of the bladder. *Clin Cancer Res* **14**, 742-749, doi:10.1158/1078-0432.CCR-07-1672 (2008).
- 36 Park, H. S. *et al.* Quantitation of Aurora kinase A gene copy number in urine sediments and bladder cancer detection. *J Natl Cancer Inst* **100**, 1401-1411, doi:10.1093/jnci/djn304 (2008).
- 37 Urquidi, V., Goodison, S., Cai, Y., Sun, Y. & Rosser, C. J. A candidate molecular biomarker panel for the detection of bladder cancer. *Cancer Epidemiol Biomarkers Prev* **21**, 2149-2158, doi:10.1158/1055-9965.EPI-12-0428 (2012).
- 38 Bongiovanni, L. *et al.* Bradeion (SEPT4) as a urinary marker of transitional cell bladder

- cancer: a real-time polymerase chain reaction study of gene expression. *J Urol* **187**, 2223-2227, doi:10.1016/j.juro.2012.01.031 (2012).
- 39 Friedrich, M. G. *et al.* Comparison of multitarget fluorescence in situ hybridization in urine with other noninvasive tests for detecting bladder cancer. *BJU Int* **92**, 911-914 (2003).
- 40 Sarosdy, M. F. *et al.* Clinical evaluation of a multi-target fluorescent in situ hybridization assay for detection of bladder cancer. *J Urol* **168**, 1950-1954, doi:10.1097/01.ju.0000034254.89258.8e (2002).
- 41 Bollmann, M., Heller, H., Bankfalvi, A., Griefingholt, H. & Bollmann, R. Quantitative molecular urinary cytology by fluorescence in situ hybridization: a tool for tailoring surveillance of patients with superficial bladder cancer? *BJU Int* **95**, 1219-1225, doi:10.1111/j.1464-410X.2005.05509.x (2005).
- 42 Kipp, B. R. *et al.* Monitoring intravesical therapy for superficial bladder cancer using fluorescence in situ hybridization. *J Urol* **173**, 401-404, doi:10.1097/01.ju.0000149825.83180.a4 (2005).
- 43 Hanke, M. *et al.* A robust methodology to study urine microRNA as tumor marker: microRNA-126 and microRNA-182 are related to urinary bladder cancer. *Urol Oncol* **28**, 655-661, doi:10.1016/j.urolonc.2009.01.027 (2010).
- 44 Puerta-Gil, P. *et al.* miR-143, miR-222, and miR-452 are useful as tumor stratification and noninvasive diagnostic biomarkers for bladder cancer. *Am J Pathol* **180**, 1808-1815, doi:10.1016/j.ajpath.2012.01.034 (2012).
- 45 Yamada, Y. *et al.* MiR-96 and miR-183 detection in urine serve as potential tumor markers of urothelial carcinoma: correlation with stage and grade, and comparison with urinary cytology. *Cancer Sci* **102**, 522-529, doi:10.1111/j.1349-7006.2010.01816.x (2011).
- 46 Wang, G. *et al.* Expression of microRNAs in the urine of patients with bladder cancer. *Clin Genitourin Cancer* **10**, 106-113, doi:10.1016/j.clgc.2012.01.001 (2012).
- 47 Eissa, S. *et al.* Measurement of Urinary Level of a Specific Competing endogenous RNA network (FOS and RCAN mRNA/ miR-324-5p, miR-4738-3p, /lncRNA miR-497-HG) Enables Diagnosis of Bladder Cancer. *Urol Oncol* **37**, 292 e219-292 e227, doi:10.1016/j.urolonc.2018.12.024 (2019).
- 48 Chen, X. MiR-101 acts as a novel bio-marker in the diagnosis of bladder carcinoma. *Medicine (Baltimore)* **98**, e16051, doi:10.1097/MD.00000000000016051 (2019).
- 49 Soloway, M. S. *et al.* Use of a new tumor marker, urinary NMP22, in the detection of occult or rapidly recurring transitional cell carcinoma of the urinary tract following surgical treatment. *J Urol* **156**, 363-367, doi:10.1097/00005392-199608000-00008 (1996).
- 50 Miyake, M. *et al.* Influencing factors on the NMP-22 urine assay: an experimental model. *BMC Urol* **12**, 23, doi:10.1186/1471-2490-12-23 (2012).
- 51 Wang, Z. *et al.* Evaluation of the NMP22 BladderChek test for detecting bladder cancer: a systematic review and meta-analysis. *Oncotarget* **8**, 100648-100656, doi:10.18632/oncotarget.22065 (2017).
- 52 Guo, A. *et al.* Bladder tumour antigen (BTA stat) test compared to the urine cytology in the diagnosis of bladder cancer: A meta-analysis. *Can Urol Assoc J* **8**, E347-352, doi:10.5489/cuaj.1668 (2014).
- 53 Glas, A. S. *et al.* Tumor markers in the diagnosis of primary bladder cancer. A systematic review. *J Urol* **169**, 1975-1982, doi:10.1097/01.ju.0000067461.30468.6d (2003).
- 54 Chakraborty, A., Dasari, S., Long, W. & Mohan, C. Urine protein biomarkers for the detection, surveillance, and treatment response prediction of bladder cancer. *Am J Cancer Res* **9**, 1104-1117 (2019).
- 55 Li, H. *et al.* Identification of Apo-A1 as a biomarker for early diagnosis of bladder transitional cell carcinoma. *Proteome Sci* **9**, 21, doi:10.1186/1477-5956-9-21 (2011).
- 56 Li, C. *et al.* Discovery of Apo-A1 as a potential bladder cancer biomarker by urine proteomics and analysis. *Biochem Biophys Res Commun* **446**, 1047-1052, doi:10.1016/j.bbrc.2014.03.053 (2014).
- 57 Chen, Y. T. *et al.* Discovery of novel bladder cancer biomarkers by comparative urine

- proteomics using iTRAQ technology. *J Proteome Res* **9**, 5803-5815, doi:10.1021/pr100576x (2010).
- 58 Cai, Q. *et al.* Urine BLCA-4 exerts potential role in detecting patients with bladder cancers: a pooled analysis of individual studies. *Oncotarget* **6**, 37500-37510, doi:10.18632/oncotarget.6061 (2015).
- 59 Eissa, S., Matboli, M., Essawy, N. O. & Kotb, Y. M. Integrative functional genetic-epigenetic approach for selecting genes as urine biomarkers for bladder cancer diagnosis. *Tumour Biol* **36**, 9545-9552, doi:10.1007/s13277-015-3722-6 (2015).
- 60 Pham, H. T., Block, N. L. & Lokeshwar, V. B. Tumor-derived hyaluronidase: a diagnostic urine marker for high-grade bladder cancer. *Cancer Res* **57**, 778-783 (1997).
- 61 Gourin, C. G., Zhi, W. & Adam, B. L. Proteomic identification of serum biomarkers for head and neck cancer surveillance. *Laryngoscope* **119**, 1291-1302, doi:10.1002/lary.20279 (2009).
- 62 Yang, H. H. *et al.* Lipoprotein(a) level and its association with tumor stage in male patients with primary lung cancer. *Clin Chem Lab Med* **47**, 452-457, doi:10.1515/CCLM.2009.094 (2009).
- 63 Goodison, S., Chang, M., Dai, Y., Urquidi, V. & Rosser, C. J. A multi-analyte assay for the non-invasive detection of bladder cancer. *PLoS One* **7**, e47469, doi:10.1371/journal.pone.0047469 (2012).
- 64 Frantzi, M. & Vlahou, A. Ten Years of Proteomics in Bladder Cancer: Progress and Future Directions. *Bladder Cancer* **3**, 1-18, doi:10.3233/BLC-160073 (2017).
- 65 Urquidi, V. *et al.* CCL18 in a multiplex urine-based assay for the detection of bladder cancer. *PLoS One* **7**, e37797, doi:10.1371/journal.pone.0037797 (2012).
- 66 Magalhaes, T. F., Baracat, E. C., Doumouchsis, S. K. & Haddad, J. M. Biomarkers in the diagnosis and symptom assessment of patients with bladder pain syndrome: a systematic review. *Int Urogynecol J*, doi:10.1007/s00192-019-04075-9 (2019).
- 67 Tonyali, S. *et al.* Urine nerve growth factor (NGF) level, bladder nerve staining and symptom/problem scores in patients with interstitial cystitis. *Adv Clin Exp Med* **27**, 159-163, doi:10.17219/acem/69231 (2018).
- 68 Corcoran, A. T. *et al.* Mapping the cytokine profile of painful bladder syndrome/interstitial cystitis in human bladder and urine specimens. *World J Urol* **31**, 241-246, doi:10.1007/s00345-012-0852-y (2013).
- 69 Vera, P. L. *et al.* Elevated Urine Levels of Macrophage Migration Inhibitory Factor in Inflammatory Bladder Conditions: A Potential Biomarker for a Subgroup of Interstitial Cystitis/Bladder Pain Syndrome Patients. *Urology* **116**, 55-62, doi:10.1016/j.urology.2018.02.039 (2018).
- 70 Lamale, L. M., Lutgendorf, S. K., Zimmerman, M. B. & Kreder, K. J. Interleukin-6, histamine, and methylhistamine as diagnostic markers for interstitial cystitis. *Urology* **68**, 702-706, doi:10.1016/j.urology.2006.04.033 (2006).
- 71 Keay, S. *et al.* Antiproliferative factor, heparin-binding epidermal growth factor-like growth factor, and epidermal growth factor in men with interstitial cystitis versus chronic pelvic pain syndrome. *Urology* **63**, 22-26, doi:10.1016/j.urology.2003.08.024 (2004).
- 72 Byrne, D. S. *et al.* The urinary glycoprotein GP51 as a clinical marker for interstitial cystitis. *J Urol* **161**, 1786-1790, doi:10.1097/00005392-199906000-00010 (1999).
- 73 Pasikanti, K. K. *et al.* Urinary metabotyping of bladder cancer using two-dimensional gas chromatography time-of-flight mass spectrometry. *J Proteome Res* **12**, 3865-3873, doi:10.1021/pr4000448 (2013).
- 74 Pasikanti, K. K. *et al.* Noninvasive urinary metabonomic diagnosis of human bladder cancer. *J Proteome Res* **9**, 2988-2995, doi:10.1021/pr901173v (2010).
- 75 Wittmann, B. M. *et al.* Bladder cancer biomarker discovery using global metabolomic profiling of urine. *PLoS One* **9**, e115870, doi:10.1371/journal.pone.0115870 (2014).
- 76 Srivastava, S. *et al.* Taurine - a possible fingerprint biomarker in non-muscle invasive bladder cancer: A pilot study by 1H NMR spectroscopy. *Cancer Biomark* **6**, 11-20,

- doi:10.3233/CBM-2009-0115 (2010).
- 77 Huang, Z. *et al.* Bladder cancer determination via two urinary metabolites: a biomarker pattern approach. *Mol Cell Proteomics* **10**, M111 007922, doi:10.1074/mcp.M111.007922 (2011).
- 78 Jin, X. *et al.* Diagnosis of bladder cancer and prediction of survival by urinary metabolomics. *Oncotarget* **5**, 1635-1645, doi:10.18632/oncotarget.1744 (2014).
- 79 Liu, X. *et al.* Investigation of the urinary metabolic variations and the application in bladder cancer biomarker discovery. *Int J Cancer* **143**, 408-418, doi:10.1002/ijc.31323 (2018).
- 80 Parker, K. S. *et al.* Urinary Metabolomics Identifies a Molecular Correlate of Interstitial Cystitis/Bladder Pain Syndrome in a Multidisciplinary Approach to the Study of Chronic Pelvic Pain (MAPP) Research Network Cohort. *EBioMedicine* **7**, 167-174, doi:10.1016/j.ebiom.2016.03.040 (2016).
- 81 Esteller, M. Epigenetics in cancer. *N Engl J Med* **358**, 1148-1159, doi:10.1056/NEJMra072067 (2008).
- 82 Kim, W. J. & Kim, Y. J. Epigenetic biomarkers in urothelial bladder cancer. *Expert Rev Mol Diagn* **9**, 259-269, doi:10.1586/erm.09.5 (2009).
- 83 Besaratinia, A., Cockburn, M. & Tommasi, S. Alterations of DNA methylome in human bladder cancer. *Epigenetics* **8**, 1013-1022, doi:10.4161/epi.25927 (2013).
- 84 Kandimalla, R., van Tilborg, A. A. & Zwarthoff, E. C. DNA methylation-based biomarkers in bladder cancer. *Nat Rev Urol* **10**, 327-335, doi:10.1038/nrurol.2013.89 (2013).
- 85 Chan, M. W. *et al.* Hypermethylation of multiple genes in tumor tissues and voided urine in urinary bladder cancer patients. *Clin Cancer Res* **8**, 464-470 (2002).
- 86 Friedrich, M. G. *et al.* Detection of methylated apoptosis-associated genes in urine sediments of bladder cancer patients. *Clin Cancer Res* **10**, 7457-7465, doi:10.1158/1078-0432.CCR-04-0930 (2004).
- 87 Hoque, M. O. *et al.* Quantitation of promoter methylation of multiple genes in urine DNA and bladder cancer detection. *J Natl Cancer Inst* **98**, 996-1004, doi:10.1093/jnci/djj265 (2006).
- 88 Renard, I. *et al.* Identification and validation of the methylated TWIST1 and NID2 genes through real-time methylation-specific polymerase chain reaction assays for the noninvasive detection of primary bladder cancer in urine samples. *Eur Urol* **58**, 96-104, doi:10.1016/j.eururo.2009.07.041 (2010).
- 89 Abern, M. R., Owusu, R. & Inman, B. A. Clinical performance and utility of a DNA methylation urine test for bladder cancer. *Urol Oncol* **32**, 51 e21-56, doi:10.1016/j.urolonc.2013.08.003 (2014).
- 90 Fantony, J. J. *et al.* Multi-institutional external validation of urinary TWIST1 and NID2 methylation as a diagnostic test for bladder cancer. *Urol Oncol* **33**, 387 e381-386, doi:10.1016/j.urolonc.2015.04.014 (2015).
- 91 Reinert, T. *et al.* Comprehensive genome methylation analysis in bladder cancer: identification and validation of novel methylated genes and application of these as urinary tumor markers. *Clin Cancer Res* **17**, 5582-5592, doi:10.1158/1078-0432.CCR-10-2659 (2011).
- 92 Reinert, T. *et al.* Diagnosis of bladder cancer recurrence based on urinary levels of EOMES, HOXA9, POU4F2, TWIST1, VIM, and ZNF154 hypermethylation. *PLoS One* **7**, e46297, doi:10.1371/journal.pone.0046297 (2012).
- 93 Su, S. F. *et al.* A panel of three markers hyper- and hypomethylated in urine sediments accurately predicts bladder cancer recurrence. *Clin Cancer Res* **20**, 1978-1989, doi:10.1158/1078-0432.CCR-13-2637 (2014).
- 94 Yu, J. *et al.* A novel set of DNA methylation markers in urine sediments for sensitive/specific detection of bladder cancer. *Clin Cancer Res* **13**, 7296-7304, doi:10.1158/1078-0432.CCR-07-0861 (2007).
- 95 Brait, M. *et al.* Aberrant promoter methylation of multiple genes during pathogenesis of bladder cancer. *Cancer Epidemiol Biomarkers Prev* **17**, 2786-2794, doi:10.1158/1055-



- 9965.EPI-08-0192 (2008).
- 96 Costa, V. L. *et al.* Three epigenetic biomarkers, GDF15, TMEFF2, and VIM, accurately predict bladder cancer from DNA-based analyses of urine samples. *Clin Cancer Res* **16**, 5842-5851, doi:10.1158/1078-0432.CCR-10-1312 (2010).
- 97 van der Heijden, A. G. *et al.* Urine cell-based DNA methylation classifier for monitoring bladder cancer. *Clin Epigenetics* **10**, 71, doi:10.1186/s13148-018-0496-x (2018).
- 98 Bradley, M. S. *et al.* A genome-scale DNA methylation study in women with interstitial cystitis/bladder pain syndrome. *NeuroUrol Urodyn* **37**, 1485-1493, doi:10.1002/nau.23489 (2018).
- 99 Kim, Y. J. & Kim, W. J. Can we use methylation markers as diagnostic and prognostic indicators for bladder cancer? *Investig Clin Urol* **57 Suppl 1**, S77-88, doi:10.4111/icu.2016.57.S1.S77 (2016).
- 100 Hanno, P., Keay, S., Moldwin, R. & Van Ophoven, A. International Consultation on IC - Rome, September 2004/Forging an International Consensus: progress in painful bladder syndrome/interstitial cystitis. Report and abstracts. *International urogynecology journal and pelvic floor dysfunction* **16 Suppl 1**, S2-S34, doi:10.1007/s00192-005-1301-x (2005).
- 101 Nordling, J. *et al.* Primary evaluation of patients suspected of having interstitial cystitis (IC). *European urology* **45**, 662-669, doi:10.1016/j.eururo.2003.11.021 (2004).
- 102 Hanno, P. M. *et al.* AUA guideline for the diagnosis and treatment of interstitial cystitis/bladder pain syndrome. *J Urol* **185**, 2162-2170, doi:10.1016/j.juro.2011.03.064 (2011).
- 103 Urinology Think Tank Writing, G. Urine: Waste product or biologically active tissue? *NeuroUrol Urodyn* **37**, 1162-1168, doi:10.1002/nau.23414 (2018).
- 104 Wen, H. *et al.* Urinary metabolite profiling combined with computational analysis predicts interstitial cystitis-associated candidate biomarkers. *J Proteome Res* **14**, 541-548, doi:10.1021/pr5007729 (2015).
- 105 Kind, T. *et al.* Interstitial Cystitis-Associated Urinary Metabolites Identified by Mass-Spectrometry Based Metabolomics Analysis. *Sci Rep* **6**, 39227, doi:10.1038/srep39227 (2016).
- 106 Shahid, M. *et al.* Menthol, a unique urinary volatile compound, is associated with chronic inflammation in interstitial cystitis. *Sci Rep* **8**, 10859, doi:10.1038/s41598-018-29085-3 (2018).
- 107 Cahan, E. M., Hernandez-Boussard, T., Thadaney-Israni, S. & Rubin, D. L. Putting the data before the algorithm in big data addressing personalized healthcare. *NPJ Digit Med* **2**, 78, doi:10.1038/s41746-019-0157-2 (2019).
- 108 Tolles, J. & Meurer, W. J. Logistic regression: relating patient characteristics to outcomes. *Jama* **316**, 533-534 (2016).
- 109 Cortes, C. & Vapnik, V. Support-vector networks. *Machine learning* **20**, 273-297 (1995).
- 110 Platt, J. Sequential minimal optimization: A fast algorithm for training support vector machines. (1998).
- 111 Lin, Y., Lee, Y. & Wahba, G. Support vector machines for classification in nonstandard situations. *Machine learning* **46**, 191-202 (2002).
- 112 Tibshirani, R. Regression shrinkage and selection via the lasso. *Journal of the Royal Statistical Society: Series B (Methodological)* **58**, 267-288 (1996).
- 113 Ng, A. Y. in *Proceedings of the twenty-first international conference on Machine learning*. 78.
- 114 Vehtari, A., Gelman, A. & Gabry, J. Practical Bayesian model evaluation using leave-one-out cross-validation and WAIC. *Statistics and computing* **27**, 1413-1432 (2017).
- 115 Esteva, A. *et al.* A guide to deep learning in healthcare. *Nat Med* **25**, 24-29, doi:10.1038/s41591-018-0316-z (2019).
- 116 Miotto, R., Wang, F., Wang, S., Jiang, X. & Dudley, J. T. Deep learning for healthcare: review, opportunities and challenges. *Brief Bioinform* **19**, 1236-1246, doi:10.1093/bib/bbx044 (2018).

- 117 Zampieri, G., Vijayakumar, S., Yaneske, E. & Angione, C. Machine and deep learning meet genome-scale metabolic modeling. *PLoS Comput Biol* **15**, e1007084, doi:10.1371/journal.pcbi.1007084 (2019).
- 118 Bordbar, A., Monk, J. M., King, Z. A. & Palsson, B. O. Constraint-based models predict metabolic and associated cellular functions. *Nat Rev Genet* **15**, 107-120, doi:10.1038/nrg3643 (2014).
- 119 Cuperlovic-Culf, M. Machine Learning Methods for Analysis of Metabolic Data and Metabolic Pathway Modeling. *Metabolites* **8**, doi:10.3390/metabo8010004 (2018).
- 120 Angermueller, C., Parnamaa, T., Parts, L. & Stegle, O. Deep learning for computational biology. *Mol Syst Biol* **12**, 878, doi:10.15252/msb.20156651 (2016).
- 121 Min, S., Lee, B. & Yoon, S. Deep learning in bioinformatics. *Brief Bioinform* **18**, 851-869, doi:10.1093/bib/bbw068 (2017).
- 122 Vamathevan, J. *et al.* Applications of machine learning in drug discovery and development. *Nat Rev Drug Discov* **18**, 463-477, doi:10.1038/s41573-019-0024-5 (2019).
- 123 Jing, Y., Bian, Y., Hu, Z., Wang, L. & Xie, X. Q. Deep Learning for Drug Design: an Artificial Intelligence Paradigm for Drug Discovery in the Big Data Era. *AAPS J* **20**, 58, doi:10.1208/s12248-018-0210-0 (2018).
- 124 Klauschen, F. *et al.* Scoring of tumor-infiltrating lymphocytes: From visual estimation to machine learning. *Semin Cancer Biol* **52**, 151-157, doi:10.1016/j.semcancer.2018.07.001 (2018).
- 125 Baptista, D., Ferreira, P. G. & Rocha, M. Deep learning for drug response prediction in cancer. *Brief Bioinform*, doi:10.1093/bib/bbz171 (2020).
- 126 Tolios, A. *et al.* Computational approaches in cancer multidrug resistance research: Identification of potential biomarkers, drug targets and drug-target interactions. *Drug Resist Updat* **48**, 100662, doi:10.1016/j.drug.2019.100662 (2020).
- 127 Wong, N. C., Lam, C., Patterson, L. & Shayegan, B. Use of machine learning to predict early biochemical recurrence after robot-assisted prostatectomy. *BJU Int* **123**, 51-57, doi:10.1111/bju.14477 (2019).
- 128 Madhukar, N. S. *et al.* A Bayesian machine learning approach for drug target identification using diverse data types. *Nat Commun* **10**, 5221, doi:10.1038/s41467-019-12928-6 (2019).
- 129 Saeed, K. *et al.* Comprehensive Drug Testing of Patient-derived Conditionally Reprogrammed Cells from Castration-resistant Prostate Cancer. *Eur Urol* **71**, 319-327, doi:10.1016/j.eururo.2016.04.019 (2017).
- 130 Obermeyer, Z. & Emanuel, E. J. Predicting the Future - Big Data, Machine Learning, and Clinical Medicine. *N Engl J Med* **375**, 1216-1219, doi:10.1056/NEJMp1606181 (2016).
- 131 Kourou, K., Exarchos, T. P., Exarchos, K. P., Karamouzis, M. V. & Fotiadis, D. I. Machine learning applications in cancer prognosis and prediction. *Comput Struct Biotechnol J* **13**, 8-17, doi:10.1016/j.csbj.2014.11.005 (2015).
- 132 Komura, D. & Ishikawa, S. Machine learning approaches for pathologic diagnosis. *Virchows Arch* **475**, 131-138, doi:10.1007/s00428-019-02594-w (2019).
- 133 Suarez-Ibarrola, R., Hein, S., Reis, G., Gratzke, C. & Miernik, A. Current and future applications of machine and deep learning in urology: a review of the literature on urolithiasis, renal cell carcinoma, and bladder and prostate cancer. *World J Urol*, doi:10.1007/s00345-019-03000-5 (2019).
- 134 Sheyn, D. *et al.* Development and Validation of a Machine Learning Algorithm for Predicting Response to Anticholinergic Medications for Overactive Bladder Syndrome. *Obstet Gynecol* **134**, 946-957, doi:10.1097/AOG.0000000000003517 (2019).
- 135 Davis, N. F., Brady, C. M. & Creagh, T. Interstitial cystitis/painful bladder syndrome: epidemiology, pathophysiology and evidence-based treatment options. *Eur J Obstet Gynecol Reprod Biol* **175**, 30-37, doi:10.1016/j.ejogrb.2013.12.041 (2014).
- 136 Fall, M. *et al.* EAU guidelines on chronic pelvic pain. *Eur Urol* **57**, 35-48, doi:10.1016/j.eururo.2009.08.020 (2010).

- 137 Hanno, P. *et al.* Bladder Pain Syndrome Committee of the International Consultation on  
Incontinence. *Neurourol Urodyn* **29**, 191-198, doi:10.1002/nau.20847 (2010).
- 138 van de Merwe, J. P. *et al.* Diagnostic criteria, classification, and nomenclature for painful  
bladder syndrome/interstitial cystitis: an ESSIC proposal. *Eur Urol* **53**, 60-67,  
doi:10.1016/j.eururo.2007.09.019 (2008).
- 139 Akiyama, Y. *et al.* Molecular Taxonomy of Interstitial Cystitis/Bladder Pain Syndrome  
Based on Whole Transcriptome Profiling by Next-Generation RNA Sequencing of Bladder  
Mucosal Biopsies. *J Urol* **202**, 290-300, doi:10.1097/JU.000000000000234 (2019).
- 140 Peters, K. M., Killinger, K. A., Mounayer, M. H. & Boura, J. A. Are ulcerative and  
nonulcerative interstitial cystitis/painful bladder syndrome 2 distinct diseases? A study of  
coexisting conditions. *Urology* **78**, 301-308, doi:10.1016/j.urology.2011.04.030 (2011).
- 141 Seyhan, A. A. & Carini, C. Are innovation and new technologies in precision medicine  
paving a new era in patients centric care? *J Transl Med* **17**, 114, doi:10.1186/s12967-019-  
1864-9 (2019).
- 142 Clish, C. B. Metabolomics: an emerging but powerful tool for precision medicine. *Cold  
Spring Harb Mol Case Stud* **1**, a000588, doi:10.1101/mcs.a000588 (2015).
- 143 Kuehnbaum, N. L. & Britz-McKibbin, P. New advances in separation science for  
metabolomics: resolving chemical diversity in a post-genomic era. *Chem Rev* **113**, 2437-  
2468, doi:10.1021/cr300484s (2013).
- 144 Griffin, J. L. & Shockcor, J. P. Metabolic profiles of cancer cells. *Nat Rev Cancer* **4**, 551-  
561, doi:10.1038/nrc1390 (2004).
- 145 Vander Heiden, M. G. Targeting cancer metabolism: a therapeutic window opens. *Nat Rev  
Drug Discov* **10**, 671-684, doi:10.1038/nrd3504 (2011).
- 146 Pereira, M. M., Shori, D. K., Dormer, R. L. & McPherson, M. A. Studies on phosphorylation  
of calcineurin. *Biochem Soc Trans* **18**, 447, doi:10.1042/bst0180447 (1990).
- 147 Gatenby, R. A. & Gillies, R. J. Why do cancers have high aerobic glycolysis? *Nat Rev  
Cancer* **4**, 891-899, doi:10.1038/nrc1478 (2004).
- 148 Han, X. Lipidomics for studying metabolism. *Nat Rev Endocrinol* **12**, 668-679,  
doi:10.1038/nrendo.2016.98 (2016).
- 149 Lydic, T. A. & Goo, Y. H. Lipidomics unveils the complexity of the lipidome in metabolic  
diseases. *Clin Transl Med* **7**, 4, doi:10.1186/s40169-018-0182-9 (2018).
- 150 Blanksby, S. J. & Mitchell, T. W. Advances in mass spectrometry for lipidomics. *Annu Rev  
Anal Chem (Palo Alto Calif)* **3**, 433-465, doi:10.1146/annurev.anchem.111808.073705  
(2010).
- 151 Emwas, A. H. *et al.* NMR Spectroscopy for Metabolomics Research. *Metabolites* **9**,  
doi:10.3390/metabo9070123 (2019).
- 152 Fiehn, O. & Kim, J. Metabolomics insights into pathophysiological mechanisms of  
interstitial cystitis. *International neurology journal* **18**, 106-114,  
doi:10.5213/inj.2014.18.3.106 (2014).
- 153 Clemens, J. Q. *et al.* The MAPP research network: a novel study of urologic chronic pelvic  
pain syndromes. *BMC Urol* **14**, 57, doi:10.1186/1471-2490-14-57 (2014).
- 154 Fukui, Y., Kato, M., Inoue, Y., Matsubara, A. & Itoh, K. A metabonomic approach identifies  
human urinary phenylacetylglutamine as a novel marker of interstitial cystitis. *J  
Chromatogr B Analyt Technol Biomed Life Sci* **877**, 3806-3812,  
doi:10.1016/j.jchromb.2009.09.025 (2009).
- 155 Antoni, S. *et al.* Bladder Cancer Incidence and Mortality: A Global Overview and Recent  
Trends. *Eur Urol* **71**, 96-108, doi:10.1016/j.eururo.2016.06.010 (2017).
- 156 Nielsen, M. E. *et al.* Trends in stage-specific incidence rates for urothelial carcinoma of  
the bladder in the United States: 1988 to 2006. *Cancer* **120**, 86-95,  
doi:10.1002/cncr.28397 (2014).
- 157 Morales, A., Eidinger, D. & Bruce, A. W. Intracavitary Bacillus Calmette-Guerin in the  
treatment of superficial bladder tumors. *J Urol* **116**, 180-183, doi:10.1016/s0022-  
5347(17)58737-6 (1976).

- 158 Carosella, E. D., Ploussard, G., LeMaout, J. & Desgrandchamps, F. A Systematic Review of Immunotherapy in Urologic Cancer: Evolving Roles for Targeting of CTLA-4, PD-1/PD-L1, and HLA-G. *Eur Urol* **68**, 267-279, doi:10.1016/j.eururo.2015.02.032 (2015).
- 159 Kates, M. *et al.* Intravesical BCG Induces CD4(+) T-Cell Expansion in an Immune Competent Model of Bladder Cancer. *Cancer Immunol Res* **5**, 594-603, doi:10.1158/2326-6066.CIR-16-0267 (2017).
- 160 Bunimovich-Mendrazitsky, S., Shochat, E. & Stone, L. Mathematical model of BCG immunotherapy in superficial bladder cancer. *Bull Math Biol* **69**, 1847-1870, doi:10.1007/s11538-007-9195-z (2007).
- 161 Wang, X. *et al.* Cancer-FOXP3 directly activated CCL5 to recruit FOXP3(+)Treg cells in pancreatic ductal adenocarcinoma. *Oncogene* **36**, 3048-3058, doi:10.1038/onc.2016.458 (2017).
- 162 Cortes, C., Mohri, M. & Rostamizadeh, A. L2 regularization for learning kernels. *arXiv preprint arXiv:1205.2653* (2012).
- 163 Furey, T. S. *et al.* Support vector machine classification and validation of cancer tissue samples using microarray expression data. *Bioinformatics* **16**, 906-914 (2000).
- 164 LeCun, Y., Bengio, Y. & Hinton, G. Deep learning. *nature* **521**, 436-444 (2015).
- 165 Bengio, Y., Courville, A. & Vincent, P. Representation learning: A review and new perspectives. *IEEE transactions on pattern analysis and machine intelligence* **35**, 1798-1828 (2013).
- 166 Schmidhuber, J. Deep learning in neural networks: An overview. *Neural networks* **61**, 85-117 (2015).
- 167 Crammer, K. & Singer, Y. On the algorithmic implementation of multiclass kernel-based vector machines. *Journal of machine learning research* **2**, 265-292 (2001).
- 168 Kohavi, R. in *Ijcai*. 1137-1145 (Montreal, Canada).
- 169 Kingma, D. P. & Ba, J. Adam: A method for stochastic optimization. *arXiv preprint arXiv:1412.6980* (2014).
- 170 Mlynska, A. *et al.* A gene signature for immune subtyping of desert, excluded, and inflamed ovarian tumors. *Am J Reprod Immunol* **84**, e13244, doi:10.1111/aji.13244 (2020).
- 171 Song, B. N. *et al.* Identification of an immunotherapy-responsive molecular subtype of bladder cancer. *EBioMedicine* **50**, 238-245, doi:10.1016/j.ebiom.2019.10.058 (2019).
- 172 Xu, X. *et al.* Three-dimensional texture features from intensity and high-order derivative maps for the discrimination between bladder tumors and wall tissues via MRI. *Int J Comput Assist Radiol Surg* **12**, 645-656, doi:10.1007/s11548-017-1522-8 (2017).
- 173 Jagodinsky, J. C., Harari, P. M. & Morris, Z. S. The Promise of Combining Radiation Therapy With Immunotherapy. *Int J Radiat Oncol Biol Phys* **108**, 6-16, doi:10.1016/j.ijrobp.2020.04.023 (2020).
- 174 Institute, N. C.  
<https://www.cancer.gov/aboutcancer/treatment/types/immunotherapy#what-are-the-types-of-immunotherapy>. (2020).
- 175 Kim, T. J., Cho, K. S. & Koo, K. C. Current Status and Future Perspectives of Immunotherapy for Locally Advanced or Metastatic Urothelial Carcinoma: A Comprehensive Review. *Cancers (Basel)* **12**, doi:10.3390/cancers12010192 (2020).
- 176 Powles, T. *et al.* Atezolizumab versus chemotherapy in patients with platinum-treated locally advanced or metastatic urothelial carcinoma (IMvigor211): a multicentre, open-label, phase 3 randomised controlled trial. *Lancet* **391**, 748-757, doi:10.1016/S0140-6736(17)33297-X (2018).
- 177 Balar, A. V. *et al.* Atezolizumab as first-line treatment in cisplatin-ineligible patients with locally advanced and metastatic urothelial carcinoma: a single-arm, multicentre, phase 2 trial. *Lancet* **389**, 67-76, doi:10.1016/S0140-6736(16)32455-2 (2017).
- 178 Josefowicz, S. Z., Lu, L. F. & Rudensky, A. Y. Regulatory T cells: mechanisms of differentiation and function. *Annu Rev Immunol* **30**, 531-564,

- doi:10.1146/annurev.immunol.25.022106.141623 (2012).
- 179 Togashi, Y., Shitara, K. & Nishikawa, H. Regulatory T cells in cancer immunosuppression  
- implications for anticancer therapy. *Nat Rev Clin Oncol* **16**, 356-371,  
doi:10.1038/s41571-019-0175-7 (2019).
- 180 Winerdal, M. E. *et al.* FOXP3 and survival in urinary bladder cancer. *BJU Int* **108**, 1672-  
1678, doi:10.1111/j.1464-410X.2010.10020.x (2011).
- 181 Jou, Y. C. *et al.* Foxp3 enhances HIF-1alpha target gene expression in human bladder  
cancer through decreasing its ubiquitin-proteasomal degradation. *Oncotarget* **7**, 65403-  
65417, doi:10.18632/oncotarget.11395 (2016).
- 182 Tavazoie, M. F. *et al.* LXR/ApoE Activation Restricts Innate Immune Suppression in  
Cancer. *Cell* **172**, 825-840 e818, doi:10.1016/j.cell.2017.12.026 (2018).
- 183 Kim, K. *et al.* Single-cell transcriptome analysis reveals TOX as a promoting factor for T  
cell exhaustion and a predictor for anti-PD-1 responses in human cancer. *Genome Med*  
**12**, 22, doi:10.1186/s13073-020-00722-9 (2020).
- 184 Guo, L. *et al.* TOX correlates with prognosis, immune infiltration, and T cells exhaustion in  
lung adenocarcinoma. *Cancer Med*, doi:10.1002/cam4.3324 (2020).

Research Paper

# Alendronate-induced Perturbation of the Bone Proteome and Microenvironmental Pathophysiology

Jayoung Kim<sup>1,2,✉</sup>, Austin Yeon<sup>1</sup>, Sarah J. Parker<sup>3</sup>, Muhammad Shahid<sup>1</sup>, Aissatou Thiombane<sup>1</sup>, Eunho Cho<sup>1</sup>, Sungyong You<sup>1</sup>, Hany Emam<sup>4</sup>, Do-Gyoon Kim<sup>5</sup>, Minjung Kim<sup>6</sup>

1. Departments of Surgery and Biomedical Sciences, Cedars-Sinai Medical Center, Los Angeles, CA, USA
2. Department of Medicine, University of California Los Angeles, CA, USA
3. Smidt Heart Institute, Department of Cardiology, Cedars-Sinai Medical Center, Los Angeles, CA, USA
4. Division of Orthodontics, College of Dentistry, The Ohio State University, Columbus, OH, USA
5. Division of Oral Surgery, College of Dentistry, The Ohio State University, Columbus, OH, USA
6. Department of Cell Biology, Microbiology, and Molecular Biology, University of South Florida, Tampa, FL, USA

✉ Corresponding author: Jayoung Kim, PhD. Departments of Surgery and Biomedical Sciences, Cedars-Sinai Medical Center, Davis 5071, 8700 Beverly Blvd., Los Angeles, CA 90048. Tel: +1-310-423-7168; Fax: +1-310-967-3809; E-mail: Jayoung.kim@csmc.edu

© The author(s). This is an open access article distributed under the terms of the Creative Commons Attribution License (<https://creativecommons.org/licenses/by/4.0/>). See <http://ivyspring.com/terms> for full terms and conditions.

Received: 2021.04.14; Accepted: 2021.07.11; Published: 2021.07.23

## Abstract

**Objectives:** Bisphosphonates (BPs) are powerful inhibitors of osteoclastogenesis and are used to prevent osteoporotic bone loss and reduce the risk of osteoporotic fracture in patients suffering from postmenopausal osteoporosis. Patients with breast cancer or gynecological malignancies being treated with BPs or those receiving bone-targeted therapy for metastatic prostate cancer are at increased risk of bisphosphonate-related osteonecrosis of the jaw (BRONJ). Although BPs markedly ameliorate osteoporosis, their adverse effects largely limit the clinical application of these drugs. This study focused on providing a deeper understanding of one of the most popular BPs, the alendronate (ALN)-induced perturbation of the bone proteome and microenvironmental pathophysiology.

**Methods:** To understand the molecular mechanisms underlying ALN-induced side-effects, an unbiased and global proteomics approach combined with big data bioinformatics was applied. This was followed by biochemical and functional analyses to determine the clinicopathological mechanisms affected by ALN.

**Results:** The findings from this proteomics study suggest that the RIPK3/Wnt/GSK3/β-catenin signaling pathway is significantly perturbed upon ALN treatment, resulting in abnormal angiogenesis, inflammation, anabolism, remodeling, and mineralization in bone cells in an *in vitro* cell culture system.

**Conclusion:** Our investigation into potential key signaling mechanisms in response to ALN provides a rational basis for suppressing BP-induced adverse effect and presents various therapeutic strategies.

Key words: Osteonecrosis of the jaw; bisphosphonate; GSK signaling; clinical cone beam computed tomography; bone mineral density; proteomics; biomarker

## Introduction

Bone tissue undergoes continuous cycles of bone resorption by osteoclasts and bone formation by osteoblasts, which were orchestrated by osteocytes[1]. Bone tissue is also highly vascularized providing O<sub>2</sub>, nutrients, and precursor cells for bone remodeling and serving as routes for blood and immune cells into bone tissue. Regulatory interactions between cells of these hematopoietic, immune, and skeletal (bone) systems closely regulate bone remodeling and repair processes via secreted factors such as VEGF, M-CSF,

RANKL, Wnt3a, and Osteoprotegerin, etc. and their cell surface receptors.

Several key signal pathway has been shown to play pivotal roles in bone remodeling/repair processes, enhancing osteoblast differentiation and angiogenesis and modulating immune cell functions[2]. Specifically, Wnt pathway activation via GSK3 inactivation leads to osteoblast differentiation and stimulates bone anabolism while GSK3 gain-of-function promotes osteogenesis of adipose-



derived stromal cells, making GSK3 as a possible therapeutic target for bone diseases [3-5]. Mice expressing constitutively active GSK3 $\beta$  (GSK3 $\beta$  S9A) mutant, exhibited a marked increase in osteogenesis, whereas ones with catalytically inactive GSK3 $\beta$  (GSK3 $\beta$  K85A) showed decreased osteogenic differentiation by regulating  $\beta$ -catenin[5]. Wnt/GSK3/ $\beta$ -catenin pathway also plays important roles in angiogenesis and vasculogenesis, supporting wound healing and regeneration of oral mucosa and jaw tissue [6]. Wnt signaling activation by Wnt1, VEGF, or CHIR99021 (GSK3 $\beta$  inhibitor) enhanced, while its inactivation by JW67 (targeting APC/GSK3/ $\beta$ -catenin complex) or  $\beta$ -catenin kinase dead form suppressed, vascular differentiation of mesenchymal stem cells (MSCs) derived from dental pulp [7]. GSK3 $\beta$  regulates  $\beta$ -catenin level in endothelial cells. Expression of  $\beta$ -catenin in HUVEC cells increases VEGF-A and -C level and induces capillary formation [8].

Bisphosphonates (BPs) have been suggested to modulate the proliferation and differentiation rates of osteoblasts and trigger survival signaling leading to bone homeostasis and antiresorptive effect [9-11]. First approved by the FDA in 1995, alendronate (ALN) is currently one of the most used BPs in the medical field[12]. ALN has been used successfully for the treatment of osteoporosis [13]. Several pieces of evidence indicate that there is a strong association between ALN and lower risk of bone metastases in postmenopausal women with early breast cancer [14, 15]. Cancer patients undergoing BPs-based treatments are at a 10-fold greater risk of developing bisphosphonate-related osteonecrosis of the jaw (BRONJ) [16], which is suggested to be a result of osteoclast inhibition and apoptosis[17]. Due to the prevalent usage of BPs in many bone-related diseases, more understanding on underlying mechanisms of adverse effect caused by BPs is crucial in providing better care and improving patient quality of life [18]. In oncology patients, incidence of BRONJ has been estimated to be as high as 18.6%[19], and risk of developing BRONJ increases with longer duration or higher dosages of BPs-based therapy[20].

This study sought to understand the pathogenesis of BP-associated adverse effects by looking into proteome perturbation and potential molecular biomarkers and mechanisms using an *in vitro* cell culture system.

## Materials and Methods

### Reagents and cell culture

Several cell lines, including MG-63, SCC-9, SCC-15, and HUVEC cells, were obtained from the

American Type Culture Collection (ATCC) (Manassas, VA). Culture condition, antibodies and reagents used for this study are available in Supplementary Materials.

### Quantitative proteomics

Sample preparation methods for this study are available in Supplementary Materials. For protein quantification and statistical analysis, mapDIA was used. Data was analyzed based on the established workflows previously described [21, 22]. Briefly, peptides were identified using the openSWATH workflow [23], searched against the pan human library [24] with decoy sequences appended for false discovery rate calculation using the pyprophet algorithm [25]. Peptides with no greater than 5% identified false discovery rate (FDR) across all samples were compiled into the final experimental results using the TRIC alignment algorithm [26]. Following removal of non-proteotypic peptides (e.g., sequences matching more than one gene product from the Pan Human Library), the final aligned results were analyzed using mapDIA to select only high-quality performing fragments for quantification and to compile fragment level data into peptide and protein level abundance estimates [27]. The mapDIA software was also used to perform pairwise comparisons between ALN and control groups, including adjustment for multiple testing effects to produce a comparison FDR, which filtered proteins with significant or non-significant differential abundance in response to ALN treatment. The MS proteomics data has been deposited to the PRIDE repository with the dataset identifier, PXD024585.

### Identification of differentially expressed proteins (DEPs)

Proteins with more than 3 nonredundant peptides in each sample were selected. Further selection of proteins detected in at least 2 samples in the same group was performed for statistical testing. A median difference test and Welch's t-test were performed separately, and the resulting two p-values were combined to compute adjusted p-values using Stouffer's method. The DEPs were identified based on an adjusted p-values<0.05 and absolute log<sub>2</sub> fold-change (FC)  $\geq$ 0.58.

### VEGF ELISA assay

To determine vascular endothelial growth factor (VEGF-A) levels of conditioned medium from MG-63 cells incubated with ALN, supernatants from cell cultures were analyzed using the Human VEGF Quantikine ELISA Kit (R&D Systems, Minneapolis, Mass).

## Cytokine array

Cell lysates and conditioned media from RAW 264.7 macrophages were collected and analyzed using a cytokine array, per standard provided protocols (R&D Systems, Minneapolis, MN, USA). ImageJ was used to measure the signal intensities.

## Mineralization assay using Alizarin Red-S staining

The formation of calcium phosphate was quantified in MG-63 bone cells via Alizarin Red-S mineralization assay. Optical density was detected at an absorbance of 562 nm.

## Statistical analysis

Most of the experiments were repeated at least six (6) times with independent treatments, while all the cases were repeated at least three times. Each of the experiments did not show significantly different results across replications. Statistical analyses were conducted using GraphPad Prism, version 7.03 (GraphPad Software Inc., La Jolla, CA). Mean values from technical replicates were used for statistical analyses, and all data were presented as the mean  $\pm$  standard deviation (SD). A one-way analysis of variance (ANOVA) or Student's t-test was conducted to compare the groups of data. Differences were considered statistically significant when  $P < 0.05$ .

## Results

### Comprehensive analysis with large unbiased global proteomic assays suggested perturbed proteins in response to BP in bone cells

Mass spectrometry (MS) has several important attributes that make it amenable to providing reproducible and accurate assays for proteins and metabolites. It provides a scalable number of analytes quantified in a single assay and absolute quantification, which leads to a standardized path from assay development to validation of new candidate biomarkers applicable in any clinical chemistry laboratory. To understand the molecular mechanisms underlying specific diseases, an unbiased and global omics approach combined with big data analysis using bioinformatics is critical.

As described in the Materials and Methods, a proteomics approach was implemented (Fig 1A). The top 10 most abundant protein classes are shown in Fig 1B. Global proteomics analysis identified a highly confident and comprehensive list of perturbed proteins in MG-63 bone cells treated with ALN. Protein quantification and statistical analysis using mapDIA identified perturbed proteins in MG-63 cells treated with 10  $\mu$ M ALN. A total of 2,865 proteins

with UniProtKB IDs were identified. Further analysis with the PANTHER Protein Classification Tool revealed that the most abundant top 10 proteins classes included extracellular matrix, metabolite interconversion, nucleic acid metabolism, protein modification, translational regulation, cytoskeletal, transporter, protein-binding activity modulator, membrane traffic, and scaffold/adaptor[28]. To identify DEPs, the integrated hypothesis testing method was applied. Briefly, the median difference test and Welch's t-test was performed on high confidence proteins, which in the case of this experiment, were proteins detected with more than 3 non-redundant peptides encompassing at least 2 samples in the same group. The median test p-value and Welch's t-test p-value were then combined to adjust for multiple testing errors. Finally, 27 up- and 31 downregulated DEPs were selected for based on adjusted p-values  $< 0.05$  and  $\log_2$  FC  $\geq 0.58$ . Significant expression was assessed using a volcano plot (Fig 1C and Fig 1D) and heatmap (Fig 1E). The DEPs are listed in Table 1.

### Angiogenesis alteration in response to ALN treatment

When verifying proteins associated with angiogenesis-related Gene Ontology Biological Processes (GOBPs), several proteins were identified, including ETS proto-oncogene 1 (ETS1) ( $\log_2$  FC, 1.1566), integrin subunit alpha 5 (ITGA5) ( $\log_2$  FC, 0.6102), and milk fat globule-EGF factor 8 (MFG8) ( $\log_2$  FC, -0.7468) (Table 1). To further investigate these findings, the effects of ALN on several well-known angiogenic factors were investigated. Secretion of VEGF-A, a potent angiogenic factor, was examined in bone cells after stimulation with ALN. Consistent with similarly designed work from previous trials [29], treatment of MG-63 cells with ALN led to a statistically significant but modest decrease (approximately 30%) of VEGF secretion into the conditioned medium compared to control (Fig 2A). Furthermore, HUVEC stimulation in the collected culture medium also exhibited modest but meaningful suppression of proliferation (Fig 2B). Collectively, the reduction of VEGF secretion and HUVEC proliferation by ALN strongly implies angiogenic signals to vessel cells from bone cells. This finding suggests the potential microenvironment-level regulation of bone remodeling in ONJ. For proteomics profiling, necrotic and apoptotic conditions were avoided to fully investigate the effects of ALN on bone cells. Additional analysis confirmed that there was no induced cell death with ALN treatment in MG-63 cells. Cell viability and proliferation rates, which were determined using



MTT (Fig 2C) and crystal violet staining assays (Fig 2D), showed no cytotoxicity.

**Table 1.** List of differentially expressed proteins (DEPs) with corresponding statistics.

Uniprot ID	Gene Symbol	Full Name	Log2 FC (ALN/ Ctrl)	Median P-Value	T Test P-Value	Adj. P
Q86VN1	VPS36	Vacuolar protein-sorting-associated protein 36	2.3697	0.0191	0.3002	0.0332
Q9BXR6	CFHR5	Complement factor H-related protein 5	1.5412	0.0306	0.0824	0.0106
Q8N350	CBARP	Voltage-dependent calcium channel beta subunit-associated regulatory protein	1.23	0.0776	0.0415	0.0129
P48163	ME1	NADP-dependent malic enzyme	1.2145	0.1359	0.0149	0.0103
Q9ULH7	MRTFB	Myocardin-related transcription factor B	1.1752	0.1301	0.0877	0.0397
P14921	ETS1	Protein C-ets-1	1.1566	0.1653	0.0497	0.0319
Q9H0V9	LMAN2L	VIP36-like protein	1.1446	0.013	0.1852	0.0136
Q15427	SF3B4	Splicing factor 3B subunit 4	1.0902	0.3234	0.0296	0.0487
Q9H223	EHD4	EH domain-containing protein 4	0.8995	0.113	0.1213	0.0463
Q07021	C1QBP	Complement component 1 Q subcomponent-binding protein, mitochondrial	0.8848	0.1071	0.1049	0.0388
Q9UJW2	TINAG	Tubulointerstitial nephritis antigen	0.8833	0.0976	0.1428	0.0474
P56192	MARS1	Methionine--tRNA ligase, cytoplasmic	0.8772	0.0039	0.1283	0.0037
P08579	SNRNPB2	U2 small nuclear ribonucleoprotein B	0.8721	0.0322	0.2438	0.0361
Q9H4B7	TUBB1	Tubulin beta-1 chain	0.8644	0.0467	0.0944	0.0172
Q9H2H8	PPIL3	Peptidyl-prolyl cis-trans isomerase-like 3 (PP1ase)	0.8257	0.1129	0.1055	0.0408
P00439	PAH	Phenylalanine-4-hydroxylase (PAH)	0.8024	0.0475	0.1114	0.0206
Q5JTZ9	AARS2	Alanine--tRNA ligase, mitochondrial	0.7071	0.0877	0.0325	0.0118
Q9UKN8	GTF3C4	General transcription factor 3C polypeptide 4	0.6861	0.0038	0.1761	0.0055
Q92747	ARPC1A	Actin-related protein 2/3 complex subunit 1A (SOP2-like protein)	0.6813	0.1877	0.0156	0.0158
P99999	CYCS	Cytochrome c	0.664	0.0456	0.1572	0.0283
Q7Z2W4	ZC3HAV1	Zinc finger CCCH-type antiviral protein 1	0.6468	0.1397	0.0465	0.0254
Q9Y5M8	SRPRB	Signal recognition particle receptor subunit beta	0.645	0.0983	0.1459	0.0486
P62191	PSMC1	26S proteasome regulatory subunit 4	0.6447	0.1717	0.0328	0.0243
P43251	BTD	Biotinidase (Biotinase)	0.6273	0.1495	0.0734	0.0392
P08648	ITGA5	Integrin alpha-5	0.6102	0.0891	0.1285	0.0398
Q07955	SRSF1	Serine/ arginine-rich splicing factor 1	0.6084	0.0123	0.0315	0.0018
P18754	RCC1	Regulator of chromosome condensation	0.5984	0.1047	0.008	0.0048
P62140	PPP1CB	Serine/ threonine-protein phosphatase PP1-beta catalytic subunit	-0.6001	0.1545	0.0111	0.0097
Q9NX40	OCIAD1	OCIA domain-containing protein 1	-0.601	0.0912	0.1301	0.041
Q14244	MAP7	Microtubule-associated protein 7	-0.6115	0.0198	0.1806	0.0178
Q9Y572	RIPK3	Receptor-interacting serine/ threonine-protein kinase 3	-0.6157	0.0717	0.0554	0.0153
Q06187	BTK	Bruton tyrosine kinase	-0.6434	0.2767	0.0165	0.027
Q8IW35	CEP97	Centrosomal protein of 97 kDa	-0.6669	0.0989	0.1153	0.0394
Q969G5	CAVIN3	Caveolae-associated protein 3	-0.6891	0.0308	0.0337	0.0045
O96033	MOC52	Molybdopterin synthase sulfur carrier subunit	-0.6914	0.0731	0.0987	0.0262
P13798	APEH	Acyl-peptide hydrolase	-0.6929	0.0508	0.239	0.0485
Q9H3H3	C11orf68	UPF0696 protein C11orf68	-0.7029	0.0819	0.1651	0.0471
Q08431	MFG8	Milk fat globule-EGF factor 8	-0.7468	0.1464	0.0932	0.0466
Q9NYJ8	TAB2	TGF-beta-activated kinase 1	-0.7572	0.1619	0.0095	0.0092
O95218	ZRANB2	Zinc finger Ran-binding domain-containing protein 2	-0.8387	0.1273	0.054	0.0261
Q93074	MED12	Mediator of RNA polymerase II transcription subunit 12	-0.91	0.0239	0.2422	0.0291
Q15047	SETDB1	Histone-lysine N-methyltransferase SETDB1	-0.9105	0.2702	0.0382	0.0459
P33241	LSP1	Lymphocyte-specific protein 1	-0.9375	0.0021	0.242	0.0058
Q9H3M7	TXNIP	Thioredoxin-interacting protein	-0.9387	0.0348	0.086	0.0123
P22307	SCP2	Sterol carrier protein X	-1.0061	0.1877	0.0682	0.0465
Q96A49	SYAP1	Synapse-associated protein 1	-1.0203	0.0638	0.0634	0.0155
Q5T1M5	FKBP15	FK506-binding protein 15	-1.0953	0.0796	0.135	0.0379
Q9NR77	PXMP2	Peroxisomal membrane protein 2	-1.1041	0.397	0.0075	0.0284
Q6P4R8	NFRKB	Nuclear factor related to kappa-B-binding protein	-1.131	0.0431	0.1973	0.0347
A6ND91	ASPDH	Aspartate dehydrogenase domain-containing protein	-1.2357	0.0503	0.2253	0.0451
Q9Y320	TMX2	Thioredoxin-related transmembrane protein 2	-1.3223	0.1468	0.0342	0.0211
Q9BRK0	REEP2	Receptor expression-enhancing protein 2	-1.3431	0.0303	0.0738	0.0094
Q9UHK6	AMACR	Alpha-methylacyl-CoA racemase	-1.3986	0.0022	0.2013	0.0046
P49407	ARRB1	Beta-arrestin-1 (Arrestin beta-1)	-1.4064	0.1261	0.016	0.01
Q92630	DYRK2	Dual specificity tyrosine-phosphorylation-regulated kinase 2	-1.4443	0.0139	0.0418	0.0027
Q9BRU9	UTP23	rRNA-processing protein UTP23 homolog	-1.8162	0.0833	0.0247	0.009
O14617	AP3D1	AP-3 complex subunit delta-1	-1.9901	0.0471	0.0127	0.0029
Q9C073	FAM117A	Protein FAM117A (C/EBP-induced protein)	-3.5266	0.0051	0.308	0.015

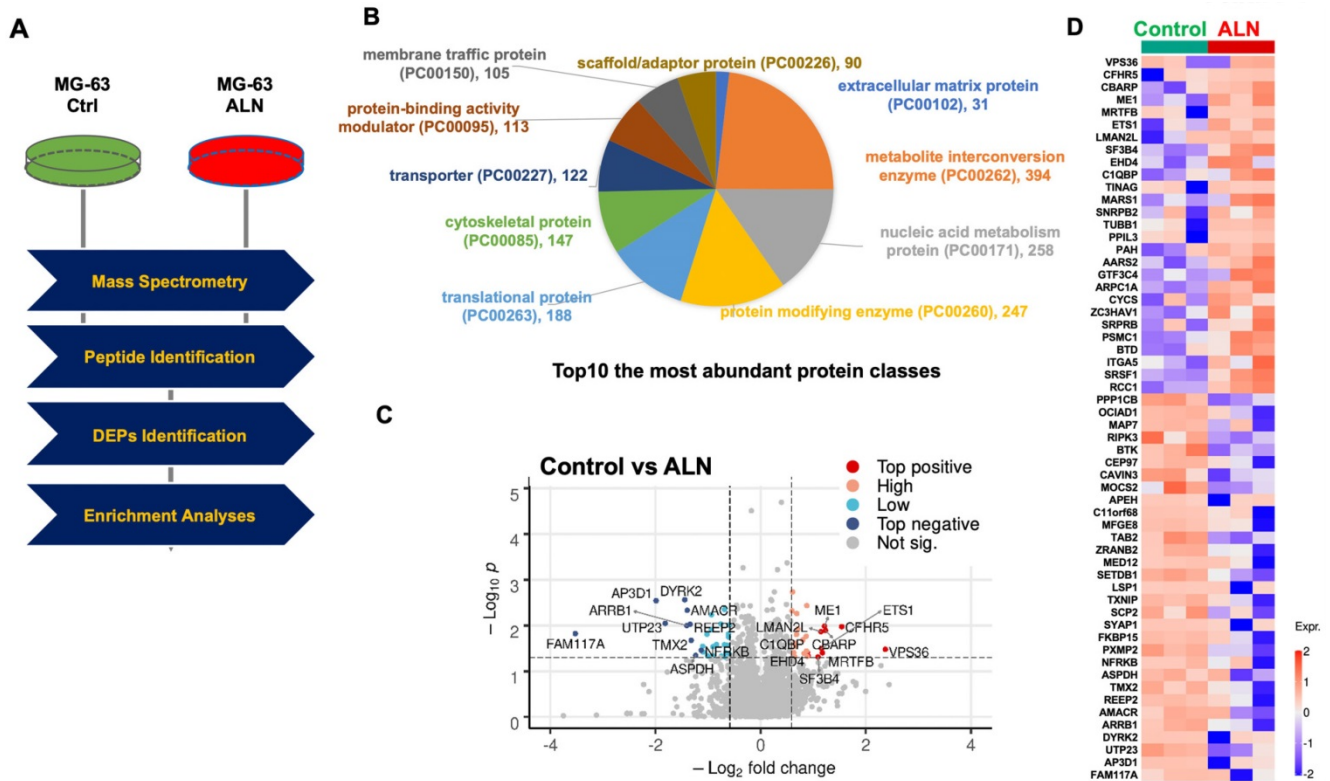


**Figure 1. Proteomics profiling revealing alendronate (ALN)-induced protein alteration in the global proteome of MG-63 bone cells. (A)** Experimental mass spectrometry (MS) workflow for this study. **(B)** Top 10 most abundant protein classes. **(C)** Volcano plot shows DEPs. **(D)** Heatmap depicts the differential expression patterns of proteins in response to ALN. Red and blue dots represent upregulated and downregulated proteins, respectively. Per row z-score of protein intensity is calculated. Each dot represents one protein. Proteins used are identical with those in the volcano plot. Experiments were done in triplicate.

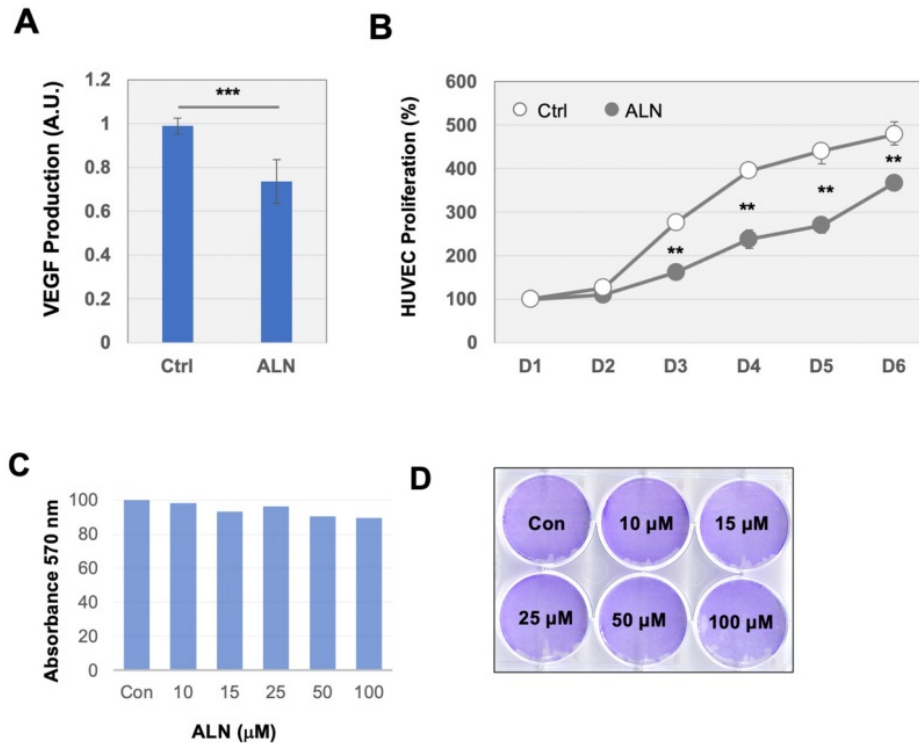


**Figure 2. Angiogenic pathways may be upregulated by ALN treatment. (A)** Secretion of VEGF in MG-63 bone cells treated with ALN. Effect of ALN treatment on the secreted VEGF levels into conditioned medium by MG-63 cells. Values (mean and standard deviation (SD)) are expressed as fold-changes compared to untreated cells (Ctrl, control). **(B)** Proliferation of HUVEC in the collected media of MG-63 cells.  $***p < 0.001$ , compared to control (Student's t-test). **(C-D)** No apoptosis was observed within the treatment period of 6 h. **(C)** Cell viability of MG-63 cells. MTT assay revealed no viability changes by ALN treatment. **(D)** Crystal violet staining assay showed no cell mass changes in response to varying concentration of ALN for 6 days. Experiments were done 6 times. Representative images were shown.

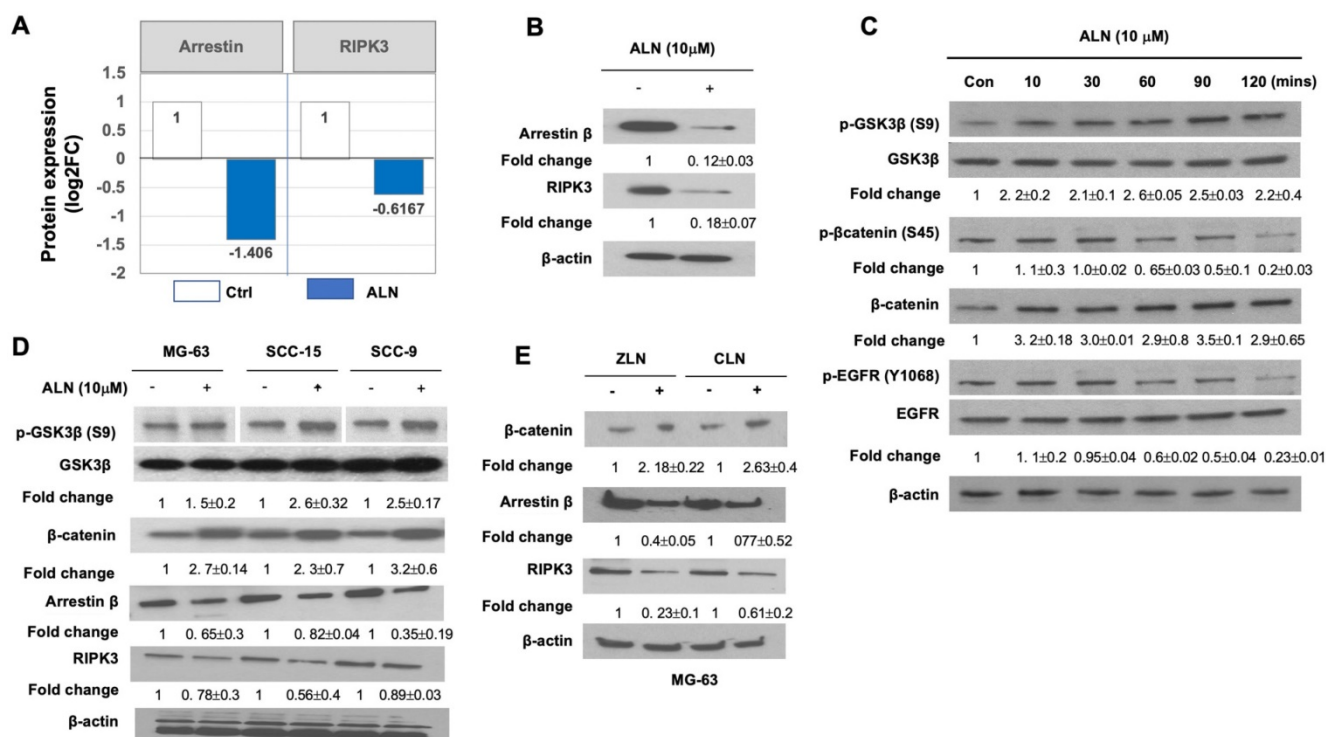


**Figure 3. The RIPK3/arrestin/GSK3β/β-catenin/VEGF pathway is altered by ALN treatment. (A-B).** Quantification results showed that arrestin β and RIPK3 are significantly suppressed with ALN treatment. **(A)** Data from proteomics profiling, DEP levels obtained from proteomics analysis are shown in Table 1. **(B)** Western blot analysis to measure the expression levels of arrestin β and RIPK3 proteins in the presence or absence of ALN. β-actin was used as the loading control. **(C)** ALN-induced phosphorylation of GSK3β (S9) and β-catenin (S45) led to stabilization of β-catenin in MG-63 cells. **(D)** Comparison of phosphorylation of GSK3β and expression of β-catenin, arrestin β, and RIPK3 in MG-63, SCC-15, and SCC-9 cells after treatment with ALN. **(E)** Effects of several BPs (ZLN and CLN) on β-catenin, arrestin β, and RIPK3 in MG-63 cells. After stimulation with 10 μM of ALN, ZLN, or CLN at various times, cells were harvested for protein extraction and western blot analysis. Representative western blot images were selected after experiments were repeated 6 times.

### Receptor-interacting protein kinase 3 (RIPK3), a necroptosis factor, is altered in the ALN-treated proteome

Among the DEPs regulated by ALN treatment, proteins involved in angiogenesis, inflammation, and necrosis were of particular interest due to their relevance in ONJ. Proteomics profiling revealed downregulation of RIPK3 in MG63 cells treated with ALN (Fig 3A). RIPK3 has recently been reported as a mediator of necroptosis, programmed non-apoptotic cell death, and necroinflammation in response to immune signaling and cytokines, such as TNF-α [30]. The inhibition of RIPK3 activity suppressed *Enterococcus faecalis* infection-induced cell death in MG-63 cells [31]. RIPK3 expression is inhibited by hypoxia, which contributes to angiogenesis [32]. Loss of RIPK3 leads to the activation of the Wnt/β-catenin signaling pathway in the *ripk3*<sup>-/-</sup> colon cancer mouse model, and enhances inflammation, immune cell infiltration, and angiogenesis [33].

Western blot analysis was able to validate that the protein expression levels of arrestin β1 (ARRB1) was significantly diminished by ALN treatment (Fig 3B), which was consistent with proteomics analysis. Given that ARRB1 is reported as a necessary

component for Wnt/β-catenin signaling and as a regulator of GSK-3β activation/inactivation [34], the effects of ALN and ARRB1 on the Wnt/GSK3/β-catenin signaling cascades were another point of interest. Proteomics profiling and biochemical analysis revealed the downregulation of RIPK3 and ARRB1 by ALN treatment, which suggests that the effects of ALN on MG-63 cells are likely to be mediated by the Wnt/GSK3/β-catenin signaling pathway.

### The glycogen synthase kinase 3 (GSK3) network is an ALN regulatory signaling pathway

To understand the activation of signaling cascades in response to BP treatment in bone cells, the phosphorylation of important signaling proteins in MG-63 cells treated with ALN was assessed. The involvement of Wnt/GSK3/β-catenin signaling aberration was first determined, and the downstream secreted effectors of the Wnt pathway were evaluated as a part of the ALN signaling pathway.

Based on previous findings in literature, the Wnt/GSK3/β-catenin pathway has been shown to play a pivotal role in bone remodeling/repair processes, enhancement of osteoblast differentiation,

angiogenesis, and modulation of immune cell functions[2]. This evaluation further suggests that the Wnt/GSK3/ $\beta$ -catenin pathway may play a key role in the biological effects of response to ALN treatment in MG-63 cells.

After treatment with ALN at varying incubation times (0, 20, 30, 60, 90, and 120 min), the phosphorylation status of a series of crucial signaling molecules was evaluated using western blot analysis. The phosphorylation of GSK-3 $\beta$  (S9) increased with ALN treatment (Fig 3C). GSK-3, a serine/threonine protein kinase that phosphorylates and inactivates glycogen synthase, is a key downstream regulator of the PI3K/Akt pathway. GSK-3 signaling is inactivated by phosphorylation of Ser9 in GSK-3 $\beta$ . Since the phosphorylation of GSK-3 $\beta$  (S9) increased, this suggests that ALN treatment inactivates GSK-3 signaling in MG-63 cells.

As an important downstream effector of the Wnt signaling pathway,  $\beta$ -catenin is phosphorylated at S45 by a complex of axin and casein kinase I (CKI), which initiates the  $\beta$ -catenin phosphorylation–degradation cascade [35]. While the phosphorylation of GSK-3 $\beta$  (S9) increased with ALN treatment, phosphorylation of  $\beta$ -catenin (S45) and EGFR (Y1068) decreased (Fig 3C). The decreased phosphorylation of  $\beta$ -catenin may increase protein stability and protein expression (Fig

3B). Increased phosphorylation of GSK-3 $\beta$  (S9) was consistently observed in other cells, including SCC-9 and SCC-15, with ALN, zoledronic acid (ZLN), or clodronate (CLN) treatment (Fig 3D and Fig 3E). These results suggest that ANL suppresses ARRB1, inactivates GSK-3 $\beta$ , and stabilizes  $\beta$ -catenin. The RIPK3/arrestin/Wnt/GSK/ $\beta$ -catenin network may be a potential molecular regulatory network whose activation is altered upon ALN therapy.

### Cytokine production and secretion in RAW 264.7 macrophages may be enhanced by ALN treatment

To test the effects of ALN on the immune system, a commercially available cytokine array was used to screen for potentially stimulated cytokines. RAW 264.7 macrophages were incubated with ALN both with and without the presence of lipopolysaccharides (LPS) (100 ng/ml) for 24 h. As shown in figure 4A, the production of tumor necrosis factor alpha (TNF- $\alpha$ ) was stimulated by LPS and the levels of TNF- $\alpha$  were significantly increased with ALN. Western blot analysis also supported these findings (Fig 4B). The secretion of IL-6 also greatly increased with ALN (Fig 4C). However, there were no dramatic additional effects across other cytokines.

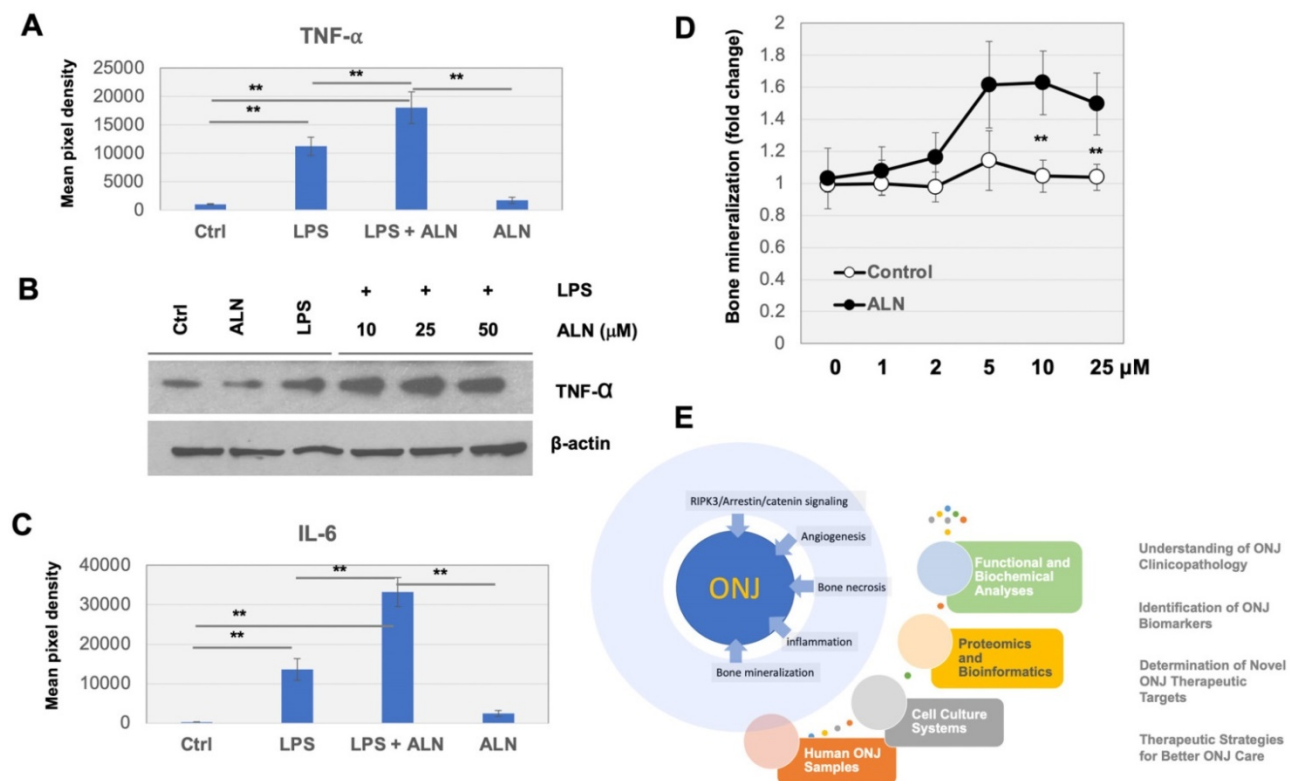


**Figure 4. Pro-inflammatory cytokines are produced and secreted in response to ALN treatment in RAW 264.7 macrophage cells. (A-B)** Cytokine array was conducted as described in Materials and Methods. Production of TNF- $\alpha$  (A) and secretion of IL-6 (B) increased with ALN treatment. (C) Western blot analysis for further validation. \*\*\* $p < 0.001$  and \*\* $p < 0.001$ , compared to control (Student's t-test). Representative images are shown. (D) ALN treatment impaired homeostasis in bone mineralization. Quantification of mineral deposition by Alizarin Red-S staining shown as a graph. Data represent average $\pm$ SD (n= 6). Statistical analysis was compared between ALN and vehicle only (ctrl) (p-value<0.05).



### Abnormalities in calcium phosphate formation in bone cells and bone mineral density (BMD) distribution in ONJ-associated osteonecrosis

ALN is regularly used to help osteoporosis patients with bone mineralization loss. To test the effects of ALN on the quantification of mineral deposition, Alizarin Red-S staining assays were used to further assess mineralization levels after treatment. MG-63 cells were incubated with ALN or vehicle control (0, 1, 5, 10, and 25  $\mu$ M) for 2 days. Incubation of cells with ALN led to a marked increase in mineralization (to ~1.6 fold) compared to controls (Fig 4D).

### Discussion

Our proteomics profiling revealed the downregulation of RIPK3 in response to ALN treatment in MG-63 bone cells. RIPK3 has been reported to play a fundamental role in inhibiting inflammation and mediating necroptosis and necroinflammation through the RIPK3-MLKL (mixed lineage kinase domain-like protein) pathway [30]. Inhibitors of RIPK3 and MLKL suppressed cell death from *Enterococcus faecalis* infection in MG-63 cells [31]. Although not encompassed in the current study, the role, and mechanisms of RIPK3 and its downstream signaling cascades in ALN-induced bone biology are under further investigation by our group. In addition, this study showed that the presence of ALN enhanced production or secretion of inflammatory cytokines in LPS-activated macrophage cells. A previous study found that ZLN, a potent BP, stimulated and increased inflammatory osteoclastic mediators [36]. Furthermore, ZLN was found to suppress proliferation and migration of vascular endothelial cells [37]. Expression of VEGF receptor 2 in vascular endothelial cells was also reported in response to treatment with ZLN [38]. In our experimental system, we observed modest decreases in VEGF secretion in response to ALN treatment.

The experimental data further suggested the potential role of the Wnt/GSK3/ $\beta$ -catenin signaling pathway in the BP-perturbed proteome and its effects on bone homeostasis. This study demonstrated that the Wnt/GSK3/ $\beta$ -catenin signaling pathways may play a fundamental role in bone metabolism, homeostasis, and remodeling. Multifaceted roles of GSK3 under each cellular context have been reported. In cytotoxic T lymphocytes (CTL), GSK3 inhibition blocks programmed cell death protein-1 (PD-1) transcription; thereby, enhancing CTL functioning [39]. GSK3 is a serine/threonine kinase that regulates Wnt/ $\beta$ -catenin, PI3K/PTEN/AKT, RAS/RAF/MAPK, hedgehog, Notch, and other signaling

pathways and has been implicated in multiple diseases [40, 41]. Phosphorylation of GSK-3 $\alpha/\beta$  at multiple serine and threonine sites inactivates the kinase, while Tyr279/216 phosphorylation (pY) activates the kinase. GSK3 is reported to have both tumor promoting (glioblastoma, pancreatic, ovarian, and blood cancers) and tumor suppressive (breast and skin cancers) roles [42]. GSK3 stabilizes anti-apoptotic Bcl2, Bcl2L12A, c-Myb, Mcl-1, and VEGF, promoting tumors. On the other hand, GSK3 phosphorylates and destabilizes  $\beta$ -catenin leading to the downregulation of c-Myc and cyclin D1. GSK3 also phosphorylates T286 on cyclin D1, leading to its nuclear export and degradation [43]. Consistent with this study, previous findings have suggested an important role for the Wnt/GSK-3 signaling pathway in osteogenesis; inhibition of Wnt/GSK-3 activity induced osteoblast differentiation and significantly increased BMD in an ovariectomized rat model [44].

Experimental observation from this study suggests that a systematic overview of changes in the microenvironmental landscape is important for understanding ALN-induced pathophysiology in bone cells (Fig 4E). Treatment with ALN also leads to alterations in bone mineralization, which may further impair bone biology. In ONJ patients, our previous studies quantifying bone density and mineralization found that cone-beam computed tomography (CBCT) and micro-computed tomography image-based histomorphometric evaluation may be an efficient method to check bone health [45]. Abnormal BMD distribution in ONJ-associated osteonecrosis was observed by clinical CBCT imaging [46]. It would be worthwhile to determine if the patterns and severity of abnormal mineralization densities within jaw-bone biopsy samples can be implemented in ONJ patient care.

Collectively, the main innovative deliverables from this study are expected to lead to a better understanding of the mechanisms underlying ALN-induced pathological effects on bone and immune cells. The findings in this paper are promising but have several limitations; (1) the effects of BPs on osteoblast function are throughout the skeleton, and (2) ALN targets osteoclasts, not osteoblasts. In conjunction with standard diagnostic procedures, the more mechanistic data related to the adverse effects of ALN can also act as an applicable supplement for clinical judgment.

### Supplementary Material

Supplementary methods.

<http://www.medsci.org/v18p3261s1.pdf>

## Acknowledgments

This research was supported by the Samuel Oschin Comprehensive Cancer Institute (SOCCI) at Cedars-Sinai Medical Center through 2019 Lucy S. Gonda Award. We appreciate technical support from the Cedars-Sinai Proteomics and Metabolomics Core.

Kim J: Contributed to conception or design, drafted the manuscript, and critically revised the manuscript.

Yeon A: Contributed to analysis, drafted the manuscript, and critically revised the manuscript.

Parker SJ: Contributed to analysis, drafted the manuscript, and critically revised the manuscript.

Shahid M: Contributed to analysis, and critically revised the manuscript.

Thiombane A: Contributed to analysis, and critically revised the manuscript.

Cho E: Contributed to analysis, and critically revised the manuscript.

You S: Contributed to analysis, drafted the manuscript, and critically revised the manuscript.

Emam H: Contributed to analysis, drafted the manuscript, and critically revised the manuscript.

Kim D-G: Contributed to conception or design, drafted the manuscript, and critically revised the manuscript.

Kim M: contributed to conception or design, drafted the manuscript, and critically revised the manuscript.

## Funding

This research was funded by National Institutes of Health (1U01DK103260, 1R01DK100974, U24 DK097154, NIH NCATS UCLA CTSI UL1TR000124), Department of Defense (W81XWH-15-1-0415 and W81XWH-19-1-0109), Centers for Disease Controls and Prevention (1U01DP006079), and the U.S.-Egypt Science and Technology Development Fund by the National Academies of Sciences, Engineering, and Medicine (all to J.K.). This article is derived from the Subject Data funded in whole or part by National Academies of Sciences, Engineering, and Medicine (NAS) and The United States Agency for International Development (USAID). Any opinions, findings, conclusions, or recommendations expressed in this article are those of the authors alone, and do not necessarily reflect the views of USAID or NAS.

## Competing Interests

The authors have declared that no competing interest exists.

## References

1. Florencio-Silva R, Sasso GR, Sasso-Cerri E, Simoes MJ, Cerri PS. Biology of Bone Tissue: Structure, Function, and Factors That Influence Bone Cells. *Biomed Res Int.* 2015; 2015: 421746.

2. Issack PS, Helfet DL, Lane JM. Role of Wnt signaling in bone remodeling and repair. *HSS J.* 2008; 4: 66-70.
3. Bertacchini J, Magaro MS, Poti F, Palumbo C. Osteocytes Specific GSK3 Inhibition Affects In Vitro Osteogenic Differentiation. *Biomedicines.* 2018; 6.
4. Schoeman MA, Moester MJ, Oostlander AE, Kaijzel EL, Valstar ER, Nelissen RG, et al. Inhibition of GSK3beta Stimulates BMP Signaling and Decreases SOST Expression Which Results in Enhanced Osteoblast Differentiation. *J Cell Biochem.* 2015; 116: 2938-46.
5. Huh JE, Ko R, Jung HJ, Lee SY. Glycogen synthase kinase 3beta promotes osteogenic differentiation of murine adipose-derived stromal cells. *PLoS one.* 2013; 8: e54551.
6. Pabst AM, Kruger M, Blatt S, Ziebart T, Rahimi-Nejdat R, Goetze E, et al. Angiogenesis in the Development of Medication-Related Osteonecrosis of the Jaws: An Overview. *Dent J (Basel).* 2016; 5.
7. Zhang Z, Nor F, Oh M, Cucco C, Shi S, Nor JE. Wnt/beta-Catenin Signaling Determines the Vasculogenic Fate of Postnatal Mesenchymal Stem Cells. *Stem Cells.* 2016; 34: 1576-87.
8. Skurk C, Maatz H, Rocnik E, Bialik A, Force T, Walsh K. Glycogen-Synthase Kinase3beta/beta-catenin axis promotes angiogenesis through activation of vascular endothelial growth factor signaling in endothelial cells. *Circ Res.* 2005; 96: 308-18.
9. Bellido T, Plotkin LI. Novel actions of bisphosphonates in bone: preservation of osteoblast and osteocyte viability. *Bone.* 2011; 49: 50-5.
10. Plotkin LI, Manolagas SC, Bellido T. Dissociation of the pro-apoptotic effects of bisphosphonates on osteoclasts from their anti-apoptotic effects on osteoblasts/osteocytes with novel analogs. *Bone.* 2006; 39: 443-52.
11. Plotkin LI, Weinstein RS, Parfitt AM, Roberson PK, Manolagas SC, Bellido T. Prevention of osteocyte and osteoblast apoptosis by bisphosphonates and calcitonin. *J Clin Invest.* 1999; 104: 1363-74.
12. Wilkins Parker LR, Preuss CV. *Alendronate*. StatPearls. Treasure Island (FL); 2021.
13. Weinstein RS, Roberson PK, Manolagas SC. Giant osteoclast formation and long-term oral bisphosphonate therapy. *N Engl J Med.* 2009; 360: 53-62.
14. Rouach V, Goldshtein I, Wolf I, Catane R, Chodick G, Iton A, et al. Exposure to alendronate is associated with a lower risk of bone metastases in osteoporotic women with early breast cancer. *J Bone Oncol.* 2018; 12: 91-5.
15. Jackson C, Freeman ALJ, Szlamka Z, Spiegelhalter DJ. The adverse effects of bisphosphonates in breast cancer: A systematic review and network meta-analysis. *PLoS one.* 2021; 16: e0246441.
16. Dodson TB. The Frequency of Medication-related Osteonecrosis of the Jaw and its Associated Risk Factors. *Oral Maxillofac Surg Clin North Am.* 2015; 27: 509-16.
17. George EL, Lin YL, Saunders MM. Bisphosphonate-related osteonecrosis of the jaw: a mechanobiology perspective. *Bone Rep.* 2018; 8: 104-9.
18. Zymperdikas VF, Yavropoulou MP, Kaklamanos EG, Papadopoulos MA. Bisphosphonates as Supplement to Dental Treatment: A Network Meta-Analysis. *J Dent Res.* 2021; 100: 341-51.
19. Khan A, Morrison A, Cheung A, Hashem W, Compston J. Osteonecrosis of the jaw (ONJ): diagnosis and management in 2015. *Osteoporos Int.* 2016; 27: 853-9.
20. Fung P, Bedogni G, Bedogni A, Petrie A, Porter S, Campisi G, et al. Time to onset of bisphosphonate-related osteonecrosis of the jaws: a multicentre retrospective cohort study. *Oral Dis.* 2017; 23: 477-83.
21. Parker SJ, Venkatraman V, Van Eyk JE. Effect of peptide assay library size and composition in targeted data-independent acquisition-MS analyses. *Proteomics.* 2016; 16: 2221-37.
22. Parker SJ, Stotland A, MacFarlane E, Wilson N, Orosco A, Venkatraman V, et al. Proteomics reveals Rictor as a noncanonical TGF-beta signaling target during aneurysm progression in Marfan mice. *Am J Physiol Heart Circ Physiol.* 2018; 315: H1112-H126.
23. Rost HL, Rosenberger G, Navarro P, Gillet L, Miladinovic SM, Schubert OT, et al. OpenSWATH enables automated, targeted analysis of data-independent acquisition MS data. *Nat Biotechnol.* 2014; 32: 219-23.
24. Rosenberger G, Koh CC, Guo T, Rost HL, Kouvonon P, Collins BC, et al. A repository of assays to quantify 10,000 human proteins by SWATH-MS. *Sci Data.* 2014; 1: 140031.
25. Teleman J, Rost HL, Rosenberger G, Schmitt U, Malmstrom L, Malmstrom J, et al. DIANA--algorithmic improvements for analysis of data-independent acquisition MS data. *Bioinformatics.* 2015; 31: 555-62.
26. Rost HL, Liu Y, D'Agostino G, Zanella M, Navarro P, Rosenberger G, et al. TRIC: an automated alignment strategy for reproducible protein quantification in targeted proteomics. *Nat Methods.* 2016; 13: 777-83.
27. Teo G, Kim S, Tsou CC, Collins B, Gingras AC, Nesvizhskii AI, et al. mapDIA: Preprocessing and statistical analysis of quantitative proteomics data from data independent acquisition mass spectrometry. *J Proteomics.* 2015; 129: 108-20.
28. Mi H, Ebert D, Muruganujan A, Mills C, Albuo LP, Mushayamaha T, et al. PANTHER version 16: a revised family classification, tree-based classification tool, enhancer regions and extensive API. *Nucleic Acids Res.* 2021; 49: D394-D403.
29. Ishtiaq S, Edwards S, Sankaralingam A, Evans BA, Elford C, Frost ML, et al. The effect of nitrogen containing bisphosphonates, zoledronate and alendronate, on the production of pro-angiogenic factors by osteoblastic cells. *Cytokine.* 2015; 71: 154-60.

30. Chen H, Fang Y, Wu J, Chen H, Zou Z, Zhang X, et al. RIPK3-MLKL-mediated necroinflammation contributes to AKI progression to CKD. *Cell Death Dis.* 2018; 9: 878.
31. Dai X, Deng Z, Liang Y, Chen L, Jiang W, Zhao W. Enterococcus faecalis induces necroptosis in human osteoblastic MG63 cells through the RIPK3 / MLKL signalling pathway. *Int Endod J.* 2020; 53: 1204-15.
32. Moriwaki K, Bertin J, Gough PJ, Orłowski GM, Chan FK. Differential roles of RIPK1 and RIPK3 in TNF-induced necroptosis and chemotherapeutic agent-induced cell death. *Cell Death Dis.* 2015; 6: e1636.
33. Bozec D, Iuga AC, Roda G, Dahan S, Yeretssian G. Critical function of the necroptosis adaptor RIPK3 in protecting from intestinal tumorigenesis. *Oncotarget.* 2016; 7: 46384-400.
34. Li H, Sun X, LeSage G, Zhang Y, Liang Z, Chen J, et al. beta-arrestin 2 regulates Toll-like receptor 4-mediated apoptotic signalling through glycogen synthase kinase-3beta. *Immunology.* 2010; 130: 556-63.
35. Amit S, Hatzubai A, Birman Y, Andersen JS, Ben-Shushan E, Mann M, et al. Axin-mediated CKI phosphorylation of beta-catenin at Ser 45: a molecular switch for the Wnt pathway. *Genes Dev.* 2002; 16: 1066-76.
36. Tamari T, Elimelech R, Cohen G, Cohen T, Doppelt O, Eskander-Hashoul L, et al. Endothelial Progenitor Cells inhibit jaw osteonecrosis in a rat model: A major adverse effect of bisphosphonate therapy. *Sci Rep.* 2019; 9: 18896.
37. Lang M, Zhou Z, Shi L, Niu J, Xu S, Lin W, et al. Influence of zoledronic acid on proliferation, migration, and apoptosis of vascular endothelial cells. *Br J Oral Maxillofac Surg.* 2016; 54: 889-93.
38. Basi DL, Lee SW, Helfman S, Mariash A, Lunos SA. Accumulation of VEGFR2 in zoledronic acid-treated endothelial cells. *Mol Med Rep.* 2010; 3: 399-403.
39. Taylor A, Harker JA, Chanthong K, Stevenson PG, Zuniga EI, Rudd CE. Glycogen Synthase Kinase 3 Inactivation Drives T-bet-Mediated Downregulation of Co-receptor PD-1 to Enhance CD8(+) Cytolytic T Cell Responses. *Immunity.* 2016; 44: 274-86.
40. McCubrey JA, Steelman LS, Bertrand FE, Davis NM, Abrams SL, Montalto G, et al. Multifaceted roles of GSK-3 and Wnt/beta-catenin in hematopoiesis and leukemogenesis: opportunities for therapeutic intervention. *Leukemia.* 2014; 28: 15-33.
41. McCubrey JA, Steelman LS, Bertrand FE, Davis NM, Sokolosky M, Abrams SL, et al. GSK-3 as potential target for therapeutic intervention in cancer. *Oncotarget.* 2014; 5: 2881-911.
42. Beurel E, Jope RS. The paradoxical pro- and anti-apoptotic actions of GSK3 in the intrinsic and extrinsic apoptosis signaling pathways. *Prog Neurobiol.* 2006; 79: 173-89.
43. Alao JP. The regulation of cyclin D1 degradation: roles in cancer development and the potential for therapeutic invention. *Mol Cancer.* 2007; 6: 24.
44. Kulkarni NH, Onyia JE, Zeng Q, Tian X, Liu M, Halladay DL, et al. Orally bioavailable GSK-3alpha/beta dual inhibitor increases markers of cellular differentiation in vitro and bone mass in vivo. *J Bone Miner Res.* 2006; 21: 910-20.
45. Kim DG. Can dental cone beam computed tomography assess bone mineral density? *Journal of bone metabolism.* 2014; 21: 117-26.
46. Nye SN CE, Emam H, Kim D-G. Heterogeneity of Bone Mineral Density in Osteonecrosis of the Jaw. 2018 AADR/CADR Annual Meeting (Fort Lauderdale, Florida). 2018.



## Review Article

Int Neurourol J 2021;25(Suppl 1):S3-7  
<https://doi.org/10.5213/inj.2142174.087>  
pISSN 2093-4777 · eISSN 2093-6931



# Irreversible Bladder Remodeling Induced by Fibrosis

Su Jin Kim<sup>1</sup>, Jayoung Kim<sup>2,3,4,5</sup>, Yong Gil Na<sup>6</sup>, Khae Hawn Kim<sup>6</sup>

<sup>1</sup>Department of Urology, Yonsei University Wonju College of Medicine, Wonju, Korea

<sup>2</sup>Departments of Surgery and Biomedical Sciences, Cedars-Sinai Medical Center, Los Angeles, CA, USA

<sup>3</sup>Samuel Oschin Comprehensive Cancer Institute, Cedars-Sinai Medical Center, Los Angeles, CA, USA

<sup>4</sup>University of California Los Angeles, Los Angeles, CA, USA

<sup>5</sup>Department of Urology, Ga Cheon University College of Medicine, Incheon, Korea

<sup>6</sup>Department of Urology, Chungnam National University Sejong Hospital, Chungnam National University College of Medicine, Sejong, Korea

Underactive bladder and impaired bladder compliance are irreversible problems associated with bladder fibrosis. Remodeling of the extracellular matrix is regarded as an important mechanism associated with bladder fibrosis. However, various risk factors and conditions contribute to the functional impairment of the bladder associated with fibrosis, and there is limited knowledge about bladder fibrosis-associated problems in the field of neurourology. Further studies are thus necessary to elucidate the underlying mechanism of bladder fibrosis and to identify effective treatment.

**Keywords:** Urinary bladder; Fibrosis; Extracellular matrix; Lower urinary tract symptoms; Collagen


- **Fund/Grant Support:** This research was supported by the Basic Science Research Program through the National Research Foundation of Korea (NRF) funded by the Ministry of Education (2018R1D1A3B07048492).
- **Conflict of Interest:** SJK and KHK, associate editors of *International Neurourology Journal*, are the authors of this article. However, they played no role whatsoever in the editorial evaluation of this article or the decision to publish it. Except for that, no potential conflict of interest relevant to this article was reported.

## INTRODUCTION

Bladder trabeculation refers to morphological changes of the bladder detrusor, including smooth muscle hypertrophy and increased collagen deposition in the detrusor extracellular matrix (ECM), resulting in fibrosis of the bladder [1,2]. These morphological changes of the bladder can be observed in patients with various voiding problems, such as neurogenic bladder and bladder outlet obstruction (BOO) [3-6]. Lower urinary tract symptoms (LUTS) in the men with benign prostatic hyperplasia (BPH) are associated with BOO, and the increased intravesical pressure that occurs in men with BOO induces hypertrophy of the bladder detrusor to overcome BOO. If BOO is

not relieved, irreversible morphological changes of the bladder, such as increased collagen accumulation and fibrosis of the bladder, occur. Fibrosis of the bladder causes the loss of normal detrusor contractility; and therefore, affected patients cannot urinate by themselves [6]. In addition to BOO associated with BPH, many other conditions are associated with fibrotic changes of the bladder, such as dementia, stroke, cerebral hemorrhage, spinal cord injury, diabetes mellitus, and aging [7].

Common LUTS associated with bladder fibrosis are a weak urinary stream, intermittency, increased residual urine sensation, and abdominal straining during urination because the fibrotic bladder loses normal contractility for expelling urine from the bladder. Medical therapies using parasympathomi-

**Corresponding author:** Khae Hawn Kim  <https://orcid.org/0000-0002-7045-8004>  
Department of Urology, Chungnam National University Sejong Hospital,  
Chungnam National University College of Medicine, 20 Bodeum 7-ro, Sejong  
30099, Korea

Email: kimcho99@cnuh.co.kr

**Submitted:** April 2, 2021 / **Accepted after revision:** May 10, 2021



This is an Open Access article distributed under the terms of the Creative Commons Attribution Non-Commercial License (<http://creativecommons.org/licenses/by-nc/4.0/>) which permits unrestricted non-commercial use, distribution, and reproduction in any medium, provided the original work is properly cited.



metics and alpha blockers have been attempted to help urination; however, inconsistent results have been reported regarding the effects of these treatments, and there is no clear evidence that they improve bladder contractility [8-11]. Some patients showed improvement of LUTS and the ability to urinate by themselves, but most patients continue to need indwelling urethral and suprapubic catheters to expel urine from their bladder due to an irreversible loss of bladder contractility [12-15].

At present, no effective treatment methods are available to prevent bladder fibrosis and to recover the impaired bladder contractility associated with bladder fibrosis. Thus, this review deals with the pathophysiology of bladder fibrosis and upcoming treatment based on a literature review.

### LUTS AND DECREASED CONTRACTILITY AND COMPLIANCE OF THE BLADDER DETRUSOR ASSOCIATED WITH BLADDER FIBROSIS

Underactive bladder (UAB) is a LUTS complex characterized by incomplete bladder emptying with a decreased urinary flow rate and increased postvoid residual urine volume [15]. UAB is associated with detrusor underactivity (DU) or acontractile detrusor observed in a urodynamic study. Morphological changes such as bladder fibrosis induced by increased collagen deposition in the detrusor ECM can induce DU and impairment of bladder contractility. According to a study reporting urodynamic results in UAB patients, detrusor hyperreflexia with impaired detrusor contractility (DHIC) was observed, as well as DU or acontractile detrusor [16]. Patients with DHIC experienced storage symptoms such as incontinence or urgency with accompanying symptoms induced by incomplete emptying [17]. These findings suggest that contractile changes associated with bladder fibrosis constitute a complicated process that results in impaired bladder contractility with or without detrusor overactivity. Furthermore, the process of a coexistent voiding problem that is not associated with bladder fibrosis (e.g., stress urinary incontinence) can be a factor that induces incontinence [18-20]. Moreover, Uren et al. [21] reported that patients diagnosed with DU using a urodynamic study showed nocturia, frequent daytime urination, urgency, and incontinence, as well as a weak urinary stream, hesitancy, and abdominal straining during urination. However, Uren et al. [21] did not investigate the etiology of DU, making it impossible to know whether the patients with storage LUTS had other voiding problems unrelated to DU.

Decreased bladder compliance is a change associated with bladder fibrosis. Bladder compliance can be conceptualized as the relationship between a change in bladder volume and a change in detrusor pressure. In general, bladder compliance is expressed as an increase in bladder volume per increment of intravesical pressure [22]. Thus, bladder compliance reflects the flexibility of the bladder. Fibrotic changes of the bladder reduce its flexibility and induce stiffness of the bladder and low bladder compliance. As a result, the intravesical pressure of a stiff bladder with low compliance is increased, and prolonged high intravesical pressure adversely affects renal function [23-26]. Therefore, it is important to improve bladder compliance and reduce the intravesical pressure of the bladder to prevent impairment of renal function. Patients with impaired bladder compliance show urge urinary incontinence [27].

Both UAB and impaired bladder compliance are associated with bladder fibrosis. However, it is unclear about why the consequences of bladder fibrosis sometimes appear as UAB or impaired bladder compliance. Previous studies have suggested that there may be a difference in the subtype of collagen deposition between UAB and impaired bladder compliance, and that increased proteoglycan deposition in the ECM may also be related factor (Fig. 1) [28-31].

### UNDERLYING MECHANISM ASSOCIATED WITH BLADDER FIBROSIS

Remodeling of the ECM and increased levels of transforming growth factor- $\beta$ 1 (TGF- $\beta$ 1) are regarded as the mechanism underlying bladder fibrosis [32]. The ECM of the bladder consists of collagen, elastin, fibronectins, and proteoglycans. Collagen is the major fibrous protein of the ECM and plays a role in providing tensile strength to the bladder. Collagen types I and III are the most important subtypes of collagen in the ECM [33-35]. Unlike collagen, elastin induces recoil of the ECM after stretching during urination. Conditions such as BOO and neurogenic bladder associated with mechanical or chemical stresses induce fibroblastic and inflammatory responses in the ECM. These responses dysregulate fibroblast secretion of matrix metalloproteinases (MMPs) and tissue inhibitors of MMPs (TIMPs) and increase ECM deposition. Prolonged ECM deposition increases the production of TIMPs which are associated with fibrosis and fibrotic changes of the bladder occur [36-38]. Moreover, increased levels of TGF- $\beta$ 1 induce fibrosis by stimulating collagen production through binding to serine/threonine ki-

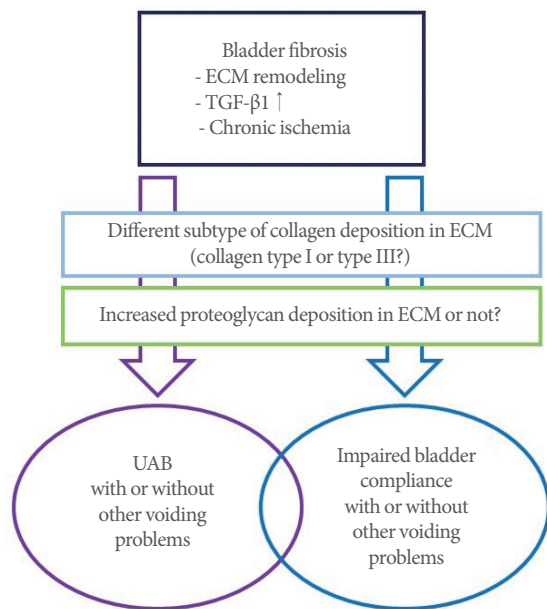


**Fig. 1.** Potential theoretical mechanism of bladder fibrosis-associated voiding problems. ECM, extracellular matrix; TGF- $\beta$ 1, transforming growth factor- $\beta$ 1; UAB, underactive bladder.

nase receptors on the cell surface, cause the phosphorylation of intracellular Smad2/3 transcription factors [39,40].

Chronic bladder ischemia may be a factor associated with bladder fibrosis. Previous studies have suggested that cardiovascular and metabolic diseases related to endothelial dysfunction decrease blood flow to the bladder. In turn, chronic ischemia of the bladder was found to increase oxidative stress and inflammatory cytokine levels, which might be associated with bladder fibrosis induced by nerve damage [41].

## UPCOMING THERAPEUTIC METHODS TO PREVENT AND TREAT BLADDER FIBROSIS

There is currently no effective treatment for LUTS associated with bladder fibrosis. Conventional medical treatment fails in most patients with voiding problems induced by bladder fibrosis, and these patients require catheterization to expel urine from the bladder. Therefore, studies have aimed to prevent and restore bladder fibrosis using antifibrotic agent such as relaxin. Ikeda et al. [42] showed that human relaxin-2 reversed fibrosis, decreased collagen deposition, and increased bladder compliance and detrusor contractility in patients with radiation-induced bladder fibrosis. A recent study reported that relaxin receptors were present in the dome and trigone of the human

bladder and that in vitro relaxin stimulation upregulated MMP-2 and decreased TGF- $\beta$ 1 [43].

Efforts have been made to apply stem cell and gene therapy to improve UAB associated with bladder fibrosis [20]. Several preclinical studies used various types of stem cells and showed improvements in detrusor contractility. A pilot study by Levanovich et al. [44] showed enhanced urination and a reduced need for clean intermittent catheterization in a patient with UAB after an intradetrusor injection of autologous muscle-derived stem cells.

## CONCLUSIONS

Bladder fibrosis is an irreversible change of the bladder that is associated with UAB and impaired bladder compliance. Although bladder fibrosis is a serious problem, it has been difficult to elucidate its exact underlying mechanism and risk factors. Moreover, the progression of voiding problems associated with bladder fibrosis cannot be predicted due to the unknown characteristics of conditions associated with bladder fibrosis. These problematic characteristics are also obstacles to the prevention and treatment of bladder fibrosis. Therefore, further studies are essential to elucidate the underlying mechanism of bladder fibrosis and to identify effective treatments.

## AUTHOR CONTRIBUTION STATEMENT

- Conceptualization: *SJK*
- Data curation: *JK*
- Formal analysis: *YGN*
- Funding acquisition: *KHK*
- Methodology: *JK*
- Project administration: *KHK*
- Visualization: *YGN*
- Writing-original draft: *SJK*
- Writing-review & editing: *SJK*

## ORCID

- |               |   |
|---------------|---|
| Su Jin Kim    | <a href="https://orcid.org/0000-0002-1917-2780">https://orcid.org/0000-0002-1917-2780</a> |
| Jayoung Kim   | <a href="https://orcid.org/0000-0002-3683-4627">https://orcid.org/0000-0002-3683-4627</a> |
| Yong Gil Na   | <a href="https://orcid.org/0000-0002-0794-5459">https://orcid.org/0000-0002-0794-5459</a> |
| Khae Hawn Kim | <a href="https://orcid.org/0000-0002-7045-8004">https://orcid.org/0000-0002-7045-8004</a> |

## REFERENCES

1. Barnard RJ, Dixon JS, Gosling JA. A clinical and morphological evaluation of the trabeculated urinary bladder. *Prog Clin Biol Res* 1981;78:285-8.
2. Jung JH, Cho SY, Yoo C, Oh SJ. Establishment of the novel cystoscopic classification for bladder trabeculation of neurogenic bladder. *Urology* 2014;84:515-9.
3. Selby B, Hidas G, Chuang KW, Soltani T, Billimek J, Kaplan S, et al. Development and validation of a bladder trabeculation grading system in pediatric neurogenic bladder. *J Pediatr Urol* 2020;16:367-70.
4. Hoffberg HJ, Cardenas DD. Bladder trabeculation in spinal cord injury. *Arch Phys Med Rehabil* 1986;67:750-3.
5. Bai SW, Park SH, Chung DJ, Park JH, Shin JS, Kim SK, et al. The significance of bladder trabeculation in the female lower urinary system: an objective evaluation by urodynamic studies. *Yonsei Med J* 2005;46:673-8.
6. Fusco F, Creta M, De Nunzio C, Iacovelli V, Mangiapia F, Li Marzi V, et al. Progressive bladder remodeling due to bladder outlet obstruction: a systematic review of morphological and molecular evidences in humans. *BMC Urol* 2018;18:15.
7. Santos-Pereira M, Charrua A. Understanding underactive bladder: a review of the contemporary literature. *Porto Biomed J* 2020;5:e070.
8. Gaitonde S, Malik RD, Christie AL, Zimmern PE. Bethanechol: is it still being prescribed for bladder dysfunction in women? *Int J Clin Pract* 2019;73:e13248.
9. Osman NI, Chapple CR. Are there pharmacotherapeutic options for underactive bladder? *Eur Urol Focus* 2018;4:6-7.
10. Yamanishi T, Yasuda K, Kamai T, Tsujii T, Sakakibara R, Uchiyama T, et al. Combination of a cholinergic drug and an  $\alpha$ -blocker is more effective than monotherapy for the treatment of voiding difficulty in patients with underactive detrusor. *Int J Urol* 2004;11:88-96.
11. Chang SJ, Chiang IN, Yu HJ. The effectiveness of tamsulosin in treating women with voiding difficulty. *Int J Urol* 2008;15:981-5.
12. Bayrak Ö, Dmochowski RR. Underactive bladder: a review of the current treatment concepts. *Turk J Urol* 2019;45:401-9.
13. Aggarwal H, Zimmern PE. Underactive bladder. *Curr Urol Rep* 2016;17:17.
14. Dewulf K, Abraham N, Lamb LE, Griebeling TL, Yoshimura N, Tyagi P, et al. Addressing challenges in underactive bladder: recommendations and insights from the Congress on Underactive Bladder (CURE-UAB). *Int Urol Nephrol* 2017;49:777-85.
15. Chapple CR, Osman NI, Birder L, Dmochowski R, Drake MJ, van Koevinge G, et al. Terminology report from the International Continence Society (ICS) Working Group on Underactive Bladder (UAB). *Neurourol Urodyn* 2018;37:2928-31.
16. Li X, Liao LM, Chen GQ, Wang ZX, Lu TJ, Deng H. Clinical and urodynamic characteristics of underactive bladder: data analysis of 1726 cases from a single center. *Medicine (Baltimore)* 2018;97:e9610.
17. Uren AD, Drake MJ. Definition and symptoms of underactive bladder. *Investig Clin Urol* 2017;58(Suppl 2):S61-7.
18. Natale F, Illiano E, Zucchi A, Balzarro M, La Penna C, Costantini E. Transobturator mid-urethral sling in females with stress urinary incontinence and detrusor underactivity: effect on voiding phase. *Int Urogynecol J* 2019;30:1519-25.
19. Ko KJ, Suh YS, Sung HH, Ryu GH, Lee M, Lee KS. Assessing the readjustable sling procedure (Remeex system) for female stress urinary incontinence with detrusor underactivity. *Int Neurourol J* 2017;21:116-20.
20. Cho KJ, Kim JC. Management of urinary incontinence with underactive bladder: a review. *Int Neurourol J* 2020;24:111-7.
21. Uren AD, Cotterill N, Harding C, Hillary C, Chapple C, Klaver M, et al. Qualitative exploration of the patient experience of underactive bladder. *Eur Urol* 2017;72:402-7.
22. Abrams P, Cardozo L, Fall M, Griffiths D, Rosier P, Ulmsten U, et al. The standardisation of terminology of lower urinary tract function: report from the Standardisation Sub-committee of the International Continence Society. *Neurourol Urodyn* 2002;21:167-78.
23. Nseyo U, Santiago-Lastra Y. Long-term complications of the neurogenic bladder. *Urol Clin North Am* 2017;44:355-66.
24. Holmdahl G, Sillen U, Hellström AL, Sixt R, Sölsnes E. Does treatment with clean intermittent catheterization in boys with posterior urethral valves affect bladder and renal function? *J Urol* 2003;170:1681-5.
25. Ghoniem GM, Bloom DA, McGuire EJ, Stewart KL. Bladder compliance in meningomyelocele children. *J Urol* 1989;141:1404-6.
26. Prakash NS, Lopategui DM, Gomez C. Changes in management of poorly compliant bladder in botulinum toxin A era. *Curr Urol Rep* 2017;18:64.
27. Truss MC, Stief CG, Uckert S, Becker AJ, Schultheiss D, Machtens S, et al. Initial clinical experience with the selective phosphodiesterase-I isoenzyme inhibitor vinpocetine in the treatment of urge incontinence and low compliance bladder. *World J Urol* 2000;18:439-43.
28. Lee BR, Perlman EJ, Partin AW, Jeffs RD, Gearhart JP. Evaluation of smooth muscle and collagen subtypes in normal newborns and those with bladder exstrophy. *J Urol* 1996;156:2034-6.

29. Imamura M, Kanematsu A, Yamamoto S, Kimura Y, Kanatani I, Ito N, et al. Basic fibroblast growth factor modulates proliferation and collagen expression in urinary bladder smooth muscle cells. *Am J Physiol Renal Physiol* 2007;293:F1007-17.
30. Asgari M, Latifi N, Heris HK, Vali H, Mongeau L. In vitro fibrillogenesis of tropocollagen type III in collagen type I affects its relative fibrillar topology and mechanics. *Sci Rep* 2017;7:1392.
31. Iozzo RY, Schaefer L. Proteoglycan form and function: a comprehensive nomenclature of proteoglycans. *Matrix Biol* 2015;42:11-55.
32. Koeck I, Burkhard FC, Monastyrskaya K. Activation of common signaling pathways during remodeling of the heart and the bladder. *Biochem Pharmacol* 2016;102:7-19.
33. Rozario T, DeSimone DW. The extracellular matrix in development and morphogenesis: a dynamic view. *Dev Biol* 2010;341:126-40.
34. Schaefer L, Schaefer RM. Proteoglycans: from structural compounds to signaling molecules. *Cell Tissue Res* 2010;339:237-46.
35. Almalki SG, Agrawal DK. Effects of matrix metalloproteinases on the fate of mesenchymal stem cells. *Stem Cell Res Ther* 2016;7:129.
36. Craig VJ, Zhang L, Hagood JS, Owen CA. Matrix metalloproteinases as therapeutic targets for idiopathic pulmonary fibrosis. *Am J Respir Cell Mol Biol* 2015;53:585-600.
37. Arpino V, Brock M, Gill SE. The role of TIMPs in regulation of extracellular matrix proteolysis. *Matrix Biol* 2015;44-46:247-54.
38. da Costa AWF, do Carmo Neto JR, Braga YLL, Silva BA, Lamounier AB, Silva BO, et al. Cardiac Chagas disease: MMPs, TIMPs, Galectins, and TGF- $\beta$  as tissue remodelling players. *Dis Markers* 2019;2019:3632906.
39. He R, Zhang J, Luo D, Yu Y, Chen T, Yang Y, et al. Upregulation of transient receptor potential canonical type 3 channel via AT1R/TGF- $\beta$ 1/Smad2/3 induces atrial fibrosis in aging and spontaneously hypertensive rats. *Oxid Med Cell Longev* 2019;2019:4025496.
40. Song S, Zhang R, Cao W, Fang G, Yu Y, Wan Y, et al. Foxm1 is a critical driver of TGF- $\beta$ -induced EndMT in endothelial cells through Smad2/3 and binds to the Snail promoter. *J Cell Physiol* 2019;234:9052-9064.
41. Yoshida M, Yamaguchi O. Detrusor underactivity: the current concept of the pathophysiology. *Low Urin Tract Symptoms* 2014;6:131-7.
42. Ikeda Y, Zabarova IV, Birder LA, Wipf P, Getchell SE, Tyagi P, et al. Relaxin-2 therapy reverses radiation-induced fibrosis and restores bladder function in mice. *Neurourol Urodyn* 2018;37:2441-51.
43. Diaz EC, Briggs M, Wen Y, Zhuang G, Wallace SL, Dobberfuhl AD, et al. Characterizing relaxin receptor expression and exploring relaxin's effect on tissue remodeling/fibrosis in the human bladder. *BMC Urol* 2020;20:44.
44. Levanovich PE, Diokno A, Hasenau DL, Lajiness M, Pruchnic R, Chancellor MB. Intradetrusor injection of adult muscle-derived cells for the treatment of underactive bladder: pilot study. *Int Urol Nephrol* 2015;47:465-7.

# Applications of artificial intelligence in urological setting: a hopeful path to improved care

Sung-Jong Eun<sup>1</sup>, Jayoung Kim<sup>2</sup>, Khae Hawn Kim<sup>3,\*</sup>

<sup>1</sup>Digital Health Industry Team, National IT Industry Promotion Agency, Jincheon, Korea

<sup>2</sup>Departments of Surgery and Biomedical Sciences, Cedars-Sinai Medical Center, Los Angeles, CA, USA

<sup>3</sup>Department of Urology, Chungnam National University Sejong Hospital, Chungnam National University School of Medicine, Sejong, Korea

Artificial intelligence (AI) has been introduced in urology research and practice. Application of AI leads to better accuracy of disease diagnosis and predictive model for monitoring of responses to medical treatments. This mini-review article aims to summarize current applications and development of AI in urology setting, in particular for diagnosis and treatment of urological diseases. This review will introduce that ma-

chine learning algorithm-based models will enhance the prediction accuracy for various bladder diseases including interstitial cystitis, bladder cancer, and reproductive urology.

**Keywords:** Artificial intelligence, Machine learning, Urology, Urological diseases

## INTRODUCTION

The advent of artificial intelligence (AI) marked one of the greatest advancements in technology. From smartphones to surgical robotics, AI has changed society in monumental ways. As AI technology continues to improve and advance, its applications in medicine will only expand even more (Mao and Vinson, 2018). AI in medicine can be divided into two classes: virtual and physical. Virtual AI includes informatics and systems-based learning, such as deep learning management of symptoms to guide treatment decisions. On the other hand, physical AI includes robots and nanotechnology for enhanced drug delivery (Hamet and Tremblay, 2017). Both branches of AI can contribute to incredible improvements in both patient care and healthcare management. These new tools and capabilities are particularly bound to make much-needed impacts in the field of urology.

Applications of AI would be beneficial across all relevant urological subdivisions, including benign urology and cancer. This reigns especially certain for analyzing massive amounts of pertinent data for diagnostics and prognostics. Machine learning (ML)

is a discipline of AI that integrates statistics with algorithms to find relationships from data (O'Mahony et al., 2014). Such a tool can be applied to clinical data and creates robust risk models and redefines classifications of diseases. As medicine advances to an era of "big data" with an increasing amount of complex healthcare data, ML can be a powerful resource in navigating, elucidating, and applying information (Checcucci et al., 2020). This present review paper will provide an overview of the current state of AI in urology as well as future prospective and limitations.

## APPLICATION OF ARTIFICIAL INTELLIGENCE IN UROLOGICAL SETTING

### AI in urine analysis

Urine can provide a wealth of information for a variety of diseases and conditions, including interstitial cystitis and urolithiasis. Cytology of the urine can even detect high-grade malignancies of the urinary tract (McIntire et al., 2019). However, the lack of standardized screening and poor accuracy due to manual observation can lead to unreliable and variable results (McCroskey et al.,

\*Corresponding author: Khae Hawn Kim  <https://orcid.org/0000-0002-7045-8004>

Department of Urology, Chungnam National University Sejong Hospital, Chungnam National University School of Medicine, 20 Bodeum 7-ro, Sejong 30099, Korea

Email: kimcho99@cnuh.co.kr

Received: September 12, 2021 / Accepted: October 10, 2021



2015). Noting this discrepancy and need, Sanghvi et al. (2019) successfully developed an AI algorithm capable of accurately analyzing urine samples for high-grade urothelial carcinoma. Urinalysis is also particularly important for addressing urinary tract infections (UTIs), the most common outpatient infections in the United States (Medina and Edgardo, 2019). Accurate and quick identification of the microbes underlying the infection is essential for providing the right antibiotics. However, culturing of the urine can take a prolonged period of time. A study developed a new strategy for urinalysis of UTI by integrating mass spectrometry with ML, which allowed for accurate bacterial identification in less than 4 hours (Florence et al., 2019).

### AI in benign urological conditions and diseases

In addition to urinalysis, AI can integrate into how other benign urological conditions and diseases are treated. For instance, Kadlec et al. (2014) developed an artificial neural network (ANN) that predicted patient outcomes after endourologic interventions for kidney stones. A separate study by Aminsharifi et al. (2017) developed a different ANN-based model that predicted outcomes for patients after percutaneous nephrolithotomy. Beyond predicting outcomes, various groups have also used AI to support physicians in diagnostics and treatment decisions. One study by Långkvist et al. (2018) created a deep convolutional neural network to help differentiate kidney stones from phleboliths in computed tomography (CT) scans.

### Big data-based ML application in urological cancers

Big data-based ML is a subfield of AI, which involves the development and deployment of dynamic algorithms to analyze data and facilitate complex pattern recognition. The basic prediction models of ML include adaptive boosted trees (AdaBoost), gradient boosted trees, k-nearest neighbor, support vector machines (SVMs), bagged SVM, and random forest. In the field of healthcare, ML has been increasingly successfully applied to preventive medicine, image recognition, diagnosis, personalized medicine, and clinical decision-making. In predicting urological cancers, ML has many applications, such as assisting in diagnosis, judging the stage and grade, providing reliable prognosis, predicting the incidence of postoperative complications, and evaluating the responses in individual therapy.

When compared with traditional statistical methods, AI application showed significantly better accuracy, suggesting that AI might assist the decision-making process of urologists (Catto et al., 2003). Authors found that the predictive capacities of relapse

accuracy using ANN or Neuro-fuzzy modeling were much better (88% and 95%, respectively) than traditional statistical methods (71%–77%). Xu et al. (2017) used a ML model to analyze the 3-dimensional bladder wall texture features based on CT/magnetic resonance imaging (MRI) images, which can accurately distinguish tumor and normal bladder wall tissue. This method can reduce the number of invasive examinations, such as cystoscopy and pathology. Kouznetsova et al. (2019) established a ML model to predict early and late stages bladder cancer (BC) by identifying metabolites that characterize different stages of BC. Other groups have used a ML model to predict the BC stage and grade before operation combined with CT or MRI technology (Wang et al., 2019). Song et al. (2020) developed a computational model that can use population-based BC data to predict 10-year overall survival without considering tumor grade.

ML algorithms can create recurrence and survival prediction models based on imaging and surgical data to evaluate the recurrence and survival rates of patients following 1, 3, and 5 years after cystectomy (Hasnain et al., 2019). Klén et al. (2019) created a ML model to assess potential risk factors for postoperative and surgical related mortality by analyzing patients at high risk of early death after radical cystectomy. Congestive heart failure and chronic lung disease were added to previously known independent prognostic risk factors for early death after cystectomy. This method only used preoperative data and can be used before surgery. Computer evaluation was evaluated on radiology information extracted from CT images of BC patients, and established a ML model to evaluate whether patients are sensitive to chemotherapy. This method significantly improves the diagnostic accuracy, helps reduce unnecessary complications, improves quality of life, and reduces costs.

Although ML is widely used in BC, there are still some limitations, such as the difficulty in quantitative analysis of observed endpoints or the inapplicability of generalizability in other data sets. Therefore, we need further verification to improve its accuracy and versatility. In this study, we aimed to identify the potential predictive features to immunotherapy specific to BC.

### AI in bladder diary

To manage patients with voiding dysfunction, hospitals have used various tools for patient management assistance, such as voiding charts. The void chart is one of the methods for doctors to objectively monitor the subjective symptoms of patients with voiding dysfunction. Since the diagnosis or treatment proceeds after doctors objectively patients' symptoms, the void chart is the start-

ing point of studies on voiding dysfunction, thereby being one of the most important diagnostic methods.

Many studies show that even if patients write the charts after being well educated, these data are inaccurate (Jarvis et al., 1980; Kim et al., 2014; Webb et al., 1992). There are many variables that can be monitored in the voiding charts, but it is clinically impossible to apply this method to all patients. In other words, there are many variables in voiding charts due to the issue of handwriting by patients with various abilities, so it is difficult to manage through accurate voiding charts. If accurate sensing technology based on AI technology and monitoring function to manage the voiding charts are implemented, systematic and efficient management of patient urination will be possible. If patients can carry their voiding charts like a watch or beeper and automatically record urination, it will be helpful in studying symptoms and mechanisms that have not been revealed in many patients.

Most of study based on AI, it proposes a technology to recognize the movement of urination by analyzing the data of acceleration signals and gyro signals collected from smart bands. Various methods and learning algorithms for motion recognition have been proposed. Most studies have used static algorithms such as ANNs (Karmonik et al., 2019; Kim et al., 2020; Nikkola et al., 2020; Prabhakar et al., 2019) and K-means clustering (Baser et al., 2020; Fraley and Raftery, 2002; Moon and Cho, 2021), or dynamic time warping (Powar and Chemmangat, 2019) in combination with algorithms. However, a time series algorithm should be used to predict or classify dynamically changing time series data. Typical

time series algorithms include dynamic Bayesian networks (Kamalabad and Grzegorzczuk, 2020), hidden Markov models (HMMs) (Sonnhammer et al., 1998), and recurrent neural networks (RNNs) (LeCun et al., 2015). The HMM and RNN methods have been widely used for time series data. However, HMMs are not appropriate for learning sequential data because each step is only influenced by the previous one. In concerned, it applied an RNN-based long short-term memory (Hochreiter and Schmidhuber, 1997) method to process patient urination recognition. It aims to improve the recognition rate of the user's urination and efficiently solve the existing issues such as the problem of not applying the past data. Thus, it developing an analytical technique for high accuracy while solving the limitation of existing studies.

The presented recognition technology of the patients' urination is an extension of the existing pattern recognition technology based on signal processing. This technology is similar to the technology of recognizing specific motions in the smart home care service. The proposed technology also recognizes the signal pattern of urination and measures the frequency and time of urination to automatically record the urination information of the patients. This study based on AI aims to develop a technology for recognizing patients' urination by collecting and analyzing sensed movement (acceleration and tilt angle) information in the patients' smart bands. This development is expected to lead to the implementation of the end-user's urination management monitoring system (Eun et al., 2021). Fig. 1 shows an example of a urination management monitoring system.

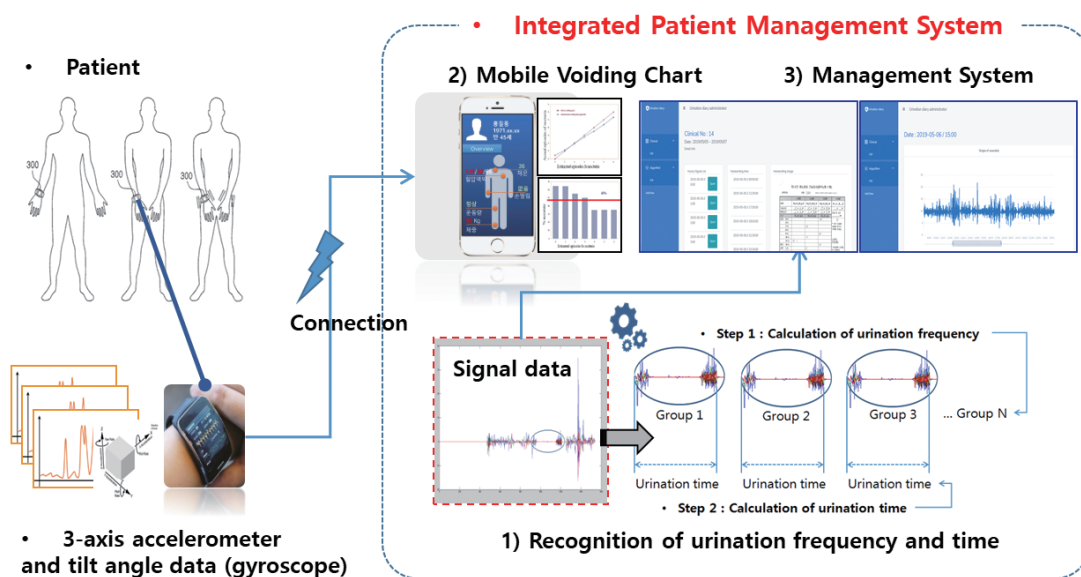


Fig. 1. The example of urination management monitoring system.

### AI applications in reproductive urology

The possibility of AI in medicine has been widely theorized over the past decades (Chung et al., 2019; Myung et al., 2019). Reproductive urology is a subfield where AI can contribute greatly because it has several limitations in the current predictive model and subjectivity within the field. Early AI application in reproductive urology focused on predicting semen parameters based on questionnaires identifying potential environmental factors and/or lifestyle influencing male fertility rates. AI has shown that genetic testing for anhydrosis has succeeded in predicting the number of patients most likely to need. With the recent development of image processing, automated sperm detection is a reality. The semen analysis, once a laboratory-only diagnostic test, has shifted to health consumer families with the emergence of AI. The prospects for AI in medicine are significant and have strong potential for AI in reproductive urology. Research identifying factors that may affect reproductive success by natural or assisted reproduction is of utmost importance to advance this field.

### CONCLUSIONS

This mini-review article aims to summarize the current application and development of AI, especially in the urology environment for the diagnosis and treatment of urology diseases. The emergence of AI marked one of the biggest advances in technology. From smartphones to surgical robotics, AI has transformed society in a monumental way. As AI technology continues to develop and expand, its applications in the medical field will expand even further. AI in medicine can be divided into two types: virtual and physical. Virtual AI includes informatics and system-based learning, such as in-depth learning management of symptoms that guide treatment decisions. On the other hand, physical AI includes robots and nanotechnology to strengthen drug delivery. Both areas of AI can contribute to remarkable improvements in both patient care and medical care. These new tools and functions are bound to have a very necessary impact, especially on the urology field. The application of AI will be beneficial across all relevant urology fields, including benign urology and cancer. These tools can be applied to clinical data, creating a robust risk model and redefining disease classification. As medicine develops into an era of “big data” and “artificial intelligence” where the amount of complex medical data increases, it can be a powerful resource in the search, explanation, and application of information.

### REFERENCES

- Aminsharifi A, Irani D, Pooyesh S, Parvin H, Dehghani S, Yousofi K, Fazel E, Zibaie F. Artificial neural network system to predict the postoperative outcome of percutaneous nephrolithotomy. *J Endourol* 2017;31:461-467.
- Baser A, Eliaçık S, Baykam MM, Tan FU. Clinical manifestations of overactive bladder with migraine as a comorbidity: a prospective cross-sectional study. *Int Neurourol J* 2020;24:375-381.
- Catto JWF, Linkens DA, Abbod MF, Chen M, Burton JL, Feeley KM, Hamdy FC. Artificial intelligence in predicting bladder cancer outcome: a comparison of neuro-fuzzy modeling and artificial neural networks. *Clin Cancer Res* 2003;9:4172-4177.
- Checucci E, Autorino R, Cacciamani GE, Amparore D, Cillis SD, Piana A, Piazzolla P, Vezzetti E, Fiori C, Veneziano D, Tewari A, Dasgupta P, Hung A, Gill I, Porpiglia F. Artificial intelligence and neural networks in urology: current clinical applications. *Minerva Urol Nefrol* 2020;72:49-57.
- Chung KJ, Kim JY, Whangbo TK, Kim KH. The prospect of a new smart healthcare system: a wearable device-based complex structure of position detecting and location recognition system, *Int Neurourol J* 2019;23:180-184.
- Eun SJ, Lee JY, Jung H, Kim KH. Personalized urination activity management based on an intelligent system using a wearable device. *Int Neurourol J* 2021;25:229-235.
- Florence RD, Gotti C, Leclercq M, Hélie MC, Boissinot M, Arrey TN, Daully C, Fournier F, Kelly I, Marcoux J, Julie BS, Bergeron MG, Droit A. Fast and accurate bacterial species identification in urine specimens using LC-MS/MS mass spectrometry and machine learning. *Mol Cell Proteomics* 2019;18:2492-2505.
- Fraley C, Raftery AE. Model-based clustering, discriminant analysis, and density estimation. *J Am Stat Assoc* 2002;97:611-631.
- Hamet P, Tremblay J. Artificial intelligence in medicine. *Metabolism* 2017;69S:S36-S40.
- Hasnain Z, Mason J, Gill K, Miranda G, Gill IS, Kuhn P, Newton PK. Machine learning models for predicting post-cystectomy recurrence and survival in bladder cancer patients. *PLoS One* 2019;14:e0210976.
- Hochreiter S, Schmidhuber J. Long short-term memory. *Neural Comput* 1997;9:1735-1780.
- Jarvis GJ, Hall S, Stamp S, Millar DR, Johnson A. An assessment of urodynamic examination in incontinent women. *Br J Obstet Gynaecol* 1980;87:893-896.
- Kadlec AO, Ohlander S, Hotaling J, Hannick J, Niederberger C, Turk TM. Nonlinear logistic regression model for outcomes after endourologic procedures: a novel predictor. *Urolithiasis* 2014;42:323-327.



- Kamalabad MS, Grzegorzczak M. Non-homogeneous dynamic Bayesian networks with edge-wise sequentially coupled parameters. *Bioinformatics* 2020;36:1198-1207.
- Karmonik C, Boone T, Khavari R. Data-driven machine-learning quantifies differences in the voiding initiation network in neurogenic voiding dysfunction in women with multiple sclerosis. *Int Neurourol J* 2019;23:195-204.
- Kim JK, Kim SJ, Park JM, Na YG, Kim KH. Past, present, and future in the study of neural control of the lower urinary tract. *Int Neurourol J* 2020; 24:191-199.
- Kim SH, Oh SA, Oh SJ. Voiding diary might serve as a useful tool to understand differences between bladder pain syndrome/interstitial cystitis and overactive bladder. *Int J Urol* 2014;21:179-183.
- Klén R, Salminen AP, Mahmoudian M, Syvänen KT, Elo LL, Boström PJ. Prediction of complication related death after radical cystectomy for bladder cancer with machine learning methodology. *Scand J Urol* 2019;53:325-331.
- Kouznetsova VL, Kim E, Romm EL, Zhu A, Tsigelny IF. Recognition of early and late stages of bladder cancer using metabolites and machine learning. *Metabolomics* 2019;15:94.
- Långkvist M, Jendeborg J, Thunberg P, Loutfi A, Lidén M. Computer aided detection of ureteral stones in thin slice computed tomography volumes using convolutional neural networks. *Comput Biol Med* 2018; 97:153-160.
- LeCun Y, Bengio Y, Hinton G. Deep learning. *Nature* 2015;7553:436-444.
- Mao S, Vinson V. Power couple: science and technology. *Science* 2018;316: 864-865.
- McCroskey Z, Pambuccian SE, Kleithers S, Antic T, Cohen MB, Barkan GA, Wojcik EM. Accuracy and interobserver variability of the cytologic diagnosis of low-grade urothelial carcinoma in instrumented urinary tract cytology specimens. *Am J Clin Pathol* 2015;144:902-908.
- McIntire PJ, Khan R, Hussain H, Pambuccian SE, Wojcik EM, Barkan GA. Negative predictive value and sensitivity of urine cytology prior to implementation of the Paris system for reporting urinary cytology. *Cancer Cytopathol* 2019;127:125-131.
- Medina M, Edgardo CP. An introduction to the epidemiology and burden of urinary tract infections. *Ther Adv Urol* 2019;11:1756287219832172.
- Moon JU, Cho KO. Current pharmacologic strategies for treatment of intractable epilepsy in children. *Int Neurourol J* 2021;25:58-18.
- Myung NV, Jung SY, Kim JY. Application of low-cost, easy-to-use, portable biosensor systems for diagnosing bladder dysfunctions. *Int Neurourol J* 2019;23:86-87.
- Nikkola J, Holm A, Seppänen M, Joutsu T, Rauhala E, Kaipia A. Repetitive transcranial magnetic stimulation for chronic prostatitis/chronic pelvic pain syndrome: a prospective pilot study. *Int Neurourol J* 2020;24:144-149.
- O'Mahony C, Jichi F, Pavlou M, Monserrat L, Anastasakis A, Rapezzi C, Biagini E, Gimeno JR, Limongelli G, McKenna WJ, Omar RZ, Elliott PM. A novel clinical risk prediction model for sudden cardiac death in hypertrophic cardiomyopathy (HCM risk-SCD). *Eur Heart J* 2014; 35:2010-2020.
- Prabhakar AT, Ahmed ASI, Nair AV, Mathew V, Aaron S, Sivadasan A, Alexander M. Neural correlates of urinary retention in lateral medullary infarction. *Int Neurourol J* 2019;23:205-210.
- Powar OS, Chemmangat K. Dynamic time warping for reducing the effect of force variation on myoelectric control of hand prostheses. *J Electromyogr Kinesiol* 2019;48:152-160
- Sanghvi AB, Allen EZ, Callenberg KM, Pantanowitz L. Performance of an artificial intelligence algorithm for reporting urine cytopathology. *Cancer Cytopathol* 2019;127:658-666.
- Song Q, Seigne JD, Schned AR, Kelsey KT, Karagas MR, Hassanpour S. A machine learning approach for long-term prognosis of bladder cancer based on clinical and molecular features. *AMIA Jt Summits Transl Sci Proc* 2020;2020:607-616.
- Sonnhammer EL, Von HG, Krogh A. A hidden markov model for predicting transmembrane helices in protein sequences. *Proc Int Conf Intell Syst Mol Biol* 1998;6:175-182.
- Wang H, Hu D, Yao H, Chen M, Li S, Chen H, Luo J, Feng Y, Guo Y. Radiomics analysis of multiparametric MRI for the preoperative evaluation of pathological grade in bladder cancer tumors. *Eur Radiol* 2019; 29:6182-6190.
- Webb RJ, Fawcett PR, Neal DE. Electromyographic abnormalities in the urethral and anal sphincters of women with idiopathic retention of urine. *Br J Urol* 1992;70:22-25.
- Xu X, Zhang X, Tian Q, Zhang G, Liu Y, Cui G, Meng J, Wu Y, Liu T, Yang Z, Lu H. Three-dimensional texture features from intensity and high-order derivative maps for the discrimination between bladder tumors and wall tissues via MRI. *Int J Comput Assist Radiol Surg* 2017;12:645-656.

Received 27 September 2021; revised 27 January 2022 and 19 March 2022; accepted 19 March 2022. Date of publication 15 April 2022; date of current version 2 May 2022. The review of this article was arranged by Associate Editor Yasemin M. Akay.

Digital Object Identifier 10.1109/OJEMB.2022.3163533

# Prediction of the Immune Phenotypes of Bladder Cancer Patients for Precision Oncology

HYUNA CHO <sup>1</sup>, FENG TONG <sup>2</sup>, SUNGYONG YOU <sup>3</sup>, SUNGYOUNG JUNG <sup>4</sup> (Senior Member, IEEE),  
 WON HWA KIM<sup>1,2,5</sup>, AND JAYOUNG KIM <sup>3,6</sup>

<sup>1</sup>Graduate School of Artificial Intelligence (GSAI), Pohang University of Science and Technology, Pohang 37673, South Korea

<sup>2</sup>Department of Computer Science and Engineering, University of Texas at Arlington, Arlington, TX 76019 USA

<sup>3</sup>Department of Surgery and Biomedical Sciences, Cedars-Sinai Medical Center, Los Angeles, CA 90048 USA

<sup>4</sup>Department of Electrical Engineering, University of Texas at Arlington, Arlington, TX 76019 USA

<sup>5</sup>Department of Computer Science and Engineering, Pohang University of Science and Technology, Pohang 37673, South Korea

<sup>6</sup>Department of Medicine, University of California Los Angeles, Los Angeles, CA 90095 USA

CORRESPONDING AUTHOR: JAYOUNG KIM (e-mail: Jayoung.kim@csmc.edu.)

The work of Jayoung Kim was supported in part by U.S.-Egypt Science and Technology Joint Fund and in part by the Samuel Oschin Comprehensive Cancer Institute at Cedars-Sinai Medical Center through 2019 Lucy S. Gonda Award. This work was supported in part by the Centers for Disease Controls and Prevention, National Institutes of Health under Grants 1U01DK103260, 1R01DK100974, U24 DK097154, 1U01DP006079, and NIH NCATS UCLA CTSI UL1TR000124, in part by the Department of Defense under Grants W81XWH-15-1-0415 and W81XWH-19-1-0109, in part by IMAGINE NO IC Research Grant, in part by the Steven Spielberg Discovery Fund in Prostate Cancer Research Career Development Award, in part by NIH under Grant R01 AG059312, in part by NSF under Grants IIS CRII 1948510 and IIS 2008602, and in part by the Korea Government (MSIT) at POSTECH under Grants IITP-2020-2015-0-00742 and IITP-2019-0-01906. The Subject Data in this work was supported in part by the National Academies of Sciences, Engineering, and Medicine, and in part by The United States Agency for International Development.

**ABSTRACT** Bladder cancer (BC) is the most common urinary malignancy; however accurate diagnosis and prediction of recurrence after therapies remain elusive. This study aimed to develop a biosignature of immunotherapy-based responses using gene expression data. Publicly available BC datasets were collected, and machine learning (ML) approaches were applied to identify a novel biosignature to differentiate patient subgroups. Immune phenotyping of BC in the IMvigor210 dataset included three subtypes: inflamed, excluded, and desert immune. Immune phenotypes were analyzed with gene expressions using traditional but powerful classification methods such as random forests, Deep Neural Networks (DNN), Support Vector Machines (SVM) together with boosting and feature selection methods. Specifically, DNN yielded the highest area under the curve (AUC) with precision and recall (PR) curves and receiver operating characteristic (ROC) curves for each phenotype ( $0.711 \pm 0.092$  and  $0.86 \pm 0.039$ , respectively) resulting in the identification of gene expression features useful for immune phenotype classification. Our results suggest significant potential to further develop and utilize machine learning algorithms for analysis of BC and its precaution. In conclusion, the findings from this study present a novel gene expression assay that can accurately discriminate BC patients from controls. Upon further validation in independent cohorts, this gene signature could be developed into a predictive test that can support clinical evaluation and patient care.

**INDEX TERMS** Artificial algorithm, biomarker, bladder cancer, gene expression, immunotherapy, machine learning.

**IMPACT STATEMENT** **Machine Learning Approaches to Predict the Immune Phenotypes in Bladder Cancer Patients:** To develop a biosignature of immunotherapy-based responses using gene expression data, Deep Neural Networks (DNN), Support Vector Machines (SVM) together with boosting and feature selection methods were applied. DNN yielded the highest area under the curve (AUC) with receiver operating characteristic (ROC) curves and precision and recall (PR) curves for each phenotype ( $0.711 \pm 0.092$  and  $0.86 \pm 0.039$  respectively). Our results suggest significant potential to further develop and utilize machine learning algorithms for analysis of bladder cancer and its precaution.

## I. INTRODUCTION

Globally, bladder cancer (BC) is the ninth most common malignant tumor. BC also accounts for 4% of all cancer-related deaths in the United States, ranking it the fifth most deadly cancer [1]. According to the American Cancer Society, there will be approximately 83730 new cases of BC (about 64280 in men and 19450 in women) and about 17200 BC-related deaths (about 12260 in men and 4940 in women) in the United States, alone, in 2021. If your paper is intended for a conference, please contact your conference editor concerning acceptable word processor formats for your particular conference.

Based on the degree of bladder muscle wall infiltration, BC can be classified as either non-muscle invasive (NMIBC) or muscle invasive (MIBC). About 70% of BC patients have NMIBC, while the other 30% have MIBC or metastatic disease [2]. Treatment for NMIBC includes endoscopic resection of the tumor followed by adjuvant intravesical treatment to reduce the possibility of recurrence or progression. The risk of recurrence and progression is affected by many factors, including tumor grade, size, staging, multiplicity, recurrence rate, and the presence of carcinoma in situ (CIS). BC requires a lifetime of close monitoring and repeated treatments, which places an immensely heavy burden on patients and the social economy. MIBC treatment options include chemotherapy and radical cystectomy. The 5-year and 10-year survival rates of MIBC are approximately 50% and 36%, respectively. However, the 5-year survival rate of metastatic BC is only 15%, and the median overall survival (OS) is about 15 months following platinum-based chemotherapy.

Immunotherapies against BC have shown encouraging results. The first immunotherapy against BC was reported in 1976, when Alvaro Morales reported 9 cases of BC that were successfully treated with *Bacillus Calmette-Guerin* (BCG), demonstrating the immunogenicity of BC [3]. Immune checkpoint inhibitors (CPIs) are leading the field of immunotherapies against BC. It includes anti-cytotoxic T lymphocyte antigen 4 (CTLA4), anti-programmed cell death 1 (PD-1), and anti-programmed cell death 1 ligand 1 (PD-L1) antibodies. Anti-CTLA4, anti-PD-1, and anti-PD-L1 CPIs can improve anti-tumor immune response by restoring T-lymphocyte activation [4]. With the rapid advancement of new immunotherapy drugs, the development and validation of biomarkers will be important. Established biomarkers can help clinicians predict whether treatments will be effective. Varying subtypes of BC may also have definitive biological differences, which can result in variable sensitivity to Immunotherapies. In order to fully optimize the benefits of immunotherapy in future treatments and to further improve its impacts, supplemental biomarkers capable of monitoring response should be integrated.

Despite the initial success of cancer immunotherapies [5], approximately 70% of patients with advanced urethral cancer are considered unresponsive to anti-PD-1 or anti-PD-L1 antibodies [6], [7].

Recent studies have employed a variety of biomarkers such as PD-L1 hyperexpression and tumor mutation burden (TMB)

to distinguish the potential immunotherapy responders from non-responders [5]. There seems to exist a link between these biomarkers and immunotherapy outcomes, but neither PD-L1 expression nor TMB was sufficient to distinguish immunotherapy responder from non-responders [8], [9]. For example, the epithelial PD-L1 expression in BC has been shown to be unrelated to immunotherapy responses [10]. In addition, there has been difficulty predicting responses using TMB as a single marker [11], although increased TMB has been linked to improved clinical outcomes of immunotherapy in bladder cancer [12]. These previous works indicate the unmet needs to identify more reliable biomarkers for the stratification of immunotherapy responders from non-responders.

IMvigor210 was an open multicenter, single-arm phase 2 clinical study designed to study whether atezolizumab could become the standard treatment for advanced urothelial cancer. This study suggested that for patients with first-line platinum-based refractory metastatic urothelial carcinoma (mUC) checkpoint inhibitors seem to be more attractive than chemotherapy [13]. Atezolizumab is now suggested to prescribe for many patients who are ineligible for cisplatin therapy. In our study we used the publicly available IMvigor210 data. Previously, IMvigor210 data has been used to test the prognostic power of gene expression signatures for basal and luminal/differentiated BC subtypes [14]. Overall survival, prognosis and response to immunotherapy were also studied in the IMvigor 210 cohort [15]. A consensus molecular classification system for MIBC was suggested by analyzing the 1750 MIBC transcriptomic profiles from datasets including IMvigor dataset, providing a tool for testing and validation of potential predictive MIBC biomarkers [16].

Big data-based ML has been increasingly used and successfully applied to preventive medicine, image recognition, diagnosis, personalized medicine, and clinical decision-making. Application of machine learning (ML) algorithms to determine the cancer-specific classifiers have been tried in a series of studies. To determine the multi-variate classifiers predicting response to paclitaxel-therapy, methylome and miRNome were used [16]. Not only in vivo multi-omics profiles [17] but also in vivo cancer molecular profiles were able to predict the drug-sensitive tumors using ML modeling approach [18].

Clinical application of conventional ML approaches has been performed for the more accurate clinical decision, which was benefited by an increased computational power and accumulated digital health data from patients [19], [20]. However, we are aware the limitations due to the complicated data processing (feature engineering) including knowledge-based training [21], [22]. ML algorithms derived from not-so-relevant data resources, low volume of patients, data with high sparsity and poor could significantly diminish enthusiasm and reduce the efficacy of ML approach [23].

Although ML is widely used in the context of BC, there are still limitations, including difficulties in quantitatively analyzing observed endpoints and the inapplicability of generalizability across data sets. Therefore, further verification is needed to improve the accuracy and versatility of ML in BC.

Therefore, in this study, we aimed to search for the potential of using ML algorithms to investigate relationships between gene expression features with immunotherapies specific to BC and identify potentials to develop and use ML algorithms for such studies. For this, we have adopted five different traditional but powerful ML classification methods (i.e., Random Forest, Deep Neural Network, Support Vector Machine, Adaboost and XGBoost) to predict BC immune phenotypes using high-dimensional gene features. With efforts to avoid pitfalls of these algorithms, e.g., overfitting, we managed to get successful classification performance identifying phenotype-specific gene features (see Section IV for detailed clinical and technical discussions). We see great possibility to further develop more sophisticated and task-specific ML algorithm for analyzing BC with gene data to provide diagnostic tool for individuals and identify BC in their early stages, or possibly even prevent the disease.

## II. MATERIALS AND METHODS

### A. ETHICS STATEMENT

For this paper, we used deposited datasets derived from previously published studies. Use of publicly deposited data does not require IRB approval.

### B. DESCRIPTION OF THE DATASET

For this study, we have used the IMvigor210 data that can be found in previous report [24] and the associated resource web site provided by Dorothee Nickles, Yasin Senbabaoglu, Daniel Sheinson at <http://research-pub.gene.com/IMvigor210CoreBiologies/>. The raw data are available at the European Genome-phenome archive (EGA) under the accession number EGAS00001002556. The IMvigor210CoreBiologies package can be downloaded at <http://research-pub.gene.com/IMvigor210CoreBiologies/IMvigor210CoreBiologies.tar.gz>. Code for data processing, analysis and plotting and the R script are available from this IMvigor210CoreBiologies package.

The IMvigor210 study was a phase 2, multicenter, single-arm, open-label, and 2 cohort trial that assessed atezolizumab as a treatment for metastatic urothelial cancer in cisplatin-ineligible patients [25]. Clinical data for the first-line cisplatin-ineligible IMvigor210 cohort was collected from 47 academic medical centers and community oncology practices across 7 countries in North America and Europe. All participants in the study consented.

The IMvigor210 dataset includes recorded responses to immune checkpoint blockade. This Illumina HiSeq 2500-based dataset contains 348 subjects (76 female and 272 male) with 17692 gene expression biomarkers (i.e., features), which were derived from genes using Entrez gene ID and gene symbol. Archival tumor tissues were collected for biomarker assessments, and gene expression was designed to be quantified for a T-effector gene signature (consisting of CD8A, GZMA, GZMB, PRF1, INFG, and TBX21) [5]. The feature values of gene information were normalized using the trimmed mean

of M-values (TMM) method. Each sample includes corresponding clinical labels, such as age, sex, PD-L1 status of immune cells, prior tobacco use, metastatic disease, best confirmed overall survival, overall response, Response Evaluation Criteria in Solid Tumor (RECIST), immune phenotype, and The Cancer Genome Atlas (TCGA) subtype. For this study, three specific immune phenotypes were investigated: immune deserts, immune-excluded, and inflamed.

All types of human cancers, including BC, can be categorized into three immune phenotypes. These phenotypes are distinguished by the strength and relationship of the immune response of T-cells acting on the tumors, and different treatments should be applied based on the individual immunological biology of each phenotype. The IMvigor210 dataset consists of 76, 134, and 74 samples of immune deserts, immune-excluded, and inflamed phenotypes, respectively. The immune desert subtype is absent of immune cells, with total lack of an immune response against the tumor. The immune-excluded subtype has an immune response with only peripheral invasion of T-cells that cannot completely overwhelm the tumor. The inflamed subtype involves an active immune response where inflammatory myeloid cells and activated CD8+ T-cells exist in the tumor [26], [27]. Since the remaining 64 samples in the dataset did not provide any information on immune phenotypes, they were disregarded for this study.

### C. CLASSIFICATION METHOD

Five powerful ML-based classification algorithms, i.e., Support Vector Machine (SVM), Random Forest, XGBoost, Adaboost and deep neural network (DNN) were adopted to investigate immune phenotypes using gene expression features [28]–[32]. We performed a supervised learning task, where each data sample consists of a feature vector and class label. In our experiment, the algorithms were trained to learn optimized mapping between the features (i.e., gene expression) and target labels (i.e., immune phenotypes).

SVM is a well-known supervised classification algorithm that can learn a decision boundary, either linear or non-linear, in a feature space. Given data samples forming individual clusters in the feature space according to class labels, SVM learns a decision boundary that maximizes the margin of distance between the decision boundary and other clusters [33]. Such a criteria intuitively makes sense as the distance between individual clusters and the learned decision boundary will be balanced. To train a linear model when the data are not linearly separable, the model requires a regularizer with a user parameter (i.e., slack variable) that controls the margin and tolerable error within the margin. Training a non-linear model requires a kernel function (e.g., Gaussian and polynomial kernels) that can map the data onto a high-dimensional space where the data can become linearly separable. Taking the trained decision boundary back to the original space will then yield an optimized non-linear decision boundary [34].

Random Forest is one of the ensemble methods for classification and regression tasks. A sole Decision Tree can perform the same tasks on supervised learning problems by asking a



series of questions regarding to the characteristics of input variables. To avoid overfitting with large trees [35], [36], Random Forest incorporates multiple Decision Trees and casts a majority vote from the results classified from each tree. This ensemble technique is known as Bagging [37], which is an abbreviation of Bootstrap Aggregation. It is a method of extracting samples multiple times (Bootstrapping [38]) and training each model to aggregate the results. Although some trees created by Random Forest can be overfitted, an overwhelming majority can suppress the flaw from having a significant impact on prediction of class labels, i.e., classification.

In addition, we adopted another ensemble method, Boosting algorithm [39], based on the Decision Tree architecture. Unlike to Bagging where each tree makes independent decisions, Boosting has a sequential prediction process in which one model influences the decision of the next tree. In this process, Boosting repeats multiple steps to create a new classification criterion by improving weights on misclassified data. Finally, it creates a strong classifier gathering weak classifiers altogether to result in the ensembled output. In this paper, we used XGBoost [40] and Adaptive Boost (AdaBoost) [41], [42]. The difference of two methods is the way to deliver information of misclassified data from previous models. For example, AdaBoost updates subsequent classifiers based on the weight values of the former models. However, the update of XGBoost is based on gradient descent with a greedy algorithm.

Lastly, for the deep learning (DL) approach, we used a DNN algorithm with multiple hidden layers [30]. This consisted of an input layer for the original data, output layer for prediction outcome (e.g., pseudo-probability for each class), and a varying number of hidden layers where the input data can be transformed and model parameters are trained to minimize prediction error, usually defined by cross-entropy. While the input and output layers contain nodes according to the input dimension and the number of class labels respectively, each hidden layer is composed of hidden nodes determined by a user. At each hidden node, the node from its previous layer becomes the input, which is connected to the hidden node via edges with corresponding edge weights. The input values and edge weights at each hidden node are first linearly combined and then fed into a non-linear activation function (e.g., sigmoid or rectified linear unit (ReLU)) to yield an output that goes into the following layer as an input. At the output layer, the outcome values from each node are normalized to yield a pseudo-probability that tells which class label is the most likely for a given data sample. The  $l_1$ - and  $l_2$ -regularizers were applied onto the model parameters for sparsity as in least absolute shrinkage and selection operator (LASSO [43], [44], depicting important features only by suppressing weights of unimportant features to 0) and to make the model stable [28].

#### D. MODEL TRAINING

In order to obtain unbiased results, we used 10-fold cross validation (CV) to conduct experiments with the two five classification algorithms [45]. For the SVM, we utilized both

linear and non-linear models. An RBF kernel was used for the non-linear classifier. The slack variable  $C$  was varied from 0.01 to 1000 to find the best performance. For Decision Tree-based models, such as Random Forest, XGBoost and AdaBoost, the number of trees per fold was kept to the same rate for comparing all results under unbiased conditions. The number of Decision Trees per fold was set to 100 and all Decision Trees were generated by allowing random sampling with replacement. The final classification was decided by majority voting incorporating outputs from every single classifier. The number of Decision Trees in all Boosting methods was set to 100. As for learning rates, XGBoost and AdaBoost were set to 0.1 and 1.0 respectively, with the highest test accuracy score for each classifier. For the DNN, we tried multiple settings by adjusting the number of hidden layers, nodes, and regularizers. The number of hidden layers varied from 0 to 3, and the number of hidden nodes in each layer varied between 16 and 1024. A drop rate ranging from 0.1 to 0.5 was applied. To measure the error of the model, cross-entropy was used. For the activation function, ReLU was used and Softmax was applied at the output layer to obtain the likelihood for each class. The overall model was trained by backpropagating the error from cross-entropy with gradient descent using the Adaptive Moment Estimation (Adam) optimizer [46].

#### E. FEATURE SELECTION

Since the data is compiled in a very high-dimensional space, statistical hypothesis tests were used to select effective features for distinguishing different groups. Statistical group analysis for each pair of phenotypes was applied on each feature, and resultant  $p$ -values were corrected for multiple comparisons using Bonferroni correction at the 0.05 confidence level. The feature selection process was applied only at the training stages (i.e., excluding test data) across each fold in CV where the phenotype labels were available; hence, avoiding circular analysis.

#### F. EVALUATION

To evaluate the performance of our classification results, we measured accuracy, precision, and recall. Accuracy was computed as the ratio of the number of correct predictions out of the total number of samples in a testing dataset. Precision and recall were considered for binary classification (i.e., positive vs. negative); precision measures how precise the prediction is for the positive class, while recall measures how much of the positive samples in the training dataset are correctly covered by the prediction. While accuracy is an intuitive and important measure for evaluation, precision and recall are also important for evaluating data with imbalanced class labels. Since precision and recall are computed for binary classification tasks, we computed them in a one-versus-all manner; out of the three immune phenotype classes, one of them is selected as positive. The other two were combined and considered the negative class. This is iterated for all the three classes as positive, yielding three individual results. We also plotted receiver operating characteristic (ROC) and precision and recall (PR) curves.

**TABLE 1. Comparison of Representative Results in Different Settings**

Classifier	Mean Train Acc	Mean Test Acc	MCC (Threshold: 0.5)	Mean Precision (std)	Mean Recall (std)	Mean AUC of PR (std)	Mean AUC of ROC (std)
SVM (Linear)	1	0.655	0.457	0.667 (0.036)	0.645 (0.048)	0.674 (0.031)	0.799 (0.083)
SVM (RBF)	1	0.655	0.456	0.655 (0.018)	0.644 (0.048)	0.678 (0.034)	0.798 (0.083)
SVM (RBF) (feature selection)	0.963	0.68	0.495	0.701 (0.035)	0.663 (0.118)	0.688 (0.034)	0.822 (0.066)
Random Forest	1	0.496	0.344	0.752 (0.099)	0.473 (0.104)	0.670 (0.045)	0.795 (0.086)
Random Forest (feature selection)	1	0.570	0.404	0.737 (0.089)	0.558 (0.051)	0.691 (0.051)	0.817 (0.077)
XGBoost	1	0.623	0.406	0.647 (0.043)	0.606 (0.103)	0.646 (0.073)	0.793 (0.081)
XGBoost (feature selection)	1	0.605	0.380	0.623 (0.029)	0.598 (0.059)	0.616 (0.055)	0.770 (0.089)
AdaBoost	0.821	0.613	0.386	0.714 (0.144)	0.547 (0.287)	0.649 (0.094)	0.776 (0.135)
AdaBoost (feature selection)	0.810	0.577	0.314	0.632 (0.116)	0.528 (0.239)	0.576 (0.110)	0.726 (0.163)
DNN (feature selection)	0.715	0.641	0.473	0.679 (0.045)	0.626 (0.101)	0.755 (0.099)	0.875 (0.054)
DNN (l1 regularizer)	0.834	0.616	0.412	0.685 (0.069)	0.590 (0.109)	0.771 (0.118)	0.870 (0.027)
DNN (feature selection, l1 regularizer)	0.719	0.666	0.488	0.722 (0.084)	0.635 (0.134)	0.771 (0.092)	0.860 (0.039)

The area under the curve (AUC) was computed for evaluation (higher AUC denotes better performance). To understand the effectiveness of a classifier on an imbalanced dataset, the AUC scores of both curves were used as quantified summaries of the model performance as well as Mathews Correlation Coefficient (MCC) at a threshold of 0.5 to determine positive and negative labels. These values ranged between 0.0 to 1.0, with larger scores suggesting that a model is more robust.

### G. IMPLEMENTATION ENVIRONMENT

All experiments were implemented in Python on a Nvidia GeForce RTX 2070 SUPER graphic card. DNN was designed based on Keras and scikit-learn machine learning libraries were utilized for the other methods. As for statistical tests, scipy library was used to derive p-values.

### III. RESULTS

Classification results on Immune Phenotypes of BC using the five classification methods are demonstrated in this section.

#### A. CLASSIFICATION OF IMMUNE PHENOTYPES WITH SVM

Immune phenotyping of BC from the Invigor210 dataset resulted in three subtypes, inflamed, immune-excluded, and immune desert; all of which are characterized by distinct T lymphocyte infiltration patterns. Immune desert tumors have

Evaluation measures were averaged across 10-fold. These values range between 0 and 1, with values closer to 1 indicating better performance. The area under the curve (AUC) of precision and recall (PR) curves accounts for the class imbalance in performance evaluation poor infiltration of immune cells (absence of pre-existing antitumor immunity),

immune-excluded tumors only exhibit retention of T lymphocytes in the reactive stroma, and inflamed tumors show infiltrated T lymphocytes [47], [48]. The overall results are summarized in Table 1.

The classification process using an SVM-based system was implemented with two types of kernel functions (i.e., linear kernel and radical basis function (RBF)). As shown in Table 1, the best accuracy scores of both SVM experiments without feature selection were 0.655 while their training accuracies were 1. This indicates that there was a serious overfitting (i.e., the model worked perfectly on the training data but significantly failed to do so for testing data). The slack variable utilized in the two cases were 100. When statistical feature selection was applied to the input data of SVM with RBF kernel, the average test accuracy across CV scored the highest (0.68) throughout all experiments, which suggests that feature selection based on statistical group tests was effective. For slack variables, the score reached a peak at 10 and decreased slightly as the variables changed. On the other hand, linear SVM with feature selection yielded poor results. The accuracy was 0.588 regardless of the slack variable.

In Fig. 1, PR and ROC curves for the three SVM experiments are described for the 3 classes, which are marked in blue (immune desert), orange (inflamed), and green (immune-excluded). Among the results with various SVMs, similar to the results of the test accuracy, SVM with RBF kernel and feature selection resulted in the highest average

AUC scores for both metrics among SVM results; 0.688 and 0.812 for the PR and ROC curves, respectively. Accordingly, MCC of 0.495 for this case was the highest as well. Notably, all of the averaged AUC scores of the PR

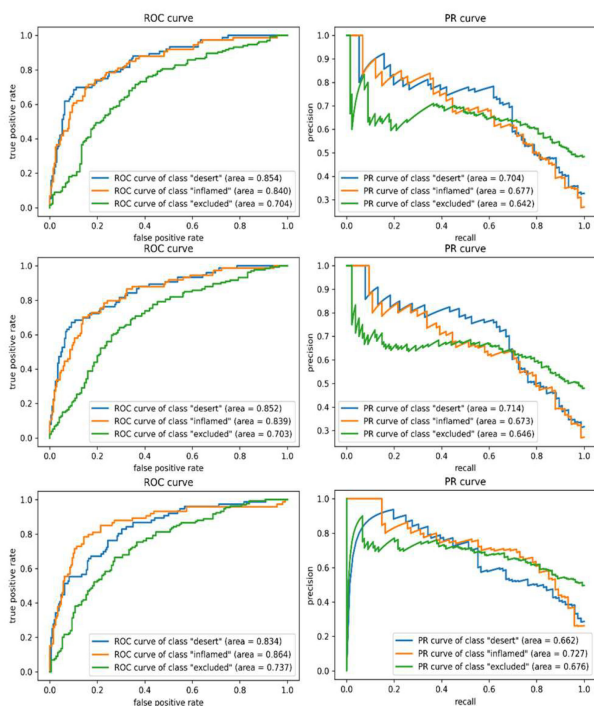


**FIGURE 1. Receiver operator characteristic (ROC) and precision and recall (PR) curves for each class using support vector machine (SVM). Top: Linear SVM, mid: SVM (RBF), bottom: SVM (RBF) with feature selection. Higher AUCs, closer to 1, indicate better performance. High AUCs with ROC curves for each phenotype indicate the model is predicting the phenotypes with low false positives. PR curves show that classification performance for the immune-excluded class is enhanced (green line) by feature selection.**

and ROC curves across SVM classes were recorded slightly smaller than the results from DNN models.

## B. CLASSIFICATION OF IMMUNE PHENOTYPES WITH RANDOM FOREST

Test accuracy of Random Forest scored the lowest throughout all experiments regardless of feature selection. Similar to SVM, training accuracies of Random Forest were 1, denoting that this algorithm has also overfitted to the input data and yielded poor test accuracy and MCC. But interestingly, we can see that mean precision recorded the highest score among all models as shown in Table 1, whether feature selection is applied or not. This highest precision value indicates that Random Forest was able to produce the lowest number of false positive samples. Notably, applying Bonferroni correction reduced the gap between precision and recall, so that the AUC scores of all classes in PR and ROC plot (shown in Fig. 2) outperformed to those of non-feature selected Random Forest.

## C. CLASSIFICATION OF IMMUNE PHENOTYPES WITH XGBOOST AND ADABOOST

For Boosting methods, the most representative Boosting algorithms, AdaBoost and XGBoost were employed and their performance curves are shown in Fig. 3. As shown in Table 1, the overall test accuracy and MCC of both Boosting

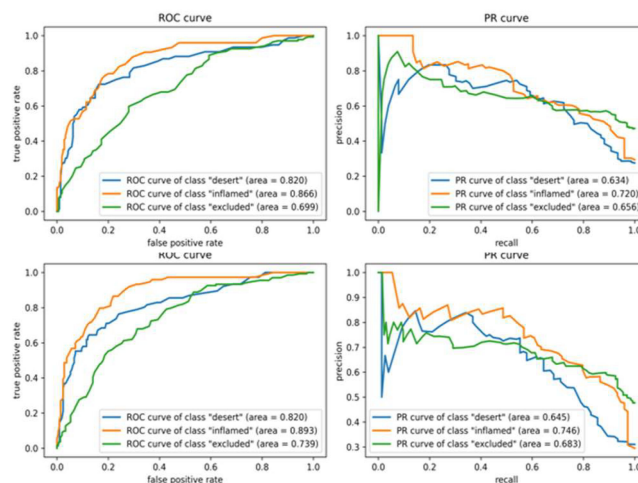


**FIGURE 2. Receiver operator characteristic (ROC) and precision and recall (PR) curves for each class using Random Forest. Top: Random Forest without feature selection, bottom: Random Forest with feature selection. Higher AUCs, closer to 1, indicate better performance. High AUCs with ROC curves for each phenotype indicate the model is predicting the phenotypes with low false positives. ROC curves show that classification performance for the immune-excluded class is enhanced (green line) by feature selection. Likewise, comparing two PR curve plots illustrates that performance of all classes with feature selection has outperformed.**

algorithms scored higher than Random Forest but lower than SVM and DNN. Although XGBoost was overfitted for training data, on the contrary to AdaBoost, the test accuracy of XGBoost was slightly higher than for AdaBoost's. Also, applying feature selection to Boosting classifiers resulted a worse performance for all metrics compared to models without Bonferroni correction.

Therefore, we can see that the feature selection was invalid in respect of Boosting algorithms that focus weights on misclassified samples for improving accuracies. In other words, the eliminated features from Bonferroni correction have had a substantial influence on decision-making processes in Boosting models, especially for identifying the attributes of incorrectly classified dataset.

## D. CLASSIFICATION OF IMMUNE PHENOTYPES WITH DNN

Various classification experiments using DNN were performed with the settings described in the Methods section. Representative results are summarized in Table 1. With a very naïve DNN model without any regularizers or techniques to make the model robust (i.e., dropout, batch normalization, and feature selection), the resultant accuracy averaged across all 10 folds was 0.549. Considering the baselines with random guess (0.33) and prediction as the dominant class (0.472), the model was properly learning to predict BC immune phenotypes. However, it suffered from overfitting and relatively low accuracy compared to the SVM-based models. Applying a dropout rate of 0.3, statistical feature selection, and l1-regularizer (with hyper parameters 0.01 and 0.08 for each layer) on two hidden layers with 32 hidden nodes, the accuracy increased to 0.666 with averaged respective precision and recall of 0.722 and 0.635 across different class labels.



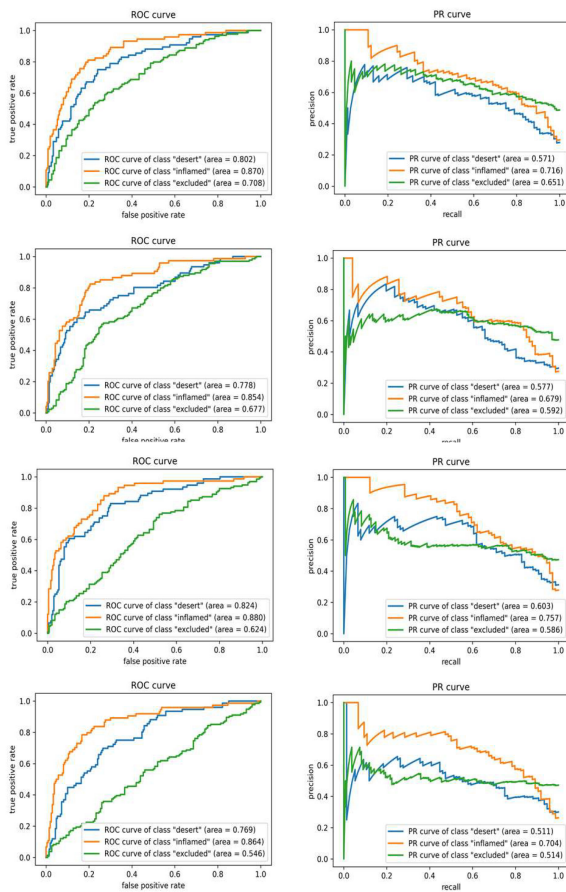


**FIGURE 3. Receiver operator characteristic (ROC) and precision and recall (PR) curves for each class using XGBoost and AdaBoost. Top: XGBoost without feature selection, second row: XGBoost with feature selection, third row: AdaBoost without feature selection, bottom: AdaBoost with feature selection. Higher AUCs, closer to 1, indicate better performance. High AUCs with ROC curves for each phenotype indicate the model is predicting the phenotypes with low false positives. Almost all classes of both Boosting algorithms without feature selection shows better AUCs of PR and ROC curves than feature selected models.**

The ROC and PR curves for individual experiments are shown in Fig. 4, where the curves for each class are given in blue (immune desert), orange (inflamed), and green (immune-excluded). All the ROC curves in the left column of Fig. 4 rapidly converged close to 1 in their true positive rate (TPR). Simultaneously, the PR curves in the right column of Fig. 4 maintained precision with respect to recall as much as possible. The respective AUCs of 0.77 and 0.87 for the PR and ROC curves demonstrated the model's feasibility in classifying different stages of immune phenotypes. The training and testing accuracies for different DNN settings are shown in Fig. 5, which demonstrates that both training (blue) and testing (orange) accuracies increase as the training progresses. After the model convergences, the middle subfigure (with l1-penalty) shows a large difference between the training and testing accuracies as opposed to the other two subfigures. These differences were due to the application of statistical feature selection using a t-test. For each fold, statistical testing

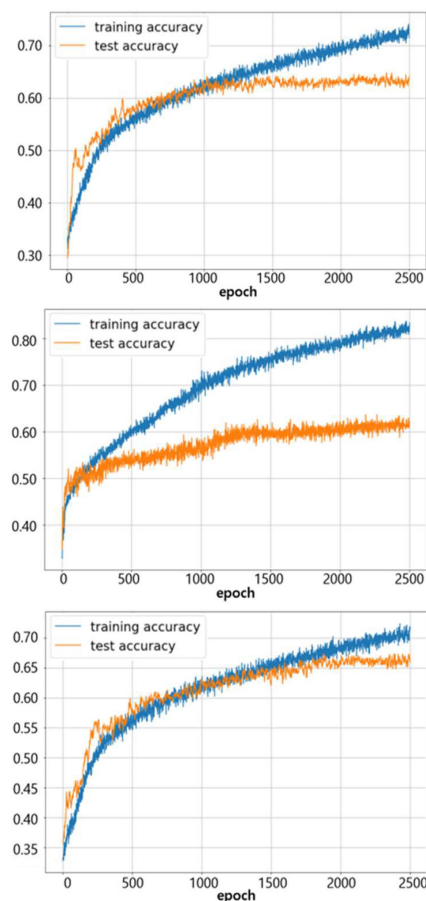


**FIGURE 4. Change of training / testing accuracy with respect to epoch in DNN training. Top: DNN (feature selection), middle: DNN (L1-norm penalty), Bottom: DNN (L1-norm penalty and feature selection). Similar training (blue) and testing (orange) accuracies indicate better generalization of the trained model to unseen testing data. As seen in the middle panel, significant overfitting (large differences between training and testing accuracies) occurs without feature selection.**

at each gene feature on the training data with Bonferroni correction at 0.05 yielded 900~1300 significant features. Given the high dimensionality of the data, without feature selection for dimension reduction, the issue of overfitting was easily seen. Although not presented in these results, we also observed overfitting occurring with an increase in hidden layers or nodes. This overfitting behavior explains the differences in MCC. As seen in Table 1, the DNN with l1-penalty only showed the lowest MCC as it was highly overfitted. On the other hand, the DNN with both l1-penalty and feature selection did not overfit and demonstrated the highest MCC of 0.488.

With the l1-regularizer at imposing sparsity at the input layer, many of the weights associated with each feature were suppressed to a value of or close to 0. From the DNN model with regularizer and feature selection, which yielded the highest accuracy and AUC for PR curves, the top 20 highest weighted gene features across all 10 folds were identified. Among them, 13 common features existed across all folds. These were named TMEM156 (Transmembrane Protein



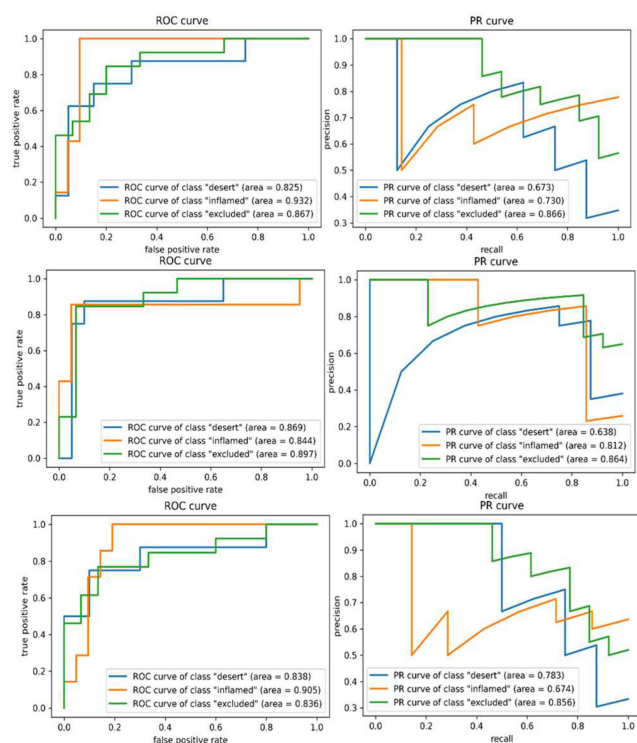


**FIGURE 5. ROC and PR curves (for each class) using deep neural network (DNN). Top: DNN (feature selection), mid: DNN (L1-norm penalty), bottom: DNN (L1-norm penalty and feature selection). Higher AUC (closer to 1) indicates better performance. High AUCs with ROC curves for each phenotype indicate the model is predicting the phenotypes with low false positives. Overall AUCs of both ROC and PR curves are higher than those from SVM analysis.**

156), TOX (Thymocyte Selection-associated High-mobility Group Box Protein), XAF1 (X-linked Inhibitor of Apoptosis-associated Factor-1), SPATC1 (Spermatogenesis and Centriole Associated 1), FOXP3 (Forehead Box P3), ARRB2 (Arestin Beta 2), TNFRSF9 (TNF Receptor Superfamily RNASE6 (Ribonuclease A Family Member K6), DBH-AS1 (DBH Antisense RNA 1), TENT5C (Terminal Nucleotidyl-transferase 5C), ID3 (DNA-binding Protein Inhibitor), APOE (Apolipoprotein E), and LAX1 (Lymphocyte Transmembrane Adaptor 1).

#### IV. DISCUSSION

In recent years, immunotherapy has come to play an increasingly important role in oncology. Immunotherapy in cancer treatment involves modifying or adding defense mechanisms to the patient's immune system. Immunotherapy is often used as a supplement to conventional cancer treatment methods, such as surgery, chemotherapy, and radiation therapy. For some specific types of lung and colorectal cancer, immunotherapy is used as the first line of treatment [49]. In urological oncology specifically, immunotherapy is used as a supplemental treatment in addition to standard of care [50]. Immunotherapy in cancer treatment involves modifying or adding defense mechanisms to the patient's immune system. Currently, immunotherapy can be divided into several types,

including immune CPIs, T cell transfer therapy, monoclonal antibodies, therapeutic vaccines, and immune system modulators [51].

Based on current research on BC therapies, immunotherapy seems to be the most promising. Because there are multiple regimens for immunotherapy, patients respond differently depending on the therapy. Currently, the US FDA has approved five anti-programmed death-1/ligand 1 (PD-1/L1) checkpoint inhibitors: atezolizumab, avelumab, durvalumab, nivolumab, and pembrolizumab [52]. Among them, atezolizumab was the first to pass approval. This approval was made based on the research results of IMvigor210. IMvigor210 was an open multicenter, single-arm phase II clinical study designed to study whether atezolizumab could become the standard treatment for advanced urothelial cancer. This study suggested that for patients with platinum-based refractory metastatic urothelial carcinoma (mUC), checkpoint inhibitors seem to be more attractive than chemotherapy [13]. Atezolizumab has shown encouraging long-term response rates, survival rates, and tolerability, supporting its therapeutic use in untreated mUC [53]. Based on the results of the study, the FDA approved atezolizumab as the first-line drug for the treatment of patients with advanced urothelial cancer who are not suitable for cisplatin chemotherapy.

Regarding Boosting methods, the key hyperparameters were the number of trees and learning rates. The number of estimators designates the scale of Random Forest. As more individual trees were included, the classification performance became better, but the whole model took longer time to be trained. A learning rate of Boosting algorithms denotes a coefficient applied to the weak classifiers when calibrating the error values sequentially. Since the learning rate directly affects the variation in the weight update, the difference in decision boundaries of multiple trees changed proportionally to the learning rate. However, it requires a large number of trees with a time-consuming ensemble process at the same time. Thus, the number of trees and learning rate has a trade-off relationship and coordinating the ratio between the two parameters was crucial to the performance of classification. Therefore, we had to manage the number of estimators at the same rate for fair comparison of the results.

In our study, Decision Tree based methods mostly tended to overfit as the training accuracies reached 1, and testing cases underperformed compared to SVM and DNN. Comparing the top-2 algorithms, although the accuracies with our DNN model were lower than that of our SVM model, the AUCs of evaluation curves (ROC and PR) were better. Specifically, the AUCs of PR curves in the DNN model were larger by 0.083 compared to the best of both models, which demonstrates that the DNN did better with imbalanced class labels. This is because the latent space for group separation found by DNN is better than SVM; while SVM with RBF kernel maps the data onto a higher dimensional space to find a linear decision boundary in that space, the DNN model mapped data onto a lower-dimensional space where group separation can be more effective and robust. The accuracy may be better in

the high-dimensional space found by SVM with RBF kernel, but the actual separation of the three immune phenotypes was more effective with DNN. This was also seen in the overfitting trend of both models. Both SVM and DNN suffered from overfitting; it was more serious for the SVM model while the DNN model was able to mitigate this issue with common techniques, such as dropout and regularizers, and this behavior was observed in MCC of individual models. As a result, there was a trade-off between training accuracy and other measures. Although SVM achieved slightly better test accuracy and MCC than those from DNNs, the precision and AUCs were significantly higher in DNN models, which we believe are more important.

Regarding the effective biomarkers found by the DNN model, downstream statistical group tests across each phenotype pairs yielded many significant p-values. As the phenotype profiles are ordered by severity, all 13 features showed very low p-values ( $<1e-6$ ) for immune desert vs. inflamed and mostly effective (i.e.,  $<0.05$ ) for other group pairs. Perhaps this was expected as our feature selection process selected important features with statistical tests at the training stage, but it was still worth analyzing them over the entire data to confirm if these biomarkers are really statistically meaningful for group comparisons.

We further investigated the 13 significant features associated with immunotherapy responsiveness in BC. FOXP3 is widely known as a key regulatory transcription factor of regulatory T cells, contributing to immune system responses [27], [54], [55]. Expression of FOXP3 in BC has been reported to negatively associated with survival of patients [56]. Recent studies have reported that FOXP3 acts as a transcriptional regulator of HIF-1 $\alpha$  gene expression in BC, suggesting the potential contribution of the FOXP3/HIF-1 $\alpha$  pathway in poorer survival [57]. APOE, an apolipoprotein related to lipoprotein-mediated lipid transport, was also found in the immunotherapy responsive molecular features. The LXR (liver X receptor)/APOE axis has been reported to regulate innate immune suppression and activation. Since this axis blocks innate immune suppression in many cancer types, it has been suggested as a therapeutic target to allow better efficacy of immunotherapy for cancer patients [58]. TOX has been found to regulate innate immunity and the tumor microenvironment. TOX expression significantly increases immune infiltration levels and is downregulated in most cancer types. Lower expression of TOX is correlated with poorer prognoses, suggesting that TOX expression can be used for stratification of non-responders to immunotherapy [59], [60].

Findings from this study suggest that the experiment we designed using ML algorithms are effective in classifying immune phenotypes of BC with gene expressions and identifying associations between specific gene expressions and the phenotypes. It also demonstrates the potential of our DNN model after improving overfitting via utilization of more samples. In addition, this study found 13 features associated with response to immunotherapy, which may all be biologically relevant.

## ACKNOWLEDGMENT

The authors would like thank the Cedars-Sinai Bioinformatics Core for technical support. Any opinions, findings, conclusions, or recommendations expressed in this article are those of the authors alone, and do not necessarily reflect the views of USAID or NAS.

## REFERENCES

- [1] S. Antoni, J. Ferlay, I. Soerjomataram, A. Znaor, A. Jemal, and F. Bray, "Bladder cancer incidence and mortality: A global overview and recent trends," *Eur. Urol.*, vol. 71, no. 1, pp. 96–108, Jan. 2017.
- [2] M. E. Nielsen *et al.*, "Trends in stage-specific incidence rates for urothelial carcinoma of the bladder in the United States: 1988 to 2006," *Cancer*, vol. 120, no. 1, pp. 86–95, Jan. 2014.
- [3] A. Morales, D. Eidinger, and A. W. Bruce, "Intracavitary Bacillus Calmette-Guerin in the treatment of superficial bladder tumors," *J. Urol.*, vol. 167, no. 2, pp. 891–894, Feb. 2002.
- [4] E. D. Carosella, G. Ploussard, J. LeMaout, and F. A. Desgrandchamps, "A systematic review of immunotherapy in urologic cancer: Evolving roles for targeting of CTLA-4, PD-1/PD-L1, and HLA-G," *Eur. Urol.*, vol. 68, no. 2, pp. 267–279, Aug. 2015.
- [5] J. J. Havel, D. Chowell, and T. A. Chan, "The evolving landscape of biomarkers for checkpoint inhibitor immunotherapy," *Nat. Rev. Cancer*, vol. 19, no. 3, pp. 133–150, Mar. 2019, doi: [10.1038/s41568-019-0116-x](https://doi.org/10.1038/s41568-019-0116-x).
- [6] A. K. Schneider, M. F. Chevalier, and L. Derre, "The multifaceted immune regulation of bladder cancer," *Nat. Rev. Urol.*, vol. 16, no. 10, pp. 613–630, Oct. 2019, doi: [10.1038/s41585-019-0226-y](https://doi.org/10.1038/s41585-019-0226-y).
- [7] M. Rouanne *et al.*, "Development of immunotherapy in bladder cancer: Present and future on targeting PD(L)1 and CTLA-4 pathways," *World J. Urol.*, vol. 36, no. 11, pp. 1727–1740, Nov. 2018, doi: [10.1007/s00345-018-2332-5](https://doi.org/10.1007/s00345-018-2332-5).
- [8] R. J. Motzer *et al.*, "Nivolumab for metastatic renal cell carcinoma: Results of a randomized phase II trial," *J. Clin. Oncol.*, vol. 33, no. 13, pp. 1430–1437, May 2015, doi: [10.1200/JCO.2014.59.0703](https://doi.org/10.1200/JCO.2014.59.0703).
- [9] C. Robert *et al.*, "Nivolumab in previously untreated melanoma without BRAF mutation," *New England J. Med.*, vol. 372, no. 4, pp. 320–330, Jan. 2015, doi: [10.1056/NEJMoa1412082](https://doi.org/10.1056/NEJMoa1412082).
- [10] A. A. Davis and V. G. Patel, "The role of PD-L1 expression as a predictive biomarker: An analysis of all US food and drug administration (FDA) approvals of immune checkpoint inhibitors," *J. Immunother. Cancer*, vol. 7, no. 1, Oct. 2019, Art. no. 278, doi: [10.1186/s40425-019-0768-9](https://doi.org/10.1186/s40425-019-0768-9).
- [11] J. D. Fumet, C. Truntzer, M. Yarchoan, and F. Ghiringhelli, "Tumour mutational burden as a biomarker for immunotherapy: Current data and emerging concepts," *Eur. J. Cancer*, vol. 131, pp. 40–50, May 2020, doi: [10.1016/j.ejca.2020.02.038](https://doi.org/10.1016/j.ejca.2020.02.038).
- [12] T. Powles *et al.*, "Atezolizumab versus chemotherapy in patients with platinum-treated locally advanced or metastatic urothelial carcinoma (IMvigor211): A multicentre, open-label, phase 3 randomised controlled trial," *Lancet*, vol. 391, no. 10122, pp. 748–757, Feb. 2018, doi: [10.1016/S0140-6736\(17\)33297-X](https://doi.org/10.1016/S0140-6736(17)33297-X).
- [13] T. Powles *et al.*, "Atezolizumab versus chemotherapy in patients with platinum-treated locally advanced or metastatic urothelial carcinoma (IMvigor211): A multicentre, open-label, phase 3 randomised controlled trial," *Lancet*, vol. 391, no. 10122, pp. 748–757, Feb. 2018.
- [14] Q. Mo, R. Li, D. O. Adeegbe, G. Peng, and K. S. Chan, "Integrative multi-omics analysis of muscle-invasive bladder cancer identifies prognostic biomarkers for frontline chemotherapy and immunotherapy," *Commun. Biol.*, vol. 3, no. 1, pp. 1–4, Dec. 2020, doi: [10.1038/s42003-020-01491-2](https://doi.org/10.1038/s42003-020-01491-2).
- [15] S. W. Baek, I. H. Jang, S. K. Kim, J. K. Nam, S. H. Leem, and I. S. Chu, "Transcriptional profiling of advanced Urothelial cancer predicts prognosis and response to immunotherapy," *Int. J. Mol. Sci.*, vol. 21, no. 5, Mar. 2020, Art. no. 1850, doi: [10.3390/ijms21051850](https://doi.org/10.3390/ijms21051850).
- [16] A. Kamoun *et al.*, "A consensus molecular classification of muscle-invasive bladder cancer," *Eur. Urol.*, vol. 77, no. 4, pp. 420–433, Apr. 2020, doi: [10.1016/j.eururo.2019.09.006](https://doi.org/10.1016/j.eururo.2019.09.006).
- [17] A. Bomane, A. Goncalves, and P. J. Ballester, "Paclitaxel response can be predicted with interpretable multi-variate classifiers exploiting DNA-methylation and miRNA data," *Front. Genet.*, vol. 10, 2019, doi: [10.3389/fgene.2019.01041](https://doi.org/10.3389/fgene.2019.01041).

- [18] S. N. L. Nguyen, A. Bomane, A. Bruna, G. Ghislat, and P. J. Ballester, "Machine learning models to predict in vivo drug response via optimal dimensionality reduction of tumour molecular profiles," Mar. 2018, Art. no. 277772, doi: <https://doi.org/10.1101/277772>.
- [19] F. Wang, L. P. Casalino, and D. Khullar, "Deep learning in medicine—promise, progress, and challenges," *JAMA Intern. Med.*, vol. 179, no. 3, pp. 293–294, Mar. 2019, doi: [10.1001/jamainternmed.2018.7117](https://doi.org/10.1001/jamainternmed.2018.7117).
- [20] P. J. Ballester and J. Carmona, "Artificial intelligence for the next generation of precision oncology," *NPJ Precis. Oncol.*, vol. 5, no. 1, pp. 1–3, Aug. 2021, doi: [10.1038/s41698-021-00216-w](https://doi.org/10.1038/s41698-021-00216-w).
- [21] C. Xiao, E. Choi, and J. Sun, "Opportunities and challenges in developing deep learning models using electronic health records data: A systematic review," *J. Amer. Med. Inform. Assoc.*, vol. 25, no. 10, pp. 1419–1428, Oct. 2018, doi: [10.1093/jamia/ocy068](https://doi.org/10.1093/jamia/ocy068).
- [22] D. Chen et al., "Deep learning and alternative learning strategies for retrospective real-world clinical data," *NPJ Digit. Med.*, vol. 2, no. 1, pp. 1–5, May 2019, doi: [10.1038/s41746-019-0122-0](https://doi.org/10.1038/s41746-019-0122-0).
- [23] R. Miotto, F. Wang, S. Wang, X. Jiang, and J. T. Dudley, "Deep learning for healthcare: Review, opportunities and challenges," *Brief Bioinf.*, vol. 19, no. 6, pp. 1236–1246, Nov. 2018, doi: [10.1093/bib/bbx044](https://doi.org/10.1093/bib/bbx044).
- [24] S. Mariathasan et al., "TGFβ attenuates tumour response to PD-L1 blockade by contributing to exclusion of T cells," *Nature*, vol. 554, no. 7693, pp. 544–548, Feb. 2018, doi: [10.1038/nature25501](https://doi.org/10.1038/nature25501).
- [25] M. Kates et al., "Intravesical BCG induces CD4+ T-cell expansion in an immune competent model of bladder cancer," *Cancer Immunol. Res.*, vol. 5, no. 7, pp. 594–603, Jul. 2017.
- [26] S. Bunimovich-Mendrazitsky, E. Shochat, and L. Stone, "Mathematical model of BCG immunotherapy in superficial bladder cancer," *Bull. Math. Biol.*, vol. 69, no. 6, pp. 1847–1870, Aug. 2007.
- [27] X. Wang et al., "Cancer-FOXP3 directly activated CCL5 to recruit FOXP3+ Treg cells in pancreatic ductal adenocarcinoma," *Oncogene*, vol. 36, no. 21, pp. 3048–3058, May 2017.
- [28] C. Cortes, M. Mohri, and A. Rostamizadeh, "L2 regularization for learning kernels," in *Proc. 25th Conf. UAI*, Jun. 2009, pp. 109–116.
- [29] T. S. Furey, N. Cristianini, N. Duffy, D. W. Bednarski, M. Schummer, and D. J. B. Haussler, "Support vector machine classification and validation of cancer tissue samples using microarray expression data," *Bioinformatics*, vol. 16, no. 10, pp. 906–914, Oct. 2000.
- [30] Y. LeCun, Y. Bengio, and G. Hinton, "Deep learning," *Nature*, vol. 521, no. 7553, pp. 436–444, May 2015.
- [31] Y. Bengio, A. Courville, and P. Vincent, "Representation learning: A review and new perspectives," *IEEE Trans. Pattern Anal. Mach. Intell.*, vol. 35, no. 8, pp. 1798–1828, Mar. 2013.
- [32] J. Schmidhuber, "Deep learning in neural networks: An overview," *Neural Networks*, vol. 61, pp. 85–117, Jan. 2015.
- [33] C. Cortes and V. Vapnik, "Support-vector networks," *Mach. Learn.*, vol. 20, no. 3, pp. 273–297, Sep. 1995.
- [34] K. Crammer and Y. Singer, "On the algorithmic implementation of multiclass kernel-based vector machines," *J. Mach. Learn. Res.*, vol. 2, no. 12, pp. 265–292, Dec. 2001.
- [35] J. Ali, R. Khan, N. Ahmad, and I. Maqsood, "Random forests and decision trees," *Int. J. Comput. Sci. Issues*, vol. 9, no. 5, Sep. 2012, Art. no. 272.
- [36] V. Svetnik, A. Liaw, C. Tong, J. C. Culberson, R. P. Sheridan, and B. P. Feuston, "Random forest: A classification and regression tool for compound classification and QSAR modeling," *J. Chem. Inf. Comput. Sci.*, vol. 43, no. 6, pp. 1947–1958, Nov. 2003.
- [37] L. Breiman, "Bagging predictors," *Mach. Learn.*, vol. 24, no. 2, pp. 123–140, Aug. 1996.
- [38] J. L. Horowitz, "The bootstrap," in *Handbook of Econometrics*, Amsterdam, Netherlands: Elsevier, vol. 5, Jan. 2001, pp. 3159–3228.
- [39] R. E. Schapire, "A brief introduction to boosting," in *Ijcai*, Princeton, NJ, USA: Citeseer, vol. 99, 1999, pp. 1401–1406.
- [40] T. Chen and C. Guestrin, "Xgboost: A scalable tree boosting system," in *Proc. 22nd ACM Sigkdd Int. Conf. Knowl. Discov. Data Mining*, Aug. 2016, pp. 785–794.
- [41] Y. Freund and R. E. Schapire, "A decision-theoretic generalization of online learning and an application to boosting," *J. Comput. Syst. Sci.*, vol. 55, no. 1, pp. 119–139, Aug. 1997.
- [42] P. Viola and M. Jones, "Rapid object detection using a boosted cascade of simple features," in *Proc. IEEE Comput. Soc. Conf. Comput. Vis. Pattern Recognit.*, Manhattan, New York, NY, USA: IEEE, vol. 1, Dec. 2001, pp. I–I.
- [43] P. Zhao and B. Yu, "On model selection consistency of lasso," *J. Mach. Learn. Res.*, vol. 7, pp. 2541–2563, Dec. 2006.
- [44] T. Park and G. Casella, "The Bayesian lasso," *J. Amer. Stat. Assoc.*, vol. 103, no. 482, pp. 681–686, Jun. 2008.
- [45] R. Kohavi, "A study of cross-validation and bootstrap for accuracy estimation and model selection," in *Proc. Int. Joint Conf. Artif. Intell.*, Montreal, Canada: American Association for Artificial Intelligence, vol. 14, no. 2, 1995, pp. 1137–1145.
- [46] D. P. Kingma and J. Ba, "Adam: A method for stochastic optimization," in *Proc. ICLR*, 2015.
- [47] A. Mlynska et al., "A gene signature for immune subtyping of desert, excluded, and inflamed ovarian tumors," *Amer. J. Reprod. Immunol.*, vol. 84, no. 1, Jul. 2020, Art. no. e13244.
- [48] B.-N. Song, S.-K. Kim, J.-Y. Mun, Y.-D. Choi, S.-H. Leem, and I.-S. J. E. Chu, "Identification of an immunotherapy-responsive molecular subtype of bladder cancer," *EBioMedicine*, vol. 50, pp. 238–245, Dec. 2019.
- [49] X. Xu et al., "Three-dimensional texture features from intensity and high-order derivative maps for the discrimination between bladder tumors and wall tissues via MRI," *Int. J. Comput. Assist. Radiol. Surg.*, vol. 12, no. 4, pp. 645–656, Apr. 2017.
- [50] J. C. Jagodinsky, P. M. Harari, and Z. S. Morris, "The promise of combining radiation therapy with immunotherapy," *Int. J. Radiat. Oncol. Biol. Phys.*, vol. 108, no. 1, pp. 6–16, Sep. 2020.
- [51] National Cancer Institute. "Immunotherapy to treat cancer," [Online]. Available: <https://www.cancer.gov/about-cancer/treatment/types/immunotherapy#what-are-the-types-of-immunotherapy>
- [52] T. J. Kim, K. S. Cho, and K. C. Koo, "Current status and future perspectives of immunotherapy for locally advanced or metastatic urothelial carcinoma: A comprehensive review," *Cancers*, vol. 12, no. 1, Jan. 2020, Art. no. 192.
- [53] A. V. Balar et al., "Atezolizumab as first-line treatment in cisplatin-ineligible patients with locally advanced and metastatic urothelial carcinoma: A single-arm, multicentre, phase 2 trial," *Lancet*, vol. 389, no. 10064, pp. 67–76, Jan. 2017.
- [54] S. Z. Josefowicz, L.-F. Lu, and A. Y. Rudensky, "Regulatory T cells: Mechanisms of differentiation and function," *Annu. Rev. Immunol.*, vol. 30, pp. 531–564, Apr. 2012.
- [55] Y. Togashi, K. Shitara, and H. Nishikawa, "Regulatory T cells in cancer immunosuppression—Implications for anticancer therapy," *Nature Rev. Clin. Oncol.*, vol. 16, no. 6, pp. 356–371, Jun. 2019.
- [56] M. E. Winerdal et al., "FOXP3 and survival in urinary bladder cancer," *BJU Int.*, vol. 108, no. 10, pp. 1672–1678, Nov. 2011.
- [57] Y.-C. Jou et al., "Foxp3 enhances HIF-1α target gene expression in human bladder cancer through decreasing its ubiquitin-proteasomal degradation," *Oncotarget*, vol. 7, no. 40, Oct. 2016, Art. no. 65403.
- [58] M. F. Tavaoie et al., "LXR/ApoE activation restricts innate immune suppression in cancer," *Cell*, vol. 172, no. 4, pp. 825–840, Feb. 2018.
- [59] K. Kim et al., "Single-cell transcriptome analysis reveals TOX as a promoting factor for T cell exhaustion and a predictor for anti-PD-1 responses in human cancer," *Genome Med.*, vol. 12, no. 1, pp. 1–16, Dec. 2020.
- [60] L. Guo, X. Li, R. Liu, Y. Chen, C. Ren, and S. Du, "TOX correlates with prognosis, immune infiltration, and T cells exhaustion in lung adenocarcinoma," *Cancer Med.*, vol. 9, no. 18, pp. 6694–6709, Sep. 2020.



**HYUNA CHO** received the B.S. degree in computer engineering from Kyung-Hee University, Seoul, South Korea, in 2020. She is currently working toward the graduation degree with the Artificial Intelligence And Medical Imaging lab, Pohang University of Science and Technology, Pohang, South Korea. During her undergraduate study, she studied machine learning from Nanyang Technological University, Singapore, and performed a research of detecting pneumonia on CT images using CNN models from Purdue University, West Lafayette, IN, USA. Her graduation thesis for medical image augmentation research won the best prize in the undergraduate thesis category of Korea Computer Congress in 2020. Her research interests mainly include accessing and solving problems in the medical field with artificial intelligence and computer vision methodologies.





**FENG TONG** received the B.E. degree in intelligent science and technology from Xidian University, Xi'an, China, in 2017, and the M.S. degree in computer science, in 2019, from the University of Texas at Arlington, Arlington, TX, USA, where he is currently working toward the Ph.D. degree with the Department of Computer Science and Engineering, supervised by Dr. Won Hwa Kim and Dr. Junzhou Huang. His research interests include machine learning, computer vision, and medical imaging.



**SUNGYONG YOU** is currently an Assistant Professor of surgery with Cedars-Sinai Medical Center. He leads the Cancer Bioinformatics Core at Cedars-Sinai and the Urologic Bioinformatics unit with the Department of Surgery as the Director. He has a strong background in computational biology and systems biology, with specific training in various Omics data analyses. Up to the present time, he has achieved a number of important career milestones as an independent Scientist, including 15 patent applications, one licensing agreement,

and more than 70 peer reviewed publications, including many papers in high-impact journals, such as *PNAS*, *Nature Medicine*, *Nature Communications*, *Journal of Clinical Investigation*, and *Science Translational Medicine*. He is currently the PI/MPI of 3 federal (NIH and DoD) grants. He is also a co-investigator on many active funded awards, including an NCI P01 program project grant.



**SUNGYOUNG JUNG** (Senior Member, IEEE) received the B.S. and M.S. degrees in electronics engineering from Yeungnam University, Gyeongsan, South Korea, in 1991 and 1993, respectively, and the Ph.D. degree in electrical engineering from the Georgia Institute of Technology, Atlanta, GA, USA, in 2002. From 2001 to 2002, he was an Advanced Circuit Engineer with Quellan Inc., Atlanta, GA, USA. He is currently an Associate Professor with the Department of Electrical Engineering, University of Texas at Arlington, Arlington, TX, USA. His research interests include IC and system design for chemical/bio-applications, RF IC and system design for wireless communications and radar applications, high-speed CMOS analog and mixed-signal circuit design, and optoelectronic IC design.



**WON HWA KIM** received the B.S. degree in information and communication engineering from Sungkyunkwan University, Seoul, South Korea, in 2008, the M.S. degree in robotics from the Korea Advanced Institute of Science and Technology, Daejeon, South Korea, in 2010, and the Ph.D. degree in computer sciences from the University of Wisconsin–Madison, Madison, WI, USA, in 2017. He has been an Assistant Professor of computer science and engineering with the Pohang University of Science and Technology, Pohang, South

Korea, since 2020 and with the University of Texas at Arlington, Arlington, TX, USA, since 2018. Prior to joining academia, he was a Researcher with Data Science Team, NEC Laboratories America in 2017. His work has been published in top-tier AI conferences, such as NeurIPS, CVPR, ICCV, ECCV, MICCAI, ISBI, as well as in high impact journals, such as *NeuroImage*, *NeuroImage: Clinical*, and *Brain Connectivity*. His research interests include computer vision and machine learning for unconventional data, and their applications in health science.



**JAYOUNG (JAY) KIM** is currently a Professor of surgery, medicine, and biomedical sciences with Cedars-Sinai Medical Center and the University of California, Los Angeles, California, CA, USA, and a Cancer Biologist by training with a broad background in medical science and specific expertise in molecular biology. Her research program has concentrated on furthering the understanding of mechanism and treatments of urological diseases. In particular, her academic career in translational science studies focuses on how to use cutting-edge

cellular, molecular, and computational tools to better understand the genitourinary tract pathophysiology. Her efforts were continued after relocating to Cedars-Sinai Medical Center/UCLA from Harvard Medical School. Her research projects have significant clinical impacts and include human specimens, clinical trials, and interventions. Her research interests include better understanding the normal and pathologic mechanisms in the urinary tract with the overarching translational goal of improving patient care through diagnosis and intervention by using various omics data, including those of the transcriptome, proteome, and metabolome, combined with comprehensive bioinformatics analysis. Her current research interests include developing molecular biomarker and machine learning algorithm-based point-of-care portable biosensor systems (usable medical devices), and validate their clinical value in digitalized health. As a PI, she holds active funding, such as the National Institutes of Health, Centers for Disease Control and Prevention, and U.S. Department of Defense.

## Disparities in Cancer Care and the Asian American Population

RICHARD J. LEE<sup>1</sup>, RAVI A. MADAN,<sup>2</sup> JAYOUNG KIM,<sup>3,4,5</sup> EDWIN M. POSADAS,<sup>6</sup> EVAN Y. YU<sup>7</sup>

<sup>1</sup>Harvard Medical School and Massachusetts General Hospital Cancer Center, Boston, Massachusetts, USA; <sup>2</sup>Genitourinary Malignancies Branch, Center for Cancer Research, National Cancer Institute, National Institutes of Health, Bethesda, Maryland, USA; Departments of <sup>3</sup>Surgery; <sup>4</sup>Biomedical Sciences; <sup>5</sup>Samuel Oschin Comprehensive Cancer Institute, Cedars-Sinai Medical Center, California, Los Angeles, USA; <sup>6</sup>University of Washington and Fred Hutchinson Cancer Research Center, Seattle, Washington, USA

Disclosures of potential conflicts of interest may be found at the end of this article.

**Key Words.** Disparities • Cancer • Asian American • Racism • Screening

### ABSTRACT

Asian Americans are the only racial/ethnic group in the U.S. for whom cancer is the leading cause of death in men and women, unlike heart disease for all other groups. Asian Americans face a confluence of cancer risks, with high rates of cancers endemic to their countries of origin due to infectious and cultural reasons, as well as increasing rates of “Western” cancers that are due in part to assimilation to the American diet and lifestyle. Despite the clear mortality risk, Asian Americans are screened for cancers at lower rates than the majority of Americans. Solutions to eliminate the disparity in cancer care are complicated by language and cultural concerns of this

very heterogeneous group. This review addresses the disparities in cancer screening, the historical causes, the potential contribution of racism, the importance of cultural perceptions of health care, and potential strategies to address a very complicated problem. Noting that the health care disparities faced by Asian Americans may be less conspicuous than the structural racism that has inflicted significant damage to the health of Black Americans over more than four centuries, this review is meant to raise awareness and to compel the medical establishment to recognize the urgent need to eliminate health disparities for all. *The Oncologist* 2021;26:453–460

**Implications for Practice:** Cancer is the leading cause of death in Asian Americans, who face cancers endemic to their native countries, perhaps because of infectious and cultural factors, as well as those faced by all Americans, perhaps because of “Westernization” in terms of diet and lifestyle. Despite the mortality rates, Asian Americans have less cancer screening than other Americans. This review highlights the need to educate Asian Americans to improve cancer literacy and health care providers to understand the important cancer risks of the fastest-growing racial/ethnic group in the U.S. Eliminating disparities is critical to achieving an equitable society for all Americans.

### INTRODUCTION

In 2020, the confluence of the COVID-19 pandemic and the outrage about the disproportionate number of deaths of Black Americans in police custody—among other egregious affronts to Black lives—exposed critical disparities in health care and structural racism faced by Black and Latinx Americans. In support of eliminating health disparities for all Americans, this review examines disparities in the delivery of cancer care for Asian Americans.

The broad brushstrokes illustrate the need to evaluate disparities in this population. Asian Americans are the fastest-growing racial/ethnic group in the U.S. Unlike every other group, for whom heart disease leads the way, cancer

is the leading cause of death in male and female Asian Americans [1, 2]. By some measures, Asian Americans have greater exposures to environmental carcinogens [3]. Despite these risks, Asian Americans have lower cancer screening rates than other groups [1, 4–7]. Taken together, there is a clear need to ensure equitable access to screening and cancer care in this vulnerable population.

### THE ASIAN AMERICAN POPULATION

Who are Asian Americans? In the broad terms “people of color” and “underrepresented minority,” Asian Americans

Correspondence: Richard J. Lee, M.D., Ph.D., Department of Medicine, Harvard Medical School, Massachusetts General Hospital Cancer Center, 55 Fruit Street, Yawkey 7E, Boston, Massachusetts 02114, USA. Telephone: 617-724-4000; e-mail: rjlee@mgh.harvard.edu Received February 1, 2021; accepted for publication February 16, 2021; published Online First on March 20, 2021. <http://dx.doi.org/10.1002/onco.13748>  
No part of this article may be reproduced, stored, or transmitted in any form or for any means without the prior permission in writing from the copyright holder. For information on purchasing reprints contact [commercialreprints@wiley.com](mailto:commercialreprints@wiley.com).

are not typically included. Asian Americans comprise 6% of the U.S. population but are not a monolith. By the current definition used by the U.S. Census Bureau (established in 1997 by the Office of Management and Budget [https://www.census.gov/topics/population/race/about.html]), the term “Asian” includes people who can trace their origin to more than 20 countries in East Asia (e.g., China, Japan, Korea), Southeast Asia (e.g., Cambodia, Philippines, Thailand, Vietnam), and the Indian subcontinent (e.g., Bangladesh, India, Pakistan) [5, 8]. As of 2015, of the more than 20 million Asian Americans, 23% were from China, 19% from India, 18% from the Philippines, 9% from Vietnam and Korea, and 7% from Japan, with the remaining 15% from all other countries [8]. Asian Americans are sometimes grouped with people with roots in the Pacific Islands (e.g., native to Hawaii, Marshall Islands). The number of countries belies the significant ethnic diversity in this heterogeneous group, with 200 languages or dialects. As such, aggregate data of “Asian Americans” often fail to capture the broad range of experience in this group.

Asian Americans are the fastest-growing racial/ethnic group in the U.S., with 72% growth between 2000 and 2015, compared with 60% for the second-fastest-growing population (Latinx Americans). Most Asian Americans (59%) were born in another country. Since 1965, one-fourth of all immigrants to the U.S. have come from Asia. Asian immigrants comprise 13% of the 11.1 million undocumented immigrants in the U.S. [8].

Social determinants of health are defined by the Centers for Disease Control and Prevention as “conditions in the places where people live, learn, work, and play” that “affect a wide range of health risks and outcomes” [9]. Asian Americans frequently settle in either central city locations or near cities [3]. Overall, the home ownership rate among Asian Americans is lower than for the U.S. overall (57% compared with 63%), with only Vietnamese and Japanese households at or above the U.S. rate [8]. More Asian Americans live in multigenerational households (26%) compared with all U.S. households (19%) [8].

Aggregate data indicate that Asian Americans fare well based on measures of economic well-being, including median household income (\$73,600 compared with \$53,600 for all U.S. households) and poverty rates (12.1% compared with 15.1%) [8]. However, disaggregated data describe a broad range among subgroups, including highest compared with lowest median household incomes (\$100,000 for Indian compared with \$36,000 for Burmese) and lowest compared with highest poverty rates (7.5% for Filipino and Indian groups compared with 35% for Burmese). In terms of education, 51% of Asian Americans over age 25 have a bachelor’s degree, compared with 30% of all Americans; however, there is a wide range among subgroups, from 9% among Bhutanese to 72% among Indians [8].

Notably, the demographics and data indicate that Asian Americans and other minority groups face different challenges related to disparities, and therefore any proposed solutions for minority groups are necessarily population specific. In addition to the wealth and poverty rates above, other measures of social inequities favor Asian Americans

over White, Black, Latinx, and Native/Indigenous Americans, including incarceration rates, health insurance rates, infant mortality, and diabetes- and heart disease–related mortality [10]. Self-reported issues such as discrimination and stress are subject to reporting bias and are less readily comparable. In terms of representation in medicine, Asians are an overrepresented minority, comprising 11.2% of U.S. primary care physicians (PCPs), compared with 6.8% Black and 5.9% Latinx PCPs [11]. By comparison, the entire U.S. population is 6% Asian, 13% Black, and 18% Latinx. Of all active U.S. physicians, 17.1% identify as Asian, with 5.0% Black and 5.8% Latinx [12]. Similar trends exist in other areas of health care requiring advanced degrees, including pharmacists (17.9% vs. 5.9% vs. 3.7%, for Asian, Black, and Latinx, respectively), dentists (14.3% vs. 3.0% vs. 6.1%), and optometrists (13.7% vs. 1.8% vs. 3.9%) [13].

### THE “MODEL MINORITY” MYTH

Given their relatively small fraction of the U.S. population, why are Asian Americans not typically clustered with other minority populations, and how does this affect their health care? In part, this may relate to the aforementioned metrics of economic well-being, in that populations that are doing well in aggregate may receive less attention. In part, this may also relate to Asians being labeled a “model minority,” a label that has impacts that may be considered positive and negative.

The U.S. has a long history of anti-Asian discrimination, including the Chinese Exclusion Act of 1882 (which was extended in 1892 as the Geary Act and then made permanent in 1902), the Immigration Act of 1917 (the Barred Zone Act), the Johnson-Reed Act (1924), and the Japanese American internment under Executive Order 9066 during World War II. The Immigration and Naturalization Act of 1965 significantly shifted the immigration barriers from Asia posed by the prior acts by lifting a national-origins quota system and allowing immigrants who were relatives of U.S. citizens or permanent residents, or those with skills that were considered useful (with a preference for those with professional degrees), or refugees of unrest. This act led to hundreds of thousands of Asians immigrating to America, with a high concentration of highly skilled and educated professionals from India and the Philippines [14]. As such, this wave of immigrants included a significant proportion fluent in English who were poised for success in the U.S.

Around the same time, the “model minority” term was coined in 1966, in two lay articles about Japanese and Chinese Americans achieving success despite the long history of anti-Asian discrimination [15, 16]. During the Civil Rights era, the portrayal of Asians as a successful minority group was used in stark contrast with the portrayal of Black Americans. The articles described how these Asian Americans overcame the above immigration policies and racism to achieve success and avoid delinquency, positing that Asian attributes such as work ethic, emphasis on education, family stability, and assimilation overcame language and other cultural barriers [3, 14]. The corollary, then, is that failures of other non-Asian minority groups are due to their lack of

such positive attributes. It was asserted that Asians historically faced even greater prejudice than Black Americans [16]. The argument as illustrated by the model minority stereotype is that opportunities are equally available and that success is achievable by anyone. Furthermore, acceptance of this stereotype undermined the perceived need to assist disadvantaged minority populations [3].

This argument must be considered a myth, given the known reinforcing structural disadvantages placed over 400 years to hinder Black American success. The Immigration Act of 1965 may have had benign motives, but the increase in skilled or professional workers with English fluency from Asia added to the established population touted as the model minority, allowing policymakers to accept a myth that America is a nonracist society and ignore the needs of Black Americans.

What are the consequences of Asian American success and this model minority stereotype? In society in general, Asian Americans are not generally considered “threatening.” In the labor market, given their high numbers in professional occupations, Asian job-seekers are not considered minority applicants. In higher education, Asian applicants for college/university are not considered an underrepresented minority and in fact may face admission quotas at certain schools. It is arguable whether this represents progress, and at its worst, this may drive a wedge between Asian Americans and other minority groups.

There are clear health care consequences from combining this model minority myth with aggregate assumptions of Asian Americans. Given economic indicators of success relative to the overall population, Asian Americans may be assumed to have similar disease risk profiles to the majority White American population. By aggregating Asian Americans in population studies, the heterogeneity of subpopulations with genetic and cultural contributions to disease risk can be masked [3]. By acceptance of the advantages of the model minority label, Asian Americans may be reluctant to disclose, or may not advocate for, their own physical or mental health concerns and needs [6]. Taken together, the consequences of this myth may lead to poor understanding of significant medical issues faced by Asian Americans and misguided policies. Poor understanding or inattention to the fastest-growing racial/ethnic group in the U.S. must be remedied to avert a significant number of cancer deaths.

---

### CANCER IS THE LEADING CAUSE OF DEATH FOR ASIAN AMERICANS

There is no question that cancer should be a significant concern for Asian Americans and their primary care providers. Cancer has been the leading cause of death for Asian Americans since 2000, with most recent data from 2017 [1, 2]. In contrast, heart disease (including coronary artery disease, arrhythmias, congestive heart failure, valvular heart disease) is the leading cause of death for all other groups in the U.S. In a study that aggregated Asian Americans, native Hawaiians, and Pacific Islanders (AANHPIs), the leading cancer causes of death in men were lung (27%), liver (14%), and colorectum (11%), and in women, they were lung (21%), breast (14%), and colorectum (11%). By comparison,

the leading causes of cancer death in all Americans in the same year were lung (27%), prostate (8%), and colorectum (8%) in men and lung (26%), breast (14%), and colorectum (8%) in women [17]. The 5-year cancer-specific survival for AANHPI men was lower compared with non-Latinx White American men (62% compared with 68%, respectively), whereas rates were similar for women (70% compared with 68%) [1]. These statistics persist despite Asian Americans having higher median household income and education levels compared with other groups [8], arguing that social determinants of health do not fully explain this disparity in the most critical outcome of survival but that it may result from the high incidence of specific malignancies in this population, such as liver and stomach cancers.

---

### CANCER PROPENSITY IN ASIAN AMERICANS

Although some of the leading cancer causes of death among Asian Americans are shared with the overall American population, understanding different cancer propensities may help eliminate disparities in outcomes.

#### Infectious Etiologies

Asian Americans have higher rates than most racial/ethnic group for cancers with infectious etiologies, including liver (hepatitis B virus [HBV]), uterine cervix (human papillomavirus [HPV]), nasopharynx (Epstein-Barr virus [EBV]), and stomach (*Helicobacter pylori*) [1, 5]. For liver cancer, chronic HBV infection among Asian Americans can be attributed to high HBV prevalence in country of origin, recent immigration, and vertical transmission [1]. The HBV infection and cancer rates vary among Asian American subpopulations. Liver cancer rates were highest among Vietnamese men and Korean women [5]. By contrast, the rising liver cancer incidence among other Americans is attributed to hepatitis C and nonalcoholic fatty liver disease [1, 18].

The cervical cancer incidence rate is slightly lower among Asian American women overall compared with non-Latinx White Americans, although rates among Cambodian Americans and Vietnamese Americans are 40%–87% higher [1]. These rates may reflect HPV prevalence in country of origin, recent immigration, and less screening with the Papanicolaou test, which may relate to health insurance status, access to care, and awareness.

Although rates of nasopharyngeal carcinoma are low in the U.S., the incidence among AANHPIs is five- to sixfold higher than among non-Latinx White Americans. Risk factors that may account for higher rates include EBV infection (with 98% of cases related to EBV), habits such as smoking, and culture-specific carcinogen exposures such as the high nitrosamine content in Cantonese salted fish [1].

Stomach cancer is the sixth and seventh leading cancer causes of death in Asian American men and women, respectively, but does not reach the top ten for Americans overall [1, 17]. Asian American men had the highest incidence and mortality from stomach cancer in the U.S. from 2010 to 2014 [18]. Incidence among Asian subpopulations is highest among Koreans followed by Japanese and Vietnamese, reflecting in part that worldwide stomach cancer rates are highest in Korea [1]. Risk factors for stomach cancer include



*H. pylori* infection, smoking, and ingestion of salt-preserved foods [1, 19]. The prevalence of *H. pylori* infection is higher in Asia and South America than the U.S. An estimated 89% of stomach cancers that originate outside of the gastric cardia are attributed to *H. pylori*. A study assessing racial/ethnic differences found that 35.6% of cases in White Americans originate in the cardia, as opposed to 10% for Asian Americans, 15% for Latinx Americans, and 11% for Black Americans. Most cases in Asian Americans (31.4%) occurred in the pyloric antrum, compared with 19.6% for all patients [20]. Consistent with the possibility that endemic infection and cultural factors contribute to risk, several studies have shown that migration from high- to low-incidence regions such as from Japan to the U.S. is associated with decreased risk of developing stomach cancer [19, 20].

### Carcinogen Exposure

Lung cancer is the leading cause of cancer-specific death in Asian Americans [1]. Although smoking is the primary risk factor for developing lung cancer, Asian Americans' cigarette use rates from 2010 to 2013 were lower (10.9%) compared with those of White Americans (24.9%), Black Americans (24.9%), and Latinx Americans (19.9%) [21]. Among Asian subpopulations, the range was broad, from Chinese and Indian Americans (7.6%) to Koreans (20.0%) [21]. That tobacco use is not more prevalent despite the increased lung cancer risk is perhaps not surprising. Whereas in the U.S., approximately 10% of patients with lung cancer are never-smokers, in Asia, >30% of patients are never-smokers, including more than half of female patients with lung cancer [22]. In this case, the biology of the disease clearly differs, with a markedly increased rate of epidermal growth factor receptor–mutant lung cancer in Asian female nonsmokers. Nonetheless, tobacco cessation remains an important recommendation to diminish cancer risk. Among smokers, only one-third of Asian Americans reported being counseled to quit smoking, compared with half of all other Americans [5].

Environmental hazards pose important, underreported health risks (e.g., heart disease, stroke, respiratory disease, cancer), most commonly for low-income and minority populations, including Asian Americans. In a national study of carcinogenic hazardous air pollutants (HAPs) based on census tracts and other available epidemiological data, Asian Americans ranked second after Black Americans for mean excess cancer incidence attributed to ambient HAP exposure, with Latinx Americans in third place [3]. When disaggregated by subpopulations, Chinese and Korean Americans had greater risks than Black Americans. Nonrace factors associated with higher cancer incidence included population density, urban setting, and renter-occupancy status (as opposed to home ownership). The byproduct of the model minority label, the authors state, is that Asian Americans are less often included in studies of environmental health disparities “based on the conventional presumption that they would have similar risk profiles to Whites.” Biologic factors may also play a role, as population differences in *CYP* gene expression, which affects activation of

carcinogens and metabolism of drugs, could contribute to cancer risk [23].

### Changing Risks with Migration and Westernization

As described above for stomach cancers, migration can affect cancer risk. Asian Americans cancer rates align with national rates within 10 years of immigration [24]. Cancer incidence patterns have been demonstrated to change among immigrants from China, Japan, Korea, and the Philippines. For example, for Korean immigrants in the U.S., incidence rates of prostate, breast, and colorectal cancers have risen compared with native South Koreans, whereas rates of stomach, liver, and gallbladder cancers have declined [25]. Rates of infection with cancer-associated viruses (HBV, HPV, EBV) or bacteria (*H. pylori*) change as a result of migration, vaccination availability and practices, health insurance availability, cancer screening, and cultural changes such as diet and lifestyle. Dietary changes (e.g., red meat consumption), more sedentary lifestyle, and consequent body composition changes (rates of overweight and obesity) may contribute to the rising rates of colorectal cancer [5]. Breast cancer incidence rates have risen fastest for Asian Americans among racial/ethnic groups, at 1.5% per year between 2012 to 2016 [26]. An understanding of the changing nature of cancer risk among Asian Americans is critical for delivery of appropriate cancer screening and care.

---

### CANCER SCREENING DISPARITIES AND SOLUTIONS

President Barack Obama signed Executive Order 13515 in October 2009, to address issues concerning the Asian American and Pacific Islander community, including strategies to reduce health disparities and improve the health of this community. Despite more than a decade since that order, significant disparities persist.

With cancer as the leading cause of death for Asian Americans, screening is of paramount importance to identify cancer cases at early, curable stages. However, screening occurs at *lower* rates for Asian Americans, the only racial/ethnic group for which cancer screening disparities compared with White Americans is not well explained by socioeconomic factors such as income, education, and access to health care [4]. This disparity holds true for each Asian subpopulation; not one group is expected to reach the national screening targets such as those in Healthy People 2020 [4].

Studies of different databases describe similar screening disparity trends [1, 5–7]. Compared with Americans overall, Asian American screening rates are lower for cervical cancer (75.4% vs. 83.0%), breast cancer (64.1% vs. 72.4%), and colorectal cancer (46.9% vs. 58.6%) [6]. These results are consistent with racial minorities receiving less provider recommendation for colon cancer screening [27]. In examining colorectal cancer screening rates among Asians in California (where approximately one-third of Asian Americans live) compared with White Americans, disparities have narrowed over time but have not been eliminated [28].

Inadequate screening is not limited to cancer. Diabetes prevalence among Asian Americans is 21%, nearly double that of White Americans, despite a lower mean body mass

index. In a survey study from 2012 to 2014, Asian Americans had a 34% lower adjusted odds of receiving the recommended diabetes screening compared with White Americans (adjusted odds ratio [AOR], 0.66; 95% confidence interval [CI], 0.60–0.73), a difference that persisted despite age and body mass index cutoffs. In perhaps a rare example of minority groups receiving *more* screening, the adjusted odds of receiving appropriate diabetes screening was significantly higher for Black Americans (AOR, 1.20; 95% CI, 1.16–1.25) and Latinx Americans (AOR, 1.36; 95% CI, 1.29–1.44) compared with White Americans [29].

The disparity in screening for diseases like cancer and diabetes and the fact that fewer Asians are counseled to quit smoking raise important questions about potential barriers to eliminating disparities and improving cancer survival. In contrast to Black and Latinx Americans, it is clear that workforce disparities are not at issue, given the overrepresentation of Asian Americans in medicine compared with the overall population, as described above [11, 12].

The challenges of evaluating Asians in aggregate are obvious: there are differences among subpopulations in language, culture, education, income, insurance, and health-seeking behaviors, to name a few. Although some barriers are similar to other racial/ethnic groups, a barrier such as language may be more readily overcome for Latinx Americans given the common Spanish language (dialects notwithstanding), whereas interpreters and translated documents may be required for each language among the many countries of origin for Asian Americans. Asian Americans in aggregate may be less information-seeking than other groups [4]. They may be less forthcoming about symptoms or concerns, including mental health concerns, and less accepting of screening for disease given absence of symptoms. Indeed, statistics indicate that they are least likely among all racial/ethnic groups to have seen a physician in the prior 12 months [5].

Numerous studies have evaluated interventions that may increase acceptance and performance of screening. Importantly, the heterogeneity of the Asian American population makes a single strategy unlikely to address the unique cancer burden of this population and fix the disparity issue, and necessitates culturally appropriate interventions to target subpopulations or communities [24]. For example, a randomized study of a community-based approach involving Korean church-based organizations in the Philadelphia–New Jersey region increased colorectal cancer screening from 16% in the control group ( $n = 455$ ) to 69% in the intervention group ( $n = 470$ ) [7]. The multifaceted intervention included educational resources, health system navigation, and fecal immunochemical tests. Similarly, a study of Korean Americans identified through local community outreach in the Los Angeles Koreatown area randomized participants ( $n = 100$ ) to educational brochures in Korean and English about colorectal cancer (control group) or the same brochures coupled with a short educational seminar (intervention group) [30]. The outcome was awareness of colorectal cancer screening assessed by questionnaire, with the intervention group having significantly greater awareness of screening methods. Importantly, the intervention group was also more willing to undergo

screening in the following 6 months (88% vs. 8%). These specific studies highlight the importance of targeted intervention: colorectal cancer is now the most common cancer among Korean Americans, yet Korean Americans over age 50 have the lowest rate of colorectal cancer screening compared with other Asian American groups [31, 32].

Care navigation can significantly improve cancer screening rates. A randomized controlled trial employing lay navigators was performed in Molokai, Hawaii, to address knowledge gaps about cancer, educate about the benefits of screening, secure insurance, facilitate health care management, provide transportation to appointments, and encourage self-advocacy [33]. The population included 45% native Hawaiian, 35% Filipino, 11% Japanese, and 8% other. Compared with the control group ( $n = 246$ ), the intervention group ( $n = 242$ ) had significantly increased cervical cancer screening (57.0% vs. 26.4%), breast cancer screening (61.7% vs. 42.4%), prostate cancer screening (by prostate-specific antigen testing; 54.5% vs. 36.0%), and colorectal cancer screening (43.0% vs. 27.2%).

The absence of national guidelines for screening certain cancers that occur at higher rates in Asian Americans is a barrier to improving outcomes. Liver and stomach cancers clearly occur at higher rates in this population, with significant mortality consequences as described above. Although Asians are only 6% of the total U.S. population, an understanding of these cancer risks by primary care providers will be important for appropriate recommendations regarding smoking cessation, HBV vaccination, *H. pylori* testing and eradication, and referrals for screening of high-risk individuals [34].

---

#### CULTURAL PERCEPTIONS OF MEDICAL CARE

An important variation among Asian Americans and in contrast with other American cultures is the general attitude toward health care. Such cultural perceptions may drive patient health care decisions more than American providers realize. For example, the simple term “cancer” has been found to carry a stigma in many Asian cultures. Some of these negative associations are derived from the belief that cancer is possibly attributable to some form of fortune (e.g., luck, transgressions in a previous lifetime, or the will of a supreme power). Therefore, it is not surprising that in a survey of 94 doctors in Singapore used euphemisms for cancer such as “lump” or “growth” [35, 36]. These findings highlight that clinicians in the U.S. may need to better understand the cultural perceptions of cancer before they can even broach the subject of screening.

Even among first-generation Asian Americans from China, a study of 45 women from varied socioeconomic backgrounds and professions demonstrated common culture-based perceptions that influenced breast screening. Although these women largely understood the significant health care implications of breast cancer, there was common sentiment among the women that because they were Chinese, the risks were low. Other barriers to screening included a fatalistic view toward a cancer diagnosis and faith in traditional Chinese remedies [37]. Specific barriers to cancer screening for pelvic and breast malignancies may

be influenced by cultural perceptions of modesty among women. A parallel problem exists for Asian men faced with concerns about prostate cancer and colon cancer screening that is interlaced with concerns about preserving masculinity and sexual function.

Another key difference between western medicine and the Asian culture is the focus of the health care discussions once a diagnosis has been made. As opposed to a western emphasis on patient-centric care, many Asian cultures prefer a family-centric model where health care decisions must often be discussed with the family before decisions can be made. These attitudes often persist generations after migration to western societies [38]. It is also common for Asians who have migrated to the west to choose to shield their older relatives from a cancer diagnosis with a poor prognosis, perhaps related to cultural beliefs that the stress could lead to worse outcomes [39]. For these reasons, extra time may be required to accommodate the scheduling of multiple family members with the patient and implement a plan of care that is in keeping with their expectations while also appropriate for the patient.

For Asian Americans who do not choose a family-centric model, cultural stoicism and a desire to limit cost expenditures on health care may lead to patients deferring care or not sharing a cancer diagnosis (or poor prognosis) with family, perhaps contributing to poor outcomes [35, 37]. It is possible that even end-of-life care is affected by these cultural perceptions. Hospice use among Asian Americans has been found to be less than among other subpopulations and is possibly influenced by a combination of patient attitudes and perceptions that are not adequately addressed by hospice care as it is generally implemented [40, 41].

---

## CONCLUSION

Asian Americans face a unique cancer challenge. As the fastest-growing racial/ethnic group in the U.S. and the only group with cancer as the leading cause of death, there is an urgent need to improve cancer screening for the Asian American population. To do so, health care providers will need to be aware of these facts, including the profile of cancer risks among different Asian subpopulations, and have the necessary tools to communicate cancer risks and benefits of screening. Asian Americans will need to be educated and encouraged to be advocates for their health, which includes improving access to insurance and health care resources.

## Is This Racism?

The health care disparities faced by Asian Americans are not remotely comparable to the structural racism faced by Black Americans forged over more than four centuries [10]. By no means should this call to action imply that the needs of Asian Americans supersede those of any other group. However, disparities do exist for Asian Americans, and this may be surprising to health care providers. Therefore, the reason to raise awareness is to compel the medical establishment to recognize the urgent need to eliminate health disparities for all.

When evaluating Asian Americans in aggregate, the measures of economic and educational status, the numbers of Asian health professionals in the U.S., and the model minority label contribute to the implicit bias that Asian Americans have similar disease risk profiles to the majority White American population. Acceptance of the advantages of the model minority label (e.g., less discrimination compared with other racial/ethnic groups) may cause some Asian Americans to embody the myth of the docile, hard-working citizen who will not complain or “rock the boat”—which, when applied to health care, may lead to less information- or care-seeking for physical and mental health care needs. This acceptance by patients and providers of a stereotype leads to less advocacy, less understanding of differing disease risk profiles whether diabetes mellitus or mental health or cancer, and less screening. Hence, the disadvantages of the model minority myth, conceived in the Civil Rights era to drive a wedge between Asians and other racial/ethnic groups, *do* implicate racism as an indirect contributor to contemporary cancer disparities for Asian Americans.

Self-advocacy will be an important antidote to disparities. Past and contemporary history point to the fickle nature of public opinion and politics with respect to Asian Americans’ standing in U.S. society. For over 150 years, Asians faced discrimination in laws and immigration practice as the “Yellow Peril,” culminating in the ignominious internment of Japanese Americans during World War II. Only with the Civil Rights era, as an affront to Black Americans, were Asian Americans dubbed a “model minority.” The death of Vincent Chin in 1982 and the Los Angeles riots of 1992 made clear that this label indeed was a myth. Even the 9/11 terrorist attacks by Al-Qaeda turned South Asian Americans, by virtue of the color of their skin and for some, their religion, into perceived threats. Finally, the COVID-19 pandemic’s emergence in China and increase in racially motivated hate crimes against Asian Americans point to the potential for political rhetoric to unearth deep-seated racism [42].

## Recommendations

Elimination of cancer disparities for all racial/ethnic groups involves (a) education for patients and providers of the existence of the disparity and (b) improved access to care [4]. For Asian Americans, perhaps more so than other groups, the many languages spoken by the subpopulations necessitate the availability of cancer information and screening in all languages. Medical interpreter services are critical for accurate information delivery, as opposed to translation by a family member or friend, given the complexity of medical terminology and description of risk, as well as potential cultural barriers to using terms such as “cancer.” Given the time pressures of contemporary medical practice, the additional time and effort of employing medical interpreter services may contribute to fewer recommendations for appropriate screening. Therefore, it is important that providers receive education about the specific cancer risks faced by Asian Americans, including higher mortality, to spend the time to appropriately discuss cancer screening, smoking cessation, and vaccination for HBV and HPV.

Educational campaigns reaching Asian Americans in their communities (grocery stores, places of worship, community centers, print media, direct mail, Internet) have proven effective [24]. Engagement of English-proficient community members such as younger generations may help steer older Asian Americans to advocate for cancer screening.

Improved access to care is a straightforward recommendation with difficult implementation. Culturally appropriate, community-based interventions that meet the Asian American populations where they live are likely to be the most effective at improving access to and education about health care [24]. Lay navigators can significantly improve awareness of cancer issues, access to care, and cancer screening in a culturally sensitive and impactful fashion [33]. Access to care and encouragement for self-advocacy can normalize seeing primary care providers for routine care and screening, in a population that is least likely to have seen a physician in the prior year [5]. Partnership of major cancer centers with community health centers will align the goals of seamlessly moving patients from screening and diagnosis to appropriate oncology care and access to clinical trials. At the national level, governmental funding to focus on and eliminate disparities among Asian Americans should be

expanded [43]. Improving cancer literacy and access to care will contribute to narrowing cancer disparities and improving cancer care for Asian Americans.

#### AUTHOR CONTRIBUTIONS

**Conception/design:** Richard J. Lee

**Data analysis and interpretation:** Richard J. Lee, Ravi A. Madan, Jayoung Kim, Edwin M. Posadas, Evan Y. Yu

**Manuscript writing:** Richard J. Lee, Ravi A. Madan, Jayoung Kim, Edwin M. Posadas, Evan Y. Yu

**Final approval of manuscript:** Richard J. Lee, Ravi A. Madan, Jayoung Kim, Edwin M. Posadas, Evan Y. Yu

#### DISCLOSURES

**Richard J. Lee:** Astellas, Bayer, Dendreon, Exelixis, GE Healthcare, Janssen (C/A), Janssen (RF-institution); **Evan Y. Yu:** Janssen, Bayer, Merck, Clovis, Advanced Accelerator Applications, Exelixis, Abbvie, Sanofi (C/A), Bayer, Merck, Daiichi-Sankyo, Taiho, Dendreon, Seagen Inc, Pharmacyclics, Blue Earth (RF—institution); **Ravi A. Madan:** Janssen (RF-institution). The other authors indicated no financial relationships.

(C/A) Consulting/advisory relationship; (RF) Research funding; (E) Employment; (ET) Expert testimony; (H) Honoraria received; (OI) Ownership interests; (IP) Intellectual property rights/inventor/patent holder; (SAB) Scientific advisory board

#### REFERENCES

- Torre LA, Goding Sauer AM, Chen MS Jr et al. Cancer statistics for Asian Americans, native Hawaiians, and Pacific Islanders, 2016: Converging incidence in males and females. *CA Cancer J Clin* 2016;66:182–202.
- Centers for Disease Control and Prevention. Leading causes of death in males, 2017. Centers for Disease Control and Prevention Web site. Available at <https://www.cdc.gov/healthequity/lcod/index.htm>.
- Grineski SE, Collins TW, Morales DX. Asian Americans and disproportionate exposure to carcinogenic hazardous air pollutants: A national study. *Soc Sci Med* 2017;185:71–80.
- Jun J. Cancer/health communication and breast/cervical cancer screening among Asian Americans and five Asian ethnic groups. *Ethn Health* 2020;25:960–981.
- Chen MS Jr. Cancer health disparities among Asian Americans: What we do and what we need to do. *Cancer* 2005;104(suppl 12):2895–2902.
- Ibaraki AY, Hall NGC, Sabin JA. Asian American cancer disparities: The potential effects of model minority health stereotypes. *Asian Am J Psychol* 2014;5:75–81.
- Ma GX, Lee M, Beeber M et al. Community-clinical linkage intervention to improve colorectal cancer screening among underserved Korean Americans. *Cancer Health Disparities* 2019;3:e1–e15.
- Pew Research Center. Key Facts about Asian origin groups in the U.S. Available at <https://www.pewresearch.org/fact-tank/2019/05/22/key-facts-about-asian-origin-groups-in-the-u-s/>. Accessed December 15, 2020.
- Centers for Disease Control and Prevention. Social determinants of health: Know what affects health. Centers for Disease Control and Prevention Web site. Available at <https://www.cdc.gov/socialdeterminants/index.htm>. Accessed December 15, 2020.
- Bailey ZD, Krieger N, Agénor M et al. Structural racism and health inequities in the USA: Evidence and interventions. *Lancet* 2017;389:1453–1463.
- Xierali IM, Nivet MA. The racial and ethnic composition and distribution of primary care physicians. *J Health Care Poor Underserved* 2018;29:556–570.
- Association of American Medical Colleges. Diversity in Medicine: Facts and Figures 2019. Washington, DC: Association of American Medical Colleges, 2019. Available at <https://www.aamc.org/data-reports/workforce/report/diversity-medicine-facts-and-figures-2019>.
- U.S. Department of Health and Human Services, Health Resources and Services Administration, National Center for Health Workforce Analyses. 2017. Sex, Race, and Ethnic Diversity of U.S. Health Occupations (2011–2015). Rockville, MD: Health Resources and Services Administration, 2017. Available at <https://bhw.hrsa.gov/sites/default/files/bureau-health-workforce/data-research/diversity-us-health-occupations.pdf>. Accessed December 15, 2020.
- Yi SS, Kwon SC, Sacks R et al. Commentary: Persistence and health-related consequences of the model minority stereotype for Asian Americans. *Ethn Dis* 2016;26:133–138.
- Petersen W. Success story, Japanese-American style. *New York Times Magazine*, January 9, 1966:20–43.
- Success story of one minority group in U.S. *U.S. News and World Report*, December 26, 1966:73–76.
- Siegel RL, Miller KD, Jemal A. Cancer statistics, 2016. *CA Cancer J Clin* 2016;66:7–30.
- Ashktorab H, Kupfer SS, Brim H et al. Racial disparity in gastrointestinal cancer risk. *Gastroenterology* 2017;153:910–923.
- Crew KD, Neugut AI. Epidemiology of gastric cancer. *World J Gastroenterol* 2006;12:354–362.
- Florea A, Brown HE, Harris RB et al. Ethnic disparities in gastric cancer presentation and screening practice in the United States: Analysis of 1997–2010 Surveillance, Epidemiology, and End Results-Medicare data. *Cancer Epidemiol Biomarkers Prev* 2019;28:659–665.
- Martell BN, Garrett BE, Caraballo RS. Disparities in adult cigarette smoking — United States, 2002–2005 and 2010–2013. *MMWR Morb Mortal Wkly Rep* 2016;65:753–758.
- Ha SY, Choi SJ, Cho JH et al. Lung cancer in never-smoker Asian females is driven by oncogenic mutations, most often involving EGFR. *Oncotarget* 2015;6:5465–5474.
- Nebert DW, Dalton TP. The role of cytochrome P450 enzymes in endogenous signalling pathways and environmental carcinogenesis. *Nat Rev Cancer* 2006;6:947–960.
- Hou SI, Sealy DA, Kabiru CE. Closing the disparity gap: Cancer screening interventions among Asians — a systematic literature review. *Asian Pac J Cancer Prev* 2011;12:3133–3139.
- Lee J, Demissie K, Lu SE et al. Cancer incidence among Korean-American immigrants in the United States and native Koreans in South Korea. *Cancer Control* 2007;14:78–85.
- DeSantis CE, Ma J, Gaudet MM et al. Breast cancer statistics, 2019. *CA Cancer J Clin* 2019;69:438–451.
- May FP, Almario CV, Ponce N et al. Racial minorities are more likely than whites to report lack of provider recommendation for colon cancer screening. *Am J Gastroenterol* 2015;110:1388–1394.
- Fedewa SA, Sauer AG, Siegel RL et al. Temporal trends in colorectal cancer screening among Asian Americans. *Cancer Epidemiol Biomarkers Prev* 2016;25:995–1000.

29. Tung EL, Baig AA, Huang ES et al. Racial and ethnic disparities in diabetes screening between Asian Americans and other adults: BRFSS 2012–2014. *J Gen Intern Med* 2017;32:423–429.
30. Kim S, Yeon A, Cho E et al. Effectiveness of a tailored colorectal cancer educational seminar in enhancing the awareness, knowledge, and behavior of Korean Americans living in the Los Angeles Koreatown area. *Divers Equal Health Care* 2019;16:1–8.
31. Maxwell AE, Crespi CM. Trends in colorectal cancer screening utilization among ethnic groups in California: Are we closing the gap? *Cancer Epidemiol Biomarkers Prev* 2009;18:752–759.
32. Liu L, Wang Y, Sherman RL et al. Cancer in Los Angeles County: Trends by Race/Ethnicity, 1976–2012. Los Angeles, CA: Los Angeles Cancer Surveillance Program, University of Southern California, 2016.
33. Braun KL, Thomas WL Jr, Domingo JLB et al. Reducing cancer screening disparities in Medicare beneficiaries through cancer patient navigation. *J Am Geriatr Soc* 2015;63:365–370.
34. Taylor VM, Ko LK, Hwang JH et al. Gastric cancer in Asian American populations: A neglected health disparity. *Asian Pac J Cancer Prev* 2014;15:10565–10571.
35. Ong KJ, Back MF, Lu JJ et al. Cultural attitudes to cancer management in traditional South-East Asian patients. *Australas Radiol* 2002;46:370–374.
36. Tan TK, Teo FC, Wong K et al. Cancer: To tell or not to tell? *Singapore Med J* 1993;34:202–203.
37. Facione NC, Giancarlo C, Chan L. Perceived risk and help-seeking behavior for breast cancer: A Chinese-American perspective. *Cancer Nurs* 2000;23:258–267.
38. Blackhall LJ, Murphy ST, Frank G et al. Ethnicity and attitudes toward patient autonomy. *JAMA* 1995;274:820–825.
39. Huang X, Butow P, Meiser B et al. Attitudes and information needs of Chinese migrant cancer patients and their relatives. *Aust N Z J Med* 1999;29:207–213.
40. Crawley LM. Racial, cultural, and ethnic factors influencing end-of-life care. *J Palliat Med* 2005;8(suppl 1):S58–S69.
41. Hardy D, Chan W, Liu CC et al. Racial disparities in the use of hospice services according to geographic residence and socioeconomic status in an elderly cohort with nonsmall cell lung cancer. *Cancer* 2011;117:1506–1515.
42. Gover AR, Harper SB, Langton L. Anti-Asian hate crime during the COVID-19 pandemic: Exploring the reproduction of inequality. *Am J Crim Justice* 2020;45:647–667.
43. Chen MS Jr, Chow EA, Nguyen TT. The Asian American Network for Cancer Awareness, Research, and Training (AANCART)'s contributions toward reducing Asian American cancer health disparities, 2000–2017. *Cancer* 2018;124:1527–1534.



1  
2  
3  
4 **Research Progress of Urine Biomarkers**  
5 **in the Diagnosis, Treatment, and Prognosis of Bladder Cancer**  
6

7  
8 Feng Jin<sup>1</sup>, Muhammad Shahid<sup>1</sup>, Jayoung Kim<sup>1,2,3,4,†</sup>  
9

10  
11 <sup>1</sup>Departments of Surgery, Cedars-Sinai Medical Center, Los Angeles, CA; <sup>2</sup>Samuel Oschin  
12 Comprehensive Cancer Institute, Cedars-Sinai Medical Center, Los Angeles, CA, USA;  
13 <sup>3</sup>Departments of Surgery and Biomedical Sciences, Cedars-Sinai Medical Center, Los Angeles,  
14 CA; <sup>4</sup>University of California Los Angeles, CA, USA; <sup>5</sup>Department of Urology, Ga Cheon University  
15 College of Medicine, Incheon, Republic of Korea  
16  
17  
18  
19  
20  
21  
22  
23

24 **†Correspondence:**

25 Jayoung Kim, PhD.

26 Professor

27 Departments of Surgery and Biomedical Sciences, Cedars-Sinai Medical Center, 8700 Beverly  
28 Blvd., Los Angeles, CA 90048

29 Tel: +1-310-423-7168 Fax: +1-310-967-3809

30 E-mail: Jayoung.Kim@cshs.org  
31  
32  
33  
34  
35  
36  
37

38 **Key words:**

39 Urine; Biomarkers; Metabolomics; Bladder Cancer  
40



41 **Abstract**

42

43 Bladder cancer (BC) is one of the most common tumor with high incidence. Relative to other  
44 cancers, BC has a high rate of recurrence, which results in increased mortality. As a result, early  
45 diagnosis and life-long monitoring are clinically significant for improving the long-term survival rate  
46 of BC patients. At present, the main methods of BC detection are cystoscopy and biopsy;  
47 however, these procedures can be invasive and expensive. This can lead to patient refusal and  
48 reluctance for monitoring. There are several BC biomarkers that have been approved by the FDA,  
49 but their sensitivity, specificity, and diagnostic accuracy are not ideal. More research is needed to  
50 identify suitable biomarkers that can be used for early detection, evaluation, and observation.  
51 There has been heavy research in the proteomics and genomics of BC and many potential  
52 biomarkers have been found. Although the advent of metabonomics came late, with the recent  
53 development of advanced analytical technology and bioinformatics, metabonomics has become  
54 a widely used diagnostic tool in clinical and biomedical research. It should be emphasized that  
55 despite progress in new biomarkers for BC diagnosis, there remains challenges and limitations in  
56 metabonomics research that affects its translation into clinical practice. In this chapter, the latest  
57 literature on BC biomarkers was reviewed.

58

59

60

61 **1 Introduction**

62

63 **1.1 Bladder cancer (BC) incidence, epidemiology, and risk factors**

64

65 Bladder cancer (BC) is the fourth most common cancer in the U.S. and the second most common  
66 cancer of the urinary system, accounting for 7% of all new cancer cases. It also accounts for 4%  
67 of all cancer-related deaths in the U.S., ranking it the fifth deadliest cancer. The male to female  
68 ratio of morbidity and mortality was about 3:1[1]. Risk factors are related to the environment, diet,  
69 and lifestyle, especially smoking, exposure to aromatic amines, and genetic factors[2-4]. Other  
70 known risk factors include the ingestion of high levels of arsenic or significant usage of pain  
71 relievers containing finazepine[4, 5].

72

73 **1.2 Economic burden of BC**

74

75 The European Organization for Research and Treatment of Cancer (EORTC) has established  
76 recommended plans for low to moderate-risk BC patients. This involves a cystoscopy every three  
77 months during the first two years, every four months during the following two years, and once a  
78 year thereafter[6]. Because BC treatment is continuous, the lifetime cost of treatment and  
79 monitoring increases with time. Studies have shown that the cumulative cost of health insurance  
80 for long-term survivors (those over 16 years) is \$172,426[7]. As a result of this need for lifelong  
81 monitoring, the cost per patient when treating BC is the highest of all other cancers[8].

82

83 **1.3 Classical Classification of BC**

84

85 Based on the degree of invasion in the bladder muscle wall, BC is divided into either non-muscle  
86 invasive BC (NMIBC) or muscle invasive BC (MIBC)[9]. There may be different genetic variation  
87 underlying the difference between the two types of BC[10]. When histologically subtyping BC,  
88 there are several types. Transitional cell carcinoma (TCC), also known as urothelial carcinoma,  
89 accounts for about 90% of all BC. Squamous cell carcinoma (SCC) and adenocarcinoma account  
90 for about 10%[11]. There are various other rare types of BC as well[12]. BC can also be divided  
91 pathologically into low-grade (LG) and high-grade (HG) tumors. LG tumors are usually well-  
92 differentiated, while HG tumors are poorly differentiated[13].

93

94 **1.4 Molecular phenotyping of BC**

95

96 Recent genome mRNA expression analysis demonstrated that BC can be classified into  
97 molecular subtypes. These different subtypes of BC have distinct progression patterns, biological  
98 and clinical properties, and response to chemotherapies. There are currently five published  
99 classification methods; these include guidelines from the University of North Carolina (UNC), MD  
100 Anderson Cancer Center (MDA), The Cancer Genome Atlas (TCGA), Lund University (Lund), and  
101 Broad Institute of Massachusetts Institute of Technology and Harvard University (Broad)(Table1)

102

103 The classifications by UNC define two molecular subtypes of high-grade BC, “luminal” and  
104 “basal”, with molecular features reflecting different stages of urothelial differentiation[14]. Luminal  
105 BC expresses terminal urothelial differentiation markers, such as those seen in umbrella cells  
106 (UPK1B, UPK2, UPK3A, and KRT20), whereas basal BC expresses high levels of genes that are  
107 typical in urothelial basal cells (KRT14, KRT5, and KRT5B). The UNC study created a gene  
108 signature, BASE47, that accurately discriminates intrinsic bladder subtypes. Identified basal  
109 tumors had significantly decreased disease-specific and overall survival. In addition, among the

110 clinicopathological features available in the MSKCC dataset, only subtypes identified by BASE47  
111 were found to be significant in disease-specific survival by univariate analysis. This study also  
112 found that females have an increased incidence of basal-like BC, which is associated with a worse  
113 prognosis.

114  
115 The classification system by MDA identified three molecular subtypes of MIBC: “basal”, “luminal”,  
116 and “P53-like” [15]. Basal MIBC was associated with shorter disease-specific and overall survival,  
117 presumably because these patients tend to have more invasive and metastatic disease at  
118 presentation. Transcription factor P63 plays a central role in controlling basal gene signatures  
119 and preliminary data suggests that EGFR, Stat-3, NFκB, and Hif-1α are also involved. Luminal  
120 MIBC displays active ER/TRIM24 pathway gene expression and were enriched for FOXA1,  
121 GATA3, ERBB2, and ERBB3. Luminal MIBC contains active PPAR gene expression and  
122 activating FGFR3 mutations; thereby, PPARγ- and FGFR-3-targeted agents may be active in this  
123 subtype. Because luminal MIBC responds well to neoadjuvant chemotherapy (NAC), targeted  
124 therapies should be combined with conventional chemotherapy for maximum efficacy. The P53-  
125 like MIBC responded very poorly to NAC and were consistently resistant to frontline neoadjuvant  
126 cisplatin-based combination chemotherapy. Additionally, comparative analysis of matches gene  
127 expression profiles before and after chemotherapy revealed that all resistant tumors expressed  
128 wild-type P53 gene expression signatures. These results indicate that “P53-ness” may play a  
129 central role in BC chemoresistance.

130  
131 The classification by TCGA identified four clusters (clusters I–IV) by analyzing RNA-seq data from  
132 129 tumors[16]. Cluster I (papillary-like) is enriched in tumors with papillary morphology, FGFR3  
133 mutations, FGFR3 copy number gain, and elevated FGFR3 expression. Cluster I samples also  
134 had significantly lower expression of miR-99a, miR-100, miR-145 and miR-125b. Tumors with  
135 FGFR3 alterations and those that share similar cluster I expression profiles may respond well to  
136 inhibitors of FGFR and its downstream targets. Clusters I and II express high levels of GATA3  
137 and FOXA1. Markers of urothelial differentiation, such as uroplakins, epithelial marker E-cadherin,  
138 and members of miR-200 miRNAs are also highly expressed in clusters I and II. Clusters I and II  
139 express high HER2 levels and an elevated estrogen receptor beta signaling signature, which  
140 suggests potential targets for hormone therapies, such as tamoxifen or raloxifene. Cluster III  
141 (basal/squamous-like) express characteristic epithelial lineage genes, including KRT14, KRT5,  
142 KRT6A, and EGFR. Many of the samples in cluster III express cytokeratins (KRT14 and KRT5).  
143 Integrated expression profiling analysis of cluster III revealed a urothelial carcinoma subtype with  
144 cancer stem-cell expression features, perhaps providing another avenue for therapeutic targeting.

145  
146 The Lund classification system defines five major urothelial carcinoma subtypes: urobasal A,  
147 genomically unstable, urobasal B, squamous cell carcinoma-like (SCC-like), and infiltrated tumor  
148 class[17]. This was established using gene expression profiles from 308 tumor cases. These  
149 different molecular subtypes show significantly different prognosis. The best prognosis is the  
150 urobasal A, and the worst prognosis are urobasal B and SCC-like. The prognosis of genomically  
151 unstable and infiltrated class are between them. Urobasal A tumors were characterized by  
152 elevated expression of FGFR3, CCND1, TP63, as well as expression of KRT5 in cells at the  
153 tumor–stroma interface. The majority of urobasal A tumors were non-muscle invasive and of low  
154 pathologic grade. The genomically unstable subtype was characterized by expression of ERBB2  
155 and CCNE, low expression of cytokeratin, and frequent mutations of TP53. Genomically unstable  
156 cases represented a high-risk group, as close to 40% were MIBC. This subtype also showed low  
157 PTEN expression. The SCC-like subtype was characterized by high expression of basal keratins,  
158 which are normally not expressed in the urothelium; these include KRT4, KRT6A, KRT6B, KRT6C,  
159 KRT14, and KRT16. SCC-like tumors also had markedly bad prognoses. Furthermore, this group

160 showed a comparatively different proportion of female/male patients, reminiscent of the 1:1  
161 proportion seen in patients diagnosed with bladder SCC, suggesting that females are more likely  
162 to develop urothelial carcinomas with a keratinized/squamous phenotype, which is associated  
163 with an adverse prognosis. Urobasal B tumors showed several similarities to urobasal A tumors,  
164 such as a high FGFR3 mutation frequency, elevated FGFR3, CCND1, and TP63 levels, and  
165 expression of the FGFR3 gene signature. However, this group also showed frequent TP53  
166 mutations and expression of several keratins specific for the SCC-like subtype. Additionally, 50%  
167 of the cases were MIBC; including 5 of 9 FGFR3 mutated cases. The infiltrated subtype  
168 demonstrated a pronounced immunologic and extracellular membrane (ECM) signal, indicating  
169 the presence of immunologic and myofibroblast cells. This subtype most likely represents a  
170 heterogeneous class of tumors; immunohistochemistry (IHC) revealed the presence of tumors  
171 with genomically unstable, urobasal B, and SCC-like protein expression patterns in this group.  
172

173 The Broad classification identified four different subtypes: luminal, immune undifferentiated,  
174 luminal immune, and basal[18]. Approximately 41% of invasive BC was in the luminal subtype,  
175 with high expression of KRT20 and UPKs 2/1A/1B/3A as well as moderate to high expression of  
176 multiple pertinent transcription factors (KLF5, PPARG, and GRHL5). The luminal subtype was  
177 enriched for in male patients, papillary histology, and stage II tumors. A third (29%) of invasive  
178 BC was in the basal subtype, with high expression of KRT14, KRT5, KRT6A/B, and KRT16, and  
179 low expression of uroplakins, which is consistent with basal or undifferentiated cytokeratin  
180 expression patterns. Consistent with prior studies, the basal subtype expressed TP63, TP73,  
181 MYC, EGFR, TGM1, and SCEL, which is indicative of some degree of squamous differentiation.  
182 The basal subtype was enriched in female patients and tumors with nonpapillary histology. The  
183 basal subtype also expressed many immune genes at intermediate and somewhat variable levels.  
184 These genes include CTLA4 and CD274, which encodes for PD-L1, suggesting that there may  
185 be immune cell infiltration of tumors. A smaller percentage of cancers (11%) were grouped into a  
186 novel subtype called immune undifferentiated. These cancers showed very low expression of  
187 luminal markers, variable expression of basal cytokeratins, and relatively high expression of  
188 immune genes, including CTLA4 and CD274, which further suggests significant immune cell  
189 infiltration and possible immune evasion. Lastly, the luminal immune subtype group constitutes  
190 about 18% of all cases and is characterized by the expression of luminal genes (cytokeratins and  
191 uroplakins) and intermediate expression of immune genes. This group was notably enriched for  
192 stage N+ tumors. The luminal subtype was enriched for in cancers with FGFR3 mutations and  
193 amplification events involving PVRL4 and YWHAZ. The basal subtype was enriched for NFE2L2  
194 mutations. Both the luminal immune and immune undifferentiated subtypes had high expression  
195 levels of ZEB1, ZEB2, and TWIST1, which is characteristic of epithelial-mesenchymal transition  
196 (EMT).  
197

198 Gottfrid et al. proposed five major tumor-cell phenotypes in advanced BC: urothelial-like,  
199 genomically unstable (GU), basal/SCC-like, mesenchymal-like, and small-cell/neuroendocrine-  
200 like[19]. Urothelial-like tumors express FGFR3 and CCND1 and frequently demonstrate a loss of  
201 9p21 (CDKN2A). GU tumors express FOXM1, but not KRT5, and frequently show loss of RB1.  
202 Basal/SCC-like tumors were found to express KRT5 and KRT14, but not FOXA1 and GATA3.  
203 The mesenchymal-like BC is a new subtype that shows a tumor-cell phenotype that starkly  
204 contrasts with previously defined subtypes and is biologically different from the basal/SCC-like  
205 cases that they are clustered with. The tumor cells are mesenchymal-like and express typical  
206 mesenchymal genes, such as ZEB2 and VIM. The tumor cells were themselves mesenchymal-  
207 like and expressed the typical mesenchymal genes ZEB2 and VIM. The consensus cluster Sc/NE-  
208 like turned out to harbor two very distinct tumor-cell phenotypes. One-half of these tumors  
209 expressed markers that are typical for neuroendocrine differentiation. This part of the Sc/NE

210 consensus cluster also showed an absence of PPARG, FOXA1, and GATA3 expression, as well  
211 as of uroplakin and KRT20 expression.

212  
213 Kardos et al. reported the discovery of a claudin-low molecular subtype of high-grade BC that  
214 shares characteristics with the homonymous subtype of breast cancer[20]. Although there has  
215 been much work done on the molecular phenotyping of BC, the different emphases of different  
216 classification methods have made it difficult to consolidate a widely accepted classification  
217 method. As a result, the molecular phenotyping of BC remains to be further studied. The claudin-  
218 low subtype can be considered a subpopulation of the basal-like subtype (UNC classification  
219 system). Claudin-low bladder tumors are rich in a variety of genetic characteristics, including  
220 increased mutation rates of RB1, EP300, and NCOR1, increased the frequency of EGFR  
221 amplification, decreased mutation rates of FGFR3, ELF3, and KDM6A, and decreased the  
222 frequency of PPARG amplification. These characteristics define a molecular subtype of BC with  
223 distinct molecular features and an immunological profile that is theoretically primed for an  
224 immunotherapeutic response.

225  
226 **Figure 1** summarizes the classification of BC.

227  
228  
229

## 230 **2 Biomarker Discovery in BC**

231  
232 More than 75% of patients are diagnosed and treated for NMIBC. At the time of initial evaluation,  
233 its recurrence rate can be as high as 70%[21]. Currently, the standard and most important  
234 examination method for BC is cystoscopy, However, this procedure is invasive, uncomfortable,  
235 and expensive[22]. Furthermore, cystoscopy may miss certain lesions, particularly smaller areas  
236 of carcinoma in situ[23]. Molecular biosignatures indicative of altered cellular landscapes and  
237 functions have been casually linked to pathological conditions, suggesting the promise of BC-  
238 specific biomarkers. However, a noninvasive biomarker that is as sensitive and specific as  
239 standard cystoscopy has yet to be discovered. As we progress through the 21<sup>st</sup> century, we now  
240 have access to a number of ways to analyze diagnostic markers in-depth. The evolution of omics  
241 platforms and bioinformatics to allow for analysis of the genome, epigenome, transcriptome,  
242 proteome, lipidome, metabolome et al. enables the development of more sensitive biomarkers.  
243 These discoveries will broaden understanding of the complex biology and pathophysiology of  
244 bladder diseases, which can then be clinically translated. Biomarkers of interest can be detected  
245 in different types of samples, including serum, tissue, and urine. Urinary biomarkers are  
246 particularly attractive due to cost, time, and minimal effort. As a result, studies on urinary BC  
247 biomarkers continue to expand.

248  
249 **Figure 2** shows the overview of the multi-OMICS strategies for urine-based biomarker discovery  
250 and translational application.

### 251 252 **2.1 Proteomics-based BC biomarkers**

253  
254 In patients with hematuria, aurora A kinase (AURKA) can discriminate low-grade BC patients vs.  
255 normal patients [24]. After adjusting for patients, clinical features, and treatment with Bacillus  
256 Calmette-Guerin, the activated leukocyte cell adhesion molecule (ALCAM) is positively correlated  
257 with tumor stage and overall survival (OS)[25]. Nicotinamide N-methyltransferase has been  
258 shown to be elevated in BC patients and is correlated with histological grade[26].  
259 Apurinic/aprimidinic endonuclease 1/redox factor-1 (APE/Ref-1) levels are higher in BC, with



260 respect to non-BC, and is correlated with tumor grade and stage; moreover, it has been shown to  
261 be significantly increased in patients with historical BC recurrence[27]. The urinary cytokeratin-  
262 20 (CK20) RT-PCR assay shows that the sensitivity of urothelial BC detection was 78-87%, and  
263 the specificity was 56-80%. , with improved diagnostic accuracy in tumor progression[28].  
264 However, its performance is relatively poor in low-grade tumors. Higher urinary levels of CK8 and  
265 CK18 have been detected via UBC Rapid Test in high vs. low-grade BC[29].

266  
267 There are multiple markers that can potentially be used for BC detection; increased urinary levels  
268 of apolipoproteins, A1, A2, B, C2, C3, and E (APOA1, APOA2, APOB, APOC2, APOC3, APOE)  
269 were found in BC compared to healthy controls[30, 31]. A signature of 4 urinary fragments of  
270 uromodulin, collagen  $\alpha$ -1 (I), collagen  $\alpha$ -1 (III), and membrane-associated progesterone receptor  
271 component 1 may be able to discriminate MIBC from NMIBC[32]. Other panels employ IL-8,  
272 MMP-9/10, ANG, APOE, SDC-1,  $\alpha$ 1AT, PAI-1, VEGFA, and CA9 to indicate BC from urine  
273 samples. The advantage of these multi-urinary protein biomarkers is evident in high and low-  
274 grade and high and low-stage diseases[33]. Combined with urine markers, including midkine  
275 (MDK), MDK, synuclein G, CEACAM1, ZAG2 [34], clusterin (CLU) and angiogenin (ANG), the  
276 sensitivity and specificity of NMIBC diagnosis can be improved through immunoassay and urine  
277 cytology [35]. CK20 and insulin-like growth factor II (IGF-II) levels were found to be increased in  
278 the urine sediments of NMIBC patients compared to controls[36]. Increased levels of urinary HAI-  
279 1 and epithelial cell adhesion molecule (EpCAM) are prognostic biomarkers in high-risk NMIBC  
280 patients[37]. Urine survivin have been proved by chemiluminescence enzyme immunoassay that  
281 it is a potential biomarker for BC, which has been shown to be related to tumor stage, lymph node  
282 metastasis, and distant metastasis.[38]. Snail overexpression represents an independent  
283 prognostic factor for tumor recurrence in NMIBC[39]. CD44 in urine was found to be elevated in  
284 high-grade MIBC by glycan-affinity glycoproteomics nanoplatfoms. [40].

285  
286 Proteomics-based BC biomarkers were summarized in **Table 2**.

## 287 288 **2.2 Metabolomics-based BC biomarkers**

289  
290 Urinary metabolomics signature may be useful in detecting early stage BC. Jin X et al. analyzed  
291 urinary metabolites by high-performance liquid chromatography-quadrupole time-of-flight mass  
292 spectrometry (HPLC-QTOFMS), and found 12 metabolites that help to identify BC.[41]. Zhou Y  
293 et al. developed a urinary pseudotargeted method based on gas chromatography-mass  
294 spectrometry (GC-MS) which has been validated by a BC metabolomics study[42]. Using binary  
295 logistic regression analysis, a four-biomarker panel was defined for the diagnosis of BC. The  
296 results revealed that the urinary four-biomarker panel can be used to diagnose NMIBC or low-  
297 grade BC. Among the four metabolites, cholesterol levels were significantly increased in the BC  
298 group, while 5-hydroxyvaleric acid, 3-phosphoglyceric acid, and glycolic acid levels were  
299 markedly decreased in the BC group.

300  
301 X. Cheng et al. carried out a study based on metabolomics with liquid chromatography-high  
302 resolution mass spectrometry (LC-HRMS) to discover novel biomarkers for detecting early-stage  
303 BC. [43]. A total of 284 subjects were enrolled in the study including 117 healthy adults and 167  
304 BC patients. Metabolite panels are known to have more predictive power than a single metabolite  
305 [44]. A metabolite panel consisting of dopamine 4-sulfate, MG00/1846Z,9Z,12Z,15Z/00, aspartyl-  
306 histidine, and tyrosyl-methionine was found to have the best predictive accuracy in diagnosing  
307 NMIBC.



308  
309 A study by Yumba Mpanga A et al. developed and validated an analytical method for the  
310 simultaneous quantitative determination of metabolites using reversed phase high-performance  
311 liquid chromatography coupled with triple quadrupole mass spectrometry (RP-HPLC-  
312 QQQ/MS)[45]. The optimized and validated method was applied to urine samples from 40 BC  
313 patients and 40 healthy matched controls. Statistical analysis was done using the Student's t-test  
314 or U-Mann Whitney test. This identified 10 compounds that participate in different metabolic  
315 pathways, such as gut flora metabolism, RNA degradation, purine metabolism, etc., as being  
316 significantly different in urine between BC and control groups ( $p < 0.05$ ). These 10 compounds  
317 include acetylslysine, N-acetylneuraminic acid, pseudouridine, uridine, xanthine, 7-methylguanine,  
318 gluconic acid, glucuronic acid, 1,7 dimethylxanthine, and hippuric acid. Moreover, acid trehalose,  
319 nicotinic acid, and AspAspGlyTrp peptide were upregulated; inosinic acid, ureidosuccinic acid,  
320 and GlyCysAlaLys peptide were downregulated in BC, but not in healthy controls[46].

321  
322 Metabolomics-based BC biomarkers were summarized in **Table 3**.

## 323 324 **2.3 Genomics-based BC biomarkers**

### 325 326 **2.3.1 DNA methylation**

327  
328 Using urine sediments from BC patients, Sun and her group demonstrated that SOX-1, IRAK3,  
329 and Li-MET gene methylation status have higher recurrence predictivity than urine cytology and  
330 cystoscopy (80 vs. 35 vs. 15%, respectively) [47]. Methylated genes, such as those for APC and  
331 cyclin D2, were found to be significantly prevalent in the urine from malignant vs. benign cases[48].  
332 Hypermethylation of the GSTP1 and RAR $\beta$ 2 and APC genes have been identified in the urine of  
333 BC patients[49]. Evaluation of Twist Family BHLH Transcription Factor 1 (TWIST1) and NID2  
334 genes methylation status in urine has been shown to differentiate primary BC patients from  
335 controls with 90% sensitivity and 93% specificity[50]. Additionally, evaluation of the methylation  
336 status of NID2, TWIST1, CFTR, SALL3, and TWIST1 genes in urinary cells in combination with  
337 urine cytology has been found to increase sensitivity and have high negative predictive value in  
338 BC patients[51, 52]. Urinary methylation levels of POU4F2 and PCDH17 is able to distinguish BC  
339 from normal controls with 90% sensitivity and 94% specificity[53]. Promoter hypermethylation of  
340 HS3ST2, SEPTIN9, and SLIT2 combined with FGFR3 mutation showed 97.6% sensitivity and  
341 84.8% specificity in the diagnosis, surveillance, and risk stratification of low- and high-risk NMIBC  
342 patients[54]. Lastly, the methylation status of p14ARF, p16INK4A, RASSf1A, DAPK, and APC  
343 has been found to be correlated with BC grade and stage[55].

### 344 345 **2.3.2 miRNAs**

346  
347 Urinary levels of miR-146a-5p are significantly increased in high-grade BC[56]. MiR-126 urinary  
348 levels were found to be elevated in BC compared to healthy controls [57]. Low miR-200c  
349 expression has been shown to be correlated with tumor progression in NMIBC[58]. Chen et al.  
350 detected 74 miRNAs, of which 33 were upregulated and 41 were downregulated in BC compared  
351 to healthy patients; the most notable of these include let-7miR, mir-1268, miR-196a, miR-1, miR-  
352 100, miR-101, and miR-143[59]. By screening patients with negative cystoscopy, Eissa et al.  
353 identified miR-96 and miR-210 as being associated with BC[60]. MiR-125b, miR-30b, miR-204,  
354 miR-99a, and miR-532-3p were downregulated in the urine supernatant of BC patients[61]. MiR-  
355 9, miR-182, and miR-200b have been shown to be correlated with MIBC aggressiveness,

356 recurrence-free, and overall survival (OS)[62]. MiR-145 distinguishes NMIBC from non-BC[63].  
357 MiR-144-5p inhibits BC proliferation, affecting CCNE1, CCNE2, CDC25A, and PKMYT1 target  
358 genes[64]. Cell-free urinary miR-99a and miRNA-125b were found to be downregulated in the  
359 urine supernatants of BC patients (sensitivity 86.7%; specificity 81.1%)[65]. Urinary levels of miR-  
360 618 and miR-1255b-5p were increased in MIBC patients compared to healthy controls[66]. Whole  
361 genome analysis determined increased miR-31-5p, miR-191-5p and miR-93-5p levels in the urine  
362 of BC patients compared to controls[67].

363

364 Genomics-based BC biomarkers were shown in **Table 4**.

365

366

### 367 **3 Metabolomics and metabolic phenotypes of BC**

368

369 In biological research, the omics approach includes genomics, proteomics, and metabolomics. It  
370 probes physiological and malignant processes at the cellular and molecular levels; thereby,  
371 characterizing the global molecular quantity, structure, function, and dynamic changes within an  
372 organism. Although genomics and proteomics have helped subtype many cancers based on gene  
373 mutation or receptor status, considerable heterogeneity is observed in tumor behavior and patient  
374 outcome, even within a genomic subtype. This is due to the unique cellular processes and  
375 metabolic profiles that can only be elucidated through metabolomics[68]. Metabolomic analysis  
376 is less complex compared to genomics, transcriptomics, and proteomics due to fewer endpoints.  
377 Metabolomics measures the entire set of small molecule products of metabolic processes in a  
378 biological system. By focusing on the downstream products of genomic and proteomic processes,  
379 metabolomics summarizes the effects of other omics methods and most closely represents a  
380 system's phenotype[69].

381

382 Metabolomic studies are either untargeted, aiming to comprehensively include all measurable  
383 analytes without a prior hypothesis, or targeted, measuring only select predefined groups of  
384 metabolites[70]. Although untargeted studies deal with large complex data sets and carry the risk  
385 of false positives due to multiple testing of variables, the advantage is that they are free from  
386 assumptions. Targeted studies, on the other hand, are hypothesis-driven and offer measurements  
387 of high precision and accuracy. In metabolomic biomarker research, targeted studies are often  
388 used to validate findings from prior untargeted studies [71].

389

390 The field of blood-based genomic and proteomic cancer biomarkers are more developed than  
391 that of urine-based metabolomics because blood is considered to be an active participant in  
392 biological processes unlike urine, which is a contrast to waste product. With the advancement of  
393 urine analysis technology, urinalysis techniques have improved considerably. There are a number  
394 of methods that now enable in-depth analysis of diagnostic markers. In particular, NMR and MS-  
395 based identification of urinary metabolites are powerful techniques that can potentially diagnose  
396 a number of conditions. At present, urine metabolomic biomarker studies are being primarily  
397 conducted by either NMR or MS. Both of these tools have their strengths and limitations. The  
398 major advantage of MS is its accuracy and specificity in regard to metabolite detection. MS is  
399 more accurate compared to NMR spectrometry; however, the analytes need to be separated for  
400 detection and assimilation. In contrast, NMR-based spectrometry is more expensive and has  
401 lower sensitivity, generally limited to less than 100 analytes in biological fluids. Furthermore, NMR  
402 does not require the segregation of analytes for detection. The major advantage of NMR is that  
403 samples are not destroyed and can actually be reused[72-74].

404

405 BC has profound metabolic abnormalities. Several altered metabolic pathways play a role in  
406 bladder tumorigenesis. As a result, metabolomics can contribute substantially to understanding  
407 the relevant alterations of catabolic and anabolic metabolic processes impaired in cancer through  
408 the identification of tumor-specific metabolic biomarkers with potential diagnostic, prognostic, or  
409 predictive value [75]. Metabolomic studies have already identified various metabolites of diverse  
410 pathways (glucose, lipid, amino acid, nucleotide metabolites) as probable BC biomarkers[76].

411  
412 However, caution must be applied; clinical metabolic phenotypes (metabotypes) may be altered  
413 due to age, gender, diet, race, lifestyle, surgical intervention, and underlying pathophysiological  
414 conditions[77]. In the context of BC metabolomics, baseline characteristics, such as tumor stage  
415 and grade, hematuria (gross or micro), surgical interventions, and smoking habit should  
416 additionally be taken into consideration [78].

#### 417 418 **4 Metabolomic Platforms**

419  
420 Contrary to the genome or proteome, the human metabolome composition is still not fully defined.  
421 There are few research approaches, all of which have emerged in metabolome analysis; these  
422 include metabolic profiling, metabolic fingerprinting and metabolic footprinting[79].

423  
424 Metabolic profiling is an example of a targeted approach, focusing on identifying and quantifying  
425 predetermined groups of metabolites with similar physicochemical properties (e.g., carbohydrates,  
426 amino acids, organic acids, nucleosides) or under the same biochemical pathway (e.g., glycolysis,  
427 gluconeogenesis,  $\beta$ -oxidation or citric acid cycle)[80]. Metabolic profiling is considered to be an  
428 extension of metabolite targeted analysis, which relies on analyzing a single compound or small  
429 subset of metabolites to determine the influence of the specific stimuli on metabolism. Metabolic  
430 fingerprinting is an untargeted approach that is not driven by any preliminary assumption and  
431 aims to define changes in the whole metabolome, which occurs at a specific state in the cell,  
432 tissue or organism. Therefore, the main purpose of metabolic fingerprinting is to identify and  
433 qualify as many possible metabolites in samples. Metabolic fingerprinting is frequently used in a  
434 comparative analysis of two subject groups (i.e., healthy vs disease, one disease vs another  
435 disease), which makes it a promising tool in studies focused on disease diagnosis and  
436 prognosis[81]. Metabolic footprinting is often applied in microbiological or biotechnological studies.  
437 Compared to the other methods, this approach does not concern intracellular metabolites but  
438 focuses on compounds that are secreted or failed to be used by cells in specific media. Due to  
439 the close relationship between intracellular and extracellular metabolism, metabolic footprinting  
440 can provide an integrative interpretation of the metabolic network in a specific living system[82].

441  
442 Due to both the physicochemical diversity of the metabolome and complexity of the biological  
443 systems, no single analytical platform is able to determine all metabolites present in complex  
444 biofluids. Therefore, numerous analytical platforms are commonly used in both targeted and  
445 untargeted metabolomic studies [83]. NMR or MS coupled with different separation techniques  
446 currently dominates in metabolomics. There are at least four major analytical platforms with  
447 proven utility for metabolomic applications: NMR, GC-MS, LC-MS, and LCECA [84]. Each of  
448 these platforms has specific advantages and disadvantages (**Table 5**).

449  
450 Modern NMR makes it possible to perform rigorous structural analysis of many metabolites in  
451 crude extracts, cell suspensions, intact tissues, or whole organisms. Structural determination of  
452 known metabolites using various one-dimensional (1D) or 2D NMR methods is straight forward;  
453 in fact, de novo structural analysis of unanticipated or even unknown metabolites is also feasible.

454 NMR has high throughput capability and is particularly capable of determining the structure of  
455 metabolites, including the location of isotope labeled atoms in different isotopes produced during  
456 stable isotope tracing studies [85-88]. As a result, metabolic pathways can now be systematically  
457 mapped by NMR with unprecedented speed. In summary, NMR offers essentially universal  
458 detection, excellent quantitative precision, and the potential for high-throughput (>100  
459 samples/day is possible). NMR is an unbiased, robust, reproducible, non-destructive and  
460 selective analytical platform. In NMR analysis almost no sample pretreatment is required.  
461 However, the main disadvantages of this technique include low sensitivity and lack of analyte  
462 separation. Another disadvantage is its high initial cost; NMR instruments can cost well over a  
463 million dollars.

464  
465 MS represents a universal, sensitive tool that can be used to characterize, identify, and quantify  
466 a large number of compounds in biological samples where metabolite concentrations may  
467 constitute a broad range[89]. Liquid chromatography coupled with mass spectrometry (LC-MS),  
468 gas chromatography coupled with mass spectrometry (GC-MS) or capillary electrophoresis  
469 coupled with mass spectrometry (CE-MS) has a significantly wider application in metabolome  
470 analysis[83].

471  
472 GC, which employs high-resolution capillary columns and is combined with MS detection, is a  
473 powerful platform for determining the metabolome. GC-MS often employs either an electron  
474 impact (EI) or chemical ionization (CI) mode, which provides putative identification based on the  
475 highly reproducible mass spectra of metabolites and availability of universal structural and mass  
476 spectral libraries[90]. GC-MS can provide structural information (more informative if the  
477 compounds are present in existing libraries), reasonable quantitative precision, and high-  
478 throughput (>100 samples/day is possible). Sensitivity is at least 2 orders of magnitude higher  
479 than NMR. One limitation of GC-MS is its inability to study molecules that cannot be readily  
480 volatilized. Another limitation is its relatively low mass accuracy (unit resolution). GC-MS is a  
481 technique of choice for volatile and thermally stable analytes. Therefore, complex and time-  
482 consuming sample derivation is necessary; however, this can lead to undesirable metabolite loss.  
483 The recent development of multidimensional GC (GC x GC) has improved resolution, robustness,  
484 and sensitivity compared to conventional GC-MS.

485  
486 LC-MS is the most suitable technique for analyzing non-volatile, thermally unstable, high or low-  
487 molecular-weight compounds with a wide polarity range. most compounds can be analyzed by  
488 LC-MS. LC-MS is commonly used in the metabolomic analysis of various biofluids (urine, blood  
489 or tissue extracts)[91, 92]. One limitation of LC-MS is its relative difficulty in obtaining consistent  
490 quantitative precision. The development of the LC-NMR-MS systems combines the high-  
491 throughput capability of NMR with the high sensitivity and resolution of LC-MS[93, 94]. To  
492 improve the sensitivity of conventional LC-MS technique, nanoLC-MS was implemented in  
493 metabolomics studies[95, 96].

494  
495 Compared to LC-MS or GC-MS, CE-MS is rarely applied in metabolomic studies. However,  
496 recent significant improvements have opened CE-MS application in metabolomics. This  
497 technique is particularly useful in analyzing highly polar ionogenic metabolites in biological fluids  
498 [97]. CE-MS is a suitable method for urinary metabolomic analysis, which can be performed with  
499 relatively minimal sample preparation. However, extensive research is also being conducted in  
500 applying CE-MS to serum metabolomics [98]. CE-MS is a technique dedicated to water-soluble  
501 and charged molecules, which makes it a highly complementary platform to other separation  
502 methods, like LC-MS or GC-MS. The main advantages of CE-MS include high resolution power

503 and small sample or reagent requirements. Its main limitation is the unstable electroosmotic flow  
504 phenomenon, which can result in notable migration time shifts during analyses[99].

505  
506 LCECA is ideal for studies on the tryptophan and tyrosine pathways that lead to monoamine  
507 neurotransmitters because many metabolites within these two pathways can be measured  
508 quantitatively with LCECA. The robust nature of this platform, its reproducibility, and sensitivity  
509 have been well described in a series of peer-reviewed publications[100-104]. Preliminary  
510 experiments described later in this review demonstrate the power and promise of  
511 electrochemistry-based platforms for metabolomics analysis in defining signatures for central  
512 nervous system (CNS) disorders and treatments. The LCECA system is extremely sensitive,  
513 perhaps 2–3 orders of magnitude higher than that of GC-MS, and displays strong run-to-run  
514 precision over long periods of time. The disadvantages include the lack of structural information  
515 and low throughput (12 samples/day is the most commonly used metabolomic configuration). The  
516 system can detect molecules, such as tyrosine and tryptophan metabolites, as well as  
517 antioxidants and oxidative damage products, but it is “blind” to other molecules, such as glucose,  
518 ketoglutarate, and most fatty acids.

519  
520 **Table 5** shows the advantages and limitations of different metabolomics platforms.

## 521 522 523 **5 Metabolomics in BC Diagnosis and Prognosis and Predicting Response to Therapies**

524  
525 BC has profound metabolic anomalies that play central roles in tumor progression[105]. Metabolic  
526 pathways, such as the tricarboxylic acid (TCA) cycle, lipid synthesis, amino acid synthesis,  
527 nucleotide synthesis, and glycolysis pathway, are known to be increased in BC tissue compared  
528 to adjacent benign tissue[106].

### 529 530 **5.1 Tricarboxylic acid cycle**

531  
532 A significant decrease in citrate concentration was consistently observed in the urine and serum  
533 of BC patients[107]. One possible explanation for this is the active uptake of citrate from the  
534 extracellular medium into the tumor cell [108]. Citrate is important for lipid biosynthesis, which is  
535 crucial for tumor proliferation[109]. Therefore, the decrease in citrate levels in the urine or serum  
536 may illustrate the increased utilization of citrate in lipogenesis for the rapid proliferation of tumor  
537 cells[2].

### 538 539 **5.2 Lipid metabolism**

540  
541 Up or downregulation of carnitine species, including carnitine, carnitine C8:1, carnitine C9:0,  
542 carnitine C9:1, carnitine C10:1, carnitine C10:3, isobutyryl carnitine, acetylcarnitine, 2,6-  
543 dimethylheptanoylcarnitine, isovalerylcarnitine, glutarylcarnitine, and decanoylcarnitine, has been  
544 reported in BC[41, 110, 111]. The carnitine system plays a central role in lipid metabolism; it  
545 facilitates the entry of long-chain fatty acids into the mitochondria for utilization in energy-  
546 generating processes and removes short-chain and medium-chain fatty acids that accumulate as  
547 a byproduct[112]. It has been postulated that the dysregulation of lipid metabolism provides an  
548 environment that is beneficial to the development of BC. Additionally, altered fatty acid  
549 transportation, fatty acid  $\beta$ -oxidation, or energy metabolism might partially explain why BC  
550 patients are prone to lethargy[2].

551



552 **5.3 Amino acid metabolism**

553

554 **5.3.1 Glutathione metabolism**

555

556 Elevated glutathione (GSH) level was reported in BC tissues and cell lines via metabolomic  
557 studies [2]. Oxidative stress results in elevated GSH and overexpression of antioxidant enzymes,  
558 such as glutathione peroxidase, glutathione reductase, and glutathione-S transferase[113]. While  
559 GSH is involved in the detoxification of carcinogens, its elevation in tumors may promote  
560 chemotherapy resistance in cancer cells via conjugation with pharmacologically active drugs or  
561 metabolites[114].

562

563 **5.3.2 Tryptophan metabolism**

564

565 Upregulation of tryptophan metabolism in BC was observed with increased levels of anthranilic  
566 acid, N-acetylanthranilic acid, kynurenine, 3-hydroxykynurenine, and malonate[115-117]. The  
567 proposed underlying mechanisms include autoxidation and interaction with nitrite or transition  
568 metals to form reactive intermediates, binding as ligands to aryl hydrocarbon receptor (AHR) that  
569 plays a role in carcinogenesis[118]. Notably, Opitz et al. demonstrated that tryptophan-2,3-  
570 dioxygenase (TDO)-derived kynurenine suppresses antitumor immune responses and promotes  
571 tumor-cell survival through AHR, which in turn suggests TDO as a potential cancer therapeutic  
572 target[119].

573

574 **5.3.3 Hippuric acid & taurine metabolism**

575

576 Downregulation of hippuric acid was generally observed in BC patients and taurine was found to  
577 be elevated in BC patients compared to benign and healthy controls [107]. Taurine inactivates  
578 hypochlorous acid, which is a strong oxidant and cytotoxic agent, by forming stable taurine  
579 chloramine (Tau-Cl). In turn, Tau-Cl downregulates immunological responses via production of  
580 proinflammatory cytokines, leading to tumor progression[120].

581

582 **5.3.4 Nucleotide metabolism**

583

584 Purine and pyrimidine metabolism has been found to be perturbed in BC, leading to upregulation  
585 of guanine, hypoxanthine, cytidine monophosphate, thymine, uracil, uridine, and  
586 pseudouridine[111, 115]. Nucleosides, particularly modified nucleosides (e.g., pseudouridine),  
587 are elevated and suggested as potential biomarkers in various cancers[121]. Such elevation  
588 nucleoside levels have been postulated to be the result of increased DNA synthesis associated  
589 with enhanced cell cycle activity in cancer[122]. Modified nucleosides are excreted in urine  
590 because they cannot be recycled as nucleosides[123]. Thus, levels of modified nucleosides in  
591 urine reflect oxidative DNA damage and RNA turnover in the body.

592

593 **5.3.5 Glycolysis**

594

595 Lactate, an important end product of glycolysis, was found to be elevated in BC tissue and urine  
596 [115, 124], indicating an increased rate of glycolysis rate. The upregulation of glycolysis, resulting  
597 in increased glucose consumption, is a universal phenomenon in cancer and is termed the  
598 “Warburg effect” [125, 126]. Gatenby and Gillies proposed that the upregulation of glycolysis is  
599 an adaptation of premalignant lesions to intermittent hypoxia, but requires evolution to the



600 resultant proliferative and invasive phenotypes where resistance to acid-induced cell toxicity is  
601 also observed[125].

602  
603 Diagnosis and prognosis of various diseases are enhanced by the identification of biomarkers,  
604 which can differentiate individuals with the disease from those without. Ideal markers are easily  
605 detectable in tissue, serum, and urine, and have a high sensitivity and specificity. There are  
606 several potential applications of metabolomics in BC and other cancers; this includes improving  
607 detection, providing prognostic information, and impacting treatment.

608  
609  
610

## 611 **6 Clinically applicable BC biomarkers-based tools**

612  
613 At present, the FDA has approved six tests for detecting or monitoring BC. NMP22, NMP22  
614 BladderChek, and UroVysion have FDA approval for BC diagnosis and surveillance;  
615 Immunocytology (uCyt+), BTA-TRAK, and BTA-STAT have been approved only for surveillance  
616 [127-131]. There are also many metabolites that can be considered as potential tumor biomarkers  
617 for BC.

618  
619 By ultra-performance liquid chromatography time-of-flight mass spectrometry, imidazole-acetic  
620 acid was evidenced in BC[132]. A metabolite panel consisting of indolylacryloylglycine, N2-  
621 galacturonyl-L-lysine, and aspartyl-glutamate can discriminate high- vs. low-grade BC[133]. In  
622 addition, alterations in the metabolisms of phenylalanine, arginine, proline, and tryptophan were  
623 evidenced by UPLC-MS in NMBIC[134]. Jin X et al. confirmed through their study that carnitine  
624 acyltransferase and pyruvate dehydrogenase complex expressions are significantly altered in  
625 cancer[41]. Alberice JV et al. propose that metabolites related to the tryptophan metabolism  
626 pathway, such as kynurenine and tryptophan, are potential urinary biomarkers and therapeutic  
627 targets of BC therapy[116]. Wittmann et al. performed unbiased metabolomics on a set of urine  
628 samples from BC patients, revealing nearly 1000 distinct metabolic signatures, of which 587 have  
629 a chemical identity[135]. The authors chose a set of 25 potential biomarkers from this group and  
630 tested this panel on a second independent cohort to validate its predictive power. A new group of  
631 metabolites, including lactate, adenosine, succinate, and palmitoyl sphingomyelin, were proposed  
632 as urinary biomarkers; thus, showing the involvement of lipid metabolism in BC progression.

633  
634  
635

## 636 **7 Conclusions and Perspectives**

637  
638 At present, there is much research on biomarkers of BC. Biomarkers can be identified in tissue,  
639 blood, urine, etc. and include genes, proteins, metabolites, etc. In this paper, we summarized the  
640 research progress of BC biomarkers in recent years. Due to the advantages of urine collection,  
641 including non-invasive procedures, simplicity, easy storage, low-cost, and direct contact with  
642 bladder cancer tissue, we focused particularly on urinary biomarker research progress. Compared  
643 to genomics and proteomics, metabonomics of BC is still in its early stages. However, because  
644 of the great progress in metabonomics research in BC using NMR, GC-MS, and LC-MS,  
645 metabonomics has been widely used to propose new biomarkers. These may be applied to  
646 screening, diagnosing, treating, evaluating, and monitoring BC. Although the potential of  
647 metabonomics to improve detection and treatment of BC may be great, the main limitation is the  
648 lack of reliable validation for a large population. Current research has so far been limited to smaller

649 samples without validation and metabolites can be easily affected by various factors. For future  
650 metabonomics research, experimental design and analysis methods need to be standardized to  
651 eliminate the systemic influence of confounding variables on the measurement of metabolites,  
652 make results more comparable, verify potential biomarkers, and assist in clinical applications  
653 against BC.  
654  
655

656 **Table 1. Different classifications of BC based on molecular phenotyping. This table does**  
 657 **not contain classifications based on Gottfrid's research.**  
 658  
 659

<b>UNC</b>	<b>MDA</b>	<b>Lund</b>	<b>TCGA</b>	<b>Broad</b>
<b>Basal</b>	<b>Basal</b>	<b>UroA</b>	<b>Cluster I</b>	<b>Basal</b>
<b>Luminal</b>	<b>Luminal</b>	<b>UroB</b>	<b>Cluster II</b>	<b>Luminal</b>
	<b>P53-like</b>	<b>GU</b>	<b>Cluster III</b>	<b>Luminal immune</b>
		<b>SCCL</b>	<b>Cluster IV</b>	<b>immune undifferentiated</b>
		<b>Infiltrated</b>		

660  
 661

662  
663  
664

**Table 2. Summary of proteomics-based BC biomarkers**

Sample s	Proteins	Reference s
urine	AURKA	24
	ALCAM	25
	Nicotinamide N-methyltransferase	26
	APE/Ref-1	27
	CK20	28
	CK8, CK18	29
	APOA1, APOA2, APOB, APOC2, APOC3, APOE	30,31
	uromodulin, collagen $\alpha$ -1 (I), collagen $\alpha$ -1 (III), and membrane-associated progesterone receptor component 1	32
	IL-8, MMP-9/10, ANG, APOE, SDC-1, $\alpha$ 1AT, PAI-1, VEGFA, and CA9	33
	midkine (MDK), synuclein G or MDK, ZAG2, CEACAM1 and angiogenin, clusterin	34,35
	CK20, IGFII	36
	HAI-1, Epcam	37
	survivin	38
Snail	39	
CD44	40	

665  
666  
667  
668  
669  
670  
671  
672  
673  
674  
675  
676  
677  
678  
679  
680  
681

682  
683  
684

**Table 3. Summary of metabolomics-based BC biomarkers**

<b>Metabolites</b>	<b>Alteration</b>	<b>References</b>	
<i>Succinate</i>	↑	41	
<i>Pyruvated</i>	↑		
<i>Oxoglutarated</i>	↑		
<i>Carnitine</i>	↑		
<i>Phosphoenolpyruvate</i>	↑		
<i>Trimethyllysine</i>	↑		
<i>Melatonin</i>	↓		
<i>Isovalerylcarnitine</i>	↑		
<i>Glutarylcarnitine</i>	↓		
<i>Octenoylcarnitine</i>	↑		
<i>Decanoylcarnitine</i>	↑		
<i>Acetyl-CoA</i>	↑		
<i>Cholesterol</i>	↑		42
<i>5-hydroxyvaleric acid</i>	↓		
<i>3-phosphoglyceric acid</i>	↓		
<i>glycolic acid</i>	↓		
<i>dopamine 4-sulfate</i>	↑	43	
<i>MG00/1846Z,9Z,12Z,15Z/00</i>	↓		
<i>aspartyl-histidine</i>			
<i>tyrosyl-methionine</i>		45	
<i>acetyllysine</i>	↑		
<i>N-acetylneuraminic acid</i>	↑		
<i>pseudouridine</i>	↑		
<i>uridine</i>	↑		
<i>xanthine</i>	↑		
<i>7-methylguanine</i>	↑		
<i>gluconic acid</i>	↑		
<i>glucuronic acid</i>	↑		
<i>1,7 dimethylxanthine</i>	↓		
<i>hippuric acid</i>	↓		
<i>acid trehalose</i>	↑	46	
<i>nicotinuric acid</i>	↑		
<i>AspAspGlyTrp peptide</i>	↑		
<i>inosinic acid</i>	↓		
<i>ureidosuccinic acid</i>	↓		
<i>GlyCysAlaLys peptide</i>	↓		

685

686  
687

**Table 4. Summary of genomics-based BC biomarkers**

	<b>Biomarkers</b>	<b>Alteration</b>	<b>References</b>
<b>DNA Methylation</b>	SOX-1, IRAK3, and Li-MET		47
	APC and cyclin D2		48
	GSTP1 and RAR $\beta$ 2 and APC		49
	TWIST1 and NID2		50
	NID2 and TWIST1 or CFTR, SALL3 and TWIST1		51,52
	POU4F2 and PCDH17		53
	HS3ST2, SEPTIN9 and SLIT2		54
	p14ARF, p16INK4A, RASSF1A, DAPK, and APC tumor suppressor		55
<b>miRNAs</b>	miR-146a-5p	↑	56
	MiR-126	↑	57
	miR-200c	↓	58
	let-7miR, mir-1268, miR-196a, miR-1, miR-100, miR-101, and miR-143		59
	miR-96 and miR-210		60
	MiR-125b, miR-30b, miR-204, miR-99a, and miR-532-3p	↓	61
	MiR-9, miR-182 and miR-200b		62
	MiR-145		63
	MiR-144-5p		64
	miR-99a and miRNA-125b	↓	65
	miR-618 and miR-1255b-5p	↑	66
	miR-31-5p, miR-191-5p and miR-93-5p	↑	67

688  
689



690  
691  
692

**Table 5. Summary of the advantages and limitations of different metabolomics platforms**

	<b>STRENGTHS</b>	<b>DRAWBACKS</b>
NMR	Rapid	Lack of sensitivity
	reproducible	Multiplicity of the resonance
	Nondestructive	Difficulty of quantification-chemical noise and signal overlapping
	High-throughput	lack of an analyte separation component
	Minimal sample manipulation	high instrument cost (over one million dollars)
	Possible tissue analysis	
MS	High sensitivity	Low quantitation
	Wide detection range	Low reproducibility
	Easy metabolite identification-databases availability	Destructive
	Possibility to couple with separation techniques	High sample volume requirements
GC-MS	reasonable quantitative precision	Can't study nonvolatile molecules
	high throughput	low mass accuracy (often unit resolution)
	low instrumentation costs (\$100–\$300,000)	undesirable metabolite losses
	High sensitivity	
	volatile and thermally stable analytes	
LC-MS	high flexibility	high instruments cost(\$100,000-over one million dollars)
	tailor separations to the compounds	difficulty in obtaining consistent quantitative precision
	enable low, medium, or high mass accuracy	
	Can trade off sensitivity for throughput	
	Can determine the exact molecular composition various biofluids analytes	
CE-MS	highly polar ionogenic metabolites analytes	notable migration time shift during analyses
	minimal sample preparation	
LCECA	high resolution power	
	extremely sensitive	lack of structural information
	strong run-to-run precision	low throughput
	high specificity (tryptophan and tyrosine pathways)	low cost (under \$100,000)

693  
694

695 **Figure Legends**

696

697 **Figure 1. Schematic illustration of molecular subtypes of bladder cancer.** Based on Whole-  
698 genome mRNA expression profiling, several molecular subtypes of muscle-invasive bladder  
699 cancer (MIBC) have been identified. Molecular subtypes of MIBC might have important  
700 implications for patient prognosis and response to conventional chemotherapy and targeted  
701 agents. Four groups have shown great similarities among tumor subtype. Lund, University of  
702 Lund; MDA, MD Anderson Cancer Center; TCGA, The Cancer Genome Atlas; UNC, University  
703 of North Carolina.

704

705 **Figure 2. Overview of the multi-OMICS strategies for urinary bladder cancer biomarker**  
706 **discovery and their clinical implication.** A typical integrated multi-omic technologies workflow  
707 showing to probe the complexity of bladder cancer biology. Integration of several of omics data  
708 sources use systems biology approach build biomarker discovery.

709

Figure 1

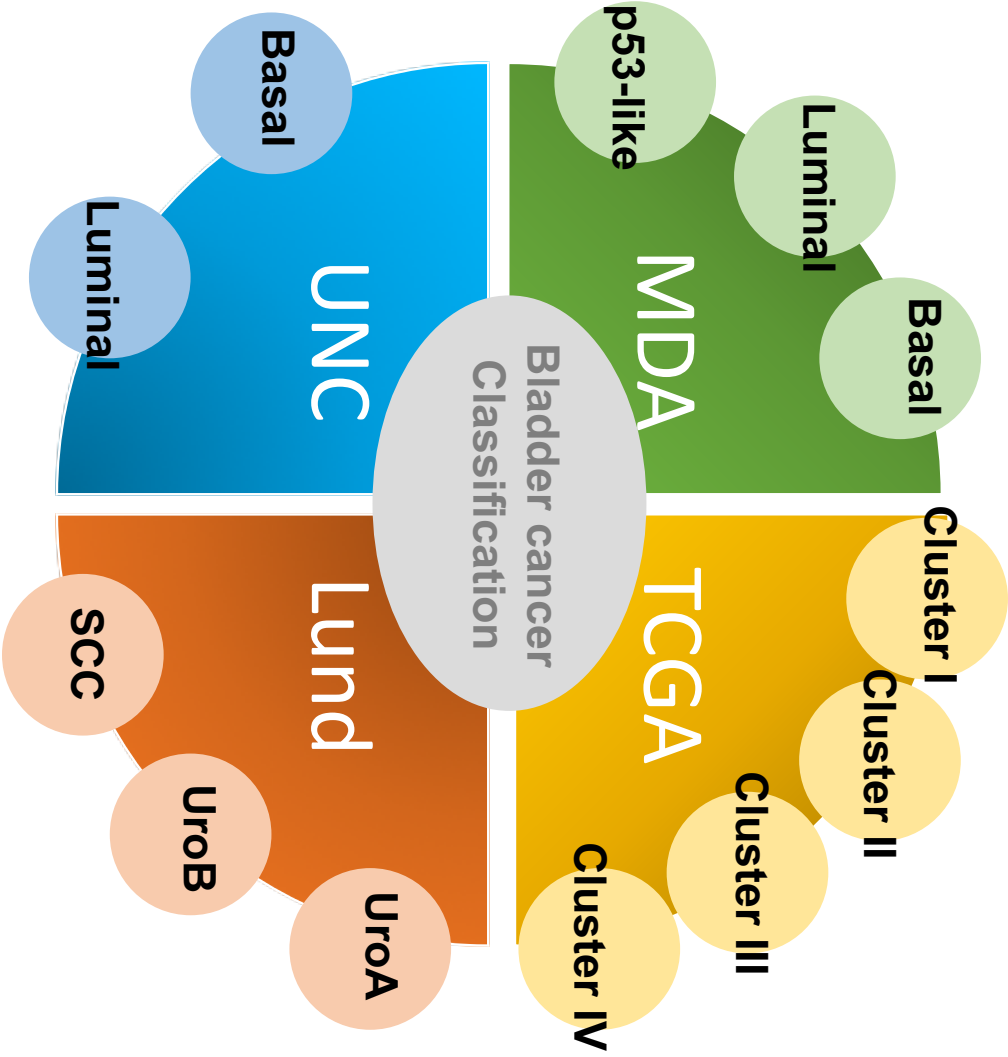
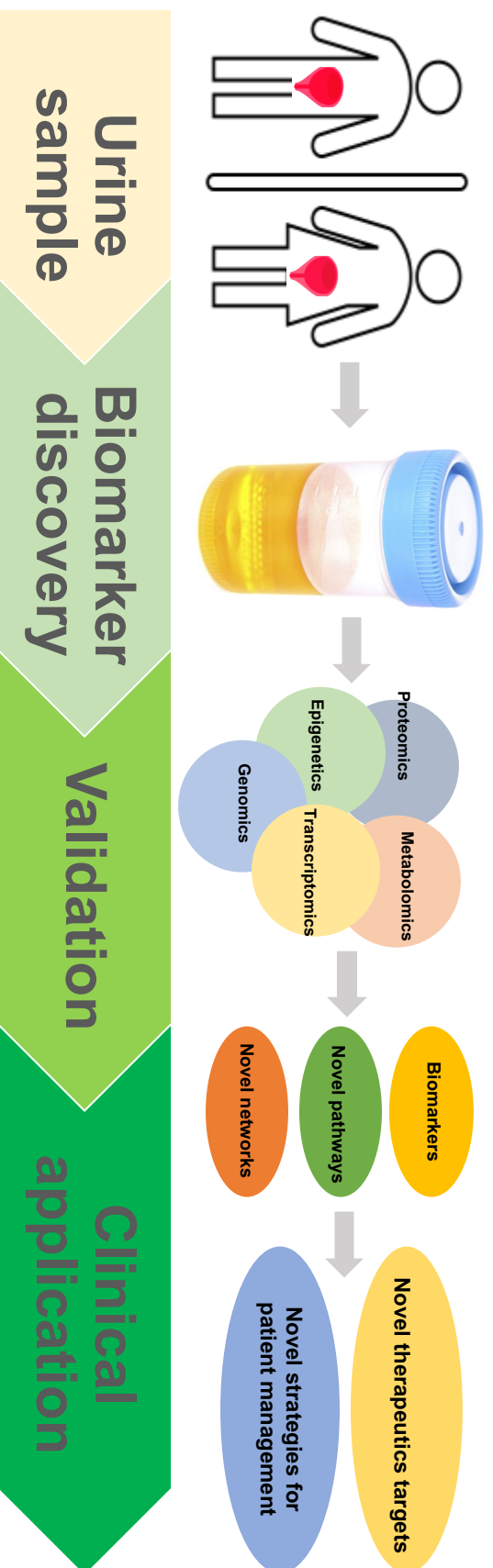


Figure 2



712 **Bibliography**

713

- 714 1. Siegel, R.L., K.D. Miller, and A. Jemal, *Cancer statistics, 2019*. CA Cancer J Clin, 2019.  
715 **69**(1): p. 7-34.
- 716 2. Mitra, A.P. and R.J. Cote, *Molecular pathogenesis and diagnostics of bladder cancer*.  
717 Annu Rev Pathol, 2009. **4**: p. 251-85.
- 718 3. Ruder, A.M., L.J. Fine, and D.S. Sundin, *National estimates of occupational exposure to*  
719 *animal bladder tumorigens*. J Occup Med, 1990. **32**(9): p. 797-805.
- 720 4. Pelucchi, C., et al., *Mechanisms of disease: The epidemiology of bladder cancer*. Nat Clin  
721 Pract Urol, 2006. **3**(6): p. 327-40.
- 722 5. Castela, J.E., et al., *Non-steroidal anti-inflammatory drugs and bladder cancer*  
723 *prevention*. Br J Cancer, 2000. **82**(7): p. 1364-9.
- 724 6. Lokeshwar, V.B., et al., *Bladder tumor markers beyond cytology: International Consensus*  
725 *Panel on bladder tumor markers*. Urology, 2005. **66**(6 Suppl 1): p. 35-63.
- 726 7. Sloan, F.A., et al., *The Cost to Medicare of Bladder Cancer Care*. Eur Urol Oncol, 2019.
- 727 8. James, A.C. and J.L. Gore, *The costs of non-muscle invasive bladder cancer*. Urol Clin  
728 North Am, 2013. **40**(2): p. 261-9.
- 729 9. Moch, H., et al., *The 2016 WHO Classification of Tumours of the Urinary System and*  
730 *Male Genital Organs-Part A: Renal, Penile, and Testicular Tumours*. Eur Urol, 2016.  
731 **70**(1): p. 93-105.
- 732 10. Eich, M.L., L. Dyrskjot, and G.J. Netto, *Toward personalized management in bladder*  
733 *cancer: the promise of novel molecular taxonomy*. Virchows Arch, 2017. **471**(2): p. 271-  
734 280.
- 735 11. Kirkali, Z., et al., *Bladder cancer: epidemiology, staging and grading, and diagnosis*.  
736 Urology, 2005. **66**(6 Suppl 1): p. 4-34.
- 737 12. Wang, G. and J.K. McKenney, *Urinary Bladder Pathology: World Health Organization*  
738 *Classification and American Joint Committee on Cancer Staging Update*. Arch Pathol Lab  
739 Med, 2019. **143**(5): p. 571-577.
- 740 13. Reuter, V.E., *The pathology of bladder cancer*. Urology, 2006. **67**(3 Suppl 1): p. 11-7;  
741 discussion 17-8.
- 742 14. Damrauer, J.S., et al., *Intrinsic subtypes of high-grade bladder cancer reflect the*  
743 *hallmarks of breast cancer biology*. Proc Natl Acad Sci U S A, 2014. **111**(8): p. 3110-5.
- 744 15. Choi, W., et al., *Identification of distinct basal and luminal subtypes of muscle-invasive*  
745 *bladder cancer with different sensitivities to frontline chemotherapy*. Cancer Cell, 2014.  
746 **25**(2): p. 152-65.
- 747 16. Cancer Genome Atlas Research, N., *Comprehensive molecular characterization of*  
748 *urothelial bladder carcinoma*. Nature, 2014. **507**(7492): p. 315-22.
- 749 17. Sjobahl, G., et al., *A molecular taxonomy for urothelial carcinoma*. Clin Cancer Res, 2012.  
750 **18**(12): p. 3377-86.
- 751 18. Kim, J., et al., *Invasive Bladder Cancer: Genomic Insights and Therapeutic Promise*. Clin  
752 Cancer Res, 2015. **21**(20): p. 4514-24.
- 753 19. Sjobahl, G., et al., *Molecular classification of urothelial carcinoma: global mRNA*  
754 *classification versus tumour-cell phenotype classification*. J Pathol, 2017. **242**(1): p. 113-  
755 125.

- 756 20. Kardos, J., et al., *Claudin-low bladder tumors are immune infiltrated and actively*  
757 *immune suppressed*. JCI Insight, 2016. **1**(3): p. e85902.
- 758 21. Hurle, R., et al., *Upper urinary tract tumors developing after treatment of superficial*  
759 *bladder cancer: 7-year follow-up of 591 consecutive patients*. Urology, 1999. **53**(6): p.  
760 1144-8.
- 761 22. Lotan, Y., R.S. Svatek, and A.I. Sagalowsky, *Should we screen for bladder cancer in a high-*  
762 *risk population?: A cost per life-year saved analysis*. Cancer, 2006. **107**(5): p. 982-90.
- 763 23. Daneshmand, S., et al., *Blue light cystoscopy for the diagnosis of bladder cancer: Results*  
764 *from the US prospective multicenter registry*. Urol Oncol, 2018. **36**(8): p. 361 e1-361 e6.
- 765 24. de Martino, M., et al., *Aurora A Kinase as a diagnostic urinary marker for urothelial*  
766 *bladder cancer*. World J Urol, 2015. **33**(1): p. 105-10.
- 767 25. Arnold Egloff, S.A., et al., *Shed urinary ALCAM is an independent prognostic biomarker of*  
768 *three-year overall survival after cystectomy in patients with bladder cancer*. Oncotarget,  
769 2017. **8**(1): p. 722-741.
- 770 26. Pozzi, V., et al., *Clinical performance and utility of a NNMT-based urine test for bladder*  
771 *cancer*. Int J Biol Markers, 2018. **33**(1): p. 94-101.
- 772 27. Choi, S., et al., *Urinary APE1/Ref-1: A Potential Bladder Cancer Biomarker*. Dis Markers,  
773 2016. **2016**: p. 7276502.
- 774 28. Mi, Y., et al., *Diagnostic accuracy of urine cytokeratin 20 for bladder cancer: A meta-*  
775 *analysis*. Asia Pac J Clin Oncol, 2019. **15**(2): p. e11-e19.
- 776 29. Ecke, T.H., et al., *UBC((R)) Rapid Test for detection of carcinoma in situ for bladder*  
777 *cancer*. Tumour Biol, 2017. **39**(5): p. 1010428317701624.
- 778 30. Chen, Y.T., et al., *Discovery of novel bladder cancer biomarkers by comparative urine*  
779 *proteomics using iTRAQ technology*. J Proteome Res, 2010. **9**(11): p. 5803-15.
- 780 31. Chen, Y.T., et al., *Multiplexed quantification of 63 proteins in human urine by multiple*  
781 *reaction monitoring-based mass spectrometry for discovery of potential bladder cancer*  
782 *biomarkers*. J Proteomics, 2012. **75**(12): p. 3529-45.
- 783 32. Schiffer, E., et al., *Prediction of muscle-invasive bladder cancer using urinary proteomics*.  
784 Clin Cancer Res, 2009. **15**(15): p. 4935-43.
- 785 33. Masuda, N., et al., *Meta-analysis of a 10-plex urine-based biomarker assay for the*  
786 *detection of bladder cancer*. Oncotarget, 2018. **9**(6): p. 7101-7111.
- 787 34. Soukup, V., et al., *Panel of Urinary Diagnostic Markers for Non-Invasive Detection of*  
788 *Primary and Recurrent Urothelial Urinary Bladder Carcinoma*. Urol Int, 2015. **95**(1): p.  
789 56-64.
- 790 35. Shabayek, M.I., et al., *Diagnostic evaluation of urinary angiogenin (ANG) and clusterin*  
791 *(CLU) as biomarker for bladder cancer*. Pathol Oncol Res, 2014. **20**(4): p. 859-66.
- 792 36. Salomo, K., et al., *Urinary transcript quantitation of CK20 and IGF2 for the non-invasive*  
793 *bladder cancer detection*. J Cancer Res Clin Oncol, 2017. **143**(9): p. 1757-1769.
- 794 37. Snell, K.I.E., et al., *Exploring the roles of urinary HAI-1, EpCAM & EGFR in bladder cancer*  
795 *prognosis & risk stratification*. Oncotarget, 2018. **9**(38): p. 25244-25253.
- 796 38. Yang, Y., J. Xu, and Q. Zhang, *Detection of urinary survivin using a magnetic particles-*  
797 *based chemiluminescence immunoassay for the preliminary diagnosis of bladder cancer*  
798 *and renal cell carcinoma combined with LAPT4B*. Oncol Lett, 2018. **15**(5): p. 7923-  
799 7933.



- 800 39. Santi, R., et al., *Snail immunohistochemical overexpression correlates to recurrence risk*  
801 *in non-muscle invasive bladder cancer: results from a longitudinal cohort study.*  
802 *Virchows Arch*, 2018. **472**(4): p. 605-613.
- 803 40. Azevedo, R., et al., *Glycan affinity magnetic nanoplatfoms for urinary glycobiomarkers*  
804 *discovery in bladder cancer.* *Talanta*, 2018. **184**: p. 347-355.
- 805 41. Jin, X., et al., *Diagnosis of bladder cancer and prediction of survival by urinary*  
806 *metabolomics.* *Oncotarget*, 2014. **5**(6): p. 1635-45.
- 807 42. Zhou, Y., et al., *Discovery and validation of potential urinary biomarkers for bladder*  
808 *cancer diagnosis using a pseudotargeted GC-MS metabolomics method.* *Oncotarget*,  
809 2017. **8**(13): p. 20719-20728.
- 810 43. Cheng, X., et al., *Metabolomics of Non-muscle Invasive Bladder Cancer: Biomarkers for*  
811 *Early Detection of Bladder Cancer.* *Front Oncol*, 2018. **8**: p. 494.
- 812 44. Tan, Y., et al., *Metabolomics study of stepwise hepatocarcinogenesis from the model rats*  
813 *to patients: potential biomarkers effective for small hepatocellular carcinoma diagnosis.*  
814 *Mol Cell Proteomics*, 2012. **11**(2): p. M111 010694.
- 815 45. Yumba Mpanga, A., et al., *Targeted metabolomics in bladder cancer: From analytical*  
816 *methods development and validation towards application to clinical samples.* *Anal Chim*  
817 *Acta*, 2018. **1037**: p. 188-199.
- 818 46. Shen, C., et al., *Developing urinary metabolomic signatures as early bladder cancer*  
819 *diagnostic markers.* *OMICS*, 2015. **19**(1): p. 1-11.
- 820 47. Su, S.F., et al., *A panel of three markers hyper- and hypomethylated in urine sediments*  
821 *accurately predicts bladder cancer recurrence.* *Clin Cancer Res*, 2014. **20**(7): p. 1978-89.
- 822 48. Pu, R.T., L.E. Laitala, and D.P. Clark, *Methylation profiling of urothelial carcinoma in*  
823 *bladder biopsy and urine.* *Acta Cytol*, 2006. **50**(5): p. 499-506.
- 824 49. Hauser, S., et al., *Serum DNA hypermethylation in patients with bladder cancer: results*  
825 *of a prospective multicenter study.* *Anticancer Res*, 2013. **33**(3): p. 779-84.
- 826 50. Renard, I., et al., *Identification and validation of the methylated TWIST1 and NID2 genes*  
827 *through real-time methylation-specific polymerase chain reaction assays for the*  
828 *noninvasive detection of primary bladder cancer in urine samples.* *Eur Urol*, 2010. **58**(1):  
829 p. 96-104.
- 830 51. Fantony, J.J., et al., *Urinary NID2 and TWIST1 methylation to augment conventional*  
831 *urine cytology for the detection of bladder cancer.* *Cancer Biomark*, 2017. **18**(4): p. 381-  
832 387.
- 833 52. van der Heijden, A.G., et al., *Urine cell-based DNA methylation classifier for monitoring*  
834 *bladder cancer.* *Clin Epigenetics*, 2018. **10**: p. 71.
- 835 53. Wang, Y., et al., *An epigenetic biomarker combination of PCDH17 and POU4F2 detects*  
836 *bladder cancer accurately by methylation analyses of urine sediment DNA in Han*  
837 *Chinese.* *Oncotarget*, 2016. **7**(3): p. 2754-64.
- 838 54. Roperch, J.P., et al., *Promoter hypermethylation of HS3ST2, SEPTIN9 and SLIT2 combined*  
839 *with FGFR3 mutations as a sensitive/specific urinary assay for diagnosis and surveillance*  
840 *in patients with low or high-risk non-muscle-invasive bladder cancer.* *BMC Cancer*, 2016.  
841 **16**: p. 704.

- 842 55. Pietrusinski, M., et al., *Detection of bladder cancer in urine sediments by a*  
843 *hypermethylation panel of selected tumor suppressor genes*. *Cancer Biomark*, 2017.  
844 **18**(1): p. 47-59.
- 845 56. Sasaki, H., et al., *Expression Level of Urinary MicroRNA-146a-5p Is Increased in Patients*  
846 *With Bladder Cancer and Decreased in Those After Transurethral Resection*. *Clin*  
847 *Genitourin Cancer*, 2016. **14**(5): p. e493-e499.
- 848 57. Hanke, M., et al., *A robust methodology to study urine microRNA as tumor marker:*  
849 *microRNA-126 and microRNA-182 are related to urinary bladder cancer*. *Urol Oncol*,  
850 2010. **28**(6): p. 655-61.
- 851 58. Wiklund, E.D., et al., *MicroRNA alterations and associated aberrant DNA methylation*  
852 *patterns across multiple sample types in oral squamous cell carcinoma*. *PLoS One*, 2011.  
853 **6**(11): p. e27840.
- 854 59. Chen, Y.H., et al., *Characterization of microRNAs expression profiling in one group of*  
855 *Chinese urothelial cell carcinoma identified by Solexa sequencing*. *Urol Oncol*, 2013.  
856 **31**(2): p. 219-27.
- 857 60. Eissa, S., et al., *Integrative functional genetic-epigenetic approach for selecting genes as*  
858 *urine biomarkers for bladder cancer diagnosis*. *Tumour Biol*, 2015. **36**(12): p. 9545-52.
- 859 61. Pospisilova, S., et al., *MicroRNAs in urine supernatant as potential non-invasive markers*  
860 *for bladder cancer detection*. *Neoplasma*, 2016. **63**(5): p. 799-808.
- 861 62. Pignot, G., et al., *microRNA expression profile in a large series of bladder tumors:*  
862 *identification of a 3-miRNA signature associated with aggressiveness of muscle-invasive*  
863 *bladder cancer*. *Int J Cancer*, 2013. **132**(11): p. 2479-91.
- 864 63. Yun, S.J., et al., *Cell-free microRNAs in urine as diagnostic and prognostic biomarkers of*  
865 *bladder cancer*. *Int J Oncol*, 2012. **41**(5): p. 1871-8.
- 866 64. Matsushita, R., et al., *Tumour-suppressive microRNA-144-5p directly targets CCNE1/2 as*  
867 *potential prognostic markers in bladder cancer*. *Br J Cancer*, 2015. **113**(2): p. 282-9.
- 868 65. Zhang, D.Z., et al., *Cell-free urinary microRNA-99a and microRNA-125b are diagnostic*  
869 *markers for the non-invasive screening of bladder cancer*. *PLoS One*, 2014. **9**(7): p.  
870 e100793.
- 871 66. Tolle, A., et al., *Identification of microRNAs in blood and urine as tumour markers for the*  
872 *detection of urinary bladder cancer*. *Oncol Rep*, 2013. **30**(4): p. 1949-56.
- 873 67. Juracek, J., et al., *Genome-wide identification of urinary cell-free microRNAs for non-*  
874 *invasive detection of bladder cancer*. *J Cell Mol Med*, 2018. **22**(3): p. 2033-2038.
- 875 68. Bathe, O.F. and F. Farshidfar, *From genotype to functional phenotype: unraveling the*  
876 *metabolomic features of colorectal cancer*. *Genes (Basel)*, 2014. **5**(3): p. 536-60.
- 877 69. Dinges, S.S., et al., *Cancer metabolomic markers in urine: evidence, techniques and*  
878 *recommendations*. *Nat Rev Urol*, 2019. **16**(6): p. 339-362.
- 879 70. Roberts, L.D., et al., *Targeted metabolomics*. *Curr Protoc Mol Biol*, 2012. **Chapter 30**: p.  
880 Unit 30 2 1-24.
- 881 71. Alonso, A., S. Marsal, and A. Julia, *Analytical methods in untargeted metabolomics: state*  
882 *of the art in 2015*. *Front Bioeng Biotechnol*, 2015. **3**: p. 23.
- 883 72. Weiss, R.H. and K. Kim, *Metabolomics in the study of kidney diseases*. *Nat Rev Nephrol*,  
884 2011. **8**(1): p. 22-33.

- 885 73. Emwas, A.H., *The strengths and weaknesses of NMR spectroscopy and mass*  
886 *spectrometry with particular focus on metabolomics research*. *Methods Mol Biol*, 2015.  
887 **1277**: p. 161-93.
- 888 74. Kalim, S. and E.P. Rhee, *An overview of renal metabolomics*. *Kidney Int*, 2017. **91**(1): p.  
889 61-69.
- 890 75. Griffin, J.L. and J.P. Shockcor, *Metabolic profiles of cancer cells*. *Nat Rev Cancer*, 2004.  
891 **4**(7): p. 551-61.
- 892 76. Cheng, Y., et al., *Metabolomics in bladder cancer: a systematic review*. *Int J Clin Exp*  
893 *Med*, 2015. **8**(7): p. 11052-63.
- 894 77. Assfalg, M., et al., *Evidence of different metabolic phenotypes in humans*. *Proc Natl Acad*  
895 *Sci U S A*, 2008. **105**(5): p. 1420-4.
- 896 78. Lotan, Y., et al., *Considerations on implementing diagnostic markers into clinical decision*  
897 *making in bladder cancer*. *Urol Oncol*, 2010. **28**(4): p. 441-8.
- 898 79. Barderas, M.G., et al., *Metabolomic profiling for identification of novel potential*  
899 *biomarkers in cardiovascular diseases*. *J Biomed Biotechnol*, 2011. **2011**: p. 790132.
- 900 80. Beckonert, O., et al., *Metabolic profiling, metabolomic and metabonomic procedures for*  
901 *NMR spectroscopy of urine, plasma, serum and tissue extracts*. *Nat Protoc*, 2007. **2**(11):  
902 p. 2692-703.
- 903 81. Ellis, D.I., et al., *Metabolic fingerprinting as a diagnostic tool*. *Pharmacogenomics*, 2007.  
904 **8**(9): p. 1243-66.
- 905 82. Mapelli, V., L. Olsson, and J. Nielsen, *Metabolic footprinting in microbiology: methods*  
906 *and applications in functional genomics and biotechnology*. *Trends Biotechnol*, 2008.  
907 **26**(9): p. 490-7.
- 908 83. Lindon, J.C. and J.K. Nicholson, *Spectroscopic and statistical techniques for information*  
909 *recovery in metabonomics and metabolomics*. *Annu Rev Anal Chem (Palo Alto Calif)*,  
910 2008. **1**: p. 45-69.
- 911 84. Kaddurah-Daouk, R., B.S. Kristal, and R.M. Weinshilboum, *Metabolomics: a global*  
912 *biochemical approach to drug response and disease*. *Annu Rev Pharmacol Toxicol*, 2008.  
913 **48**: p. 653-83.
- 914 85. Fan, X., J. Bai, and P. Shen, *Diagnosis of breast cancer using HPLC metabonomics*  
915 *fingerprints coupled with computational methods*. *Conf Proc IEEE Eng Med Biol Soc*,  
916 2005. **6**: p. 6081-4.
- 917 86. van Doorn, M., et al., *Evaluation of metabolite profiles as biomarkers for the*  
918 *pharmacological effects of thiazolidinediones in Type 2 diabetes mellitus patients and*  
919 *healthy volunteers*. *Br J Clin Pharmacol*, 2007. **63**(5): p. 562-74.
- 920 87. Clayton, T.A., et al., *Pharmaco-metabonomic phenotyping and personalized drug*  
921 *treatment*. *Nature*, 2006. **440**(7087): p. 1073-7.
- 922 88. Portilla, D., et al., *Metabolomic study of cisplatin-induced nephrotoxicity*. *Kidney Int*,  
923 2006. **69**(12): p. 2194-204.
- 924 89. Fiehn, O., *Metabolomics--the link between genotypes and phenotypes*. *Plant Mol Biol*,  
925 2002. **48**(1-2): p. 155-71.
- 926 90. Kind, T., et al., *FiehnLib: mass spectral and retention index libraries for metabolomics*  
927 *based on quadrupole and time-of-flight gas chromatography/mass spectrometry*. *Anal*  
928 *Chem*, 2009. **81**(24): p. 10038-48.

- 929 91. Becker, S., et al., *LC-MS-based metabolomics in the clinical laboratory*. J Chromatogr B  
930 Analyt Technol Biomed Life Sci, 2012. **883-884**: p. 68-75.
- 931 92. Gika, H.G., et al., *Current practice of liquid chromatography-mass spectrometry in*  
932 *metabolomics and metabonomics*. J Pharm Biomed Anal, 2014. **87**: p. 12-25.
- 933 93. Dunn, W.B., N.J. Bailey, and H.E. Johnson, *Measuring the metabolome: current analytical*  
934 *technologies*. Analyst, 2005. **130**(5): p. 606-25.
- 935 94. Zhang, A., et al., *Modern analytical techniques in metabolomics analysis*. Analyst, 2012.  
936 **137**(2): p. 293-300.
- 937 95. Myint, K.T., et al., *Polar anionic metabolome analysis by nano-LC/MS with a metal*  
938 *chelating agent*. Anal Chem, 2009. **81**(18): p. 7766-72.
- 939 96. Fernandez-Arroyo, S., et al., *Application of nanoLC-ESI-TOF-MS for the metabolomic*  
940 *analysis of phenolic compounds from extra-virgin olive oil in treated colon-cancer cells*. J  
941 Pharm Biomed Anal, 2012. **63**: p. 128-34.
- 942 97. Ramautar, R., G.W. Somsen, and G.J. de Jong, *CE-MS for metabolomics: developments*  
943 *and applications in the period 2012-2014*. Electrophoresis, 2015. **36**(1): p. 212-24.
- 944 98. Naz, S., et al., *Method development and validation for rat serum fingerprinting with CE-*  
945 *MS: application to ventilator-induced-lung-injury study*. Anal Bioanal Chem, 2013.  
946 **405**(14): p. 4849-58.
- 947 99. Moraes, E.P., et al., *Metabolomic assessment with CE-MS of the nutraceutical effect of*  
948 *Cystoseira spp extracts in an animal model*. Electrophoresis, 2011. **32**(15): p. 2055-62.
- 949 100. Shi, H., et al., *Attention to relative response across sequential electrodes improves*  
950 *quantitation of coulometric array*. Anal Biochem, 2002. **302**(2): p. 239-45.
- 951 101. Shi, H., et al., *Development of biomarkers based on diet-dependent metabolic serotypes:*  
952 *practical issues in development of expert system-based classification models in*  
953 *metabolomic studies*. OMICS, 2004. **8**(3): p. 197-208.
- 954 102. Paolucci, U., et al., *Development of biomarkers based on diet-dependent metabolic*  
955 *serotypes: concerns and approaches for cohort and gender issues in serum metabolome*  
956 *studies*. OMICS, 2004. **8**(3): p. 209-20.
- 957 103. Paolucci, U., et al., *Development of biomarkers based on diet-dependent metabolic*  
958 *serotypes: characteristics of component-based models of metabolic serotypes*. OMICS,  
959 2004. **8**(3): p. 221-38.
- 960 104. Beal, M.F., et al., *Kynurenic acid concentrations are reduced in Huntington's disease*  
961 *cerebral cortex*. J Neurol Sci, 1992. **108**(1): p. 80-7.
- 962 105. Massari, F., et al., *Metabolic phenotype of bladder cancer*. Cancer Treat Rev, 2016. **45**: p.  
963 46-57.
- 964 106. Sahu, D., et al., *Metabolomics analysis reveals distinct profiles of nonmuscle-invasive*  
965 *and muscle-invasive bladder cancer*. Cancer Med, 2017. **6**(9): p. 2106-2120.
- 966 107. Srivastava, S., et al., *Taurine - a possible fingerprint biomarker in non-muscle invasive*  
967 *bladder cancer: A pilot study by 1H NMR spectroscopy*. Cancer Biomark, 2010. **6**(1): p.  
968 11-20.
- 969 108. Anghileri, L.J., et al., *Mechanisms of gallium-67 accumulation by tumors: role of cell*  
970 *membrane permeability*. J Nucl Med, 1988. **29**(5): p. 663-8.
- 971 109. Mycielska, M.E., et al., *Citrate transport and metabolism in mammalian cells: prostate*  
972 *epithelial cells and prostate cancer*. Bioessays, 2009. **31**(1): p. 10-20.

- 973 110. Huang, Z., et al., *Bladder cancer determination via two urinary metabolites: a biomarker*  
974 *pattern approach*. Mol Cell Proteomics, 2011. **10**(10): p. M111 007922.
- 975 111. Putluri, N., et al., *Metabolomic profiling reveals potential markers and bioprocesses*  
976 *altered in bladder cancer progression*. Cancer Res, 2011. **71**(24): p. 7376-86.
- 977 112. Peluso, G., et al., *Cancer and anticancer therapy-induced modifications on metabolism*  
978 *mediated by carnitine system*. J Cell Physiol, 2000. **182**(3): p. 339-50.
- 979 113. Pelicano, H., D. Carney, and P. Huang, *ROS stress in cancer cells and therapeutic*  
980 *implications*. Drug Resist Updat, 2004. **7**(2): p. 97-110.
- 981 114. Shen, H., L. Kauvar, and K.D. Tew, *Importance of glutathione and associated enzymes in*  
982 *drug response*. Oncol Res, 1997. **9**(6-7): p. 295-302.
- 983 115. Pasikanti, K.K., et al., *Urinary metabotyping of bladder cancer using two-dimensional gas*  
984 *chromatography time-of-flight mass spectrometry*. J Proteome Res, 2013. **12**(9): p. 3865-  
985 73.
- 986 116. Alberice, J.V., et al., *Searching for urine biomarkers of bladder cancer recurrence using a*  
987 *liquid chromatography-mass spectrometry and capillary electrophoresis-mass*  
988 *spectrometry metabolomics approach*. J Chromatogr A, 2013. **1318**: p. 163-70.
- 989 117. Bansal, N., et al., *Low- and high-grade bladder cancer determination via human serum-*  
990 *based metabolomics approach*. J Proteome Res, 2013. **12**(12): p. 5839-50.
- 991 118. Chung, K.T. and G.S. Gadupudi, *Possible roles of excess tryptophan metabolites in*  
992 *cancer*. Environ Mol Mutagen, 2011. **52**(2): p. 81-104.
- 993 119. Opitz, C.A., et al., *An endogenous tumour-promoting ligand of the human aryl*  
994 *hydrocarbon receptor*. Nature, 2011. **478**(7368): p. 197-203.
- 995 120. Rosado, J.O., M. Salvador, and D. Bonatto, *Importance of the trans-sulfuration pathway*  
996 *in cancer prevention and promotion*. Mol Cell Biochem, 2007. **301**(1-2): p. 1-12.
- 997 121. Zheng, Y.F., et al., *Clinical significance and prognostic value of urinary nucleosides in*  
998 *breast cancer patients*. Clin Biochem, 2005. **38**(1): p. 24-30.
- 999 122. Wu, H., et al., *Metabolomic profiling of human urine in hepatocellular carcinoma*  
1000 *patients using gas chromatography/mass spectrometry*. Anal Chim Acta, 2009. **648**(1): p.  
1001 98-104.
- 1002 123. Nakano, K., et al., *Urinary excretion of modified nucleosides as biological marker of RNA*  
1003 *turnover in patients with cancer and AIDS*. Clin Chim Acta, 1993. **218**(2): p. 169-83.
- 1004 124. Tripathi, P., et al., *HR-MAS NMR tissue metabolomic signatures cross-validated by mass*  
1005 *spectrometry distinguish bladder cancer from benign disease*. J Proteome Res, 2013.  
1006 **12**(7): p. 3519-28.
- 1007 125. Gatenby, R.A. and R.J. Gillies, *Why do cancers have high aerobic glycolysis?* Nat Rev  
1008 Cancer, 2004. **4**(11): p. 891-9.
- 1009 126. Semenza, G.L., et al., *'The metabolism of tumours': 70 years later*. Novartis Found Symp,  
1010 2001. **240**: p. 251-60; discussion 260-4.
- 1011 127. Liang, Q., et al., *Comparison of the diagnostic performance of fluorescence in situ*  
1012 *hybridization (FISH), nuclear matrix protein 22 (NMP22), and their combination model in*  
1013 *bladder carcinoma detection: a systematic review and meta-analysis*. Onco Targets Ther,  
1014 2019. **12**: p. 349-358.

- 1015 128. Hajdinjak, T., *UroVysion FISH test for detecting urothelial cancers: meta-analysis of*  
1016 *diagnostic accuracy and comparison with urinary cytology testing*. Urol Oncol, 2008.  
1017 **26**(6): p. 646-51.
- 1018 129. Horstmann, M., et al., *Combinations of urine-based tumour markers in bladder cancer*  
1019 *surveillance*. Scand J Urol Nephrol, 2009. **43**(6): p. 461-6.
- 1020 130. Todenhofer, T., et al., *Combined application of cytology and molecular urine markers to*  
1021 *improve the detection of urothelial carcinoma*. Cancer Cytopathol, 2013. **121**(5): p. 252-  
1022 60.
- 1023 131. He, H., et al., *ImmunoCyt test compared to cytology in the diagnosis of bladder cancer: A*  
1024 *meta-analysis*. Oncol Lett, 2016. **12**(1): p. 83-88.
- 1025 132. Shao, C.H., et al., *Metabolite marker discovery for the detection of bladder cancer by*  
1026 *comparative metabolomics*. Oncotarget, 2017. **8**(24): p. 38802-38810.
- 1027 133. Liu, X., et al., *Investigation of the urinary metabolic variations and the application in*  
1028 *bladder cancer biomarker discovery*. Int J Cancer, 2018. **143**(2): p. 408-418.
- 1029 134. Loras, A., et al., *Bladder cancer recurrence surveillance by urine metabolomics analysis*.  
1030 Sci Rep, 2018. **8**(1): p. 9172.
- 1031 135. Wittmann, B.M., et al., *Bladder cancer biomarker discovery using global metabolomic*  
1032 *profiling of urine*. PLoS One, 2014. **9**(12): p. e115870.  
1033



## Research Article

# Stress-Induced Accumulation of HnRNP K into Stress Granules

Jayoung Kim<sup>1,2,3,4\*</sup>, Austin Yeon<sup>1</sup>, Woong-Ki Kim<sup>5</sup>, Khae-Hawn Kim<sup>6</sup>, Takbum Ohn<sup>7</sup>

<sup>1</sup>Departments of Surgery and Biomedical Sciences, Cedars-Sinai Medical Center, Los Angeles, CA, USA

<sup>2</sup>Samuel Oschin Comprehensive Cancer Institute, Cedars-Sinai Medical Center, Los Angeles, CA, USA

<sup>3</sup>University of California Los Angeles, CA, USA

<sup>4</sup>Department of Urology, Ga Cheon University College of Medicine, Incheon, South Korea

<sup>5</sup>Department of Microbiology and Molecular Cell Biology, Eastern Virginia Medical School, Norfolk, VA, USA

<sup>6</sup>Department of Urology, Chungnam National University Sejong Hospital, Sejong, Republic of Korea

<sup>7</sup>Department of Cellular & Molecular Medicine, College of Medicine, Chosun University, Gwangju, Republic of Korea

\***Corresponding Author:** Jayoung Kim, Departments of Surgery and Biomedical Sciences, Cedars-Sinai Medical Center, Davis 5071, 8700 Beverly Blvd., Los Angeles, CA 90048, USA, Tel: +1-310-423-7168; Fax: +1-310-967-3809

**Received:** 20 September 2021; **Accepted:** 05 October 2021; **Published:** 15 October 2021

**Citation:** Jayoung Kim, Austin Yeon, Woong-Ki Kim, Khae-Hawn Kim, Takbum Ohn. Stress-Induced Accumulation of HnRNP K into Stress Granules. Journal of Cancer Science and Clinical Therapeutics 5 (2021): 434-447.

### Abstract

Stress granules (SGs) are cytoplasmic aggregates to reprogram gene expression in response to cellular stimulus. Here, we show that while SGs are being assembled in response to clotrimazole, an antifungal medication heterogeneous nuclear ribonucleoprotein (hnRNP) K, an RNA-binding protein that mediates translational silencing of mRNAs, is rapidly accumulated in SGs in U-2OS osteosarcoma cells. Forced expression of hnRNP K induces

resistance to clotrimazole-induced apoptosis. Erk/MAPK is transiently activated in response to clotrimazole, and pharmacological suppression of the Erk/MAPK pathway sensitizes the cells to apoptosis. Inhibition of the Erk/MAPK pathway promotes the assembly of SGs. These results suggest that dynamic cytoplasmic formation of SGs and hnRNP K relocation to SGs may be defensive mechanisms against clotrimazole-induced apoptosis in U-2OS osteosarcoma cells.



**Keywords:** hnRNPK; Stress granules; Apoptosis; Erk/MAPK

**List of abbreviations:** DMEM: Dulbecco's modified Eagle's medium; FACS: Fluorescence-activated cell sorting; hnRNPs: Heterogeneous nuclear ribonucleoproteins; IF: Immunofluorescence; MAPKs: Mitogen activated protein kinases; siCTL: siRNA Control; SGs: Stress granules; SD: Standard deviation; PBs: Processing bodies; MTT: 3-(4, 5-dimethylthiazolyl-2)-2, 5-diphenyltetrazolium bromide

## 1. Introduction

Heterogeneous nuclear ribonucleoproteins (hnRNPs) play important roles both in DNA-related functions, such as transcription, recombination, and regulation of telomere length, and in RNA-related functions, such as regulation of splicing, pre-mRNA 3'-end processing, export of mRNA from the nucleus, translation, transport of mature mRNA, and mRNA turnover [1, 2]. There are approximately 20 major hnRNPs (hnRNP A1 to hnRNP U), and the location and function of each member in various cell types are distinctive [3-5]. Some hnRNPs, such as hnRNP A, hnRNP D, hnRNP E, hnRNP I, hnRNP K, and hnRNP L, shuttle between the nucleus and cytoplasm, while others mostly exist in the nucleus [6-8].

HnRNP K is an abundant and ubiquitous protein that interacts with a diverse group of molecules [2, 9]. The function of hnRNP K is modified in response to cytokines, growth factors, oxidative stress, etc. [10]. HnRNP K is also involved in multiple processes that control gene expression [11, 12]. Previous reports demonstrated altered expression and localization of hnRNP K in human tumors, including myelogenous leukemia [13] and colorectal cancer [14, 15],

suggesting the importance of mRNA metabolism regulated at the (post) translational level in cancer cells. Overexpression of hnRNP K is associated with increased transcriptional activity of oncogene c-myc and poorer survival outcomes [12], suggesting that it may have an important role in tumorigenesis. HnRNP K not only interacts with RNA, DNA, and other proteins; it also binds to factors involved in signal transduction, including mitogen activated protein kinases (MAPKs) [16]. Erk/MAPK-dependent hnRNP K phosphorylation is needed for translocation from the nucleus to cytoplasm, leading to the translational inhibition of 15-lipoxygenase. Although localization of hnRNP K is dependent on cell types, it should be noted that it may have unique motifs for nuclear/cytoplasmic shuttling. This shuttling activity of hnRNP K may be essential for biological responses that control cellular differentiation, proliferation, and survival [9, 17-20]. Electron microscopic examination revealed that hnRNP K exists in the nucleus, cytoplasm, mitochondria, and within the vicinity of the plasma membrane [21]. Interestingly, nucleus-residing hnRNP K in colon cancer cells was found to be associated with increased survival rates [22].

Post-transcriptional regulation of gene expression upon various stimuli, such as heat shock, oxidative stress, viral infection, is vital for cell survival [23]. Stress granules (SGs) are cytoplasmic sites in which translationally stalled mRNAs and numerous RNA binding proteins are nucleated upon stresses [24], and this event allows cell to reprogram gene expression [25]. SGs are signaling platforms that contribute to the coordination of cellular processes. The core constituents of SGs are small ribosomal subunits, translation initiation factors (e.g., eIF4E, eIF3, eIF4G, and PABP), and various RNA binding proteins that regulate translation or mRNA decay [26]. It has been suggested that

SGs are the sites where mRNA triage takes place to direct RNAs to be degraded or re-translated. A recent study showed that SGs also contain micro-RNA machinery, suggesting a possible link between these two pathways [27]. The SG components that contribute to the cellular responses to stress stimuli remain elusive despite recent advances in purification and molecular profiling technologies [28, 29]. In this study, we tested the hypothesis that hnRNP K is recruited to SGs in response to apoptotic stimuli, which is an essential survival mechanism. We induced apoptosis of the U-2OS osteosarcoma cells by acute treatment with clotrimazole, a broad-spectrum antimycotic drug mainly used for the treatment of fungal infections. We further tried to understand the key signaling pathways required for defense mechanism against clotrimazole-induced apoptosis.

## 2. Materials and Methods

### 2.1 Antibodies and reagents

The antibodies used in this study include the following: anti-hnRNP K (sc-28380) and anti-EIF3 $\alpha$  (sc-376651) (Santa Cruz Biotechnology, Santa Cruz, CA), anti-phospho-Erk/MAPK (9101), anti-Erk/MAPK (9102), anti-HA-Tag (3724), anti-GAPDH (5174), anti- $\beta$ -Tubulin (2146), and anti-Lamin A/C (4777) (Cell Signaling Technology, Beverly, MA). A specific MEK1 inhibitor, PD98059 (513000), and p38MAPK inhibitor, SB203580 (559389), were purchased from Sigma-Aldrich (St. Louis, MO). All other chemicals, including clotrimazole, were obtained from Sigma-Aldrich.

### 2.2 Cell culture and transfections

The U-2OS osteosarcoma cell line was procured through American Type Culture Collection and was maintained in Dulbecco's modified Eagle's medium (DMEM) (high

glucose), 10% fetal bovine serum, 100 $\mu$ g streptomycin, and 100 units/ml penicillin (Invitrogen, Carlsbad, CA) at a humidified atmosphere of 5% CO<sub>2</sub> at 37°C. U-2OS cells in 150 mm dishes at ~80% confluence were applied to electroporation with an empty vector or a hnRNPK expressing plasmid using nucleofector (Amaxa Inc., Gaithersburg, MD) followed by instructions supplied by the company. For siRNA transfection, cells were cultured in 6-well plates at a density of 1x10<sup>5</sup> cells/mL. After 24 h, cells at ~80% confluence were transiently transfected with 5-nM small interfering RNAs (siRNAs) of hnRNPK (Sigma-Aldrich) or negative control siRNA (siCTL) (Ambion, Austin, TX, USA), by using Lipofectamine RNAiMAX (Thermo Fisher Scientific Inc., Carlsbad, CA, USA), according to the manufacturer's instructions. As transfection controls, empty vector or NON-TARGET control siRNAs were used. Mock cells were treated with RNAiMAX and cultured in Opti-MEM for 6 hrs, but without siRNA.

### 2.3 Preparation of whole cell lysates and immunoblot analysis

Treated cells were washed twice in ice-cold phosphate-buffered saline (PBS) and lysed in a minimum volume of 1X cell lysis buffer [1% Nonidet P-40; 50 mM Tris pH 7.4; 10 mM NaCl; 1 mM NaF; 5 mM MgCl<sub>2</sub>; 0.1 mM EDTA; 1 mM PMSF; and COMPLETE™ protease inhibitor cocktail tablet (Roche Diagnostics Corp.)]. Protein content was determined using the Micro BCA Protein Assay Kit (Thermo Scientific, Rockford, IL). Cell extracts (10  $\mu$ g/lane) were resolved by 4-12% gradient SDS-polyacrylamide gel electrophoresis (Bio-Rad, Hercules, CA) and electro-transferred onto nitrocellulose membranes. Following the transfer, membranes were stained with Ponceau S to confirm equal protein loading. Membranes

were blocked with PBS/0.1% Tween-20 (PBST) and 10% skim milk and incubated with antibodies in PBST overnight at 4°C. Following incubation with species-specific horseradish peroxidase (HRP)-conjugated secondary antibodies, signals were detected using the SuperSignal Chemiluminescent Reagent (Pierce Chemical Co., Rockford, IL) with exposure of blots onto X-ray films.

#### **2.4 Cell proliferation assay and apoptosis analysis**

The proliferation rate was determined by counting cell numbers under the indicated conditions. Fluorescence-activated cell sorting (FACS) analysis was performed to verify the apoptotic cell population by measuring the sub-G<sub>0</sub> population. After harvesting at the indicated conditions, cells were stained with propidium iodide, and visualized by flow cytometry. Cell proliferation assays using 3-(4, 5-dimethylthiazolyl-2)-2, 5-diphenyltetrazolium bromide (MTT), and cell viability assays using crystal violet staining were performed to determine cell numbers. All experiments were performed in 6 biological replicates and mean values were calculated. TUNEL assay was performed to compare apoptotic levels in response to clotrimazole with or without PD98059, a MEK1 inhibitor, or SB203580, a p38MAPK pathway inhibitor. Cells in the cover slip were incubated in PD98059-containing medium for 1 h, followed by treatment with 20 µM clotrimazole for an additional 30 min.

#### **2.5 Immunofluorescence microscopy**

For imaging experiments, 1 x 10<sup>3</sup> cells were plated on glass cover slides (VWR, West Chester, PA) 24 h before drug treatment. Cells with 80% confluency were used for the following experiments. Pre-incubation of cells with 50 µM PD98059 for 1 h was followed by treatment with 20 µM of clotrimazole in serum-free medium. Immunostaining was

done using the following primary antibodies after clotrimazole treatment: anti-EIF3α pAb (SGs marker), or anti-hnRNP K mAb at dilutions of 1:100, 1: 50, and 1:100, respectively. Cells were fixed with 4% PFA formaldehyde for 15 min followed by ice-cold methanol for 5 min. Cells were then washed once with ice-cold PBS, and non-specific binding sites were blocked in PBS/0.1% BSA for 1 h at room temperature prior to incubation with primary antibodies. The immune reaction for each primary antibody was detected by Cy5 (blue; for EIF3α), or FITC-(green; for hnRNPK) conjugated secondary antibodies (1:250) for 30 min at room temperature. Slides were mounted in Vectashield medium-containing DAPI (Vector Laboratories, Inc., Burlingame, CA) and analyzed using AxioVision under a microscope (Carl Zeiss Inc.).

#### **2.6 Statistical analysis**

All experiments were repeated in 6 biological duplicates for statistical analysis. The data were expressed as mean ± standard deviation (SD) for continuous variables while frequencies (%) for categorical variables. Students' t test and one-way ANOVA post-hoc Tukey's test were used to compare the data from different groups. *P*<0.05 was considered statistically significant.

### **3. Results**

#### **3.1 Clotrimazole treatment induced formation of SGs and apoptosis in U-2OS sarcoma cells**

Tight control of translation is fundamental in cellular homeostasis for eukaryotic cells, and deregulation of proteins contributes to numerous human diseases. SGs and processing bodies (PBs) are the main intracellular compartments for regulating and controlling mRNA degradation, stability, and translation, which are involved in many biological responses including cell proliferation,

differentiation, apoptosis, and development [26, 30, 31]. We sought to examine in this study whether apoptosis induced by clotrimazole is linked to the functional formation of SGs, and whether hnRNPK, a potential translational regulator, is modulated during granule assembly. Clotrimazole, an antifungal drug that dissociates Hex II from the mitochondria [32], significantly induces apoptosis in U-2OS osteosarcoma cells. FACS analysis revealed that about 21.8% of cells went into the apoptotic phase 6 h after treatment with 20  $\mu$ M clotrimazole (Figure 1A). MTT assays showed a significant, dose-dependent reduction of cellular proliferation with clotrimazole (Figure 1B). TUNEL assays demonstrated increased numbers of apoptotic (green) cells detected in a dose-dependent manner (Figure 1C). When cell proliferation was measured via crystal violet staining, proliferation dramatically decreased in a time- dependent fashion, particularly with treatment with 20  $\mu$ M clotrimazole for 4 h (Figure 1D).

### **3.2 HnRNP K is necessary as a defensive mechanism against clotrimazole-induced apoptosis**

U-2OS cells formed RNA granules, such as SGs, within 30 min of being treated with clotrimazole. This was observed with immunofluorescence (IF) staining of EIF3 $\alpha$ , which indicates SGs. Representative stained images of normal and clotrimazole- stimulated conditions are shown in Figure 1E. This data demonstrated that SGs are rapidly translocated specifically to the cytoplasmic foci.

In addition, we found that cells harboring ectopic hnRNP K were more resistant to the clotrimazole-induced apoptosis, compared to cells transfected with vector plasmid (Figure 2A). In control condition, clotrimazole treatment increased apoptosis approximately 6-fold. Overexpression of hnRNP K made U-2OS cells approximately 35% more resistant to

the apoptosis induced by clotrimazole. The efficient overexpression of hnRNP K were confirmed, which was shown by Western blot analysis using anti-HA tag and anti-hnRNP K (Figure 2A, right panels). When hnRNP K expression was silenced with siRNA transfection, cells were approximately 140% more sensitized to clotrimazole treatment compared to control (Figure 2B). The knockdown of hnRNP K by siRNA transfection was confirmed using Western blot analysis with anti-hnRNP K (Figure 2B, right panels).

### **3.3 HnRNP K is recruited to cytoplasmic SGs in response to clotrimazole**

Examination of SGs in apoptotic human sarcoma cells showed that hnRNP K, which is predominantly localized to the nucleus normally, exhibited translocation upon clotrimazole treatment (Figure 3A). SGs are rapidly assembled and accumulated as cytoplasmic foci in response to clotrimazole (blue) (Figure 3A, right). These findings may suggest that translocation of hnRNP K to SGs in the cytosol could be related to the function of hnRNP K in the regulation of general translation under stress conditions. To further test the translocation of hnRNP K from the nucleus to cytosol in response to clotrimazole, cells were treated with clotrimazole and the expression of nuclear and cytoplasmic hnRNP K was examined. Subcellular fractionation and Western blot analysis showed that some part of endogenous hnRNP K (approximately 25%) moved from the nucleus to cytoplasm (Figure 3B, left). Quantitative data showing the expression % of hnRNP K in nuclear vs cytoplasmic fractions were shown in the graph (Figure 3B, right).

### **3.4 Suppression of Erk/MAPK sensitizes clotrimazole-induced apoptosis**

To investigate signal transduction pathways involved in the

assembly of SGs after treatment with clotrimazole, several signal pathways were examined. Western blot analysis using anti-phospho-Erk/MAPK antibodies demonstrated that Erk/MAPK is activated transiently 15 min after clotrimazole treatment (Figure 4A), while p38MAPK was not activated (Figure 4A). Protein levels of Erk/MAPK were not affected by clotrimazole (Figure 4A). Activation of the Erk/MAPK pathway has been linked to enhanced proliferation and anti-apoptosis of tumor cells [33].

In experiments aimed at manipulating this pathway, we used a selective inhibitor of MEK1, PD098059, and assessed the involvement of the Erk/MAPK pathway in increased apoptosis after clotrimazole treatment. Phosphorylation levels of Erk/MAPK were diminished in the presence of PD098059 (Figure 4B). Efficacy of the inhibitor was monitored by its ability to block phosphorylation of Erk/MAPK, while levels of total Erk/MAPK were not changed (Figure 4B). Both TUNEL assays (Figure 4C) and cell viability analysis (Figure 4D) showed that

suppression of the Erk/MAPK pathway enhanced apoptosis induced by clotrimazole. These results suggest that activated Erk/MAPK plays as a survival mechanism for cells against clotrimazole-induced apoptosis.

In contrast to apoptosis induction, further examination using IF staining analysis revealed that hnRNP K localization to SGs corresponded to Erk/MAPK activation (Figure 4E). The hnRNP K accumulation to foci was stimulated in response to clotrimazole treatment (CZ), which was significantly enhanced when Erk/MAPK was inhibited (CZ+PD) (Figure 4E). There was no significant change in PD98059 (PD) only, compared to control (Con). Inhibition of the p38MAPK pathway by a specific inhibitor, SB203580, had no effect on hnRNP K accumulation to foci (Figure 4E). Taken together, these experiments suggest the role of the Erk/MAPK pathway as a main mediator of clotrimazole-stimulated cell apoptosis and the formation/accumulation of SGs, but not for the formation/accumulation of PBs in U-2OS cells.

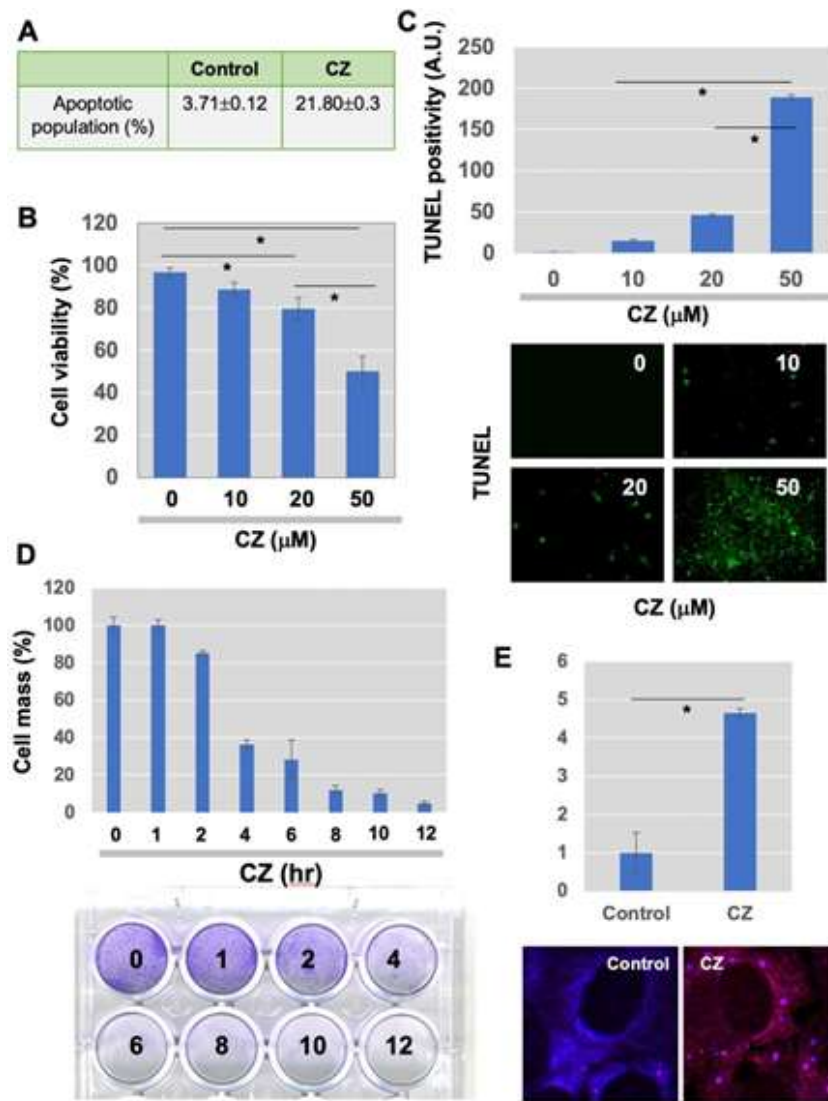


**Figure 1:** Clotrimazole treatment-induced assembly of stress granules (SGs), followed by apoptosis in U-2OS osteosarcoma cells. (A) U-2OS cells were incubated in serum-free medium containing 20 μM clotrimazole for 6 h. To measure apoptotic cell population, FACS analysis was performed after fixation and staining of cells; (B and C). (B) MTT-based proliferation assay 24 h after treatment of cells with 20 μM clotrimazole and (C) TUNEL assay were done to determine proliferation and apoptosis in response to clotrimazole (Green in Figure 1C, apoptotic cells). Bar graph representing the percentage of apoptotic cells. Error bars indicate standard errors. (n=6). \*P<0.01. (D) U-2OS cells pretreated with 20 μM clotrimazole for indicated time points (0, 1, 2, 4, 6, 8, 10, and 12 h) and crystal violet staining was performed. (E) Immunofluorescence (IF) staining analysis using marker proteins for SGs was performed 30 min after 20 μM clotrimazole treatment in serum-free medium, which was further processed for IF microscopy. The fold change of the % of accumulation into foci was shown. Scale bar, 10 μm.



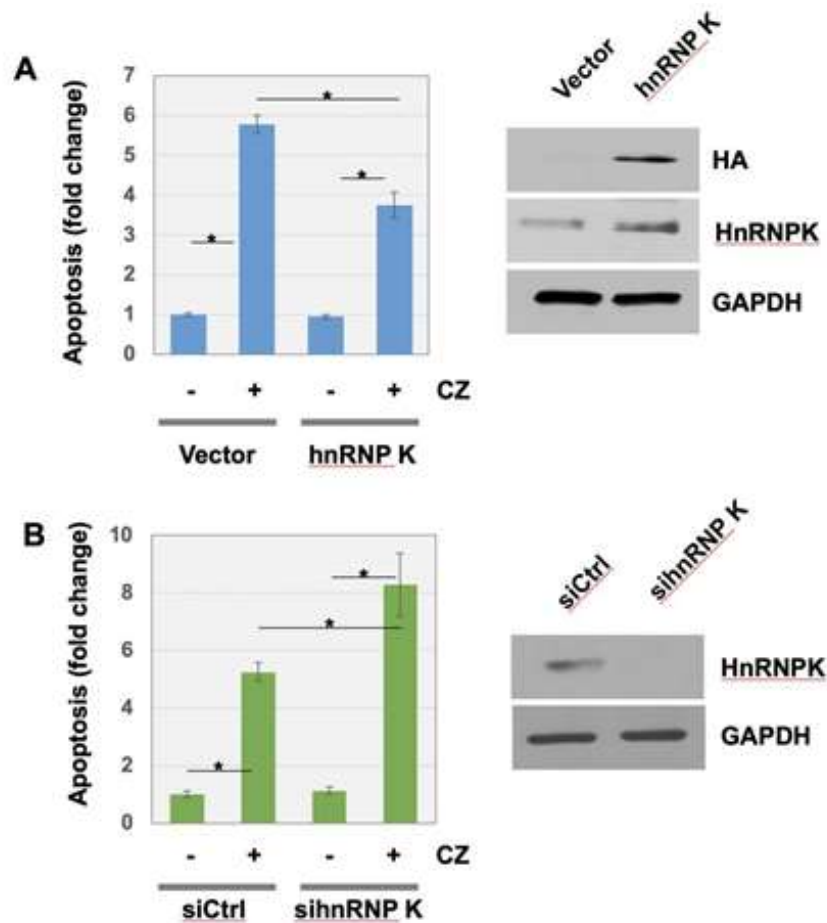


**Figure 2:** HnRNP K suppressed clotrimazole-induced apoptosis of U-2OS cells. (A) Ectopic expression of hnRNP K overexpressing construct or vector only in U-2OS cells was followed by clotrimazole treatment. The expression of HA-HnRNP K constructs were assessed by Western blot analysis using anti-HA or anti-HnRNP K antibodies. (B) U-2OS cells transiently transfected with control siRNA or si hnRNP K were treated with clotrimazole. For A and B, FACS analysis using 6 biological replicates was performed to determine apoptosis level at the indicated conditions. Error bars indicate standard derivation. \*P<0.01.



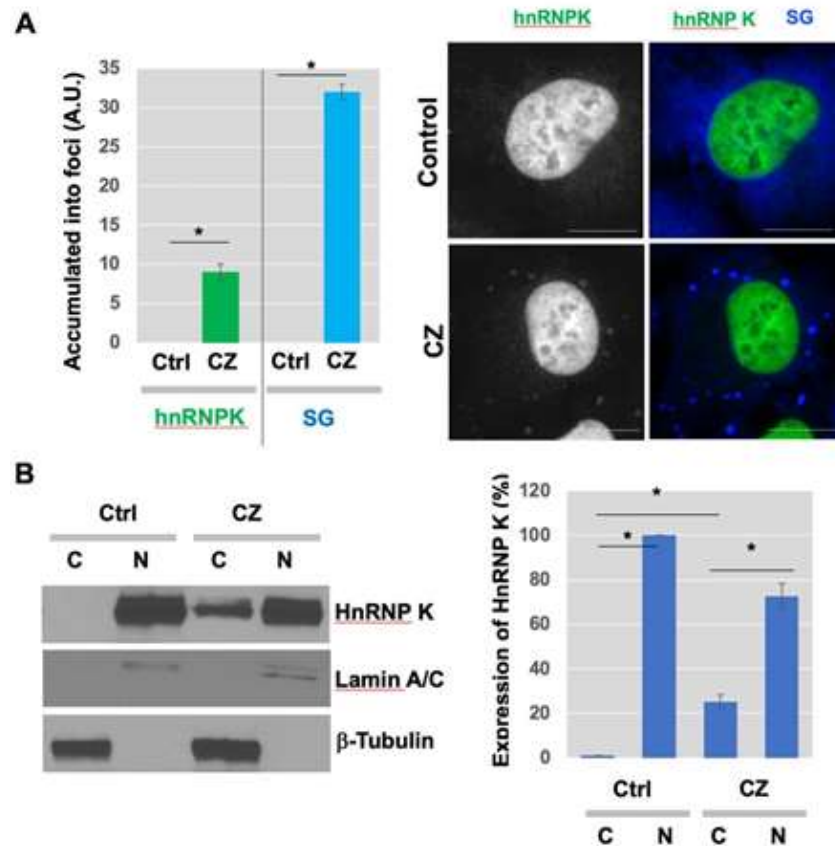


**Figure 3:** HnRNP K translocated into SGs with clotrimazole treatment. (A) Cells were incubated in serum-free medium in presence of 20  $\mu$ M clotrimazole for 30 min. After cell fixation with 4% PFA solution and methanol, cells were stained using various antibodies, as described in Materials and Methods (Gray/Green, hnRNP K; Blue, EIF3 $\alpha$ ). Scale bar, 10  $\mu$ m. (B) Cytosol accumulation of hnRNP K. U-2OS cells were treated with clotrimazole for 2 h. Western blot analysis using anti-Lamin A/C and anti- $\beta$ -Tubulin was performed and the successful subcellular fractionation for nuclear and cytoplasmic fractions was confirmed, respectively. Same concentration of proteins were used for the following Western blot analysis to measure the protein expression levels of hnRNP K in cytoplasmic vs nuclear fractions. ImageJ software was used to quantify the band intensities to determine the ratio of nuclear vs cytoplasmic hnRNP K (right).

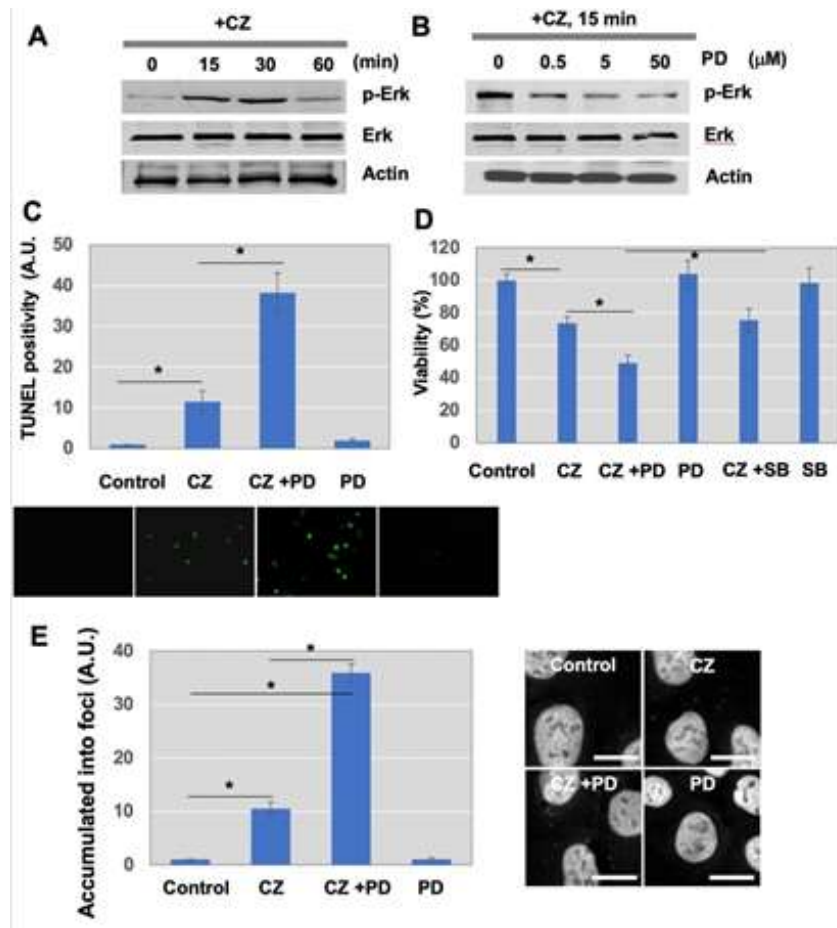


**Figure 4:** Erk/MAPK activation by clotrimazole treatment suppressed apoptosis, but not trafficking of hnRNP K. (A) Cells were treated with 20  $\mu$ M clotrimazole for the indicated times. Western blot analysis was performed to assess phosphorylation status of Erk/MAPK and p38MAPK in response to clotrimazole. The protein expression level of total Erk/MAPK and p38MAPK was also determined. (B) Inhibition of MEK1, an upstream molecule of Erk/MAPK, with PD98059 suppressed Erk/MAPK phosphorylation after treatment with clotrimazole. Cells were pretreated with 10  $\mu$ M PD98059 for 30 min and stimulated with clotrimazole for 15 min. (C) Blockage of Erk/MAPK by PD98059 increased cell apoptosis by clotrimazole. TUNEL assay was used for determination of apoptosis. Green spots indicate apoptotic cells. Representative images were shown. (D) To observe the increased apoptosis by inhibition of Erk/MAPK or p38MAPK, cells were seeded with the same density 1 day before clotrimazole treatment. Cells were pretreated with 10  $\mu$ M PD98059 or 10  $\mu$ M SB203580 for 30 min and stimulated with clotrimazole for 2 h. Cells were stained by crystal violet solution after fixation and stained cells in purple were counted as viable. (E) Cells were pretreated with 10  $\mu$ M PD98059 or 10  $\mu$ M SB203580 for 30 min, followed by incubation with 20  $\mu$ M clotrimazole for 15 min. Stained images of hnRNP K were analyzed under microscopy as described in Materials and Methods. Scale bar, 10  $\mu$ m.

#### 4. Discussion

Herein, we provide evidence that hnRNP K is translocated to cytoplasmic SGs in response to apoptotic stress induced by clotrimazole in U-2OS sarcoma cells, and that the Erk/MAPK signal pathway is activated but not required for this phenomenon. Our study is the first to address the potential role of SGs in trafficking hnRNP K in human cancer cells. SGs harbor various RNA-binding proteins and mRNAs, which play vital roles in alternative splicing. SGs are a platform of mRNA trafficking to processing bodies (PBs), where mRNA decay occurs. Our results showed that hnRNP K is present in SGs, suggesting that (1) hnRNP K binds to mRNAs to be degraded or protected from mRNA degradation upon stress stimuli, and (2) mRNA turnover can be regulated by foci formation. Microscopic examination revealed that hnRNP K accumulates dramatically and rapidly, within 30 min, to RNA granules. Being a transient phenomenon, this was consistent with previous observations that once stress is relieved, SGs disassemble [24, 34, 35]. This also supports the idea that formation of RNA granules is important in tight regulation of gene expression in response to stress. However, the complete mechanism of how these cytoplasmic foci is assembled is unknown. Our microscopic images also showed that many SGs overlap or, at the very least, assemble. Since the functions of SGs are known to be distinct, we speculated that hnRNP K in SGs would move to PBs under specific conditions via tight communication between SGs and PBs.

Cells respond to stress stimuli by activating defensive survival mechanisms to prevent damage to some extent, and, when necessary, activate apoptosis. Among the MAPK pathways, the JNK/SAPK and p38MAPK pathways are

considered to play major roles during apoptosis in response to stress stimuli. The activation of signaling pathways regulate the subcellular distribution of RNA-binding proteins and mRNA decay. The hnRNP A1, a nucleocytoplasmic shuttling protein, is translocated into SGs depending on p38MAPK and Mnk1/2-involved phosphorylation [36]. Phosphorylation of hnRNP K at serine 284 and 353 by serum-induced Erk/MAPK activation results in enhanced cytoplasmic translocation of hnRNP K and suppressed mRNA translation [16]. Our data showed that clotrimazole treatment activates Erk/MAPK, but not p38MAPK. Inhibition of Erk/MAPK or p38MAPK affect the accumulation of hnRNP K into cytoplasmic foci upon treatment with clotrimazole. However, we cannot rule out the possibility that clotrimazole may stimulate other signaling pathways resulting in the accumulation of hnRNP K into RNA granules.

Furthermore, our study found that cytoplasmic accumulation of hnRNP K is crucial for its role in metastasis by functional interference screening. Our data showed that forced expression of hnRNP K suppressed apoptosis that is induced in response to clotrimazole treatment, suggesting that hnRNP K plays an important role in stress-induced survival pathways. This observation is consistent with the previous report suggesting hnRNP K as a potential target to halt cancer progression. Although the specific role of hnRNP K sequestering to these foci is not clearly understood, it is possible that recruitment of hnRNP K to SGs may be of wider significance, considering it modulates gene expression and translation metabolism.

#### Conflicts of Interest

The authors have nothing to disclose.

## Funding

This research was funded by National Institutes of Health (1U01DK103260, 1R01DK100974, U24 DK097154, NIH NCATS UCLA CTSI UL1TR000124), Department of Defense (W81XWH-15-1-0415 and W81XWH-19-1-0109), Centers for Disease Controls and Prevention (1U01DP006079), and the U.S.-Egypt Science and Technology Development Fund by the National Academies of Sciences, Engineering, and Medicine. This article is derived from the Subject Data funded in whole or part by National Academies of Sciences, Engineering, and Medicine (NAS) and The United States Agency for International Development (USAID) (all to J.K.). This research was also supported by the National Research Foundation (NRF) funded by the Korean government (NRF- 2020R1A2C2007845 to T.O.). Any opinions, findings, conclusions, or recommendations expressed in this article are those of the authors alone, and do not necessarily reflect the views of USAID or NAS.

## Acknowledgments

The authors wish to thank Dr. Minjung Kim (University of South Florida) and Dr. Aravindh K. Jayabalan (Johns Hopkins University) for critical reading and comments. This research was supported by the Samuel Oschin Comprehensive Cancer Institute (SOCCI) at Cedars-Sinai Medical Center through the Lucy S. Gonda Award (2019).

## References

1. Krecic AM, Swanson MS. hnRNP complexes: composition, structure, and function. *Curr Opin Cell Biol* 11 (1999): 363-371.
2. Perrotti D, Neviani P. From mRNA metabolism to cancer therapy: chronic myelogenous leukemia shows the way. *Clin Cancer Res* 13 (2007): 1638-1642.
3. Burd CG, Dreyfuss G. Conserved structures and diversity of functions of RNA-binding proteins. *Science* 265 (1994): 615-621.
4. Burd CG, Dreyfuss G. RNA binding specificity of hnRNP A1: significance of hnRNP A1 high-affinity binding sites in pre-mRNA splicing. *Embo J* 13 (1994): 1197-1204.
5. Geuens T, Bouhy D, Timmerman V. The hnRNP family: insights into their role in health and disease. *Hum Genet* 135 (2016): 851-867.
6. Dreyfuss G, Matunis MJ, Pinol-Roma S, et al. hnRNP proteins and the biogenesis of mRNA. *Annu Rev Biochem* 62 (1993): 289-321.
7. Conway G, Wooley J, Bibring T, et al. Ribonucleoproteins package 700 nucleotides of pre-mRNA into a repeating array of regular particles. *Mol Cell Biol* 8 (1988): 2884-2895.
8. Wall ML, Bera A, Wong FK, et al. Cellular stress orchestrates the localization of hnRNP H to stress granules. *Exp Cell Res* 394 (2020): 112111.
9. Bomsztyk K, Denisenko O, Ostrowski J. hnRNP K: one protein multiple processes. *Bioessays* 26 (2004): 629-638.
10. Ostrowski J, Klimek-Tomczak K, Wyrwicz LS, et al. Heterogeneous nuclear ribonucleoprotein K enhances insulin-induced expression of mitochondrial UCP2 protein. *J Biol Chem* 279 (2004): 54599-54609.
11. Ostrowski J, Wyrwicz L, Rychlewski L, et al. Heterogeneous nuclear ribonucleoprotein K protein associates with multiple mitochondrial transcripts within the organelle. *J Biol Chem* 277 (2002): 6303-6310.

12. Notari M, Neviani P, Santhanam R, et al. A MAPK/HNRPK pathway controls BCR/ABL oncogenic potential by regulating MYC mRNA translation. *Blood* 107 (2006): 2507-2516.
13. Gallardo M, Lee HJ, Zhang X, et al. hnRNP K Is a Haploinsufficient Tumor Suppressor that Regulates Proliferation and Differentiation Programs in Hematologic Malignancies. *Cancer Cell* 28 (2015): 486-499.
14. Zhu XH, Wang JM, Yang SS, et al. Down-regulation of DAB2IP promotes colorectal cancer invasion and metastasis by translocating hnRNP K into nucleus to enhance the transcription of MMP2. *Int J Cancer* 141 (2017): 172-183.
15. Gao T, Liu X, He B, et al. Exosomal lncRNA 91H is associated with poor development in colorectal cancer by modifying HNRNP K expression. *Cancer Cell Int* 18 (2018): 11.
16. Habelhah H, Shah K, Huang L, et al. ERK phosphorylation drives cytoplasmic accumulation of hnRNP-K and inhibition of mRNA translation. *Nat Cell Biol* 3 (2001): 325-330.
17. Xu Y, Li R, Zhang K, et al. The multifunctional RNA-binding protein hnRNP K is critical for the proliferation and differentiation of myoblasts. *BMB Rep* 51 (2018): 350-355.
18. Li J, Chen Y, Xu X, et al. HNRNP K maintains epidermal progenitor function through transcription of proliferation genes and degrading differentiation promoting mRNAs. *Nat Commun* 10 (2019): 4198.
19. Li D, Wang X, Mei H, et al. Long Noncoding RNA pancEts-1 Promotes Neuroblastoma Progression through hnRNP K-Mediated beta-Catenin Stabilization. *Cancer Res* 78 (2018): 1169-1183.
20. Good AL, Haemmerle MW, Oguh AU, et al. Metabolic stress activates an ERK/hnRNP K/DDX3X pathway in pancreatic beta cells. *Mol Metab* 26 (2019): 45-56.
21. Mikula M, Dzwonek A, Karczmarski J, et al.: Landscape of the hnRNP K protein- protein interactome. *Proteomics* 6 (2006): 2395-2406.
22. Carpenter B, McKay M, Dundas SR, et al. Heterogeneous nuclear ribonucleoprotein K is over expressed, aberrantly localised and is associated with poor prognosis in colorectal cancer. *Br J Cancer* 95 (2006): 921-927.
23. Anderson P, Kedersha N. Stressful initiations. *J Cell Sci* 115 (2002): 3227-3234.
24. Kedersha N, Stoecklin G, Ayodele M, et al.: Stress granules and processing bodies are dynamically linked sites of mRNP remodeling. *J Cell Biol* 169: 871-884, 2005.
25. Markmiller S, Soltanieh S, Server KL, et al. Context-Dependent and Disease- Specific Diversity in Protein Interactions within Stress Granules. *Cell* 172 (2018): 590-604 e513.
26. Anderson P, Kedersha N. RNA granules. *J Cell Biol* 172 (2006): 803-808.
27. Leung AK, Calabrese JM, Sharp PA. Quantitative analysis of Argonaute protein reveals microRNA-dependent localization to stress granules. *Proc Natl Acad Sci U S A* 103 (2006): 18125-18130.
28. Mahboubi H, Stochaj U. Cytoplasmic stress granules: Dynamic modulators of cell signaling and disease. *Biochim Biophys Acta Mol Basis Dis* 1863 (2017): 884-895.
29. Ohn T, Kedersha N, Hickman T, et al. A functional RNAi screen links O-GlcNAc modification of

- ribosomal proteins to stress granule and processing body assembly. *Nat Cell Biol* 10 (2008): 1224-1231.
30. Eulalio A, Behm-Ansmant I, Izaurralde E. P bodies: at the crossroads of post-transcriptional pathways. *Nat Rev Mol Cell Biol* 8 (2007): 9-22.
31. Jakymiw A, Pauley KM, Li S, et al. The role of GW/P-bodies in RNA processing and silencing. *J Cell Sci* 120 (2007): 1317-1323.
32. Majewski N, Nogueira V, Bhaskar P, et al. Hexokinase-mitochondria interaction mediated by Akt is required to inhibit apoptosis in the presence or absence of Bax and Bak. *Mol Cell* 16 (2004): 819-830.
33. Roberts PJ, Der CJ. Targeting the Raf-MEK-ERK mitogen-activated protein kinase cascade for the treatment of cancer. *Oncogene* 26 (2007): 3291-3310.
34. Kedersha N, Anderson P. Stress granules: sites of mRNA triage that regulate mRNA stability and translatability. *Biochem Soc Trans* 30 (2002): 963-969.
35. Kedersha N, Anderson P. Mammalian stress granules and processing bodies. *Methods Enzymol* 431 (2007): 61-81.
36. Guil S, Long JC, Caceres JF. hnRNP A1 relocalization to the stress granules reflects a role in the stress response. *Mol Cell Biol* 26 (2006): 5744-5758.



This article is an open access article distributed under the terms and conditions of the [Creative Commons Attribution \(CC-BY\) license 4.0](https://creativecommons.org/licenses/by/4.0/)